IL
NUOVO CIMENTO
ORGANO DELLA SOCIETÀ ITALIANA DI FISICA
SOTTO GLI AUSPICI DEL CONSIGLIO NAZIONALE DELLE RICERCHE
E DEL COMITATO NAZIONALE PER L'ENERGIA NUCLEARE

VOL. XXII, N. 2 *Serie decima* 16 Ottobre 1961

Annihilation of Polarized Positrons in Magnetized Iron (*).

W. D. McGLINN (**)

Physics Department, Northwestern University - Evanston, Ill.

(ricevuto il 14 Ottobre 1960)

Summary. — An attempt is made to describe the integral, angular correlations for annihilation of polarized positrons in iron for a saturating magnetic field. A comparison with experiment is made. The positron wave function used to calculate the angular correlation for annihilation of the $3s$, $3p$, and $3d$ electrons of iron was that obtained by a Wigner-Seitz calculation for zero crystal momentum, the potential in the Schrödinger equation being taken as the ion core potential. The inner electron wave functions were assumed to be those of free atomic iron. The angular correlation for the conduction electron annihilation was calculated assuming a degenerate Fermi gas for the electrons and a zero-momentum wave function for the positron.

Introduction.

One of the many experiments that have been performed using the polarized beam of β-particles coming from β-decay was that of HANNA and PRESTON (1). In this experiment they observed the angular correlation of the two-γ annihilation in ferro-magnetic materials first with a saturating magnetic field in the direction of the incoming annihilating positron and then opposite to this direction. A difference in the two correlations was noted.

(*) Based on a thesis submitted to the University of Kansas in partial fulfillment of the requirements of a Ph. D. degree. The results of this paper were reported at the 1959 Annual Meeting of the American Physical Society held in New York, N. Y.

(**) Magnolia Oil Fellow.

(1) S. S. HANNA and R. S. PRESTON: *Phys. Rev.*, **109**, 3 (1958).

This work is an attempt to explain this difference semi-quantitatively and also to explain the shape of the angular correlation curve.

The very presence of an effect already indicated that at least part of the high momentum part of the two-γ correlation is due to annihilation of inner electrons in particular electrons contributing to ferro-magnetism. This is in contradiction to the belief held by some that the high momentum part is due mainly to an excluded volume effect in the positron wave function ([2]).

1. – The relation between the two-photon angular correlation and the wave function of the system.

If an initial state of the positron-electron system be given by a momentum distribution function $\theta(p_1, l_1, ..., q, s)$, where p_j, l_j, and q, s are the momentum and spin variables of electron j and the positron then the field theoretic state vector corresponding to this state will be represented by

$$(1) \qquad |I\rangle = \sum_{s} \sum_{l_1 \ldots l_n} \int_{-\infty}^{+\infty} \mathrm{d}^3q \, \mathrm{d}^3p_1 \ldots \mathrm{d}^3p_n \, \frac{\theta(p_1, l_1 \ldots, q, s)}{(N!)^{\frac{1}{2}}} \, a^*_{l_1}(p_1) \ldots b^*_s(q) \, |\Omega\rangle \, ,$$

where: $|\Omega\rangle$ = the vacuum state,

$a^*_{l_i}(p_1)$ = creation operator for an electron in a plane wave state of momentum p and spin l,

$b^*_s(q)$ = creation operator for a positron in a plane wave state of momentum q and spin s.

The part of the S operator that contributes to first order to quantum annihilation is given by

$$(2) \qquad R = \sum_{s_0} \sum_{l_0} \int M(k_1, \lambda_1, k_2, \lambda_2, p_0, l_0, q_0, s_0) \cdot$$
$$\cdot a_{l_0}(p_0) b_{s_0}(q_0) \, \mathrm{d}^3p_0 \mathrm{d}^3q_0 \int \frac{\exp\left[i(p_f - p_i)\cdot x\right]}{(2\pi)^4} \, \mathrm{d}^4x \, ,$$

(see eq. (12-30) of ref. ([3])). The notation used here is the same as ref. ([3]) except that in addition s and l are used to indicate the spin state of the positron and electron respectively.

Letting the final state vector be denoted by

$$|F\rangle = a^*_{l_1}(p'_1) a^*_{l_1}(p'_2) \ldots a^*_{l'_{n-1}}(p'_{n-1}) \, |\Omega\rangle \, ,$$

([2]) R. A. FERRELL and F. ROHRLICH: *Rev. Mod. Phys.*, **28**, 308 (1956).

([3]) J. M. JAUCH and R. ROHRLICH: *The Theory of Photons and Electrons* (Cambridge, Mass., 1955).

assuming a product-type wave function for the initial state, that is

$$\theta = \theta_+(q_0, s_0) \sum_p \frac{(-1)^p}{(N!)^{\frac{1}{2}}} \theta_1(p_0, l_0) \dots \theta_n(p_{n-1}, l_{n-1}) , \tag{3}$$

such that

$$\sum_l \int \mathrm{d}^3p\, \theta_i^*(p, l)\theta_j(p, l) = \delta_{ij} ,$$

the transition probability is given by

$$\begin{aligned} \Gamma_T = & \int \mathrm{d}k_1\, \mathrm{d}k_2 \frac{1}{(N-1)!} \int \sum_{l'_1 \dots l'_n} {}_1 |\langle F | R | I \rangle|^2 \mathrm{d}^3p'_1 \dots \mathrm{d}^3p'_{n-1} = \\ = & \frac{1}{(N-1)!} \int \mathrm{d}k_1\, \mathrm{d}k_2 \sum_j \sum_{\substack{l'_0 s'_0 \\ l_0 s_0}} \int M^*(p'_0, l'_0, q'_0, s'_0, k_1, k_2) M(p_0, l_0, q_0, s_0, k_1, k_2) \cdot \\ & \cdot \theta_j^*(p'_0, l'_0)\theta_j(p_0, l_0)\theta_+^*(q'_0, s'_0)\theta_+(q_0, s_0)\delta^4(k_1 + k_2 - p'_0 - q'_0) \cdot \\ & \cdot \delta^4(k_1 + k_2 - p_0 - q_0)\, \mathrm{d}^3p'_0\, \mathrm{d}^3q'_0\, \mathrm{d}^3p_0\, \mathrm{d}^3q_0 , \end{aligned} \tag{4}$$

where the integration of k_1 and k_2 extends over the final states to be considered. If one quantizes in a volume v, becomes

$$\begin{aligned} \Gamma = & \frac{(2\pi)^2}{V} \sum_j \sum_{\substack{l_0 k'_0 \\ l_0 s_0}} \sum_{\substack{p'_k q'_i \\ p_k q_i}} \theta_j^*(p'_k, l'_0)\theta_j(p_k, l_0)\theta_+^*(q'_i, s'_0)\theta_+(q_i, s_0) \cdot \\ & \cdot \lim_{\substack{v \to \infty \\ T \to \infty}} \int_{vT} \frac{\exp[i(p_k + q_i - p'_k - q'_i) \cdot x]}{vT} \mathrm{d}^4x \cdot \\ & \cdot \int \mathrm{d}k_1\, \mathrm{d}k_2\, M^*(p'_k, l'_0, q'_i, s'_0, k_1, k_2) M(p_k, l_0, q_i, s_0, k_1, k_2) \delta(k_1 + k_2 - p_k - q_i) . \end{aligned} \tag{5}$$

Since almost all the positrons in metals are thermalized before annihilating both the momenta of the electron and of the positron are non-relativistic upon annihilation [4]. If one makes the approximation $\bar{p}_k = \bar{q}_i = 0$ in M and M^* and that $p_{k0} = q_{i0} = m$, the integral (5) reduces to (suppressing the spin indices)

$$\begin{aligned} \Gamma = & (2\pi)^2 \int \mathrm{d}k_1\, \mathrm{d}k_2 |M(0, 0, k_1, k_2)|^2 \delta(|\bar{k}_1| + |\bar{k}_2| - 2m) \cdot \\ & \cdot \sum_{s_i} \delta(\bar{k}_1 + \bar{k}_2 - \bar{s}_i)\Phi_j(s_i)\Phi_j^*(s_i) , \end{aligned} \tag{6}$$

[4] G. E. Lee-Whiting: *Phys. Rev.*, **97**, 155 (1955).

where

$$\Phi_j(s_i) = \int \frac{\Psi_i(y)\Psi_+(y)}{v^{\frac{1}{2}}} \exp\left[-i\bar{s}_i \cdot \bar{y}\right] \mathrm{d}^3 y \,.$$

It is easily shown that $M(0, l_0, 0, s_0, k_1, k_2)$ is a constant for spins l_0 and s_0 anti-parallel and equal to zero for spins parallel. Since we are not interested in the absolute value the transition probability per unit time we can replace M^2 by $\delta_{l,-s}$, where l is the z component of the spin index of the electron and s is that of the positron.

If one assumes that the positron wave function is polarized in spin, that is the probability of finding the spin up is a^2 and spin down is b^2, $b^2 \neq a^2$, then the final transition probability, averaged over the initial spin of the positron is given by

$$(7) \qquad \Gamma = C \int \mathrm{d}k_1 \, \mathrm{d}k_2 \sum_j \left[b^2 \delta_{\lambda_j +} + a^2 \delta_{\lambda_j -}\right] \cdot \cdot \delta(|\bar{k}_1| + |\bar{k}_2| - 2m) \sum_{s_i} \delta(\bar{k}_1 + \bar{k}_2 - \bar{s}_i) \, \Phi_j(s_i) \, \Phi_j^*(s_i) \,,$$

where λ_i is the spin index of Ψ_j, Ψ_j is assumed an eigenstate of the z component of the spin, and C is a proportionality constant involving M.

2. – The positron wave function.

Since the positron is nearly always thermalized before annihilating one must obtain the crystal wave function of the positron of lowest energy. This will correspond to the lowest energy wave function with crystal momentum equal to zero. We shall use the cellular method of Wigner-Seitz for computing this wave function. Since the iron crystal is body-centered cubic we will assume the unit cell can be replaced with a sphere of equal volume. We shall assume a spherical potential within each cell that arises from atomic iron electron functions for the argon core and the electrons that are assumed present. The valence electrons we assume for this calculation are smeared uniformally throughout the crystal. Two cases will be treated, one assuming present six $3d$ electrons per atom, the second case assuming two $3d$ electrons present [5].

The boundary condition at the unit cell radius implied by the Bloch form is

$$\frac{\mathrm{d}\Psi(r_0)}{\mathrm{d}r} = 0 \,.$$

---

[5] R. J. WEISS and J. J. DE MARCO: *Rev. Mod. Phys.*, **30**, 59 (1958).

The lowest energy wave function associated with crystal momentum equal to zero is an s wave function satisfying the above boundary condition and having its first zero with decreasing r, at $r = 0$.

The electron wave functions used to calculate the effective potential were those given in ref. [6]. These should of course be altered by the fact that the $4s$ electrons are not present as such, and, for instance, in the case assuming two $3d$ electrons, not all of the $3d$ electrons are present as such. There is also the fact that the wave functions, especially the d wave functions, are altered from those of the free atom. Hopefully these corrections are small.

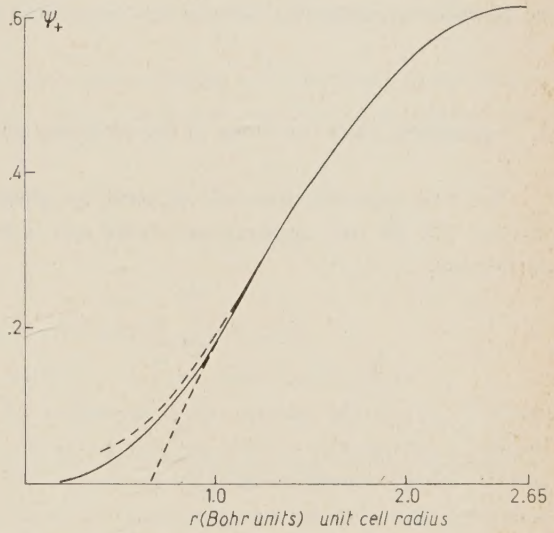

Fig. 1. – Calculated positron wave function assuming six $3d$ electrons present.

The wave equation was integrated numerically for various values of the energy until two values were found differing in the third significant figure, one that caused the wave function to cross over the axis and the other that caused the wave function to turn upwards. A curve was drawn between these two going smoothly to zero at $r = 0$. The results are indicated in Fig. 1 and 2. The normalization in these figures is not significant.

As can be seen there is considerable penetration of the core by the positron wave function for both cases. For the case of six $3d$ electrons the penetration

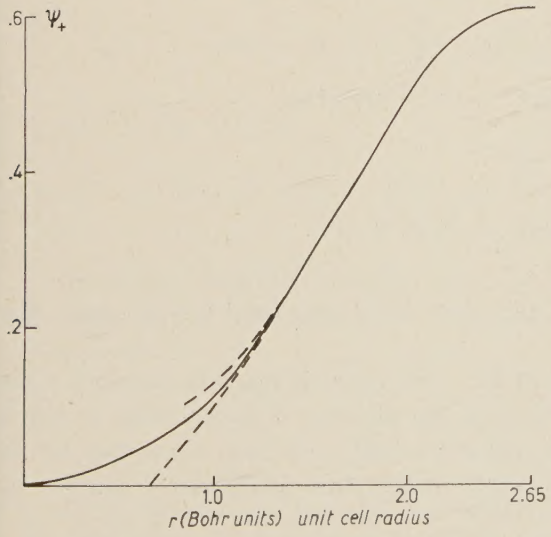

Fig. 2. – Calculated positron wave function assuming two $3d$ electrons present.

[6] M. F. MANNING and L. GOLDBERG: *Phys. Rev.*, **53**, 662 (1938).

is greater as would be expected from the fact that the repulsive potential of the nucleus is shielded more in this case than in the case of two $3d$ electrons. This large penetration contradicts some previous assumptions but is essentially in agreement with the results of DONOVAN and MARCH for copper [7].

3. – Assumed wave functions of the electrons and the resulting angular correlations.

We will consider the $3s$, $3p$, and $3d$ electrons in a tight binding approximation (2). In this approximation we can represent the electron wave functions as follows,

$$\Psi_{K,m} = \frac{1}{N^{\frac{1}{2}}} \sum_{r_n} \exp\left[iK \cdot r_m\right] \Psi_m(r - r_n) ,$$

where $\Psi_m(r)$ is the atomic wave function of a d, s or p electron with a particular z component of the angular momentum m, k is the crystal momentum and r is the position of the nucleus. We must consider as indicated in Section 1 the Fourier transform of the product of the electron wave function and the positron wave function $\Psi_+/N^{\frac{1}{2}}$, that is

$$\theta_{K,m}(k) = \int \Psi_{K,m}(\bar{r}) \frac{\Psi_+(r)}{N^{\frac{1}{2}}} \exp\left[-ik \cdot r\right] \mathrm{d}^3x .$$

Using the periodicity of $\Psi_{K,m}$ and Ψ_+, from (7) we find for the transition probability for the $3s$ level

$$\Gamma_{3s} = \frac{C}{8\pi^3} \sum_m \int \mathrm{d}k_1 \, \mathrm{d}k_2 \, \delta(|\bar{k}_1| + |\bar{k}_2| - 2m) \, |F_m(\bar{k}_1 + \bar{k}_2)|^2 , \tag{8}$$

where

$$F_m(\bar{k}) = \int \exp\left[i\bar{k} \cdot \bar{r}\right] \Psi_0 \, \Psi_m \, \mathrm{d}^3r .$$

The transition probability per unit time for the $3p$ level has of course the same form.

Because the $3d$ level is not filled for each atom, it must be handled a bit differently. Since the material in which the positron is annihilating is not a single crystal but rather many crystals randomly oriented, there can be no preferential occupation of a level corresponding to a particular z component

(7) B. DONOVAN and N. H. MARCH: *Phys. Rev.*, **110**, 582 (1958).

of the angular momentum, and we must assume they have the same probability of occupation.

For iron at magnetic saturation magnetic moment measurements indicate that there are about two more electrons in the d level aligned opposite to the field than with it.

With these considerations, for the case assuming two electrons in the d level, the transition probability per unit time when the electrons are aligned up is

$$\Gamma_{3d} = \sum_m \frac{2}{5} b^2 \frac{C}{8\pi^3} \int \mathrm{d}k_1 \, \mathrm{d}k_2 \, \delta(|\bar{k}_1| + |\bar{k}_2| - 2m) \, |F_m(\bar{k}_1 + \bar{k}_2)|^2 , \tag{9}$$

and when aligned down is

$$\Gamma_{3d} = \sum_m \frac{2}{5} a^2 \frac{C}{8\pi^3} \int \mathrm{d}k_1 \, \mathrm{d}k_2 \, \delta(|\bar{k}_1| + |\bar{k}_2| - 2m) \, |F_m(\bar{k}_1 + \bar{k}_2)|^2 . \tag{10}$$

In the case where six electrons are in the d level one obtains for spins aligned upward

$$\Gamma_{3d} = \frac{C}{8\pi^3} \sum_m \left(b^2 \frac{4}{5} + a^2 \frac{2}{5} \right) \int \mathrm{d}k_1 \, \mathrm{d}k_2 \, \delta(|\bar{k}_1| + |\bar{k}_2| - 2m) \, |F_m(\bar{k}_1 + \bar{k}_2)|^2 , \tag{12}$$

and when aligned down we merely interchange b and a.

Using the well known expansion

$$\exp[-ik \cdot r] = \sum_{l=0}^{\infty} (2l+1)(-i)^l j_l(kr) \, p_l(\cos\theta) ,$$

it can be shown that

$$|F(|\bar{k}|)|^2 \equiv \sum_m |F_m(\bar{k})|^2 = (2l+1) \left| \int j_l(kr) \, \Psi_+(r) \, \Psi(r) r^2 \, \mathrm{d}r \right|^2 , \tag{13}$$

In determining $F(k)$ for a particular level, we must of course know $\Psi_+(r)\Psi(r)$. In each case a particular analytic approximation is made that permits the evaluation of

$$\int j_l(kr) \, \Psi_+(r) \, \Psi(r) r^2 \, \mathrm{d}r .$$

Since we wish to compare our analysis to the experiment of HANNA and PRESTON let us now consider the geometry of that experiment. We will relate our analysis to the integral curve of Fig. 3 of ref. [1].

One photon is observed at a fixed counter used to define that two-quantum axis whose position vector to the annihilating source is perpendicular to the incoming positron beam. The other large counter observes all photons coming off at an angle greater than a minimum angle θ, which is varied.

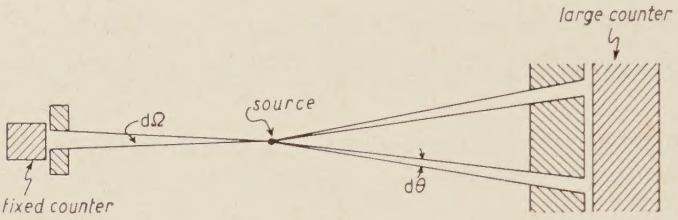

Fig. 3. – Geometry of the experiment of HANNA and PRESTON [1].

Let us first consider the transition probability per solid angle $d\Omega_1$, and $d\Omega_2$ (refer to Fig. 3). We have easily that

$$\frac{C^2}{8\pi^3}\int |F(\bar{k}_1+\bar{k}_2)|^2\delta(|\bar{k}_1|+|\bar{k}_2|-2m)k_1^2\,dk_1 k_2^2\,dk_2\,d\Omega_1\,d\Omega_2 =$$

$$= \frac{C}{4\pi^2}\,m^2 p_c\,dp_c\,d\Omega_1\int_{p_c}^{\infty} k\,|F(|\bar{k}|)|^2(k^2-p_c^2)^{\frac{1}{2}}\,dk\,,$$

where $p_c = 2^{\frac{1}{2}}m(1-\cos\theta)^{\frac{1}{2}}$. From this we see that the transition probability into all angles greater than some particular is given by

$$\Gamma = \frac{C}{4\pi^2}\,m^2\,d\Omega_1\int_{p_c}^{\infty} k\,|F(|\bar{k}|)|^2(k^2-p_c^2)^{\frac{1}{2}}\,dk\,. \tag{14}$$

The problem remaining is that of treating the conduction electrons. The angular correlation for the annihilation of these electrons is calculated assuming a degenerate Fermi gas for the electrons and a zero momentum wave function for the positron. The validity of this approximation for the positron wave function is indicated by remarks in ref. (7).

In this case the analysis is extremely simple of course and the equation for the conduction electrons analogous to (12) for the inner electrons is

$$\Gamma_c = \frac{1}{3}\,\frac{Cm^2}{4\pi^2}\,d\Omega_1(k_f^2-p_c^2)^{\frac{1}{2}}\,, \tag{15}$$

where k_f is the momentum of the Fermi surface.

4. – Comparison with experiment.

To compare with the experiment of HANNA and PRESTON, the degree of polarization of the positrons in the annihilating material at the time of annihilation must be known. It is estimated, for the iron sample used to obtain Fig. 3 of ref. ([1]) that the polarization of the positrons impinging on the sample was about .70. During thermalization before annihilating there occurs some de-polarization of the positron. No attempt is made here to estimate the de-polarization. Calculations are made assuming a polarization at annihilation of .70 and .40.

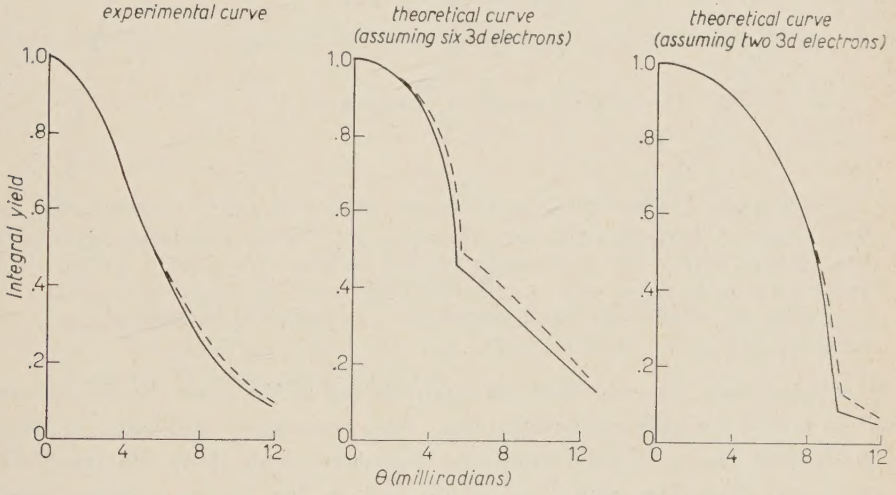

Fig. 4. – Comparison of experimental and theoretical integral angular correlations assuming 70% polarization of the positrons in the theoretical calculations.

The evaluation of the integrals over the final photon states for the inner electrons was performed on a IBM 650 computer. With these integrals evaluated contributions to the annihilation by all the inner electrons and conduction electrons are summed and the results normalized to unity at 0.

The results, and the experimental results of HANNA and PRESTON, are shown in the graphs of Fig. 5 and 6. The discontinuity in the slope of the theoretical curve is due to the method of treatment of the conduction electrons.

The comparison between the theoretical results assuming two $3d$ electrons present and the experimental results is very poor. The contribution of the conduction electrons, with the assumption that they can be treated as a degenerate Fermi gas, is too great. The Fermi level is much larger than would appear to be indicted by the experimental curve. This appears to be in disagreement with the conclusions of ref. ([8]) concerning the number of electrons in the d level.

The curves assuming six $3d$ electrons are in better agreement. The contributions to high angles is still too large, as is the difference between the curves for the parallel an anti-parallel fields, the agreement being better for the assumed polarization of .40.

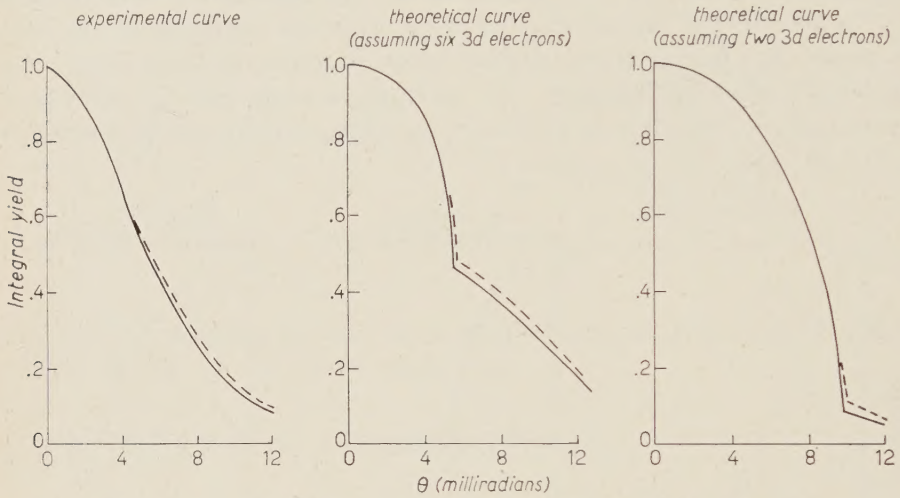

Fig. 5. – Same as Fig. 4 except 40% polarization is assumed.

It is interesting to note that the annihilation of the inner electrons is sufficient to produce a high momentum tail. This contradicts the belief expressed in ref. ([2]) that the positrons annihilate essentially only with the conduction electrons and that the high momentum tail is due to the « Swiss Cheese » structure of the positron wave function. In fact the calculations give too large a contribution at high momenta. The probable reason for this is that the approximation of using atomic $3d$ wave functions is not too good. It should be noticed that the atomic $3d$ wave functions are still fairly large at the unit cell radius, thus casting doubt on the weak binding approximation for these electrons.

RIASSUNTO (*)

Si vogliono descrivere le complete correlazioni angolari per l'annichilamento nel ferro di positoni polarizzati in presenza di un campo magnetico di saturazione. Si fa un confronto coll'esperienza. La funzione d'onda del positone usato per calcolare la correlazione angolare per l'annichilamento degli elettroni $3s$, $3p$ e $3d$ del ferro è ottenuta da un calcolo di Wigner-Seitz per momento nullo del cristallo prendendo nell'equazione di Schrödinger il potenziale uguale al potenziale del nocciolo ionico. Le funzioni d'onda degli elettroni interni furono prese uguali a quelle del ferro atomico libero. Si è calcolata la correlazione angolare per l'annichilamento dell'elettrone di conduzione assumendo per gli elettroni un gas di Fermi degenerato e per il positone una funzione d'onda di momento zero.

(*) *Traduzione a cura della Redazione.*

IL NUOVO CIMENTO Vol. XXII, N. 2 16 Ottobre 1961

Investigation of Azimuthal Effects at Multiple Particle Production.

S. A. Azimov, L. P. Chernova, G. M. Chernov, V. M. Chudakov and B. K. Nikishin

Physical-Technical Institute of the Academy of Sciences of the Uzbek SSR - Tashkent

(ricevuto il 12 Giugno 1961)

Summary. — The azimuthal angular distribution of the secondary particles produced at p-$\mathcal{N}$ collisions of 9 GeV energy and nuclear interactions of single charged cosmic ray particles in the photoemulsion have been investigated by the suggested method. The influence of the energy-momentum conservation law was estimated. The experimental results were compared with some theories and models of nuclear interactions produced by high energy nucleons.

Introduction.

Kraushaar and Marks [1] and subsequently Koba and Takagi [2] predicted the azimuthal anisotropy of secondary particles produced in nucleon-nucleon collisions of high energy as a logical consequence of the two-centre model. However, the statistical fluctuations in the angular distribution of the particles prevent the experimental detection of this effect (*). Pernegr *et al.* [3] compared the experimental data with calculations according to the Monte-Carlo method and received indication of existence of the azimuthal

(1) W. L. Kraushaar and L. J. Marks: *Phys. Rev.*, **93**, 326 (1954).

(2) Z. Koba and S. Takagi: *Nuovo Cimento*, **10**, 755 (1958).

(*) Composition of the summary shower makes no sense at the investigation of azimuthal effects.

(3) J. Pernegr, V. Petržilka and V. Šimak: *Transactions of the International Conference on Cosmic Rays*, vol. **1** (Moscow, 1960), p. 119.

anisotropy. In papers ([4-6]) original methods for the investigation of the azimuthal angular distribution of shower particles were suggested, however, the two following defects are distinctive of each of these works. Firstly, the random variables used by the authors cannot be considered as independent ones, if they belong to the same shower. For instance, in the paper of A. P. ZHDANOV *et al.* ([4]) such of random variable was a number a particles getting in the 60° interval of the azimuthal angles. These variables regarding the same shower are bounded up by linear dependence, namely, their sum is equal to the total number n_s of shower particles. The possibility of application of the Pearson test in such cases needs a substantiation. Secondly, the methods suggested in the papers mentioned above permit only to ascertain the fact of violation of the azimuthal isotropy of the shower particles or of the statistical independence of their emission angles, but they do not permit to ascertain the violation character of this conditions (asymmetry, anisotropy, etc.). These methods also do not permit to distinguish the real azimuthal effect from the apparent one connected with inaccuracy of determination of the primary direction.

In some works ([7,8]) the Pearson test was applied to each shower taken separately. Such approach has also some defects. Firstly, it is desirable ([9]) that the showers should have a large number n_s of particles and, secondly, the calculation of the Pearson probabilities for the individual showers represents, as a matter of fact, only the first stage of the work and needs generalization.

In what follows the possibility of using the χ^2-test for the uncovering of the azimuthal anisotropy of secondary particles is shown for the case of small n_s, when the shortage of particles in each shower may be compensated by a great number of showers. The method suggested is free from the mentioned defects.

1. – Method of investigation.

To investigate the angular distribution of the particles the total azimuthal angle 2π is divided into m equal intervals $\Delta\varphi$, and the number of particles n_k in every interval is calculated $\left(\sum_{k=1}^{m} n_k = n_s\right)$. As is known, the

([4]) A. P. ZHDANOV, I. M. KUKS, N. V. SKIRDA and R. M. JAKOVLEV: *Transactions of the International Conference on Cosmic Rays*, vol. **1** (Moscow, 1960), p. 87.

([5]) D. P. STERN: *Suppl. Nuovo Cimento*, **16**, 251 (1960).

([6]) E. M. FRIEDLÄNDER: *Žurn. Èksp. Theor. Fiz.*, **39**, 965 (1960).

([7]) I. I. GUREVICH, A. P. MISHAKOVA, B. A. NIKOL'SKIJ and L. V. SURKOVA: *Žurn. Èksp. Theor. Fiz.*, **34**, 265 (1958).

([8]) DEN PHEN SU, G. B. ZHDANOV and M. I. TRETJAKOVA: *Transactions of the International Conference on Cosmic Rays*, vol. **1**, (Moscow, 1960) p. 111.

([9]) N. V. SMIRNOV and I. V. DUNIN-BARKOVSKIJ: *Short Course of Mathematical Statistics for Technical Applications* (Moscow, 1959).

value

$$\chi_m^2 = \frac{m}{n_s} \sum_{k=1}^{m} \left(n_k - \frac{n_s}{m} \right)^2 = \frac{m}{n_s} \sum_{k=1}^{m} n_k^2 - n_s \,, \tag{1}$$

has χ^2-distribution with $m-1$ degrees of freedom, if n_s is great (provided that the azimuthal isotropy of shower particles and the statistical independence of their emission angles φ_i takes place in the monotonous showers with the same n_s). Taking into account the statistical independence of the φ_i, it is easy to find the expectation value of the normalized value $\alpha_m = \chi_m^2/(m-1)$ at arbitrary n_s:

$$E(\alpha_m) = 1 + \frac{m}{m-1} (n_s - 1) \sum_{k=1}^{m} \left(P_k - \frac{1}{m} \right)^2, \tag{2}$$

where P_k is the probability of the particle getting to the k-th interval $\Delta\varphi$. If the azimuthal angular distribution is isotropic, $P_k = 1/m$ and

$$E(\alpha_m) = 1 \,. \tag{3}$$

The α_m variance calculation is very cumbersome. Omitting it we give the final result corresponding to the azimuthal isotropy of shower particles and the statistical independence of its angles φ_i:

$$\sigma^2(\alpha_m) = [2/(m-1)] \cdot [(n_s - 1)/n_s] \,. \tag{4}$$

The scantiness of the variances permits to indicate the critical limit for the $\bar{\alpha}_m$ value averaging over n showers with any n_s (which don't have to be equal):

$$\bar{\alpha}_m = \sum_{i=1}^{n} \alpha_{mi} / n \,, \tag{5}$$

the exceeding probability of which is very small. For that one can use Chebyshev's inequality which overestimates naturally the critical limit of $\bar{\alpha}_m$, but it can be used for any number n of showers (*). If n is great, the random variable $\bar{\alpha}_m$ follows roughly the normal distribution law in accordance with Lyapunov's theorem, the applicability condition of which is fulfilled for the shower succession with limited number n_s of particles. The use of normal distribution reduces considerably the critical limit of $\bar{\alpha}_m$.

(*) When n is great and n_s is small, the best results are given by application of the more precising Chebyshev inequality ([10]).

([10]) S. N. BERNSTEIN: *Theory of Probabilities* (Moskow-Leningrad, 1934).

By means of the χ^2-test one can investigate the azimuthal angular distribution of shower particles as a whole, irrespective of the angle θ with the primary direction. In order to get information about the azimuthal symmetry of the particles, flying at different angles θ, one can use the following relation:

$$\alpha = \frac{n_s(\overline{\cos\theta})^2}{\overline{\sin^2\theta}}\,\mathrm{tg}^2\,\theta_0 = 1 + \sum_{i\neq j}\sin\theta_i\sin\theta_j\cos(\varphi_i-\varphi_j)\Big/\sum_{i=1}^{n_s}\sin^2\theta_i\,, \tag{6}$$

where

$$\overline{\cos\theta} = \sum_{i=1}^{n_s}\cos\theta_i/n_s\,, \qquad \overline{\sin^2\theta} = \sum_{i=1}^{n_s}\sin^2\theta_i/n_s\,.$$

θ_i is the angle of i-th particle with primary direction in the laboratory system (L.S.), φ_i is its azimuthal angle, θ_0 is the angle between the primary direction and the shower axis passing through the centre of gravity of the points of intersection of the tracks of secondary charged particles with the sphere of radius $=1$, the centre of which coincides with the shower vertex. Let $f(\theta_1, \varphi_1, \theta_2, \varphi_2, \ldots, \theta_{ns}, \varphi_{ns})$ be the probability density of the many-dimensional distribution. Assuming that the angular distribution of each particle with any θ and with the fixed directions of other n_s-1 particles is azimuthally isotropic, the expectation value of the α and its variance are respectively equal to

$$E(\alpha) = \int\alpha\cdot f(\theta_1, \varphi_1, \theta_2, \varphi_2, \ldots, \theta_{ns}, \varphi_{ns})\prod_{i=1}^{n_s}\mathrm{d}\theta_i\,\mathrm{d}\varphi_i = \tag{7}$$

$$= \int\alpha\cdot f_1(\theta_1, \theta_2, \ldots, \theta_{ns})\prod_{i=1}^{n_s}\mathrm{d}\theta_i(\mathrm{d}\varphi_i/2\pi) = 1\,,$$

and

$$\sigma^2(\alpha) = E[1 - n_s^{-1}(\overline{\sin^2\theta})^{-2}(\overline{\sin^4\theta})] < 1\,. \tag{8}$$

In a more general case when

$$f(\theta_1, \varphi_1, \theta_2, \varphi_2, \ldots, \theta_{ns}, \varphi_{ns}) = \tag{9}$$

$$= f_1(\theta_1, \theta_2, \ldots, \theta_{ns})f_2(\varphi_1)f_2(\varphi_2)\ldots f_2(\varphi_{ns})\,, \qquad \int f_2(\varphi)\,\mathrm{d}\varphi = 1\,,$$

the expectation value of α differs from 1 by the value

$$\begin{cases} E(\alpha) - 1 = aE[n_s(\overline{\sin\theta})^2(\overline{\sin^2\theta})^{-1} - 1] \geqslant 0\,, \\ a = [E(\cos\varphi)]^2 + [E(\sin\varphi)]^2\,. \end{cases} \tag{10}$$

The same properties (*i.e.* eq. (7) and ineq. (8)) are inherent to the value

$$\alpha' = \frac{n_s}{\mathrm{tg}^2\,\theta}\,\mathrm{tg}^2\,\theta_0', \tag{11}$$

where θ_0' is the angle between the primary direction and the straight line passing through the shower vertex and the centre of gravity of the points of intersection of secondary charged particles or their continuations with a plane tangent to the sphere of the radius — 1 in the point of its intersection with the continuation of the primary track. The experimental values of α' can be calculated easily with help of target-diagrams of shower particles.

2. – Influence of the momentum conservation law.

The calculation of the expectation values of α, α', α_m, which describe the azimuthal angular distribution of secondary particles, and their variances was made assuming the statistical independence of the azimuthal angles φ_i of the particles. The energy-momentum conservation law subordinates the particle's momenta and their directions to some bonds disturbing this condition. According to experimental data the transverse momenta of secondary particles slightly differ. Regarding the great value of transverse momentum of nucleons in comparison with the one of pions, the recent experimental data ([11,12]) do not confirm this possibility, which would bea ble to lead to an increase of the expectation values α, α', α_m, when the number of charged mesons is small (~ 5). If the transverse momenta of the secondary particles are of the same order, momentum conservation law interdicts the cases possible at statistical independence of angles, when the majority of charged particles have approximately the same angles φ. This symmetrization of the angular distribution must lead to reduction of the average values $\bar{\alpha}$, $\bar{\alpha}'$, $\bar{\alpha}_m$. For elucidation of the influence of the energy-momentum conservation law we have drawn the table of random stars ([13]) showing the (pp)-collisions of 9 GeV energy according to statistical theory. The results listed in Table I show clearly that the average values $\bar{\alpha}$, $\bar{\alpha}'$, $\bar{\alpha}_m$ are smaller than 1, *i.e.* smaller than their expectation values corresponding to the azimuthal isotropy of secondary charged particles and the statistical independence of their angles φ_i.

([11]) Wang Shu-Fen, T. Vishki I. M. Gramenitskii, U. G. Grishin, N. Dalkhazhav, R. M. Lebedev, A. A. Nomofilov, M. I. Podgoretskii and V. N. Stel'tson: *Žurn. Èksp. Theor. Fiz.*, **39**, 957 (1960).

([12]) E. R. T. Awunor-Renner, L. Blaskovitch, B. R. French, C. Ghesquière, I. B. de Minvielle-Devaux, W. W. Neale, C. Pelletier, P. Rivet, A. B. Sahiar and I. O. Skillicorn: *Nuovo Cimento*, **17**, 134 (1960).

([13]) G. I. Kopylov: preprint JINR, P-259 (1959).

TABLE I. *Azimuthal characteristics of random stars.* $\sigma(\bar{\alpha})$ is the standard deviation of isotropy of secondary particles and the statistical independence of their angles φ_i. P is estimated according to Lyapunov's theorem (in the brackets: the values P obtained with total numbe

No.	Characteristics of group	Azimuthal characteristics of group	α	α'	α_2	α_3
1	$2 \leqslant n_s \leqslant 6$ $n = 201$	$\bar{\alpha}(\bar{\alpha}', \bar{\alpha}_m)$	0.708	0.767	0.710	0.7
2		$\sigma(\bar{\alpha})$	< 0.071	< 0.071	0.083	0.0
3		$\lvert\bar{\alpha} - 1\rvert / \sigma(\bar{\alpha})$	> 4.1	> 3.3	3.5	3.7
4		P in %	$< 10^{-2}$ (< 6)	< 0.1 (< 9)	< 0.1 (< 5)	$\sim 10^{-}$ ($<$

It is likely that with increasing n_s the influence of the energy-momentum conservation law will weaken. Indeed, at the constancy of the transverse momentum we have two bonds laid on the azimuthal angles. If the number of shower particles is great, and if neutral particles are present, these bonds apparently are not essential.

3. – Experimental data.

The most interesting investigation is that of the azimuthal effects at the nucleon-nucleon collisions. In Table II the azimuthal characteristics of (p,N')-collisions of 9 GeV energy found in the nuclear emulsion and treated in JINR are listed. In the very high energy region there are no reliable criteria for the selection of the (N,N')-collisions. Table III contains the azimuthal characteristics of «jets» produced by single charged cosmic ray particles in the photoemulsion and having a small number of heavy prongs: $n_h + n_\nu \leqslant 5$ (the angle measurements were fulfilled in the Laboratory of J. PERNEGR). One can hope that many of these «jets» represent the (p,N')-collisions. At small multiplicities (line 1 of Table II) the influence of the momentum conservation law is appreciable. With increasing n_s this influence apparently will weaken, while the effect of azimuthal anisotropy of secondary particles becomes stronger according to eq. (2). Therefore, at $n_s \geqslant 14$ (line 5 of Table III) we observe $\bar{\alpha}_m$ values appreciably exceeding 1 for $m \geqslant 3$.

As shown above (eq. (2)) the expectation values of α_m ($m \geqslant 3$) are sensitive to the disturbance of the azimuthal isotropy of secondary particles, even

aging over n showers random value $\bar{\alpha}(\bar{\alpha}', \bar{\alpha}_m)$ which was calculated assuming the azimuthal ability of obtaining the value $\bar{\alpha}$ not greater (not smaller) than the observed one which was of Chebyshev's inequalities). Only values $|\bar{\alpha} - 1|/\sigma(\bar{\alpha}) \geqslant 1$ and $P \leqslant 10\%$ are listed. n_s is the ged particles.

α_4	α_5	α_6	α_7	α_8	α_9	α_{10}
0.779	0.839	0.894	0.874	0.899	0.917	0.935
0.048	0.041	0.037	0.034	0.031	0.029	0.028
4.6	3.9	2.9	3.7	3.3	2.9	2.3
10^{-3}	$< 10^{-2}$	~ 0.2	$\sim 10^{-2}$	< 0.1	~ 0.2	~ 1
< 0.5)	(< 2)	—	(< 3)	(< 7)	—	—

if the azimuthal angular distribution remains symmetrical. On the other hand, the expectation value of α_2 becomes greater than 1 only in the case of azimuthal asymmetry of secondary particles. For instance, the tendency of mesons to coplanarity appearing because of the presence of a great intrinsic angular momentum of the excited centre leads to the increasing of $E(\alpha_m)$ $(m \geqslant 3)$, but $E(\alpha_2)$ does not change essentially, if the angles of deviation of centres from the primary direction are small. It is to be noticed that the tendency of mesons to coplanarity can appear as the azimuthal anisotropy of secondary particles in the case, if we fix after collision the momenta of excited centres which differ from the primary direction. In the succession of the monotonous showers, the primaries of which are described by a plane wave, the azimuthal anisotropy will not take place and the tendency of mesons to coplanarity will become apparent as the statistical dependence of the angle φ_i of secondary particles acting in the direction of increasing $E(\alpha_m)$. Therefore, there is ground to speak about the physical phenomenon, for instance, about the tendency of mesons to coplanarity without specifing which condition of the two is disturbed by this phenomenon: the azimuthal isotropy of secondary particles or the statistical independence of their angles φ_i.

The expectation values of α and α' similar to $E(\alpha_2)$ are sensitive only to the disturbance of the symmetry of the azimuthal angular distribution of particles in the individual showers (see eq. (10)). However, it is necessary to emphasize the considerable difference between the α and α' values, on the one hand, and the α_2 value, on the other hand. If the symmetry for the particles of the diffuse and narrow cones taken separately in L.S. are disturbed, but the azimuthal angular distribution remains symmetrical as a whole, the

TABLE II. - *Azimuthal characteristics of p-N collisions at 9 GeV energy. n_s is the total number of secondary charged particles.*

No.	Characteristics of group	Azimuthal characteristics of group	α	α'	α_2	α_3	α_4	α_5	α_6	α_7	α_8	α_9	α_{10}
		$\bar{\alpha}(\bar{\alpha}', \bar{\alpha}_m)$	0.755	0.807	0.632	0.773	0.856	0.863	0.902	0.935	0.953	0.972	0.950
2	$2 \leqslant n_s \leqslant 5$	$\sigma(\bar{\alpha})$	<0.041	<0.041	0.046	0.033	0.027	0.023	0.021	0.019	0.018	0.016	0.015
3	$n = 597$	$\lvert\bar{\alpha} - 1\rvert/\sigma(\bar{\alpha})$	>6.0	>4.7	8.0	6.9	5.3	6.0	4.7	3.4	2.6	1.8	3.3
4		P in %	$<10^{-5}$ (<3)	$<10^{-3}$ (<5)	$<10^{-5}$ ($<10^{-}$)	$<10^{-5}$ ($<10^{-2}$)	$<10^{-5}$ (<0.1)	$<10^{-5}$ ($<10^{-}$)	$<10^{-3}$ (<0.4)	<0.1 (<6)	<1 —	~ 4 —	<0.1 (<7)
5		$\bar{\alpha}(\bar{\alpha}', \bar{\alpha}_m)$	0.92	0.94	0.77	1.01	1.04	1.00	1.07	1.04	1.05	1.08	1.04
6	$6 \leqslant n_s \leqslant 9$	$\sigma(\bar{\alpha})$	<0.12	<0.12	0.15	0.11	0.09	0.08	0.07	0.06	0.06	0.05	0.05
7	$n = 72$	$\lvert\bar{\alpha} - 1\rvert/\sigma(\bar{\alpha})$	—	—	1.5	—	—	—	1.1	—	—	1.6	—
8		P in %	—	—	~ 7	—	—	—	—	—	—	~ 6	—

TABLE III. – *Azimuthal characteristics of « jets » produced by the single charged cosmic ray particles with a small number of heavy prongs* $n_h + n_g \leqslant 5$. γ_c is the Lorentz factor of the c.m. system estimated according to the Castagnoli formula.

No.	Characteristics of group	Azimuthal characteristics of group	α	α'	α_2	α_3	α_4	α_5	α_6	α_7	α_8	α_9	α_{10}
1	$n_s \leqslant 12$	$\bar{\alpha}(\bar{\alpha}', \bar{\alpha}_m)$	0.94	0.87	0.78	0.91	0.80	0.98	1.01	0.99	0.91	1.05	0.98
2	$\bar{n}_s = 9.3$	$\sigma(\bar{\alpha})$	<0.17	<0.17	0.22	0.16	0.13	0.11	0.10	0.09	0.08	0.08	0.07
3	$\bar{\gamma}_c = 12.5$	$\lvert\bar{\alpha}-1\rvert/\sigma(\bar{\alpha})$	—	—	1.0	—	1.6	—	—	—	1.1	—	—
4	$n = 36$	P in %	—	—	—	—	~ 6	—	—	—	—	—	—
5	$n_s \geqslant 14$	$\bar{\alpha}(\bar{\alpha}', \bar{\alpha}_m)$	1.07	1.04	0.63	1.80	1.41	1.35	1.68	1.23	1.37	1.32	1.45
6	$\bar{n}_s = 19.5$	$\sigma(\bar{\alpha})$	<0.25	<0.25	0.34	0.24	0.20	0.17	0.15	0.14	0.13	0.12	0.11
7	$\bar{\gamma}_c = 12.7$	$\lvert\bar{\alpha}-1\rvert/\sigma(\bar{\alpha})$	—	—	1.1	3.3	2.1	2.0	4.4	1.7	2.9	2.7	3.9
8	$n = 16$	P in %	—	—	—	<0.1	~ 2	~ 2	$<10^{-3}$	~ 5	~ 0.2	~ 0.4	$<10^{-2}$
			—	—	—	($\leqslant 9$)	—	—	($\leqslant 5$)	—	—	—	($\leqslant 7$)

average values $\overline{\alpha}$ and $\overline{\alpha}'$ become greater (*) than 1 in contrast to $\overline{\alpha}_2$. For instance, this can be observed on condition that two equally excited nucleons flying at great angles with the primary direction are formed in the C.M.S. of collision.

From the experimental data listed in line 5 of Table III it follows that the azimuthal anisotropy of secondary particles takes place in the «jets». In this case the angular distribution apparently remains symmetrical to η at different angles θ with the primary direction. In any case the symmetry of the azimuthal angular distribution is disturbed less than the isotropy. It is not excluded that the analogous azimuthal effect takes place in (p.N)-collisions of 9 GeV energy, however, in view of the small number of particles in the showers and the appreciable influence of the momentum conservation law, the average values $\overline{\alpha}_m$ do not exceed 1. The data listed in lines 5 of Table II (where all $\overline{\alpha}_m$ are greater than 1, when $m \geqslant 3$, and $\overline{\alpha}$, $\overline{\alpha}'$, $\overline{\alpha}_2$ are smaller than 1) can give some indication of existence of this effect at 9 GeV energy. Besides that, comparison of the first lines of Tables I and II shows that the $\overline{\alpha}_m$ values ($m > 3$) of the real showers are greater than the ones of random stars, which can be attributed to the azimuthal anisotropy of secondary particles. Nevertheless, it is premature to conclude about the existence of the azimuthal effect in the (pN)-collisions at 9 GeV energy.

Measurements of angular distribution of shower particles were made by us in 55 cases of the interaction of single charged cosmic ray particles with heavy emulsion nuclei ($n_h + n_g > 8$). In the $\gamma_c < 3$ region our measurements are absolutely reliable. The results of treatment of these showers listed in Table IV agree in limits of errors with the assumptions about the azimuthal isotropy of secondary particles and the statistical independence of their angles η_i. From comparison of line 11 of Table IV and line 5 of Table III one can conclude that if the azimuthal effect even exists at the collisions with heavy nuclei of the emulsion, it is expressed considerably weaker than in the «jets» with small number of heavy prongs. That is apparently connected with the number of the nucleons of the target-nucleus participating in the collision, but not with the difference in the shower energy, since in paper (8) in each of the 11 showers with $\gamma_c \geqslant 10$, $n_h + n_s \geqslant 8$ and great number of shower tracks n_s, no deviations from isotropy by means of the Pearson test (**) were discovered.

Let us consider the influence of the apparent azimuthal effects for the results listed in line 5 of Table III. It is to be asserted that the influence of the inaccuracy of the determination of the primary direction is not essential,

(*) In connection with the increasing of angles θ_0 and θ_0' between the shower axis and the primary direction.

(**) Compare also line 5 of Table II with line I of Table III.

TABLE IV. – *Azimuthal characteristics of showers produced by the single charged cosmic ray particles with a great number of heavy prongs* $n_g + n_h > 8$.

No.	Characteristics of group	Azimuthal characteristics of group	α	α'	α_2	α_3	α_4	α_5	α_6	α_7	α_8	α_9	α_{10}
1	$\bar{n}_s = 16.8$	$\bar{\alpha}(\bar{\alpha}', \bar{\alpha}_m)$	0.87	0.99	1.22	1.02	0.94	0.97	0.94	1.00	1.04	0.95	0.98
2	$\bar{\gamma}_c = 3.8$	$\sigma(\bar{\alpha})$	< 0.14	< 0.14	0.18	0.13	0.11	0.09	0.08	0.08	0.07	0.07	0.06
3	$n = 55$	$\lvert\bar{\alpha} - 1\rvert/\sigma(\bar{\alpha})$	–	–	1.2				–	—		—	—
4	$\gamma_c < 3$	$\bar{\alpha}(\bar{\alpha}', \bar{\alpha}_m)$	0.90	0.92	1.21	1.15	1.05	1.03	1.08	1.05	1.11	0.96	1.01
5	$\bar{n}_s = 15.5$	$\sigma(\bar{\alpha})$	< 0.18	< 0.18	0.24	0.17	0.14	0.12	0.11	0.10	0.09	0.09	0.08
6	$n = 31$	$\lvert\bar{\alpha} - 1\rvert/\sigma(\bar{\alpha})$		–					–	–	1.2	—	
7	$\gamma_c < 3$	$\bar{\alpha}(\bar{\alpha}', \bar{\alpha}_m)$	0.63	0.59	1.21	0.88	1.12	0.93	0.89	1.00	1.04	0.90	0.89
8	$n_s < 14$	$\sigma(\bar{\alpha})$	< 0.28	< 0.28	0.37	0.26	0.21	0.19	0.17	0.15	0.14	0.13	0.12
9	$\bar{n}_s = 9.4$	$\lvert\bar{\alpha} - 1\rvert/\sigma(\bar{\alpha})$	> 1.4	> 1.5	–						—	–	
10	$n = 13$	P in %	< 8	< 7	–	–	–	–	–	–	—		–
11	$\gamma_c < 3$	$\bar{\alpha}(\bar{\alpha}', \bar{\alpha}_m)$	1.09	1.15	1.22	1.35	1.00	1.11	1.22	1.08	1.16	1.00	1.09
12	$n_s \geqslant 14$	$\sigma(\bar{\alpha})$	0.24	0.24	0.32	0.23	0.19	0.16	0.15	0.13	0.12	0.11	0.11
13	$\bar{n}_s = 19.9$	$\lvert\bar{\alpha} - 1\rvert/\sigma(\bar{\alpha})$				1.5			1.5		1.3		
14	$n = 18$	P in %				~ 7	–	–	~ 7		~ 10	–	

since an anisotropic, but symmetrical angular distribution is observed. The discrimination of selection of the shower particles or the inequality of the measurements over the horizontal and vertical lines on the microscope can lead to an apparent azimuthal anisotropy too. However, in this case we should observe the azimuthal effect in the showers having a great number of heavy prongs (line 11 of Table IV).

4. – Discussion of results.

The azimuthal anisotropy of secondary particles contradicts the hydrodynamical theory of the « jets » formation at the head-on collisions and corresponds to the predictions of the two-centre model ([1,2]). If the registration of the angular momentum conservation law at the « head-on » collisions of nucleons has no essential importance, our results point out the great role of the « peripherical » $(\mathcal{N}'\mathcal{N}')$-interactions at high energies. An explanation of the azimuthal anisotropy of secondary particles is apparently impossible without the registration of this conservation law.

The experimental data do not contradict the symmetry of the azimuthal angular distribution whence it appears that the deviation of the excited centres from the direction of the primary nucleons do not play an appreciable role. The indications of the deviation of the centres obtained by a number of authors ([3,14]) cannot be considered as correct ones. This result can be compared with the estimates according to the theory of the peripherical interactions of the nucleons ([15]). Let us consider the collision of one nucleon with the peripherical meson of another leading to the formation of one excited centre. The Lorentz factor of the latter in the C.M.S. of the $(\mathcal{N}'\mathcal{N}')$-collision is equal to

$$\gamma^* \approx E/2(\varepsilon E)^{\frac{1}{2}} , \tag{12}$$

where E is the energy of the nucleon before the collision in C.M.S., ε is the energy of the pion. Considering the secondary particles as relativistic ones in the system of rest of the excited centre let us estimate the half angle $\theta_{\frac{1}{2}}$ of their emission in C.M.S. from the ratio

$$\sin \theta_{\frac{1}{2}} \approx 2(\varepsilon/E)^{\frac{1}{2}} . \tag{13}$$

([14]) H. W. MEIER: *Nuovo Cimento*, **11**, 307 (1959).

([15]) JU. A. ROMANOV and D. S. CERNAVSKIJ: *Žurn. Èksp. Theor. Fiz.*, **38**, 1132 (1960); D. S. CERNAVSKIJ: *Suppl. Nuovo Cimento*, **8**, 775 (1958).

If the average value of ε/E is equal to the half of the ratio of the pion mass to the nucleon mass, the values of $\theta_{\frac{1}{2}}$ fluctuate around 33°. The transverse momentum of the excited centre is approximately equal μc (μ is the pion mass), and its deviation angle θ^* from the primary direction in C.M.S. satisfies the ratio

$$\sin\theta^* \sim \mu c^2/E \,. \tag{14}$$

At high energies the angle $\theta^* \ll \theta_{\frac{1}{2}}$, therefore, the deviation of an excited centre or of two centres from the primary direction, must not appreciably influence the angular distribution of secondary particles. The same result follows from the calculations according to the perturbation theory at 9 GeV energy ([16]).

The Polish group ([17]) proved the double-maximum character of the distribution of secondary particles over $\log \operatorname{tg}\theta$ (θ is the angle with the primary direction in L.S.) at nuclear interactions of the nucleons in the emulsion at energies greater than 10^{12} eV. Such shape of the angular distribution is connected with the independent emission of particles by two excited centres. The symmetry of the distribution over $\log \operatorname{tg}\theta$ means that the centres moving slowly and rapidly in the L.S. disintegrate at average into the same number of particles. If two maxima are observed at the (NN)-collisions, one must apparently take the well-known model of the « fire balls », moving separately from the nucleons after the collision, for the explanation of the small coefficient of inelasticity. Of course, two centres can be generated, if two nucleons of the target nucleus participate in the interaction, for instance, on account of two collisions of the virtual pions of the primary nucleon with the pions of two nucleons of the target nucleus. If such process can be subdivided into the independent (NN)-collisions, the azimuthal correlation between the planes of the preferable emission of the particles by the different centres will not be observed.

The azimuthal anisotropy of the shower particles shows the presence of the great intrinsic angular momentum of the excited centres. If one assumes the model of the revolving balls, the angular distribution of secondary particles in the system of the rest of the centre (M^*-system) can change from the isotropy in the space to the isotropy in the plane. The latter distribution corresponds to the strong anisotropy in the M^*-system in the usual sense of the word. Really, the average value $(\operatorname{cosec}\bar{\theta})_{\text{av.}}$ ($\bar{\theta}$ is the emission angle of the particle in the M^*-system) is equal to ∞ in this case, if the direction of the intrinsic angular momentum of the centre is perpendicular to the line, from

([16]) I. M. Dremin and D. S. Cernavskij: *Žurn. Èksp. Theor. Fiz.*, **38**, 229 (1960).
([17]) J. Gierula, M. Mięsowicz and P. Zielinski: *Nuovo Cimento*, **18**, 102 (1960).

which the angles θ are counted off. The model of the revolving balls as the assumption usually taken about the isotropy in the M^*-system explains readily the angular dependence of the transverse momentum in the system with symmetric angular distribution of the shower particles obtained by PERNEGR *et al.* [18]. Let us note too that the approximate constancy of the average energy of the mesons in the system of the excited centre results as before from the fact of the constancy of the average transverse momentum, when the rotation of the balls is taken into account.

We consider that the possible anisotropy of the angular distribution of particles in the M^*-system does not contradict the experimental data. The conclusion [19] about the anisotropy of this distribution has been obtained by means of the subjective selection of the « jets » and the subjective subdivision of them into the diffuse and narrow cones. As it was really shown [20] by the calculations of the fluctuations of the angular distribution according to Monte-Carlo method, this procedure is unsatisfactory.

The value $\mathscr{D}$ attaining positive values for the showers with two maxima was introduced by the Polish group [17] as a measure of the deviation of the distribution of secondary particles over $\log \operatorname{tg} \theta$ from the normal curve. The dependence of $\mathscr{D}$ from the standard deviation σ of the distribution of shower particles over $\log \operatorname{tg} \theta$ is plotted in Fig. 1. The curve I is calculated according to the model of two-centre which do not deviate from the primary direction and disintegrate into the same number of relativistic secondary praticles isotropically in the M^*-systems (*). The experimental points taken from [17] lie mainly below this curve which can be explained by the admixture of the asymmetrical (when the centres disintegrate into a different number of secondary particles) and one-centre showers. The registration of the anisotropy of the angular distribution in the M^*-system also improves the agreement with the experiment. The curve 2 of Fig. 1 corresponds to the standard deviation $\sigma_0 = 0.50$ for the angular distributions of particles of each centre and to the disintegration of the centres into the same number of secondary particles. It is to be stated that the angular distribution isotropic in the plane in the M^*-system is not badly approximated by a Gaussian distribution over $\log \operatorname{tg} \theta$ with the standard deviation $\sigma_0 \approx 0.64$. Thus, the experimental data considered here do not contradict at least the idea about the rotation of the « fire balls ».

[18] J. PERNEGR, V. ŠIMAK and M. VOTRUBA: *Nuovo Cimento*, **17**, 129 (1960).

[19] P. CIOK, T. COGHEN, J. GIERULA, R. HOŁYŃSKI, A. JURAK, M. MIĘSOWICZ and T. SANIEWSKA: *Nuovo Cimento*, **10**, 741 (1958).

[20] B. A. NICOL'SKIJ and A. P. MISHAKOVA: *Žurn. Èksp. Theor. Fiz.*, **38**, 1507 (1960).

(*) The isotropic angular distribution in the system of the rest of the centre was approximated at the calculation by the Gaussian distribution over $\log \operatorname{tg} \theta$ with $\sigma_0 = 0.36$.

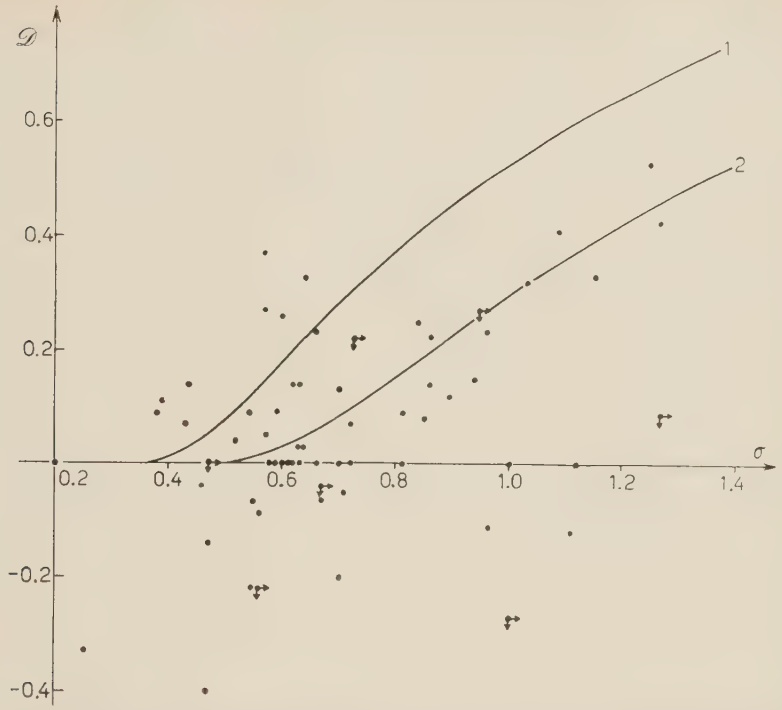

Fig. 1. – Dependence of the characteristic $\mathscr{D}$ of the angular distribution of shower particles from the standard deviation σ of this distribution. The experimental points are taken from ([17]). The curves are calculated according to the two-centre model.

The angular momentum of the « fire balls » is most simply taken into account by the thermodynamic theory of Fermi. Following KRAUSHAAR and MARKS ([1]), one can obtain the ratio for a total number N of pions, produced by the disintegration of one « fire ball »:

$$N^{\frac{1}{4}} = (2/\pi)^{\frac{1}{4}} (R/\lambda\!\!\!^{-})^{\frac{3}{4}} ab^{-\frac{3}{4}} (\overline{U}/mc^2)^{\frac{3}{4}} F_1(\varrho)[F_2(\varrho)]^{-\frac{3}{4}} , \tag{15}$$

where R is the radius of the sphere, in which the statistical equilibrium is established, $\lambda\!\!\!^{-} = \hbar/mc$ is the Compton wave length of the nucleon, $\overline{U}$ is the average energy of the pion in the M^*-system, ϱ is the parameter depending on the angular momentum of the mesons in the M^*-system and determining their azimuthal angular distribution. The values of the constants a and b, functions $F_1(\varrho)$ and $F_2(\varrho)$ and curves of the azimuthal angular distribution of secondary particles for different ϱ are listed in the work ([1]). If $\overline{U} = \text{const}$, the number of shower particles n_s singly determines the parameter ϱ. For each of 16 showers, the azimuthal characteristics of which are listed in line 5

of Table III, the expectation values were calculated by us with the help of eq. (15), the curves of paper [1] and eq. (2). The calculation was made for $\bar{U} \sim 0.5$ GeV and for the different values of R assuming that the « fire balls » do not deviate from the primary direction and disintegrate into the same number of mesons, and the planes of the preferable emission of the particles by the different centres are coinciding. It was found that the values $E(\alpha_m)$ are nearly independent from the orientation of the plane of the preferable emission of the particles at $m = 5, 7, 9$, and the agreement of the expectation values of the average values $\bar{\alpha}_m$ with the characteristics $\bar{\alpha}_m$ experimentally found is reached at $R \approx 3\hbar/\mu c$. This value of R is too great in comparison with the generally accepted one. The registration of the momentum conservation law disturbing the statistical independence of the angles q_i of secondary particles, of the admixture of asymmetrical and one-centre cases, and of the possible lack of coincidence of the planes of the preferable emission of the particles by the different centres, only redoubles our conclusion that the thermodynamical theory cannot simultaneously explain the constancy of the transverse momentum of secondary particles and the great value of the azimuthal anisotropy.

* * *

In conclusion the authors wish to thank Acad. V. I. Veksler and Dr. J. Pernegr for their assignment of the experimental data obtained in their Laboratories, M. I. Podgoretsky for the useful advices and G. I. Copylov for sending the table of random stars.

RIASSUNTO (*)

Abbiamo studiato col metodo proposto la distribuzione azimutale angolare delle particelle secondarie prodotte in collisioni p-$\mathcal{N}$ di 9 GeV e in interazioni nucleari di singole particelle cariche dei raggi cosmici nelle emulsioni fotografiche. Abbiamo valutato l'influenza della legge di conservazione dell'energia-impulso. I risultati sperimentali sono stati confrontati con alcune teorie e modelli per le interazioni nucleari prodotte da nucleoni di alta energia.

(*) *Traduzione a cura della Redazione.*

Low-Field Breakdown in n-Type Germanium (*) (**).

G. Ascarelli (***)

Department of Physics and Research Laboratory of Electronics, Massachussets Institute of Technology - Cambridge, Mass.

(ricevuto il 26 Giugno 1961)

Summary. — Measurements of the time necessary to produce low field breakdown in n-type germanium have been made as a function of the applied electric field: this time interval is proportional to E^{-2}. The experimental results presented herein, as well as the results obtained from d.c. measurements, can be explained (on the basis of the avalanche multiplication model of breakdown) if it is assumed that the distribution function of the electrons whose energy is smaller than the ionization energy of the impurities is given by $f(x) \propto (1+px) \exp[-x]$ (where p is proportional to $(\mu_0 E)^2$ with μ_0 equal to the observed low field mobility, $x = \varepsilon/kT$, where ε is the electron energy) and that the cross-section for impact ionization is constant for $\varepsilon > \varepsilon_0$ and equal to zero for $\varepsilon < \varepsilon_0$.

1. – Introduction.

Low-temperature breakdown has been observed in both n- and p-type germanium by many authors ([1-6]). However, we lack an explanation for the delay of the phenomenon after the electric field has been applied, as well as an expla-

(*) This work was performed in part at the Physics Department, University of Illinois.

(**) This work was supported in part by the U.S. Army (Signal Corps), U.S. Air Force (Office of Scientific Research, Air Research and Development Command), and the U.S. Navy (Office of Naval Research).

(***) Now at Department of Physics, Istituto Superiore di Sanità, Rome.

(1) A. N. Gerritsen: *Physica*, **15**, 427 (1949).

(2) G. Dresselhaus, A. F. Kip and C. Kittel: *Phys. Rev.*, **92**, 827 (1953).

(3) E. Burstein, J. W. Davisson, E. E. Bell, W. J. Turner and H. G. Lipson: *Phys. Rev.*, **98**, 65 (1954).

(4) F. J. Darnell and S. A. Friedberg: *Phys. Rev.*, **98**, 1860 (1955).

(5) N. Sclar and E. Burstein: *Journ. Phys. Chem. Sol.*, **2**, 1 (1957).

(6) S. H. Koenig and G. R. Gunther-Mohr: *Journ. Phys. Chem. Sol.*, **2**, 268 (1957).

nation for the origin of the high-frequency oscillations that have been observed ([5-7]) in critically compensated samples. If the breakdown mechanism proposed by SCLAR and BURSTEIN is accepted, the delay of the observed breakdown has an explanation similar to that encountered in gas discharge and is connected with the time it takes for an electron to gain sufficient energy to ionize. If, instead, the ideas proposed by KOENIG ([8]) are accepted, the time required to attain a given density is limited by the current that can be carried across the contacts. Regarding the oscillations of the current in the sample that is being broken down, SCLAR and BURSTEIN attribute them principally to contacts, while KOENIG believes that thermal effects in the bulk of the sample are responsible for the phenomenon ([9]).

Impact ionization of donor and acceptor impurities produced by the electrons « heated » by microwaves has been used in the early work on cyclotron resonance ([2]) as a means of obtaining the carrier densities necessary for the experiment. SCLAR and BURSTEIN ([5]) in their paper argue that in view of the fact that d.c. breakdown is reversible, and that it depends on the applied field rather than on the applied voltage, it should be connected with the bulk of the sample rather than the region at the contacts. On the other hand, according to KOENIG, the time delay observed in breakdown is polarity-dependent and is strongly influenced by room temperature radiation falling on the negatively biased contact ([8]).

We will use the model proposed by SCLAR and BURSTEIN for describing breakdown, using their mathematical formulation to discuss the build-up of the electron density.

2. – Experimental results.

The experimental investigation follows lines similar to those developed by MADAN *et al.* ([10]) for the study of delayed breakdown in gaseous discharges.

Our samples were mounted along the axis of a reentrant microwave cavity: the microwaves were used only as a probe to measure the conductivity of the sample and thus to determine the time at which the electron density attained an arbitrary value N. A d.c. pulse was applied to the specimen in order to

([7]) A. L. MCWHORTER and R. H. REDIKER: *Solid State Physics in Electronics and Telecommunications*, Vol. II, Eds. M. DESIRANT and J. L. MICHIELS (New York, 1960), p. 939. Also *Proc. Int. Conf. Semiconductor Physics* (Prague, 1961), p. 134.

([8]) S. H. KOENIG: *Solid State Physics in Electronics and Telecommunications*, Vol. I, Eds. M. DESIRANT and J. L. MICHIELS (New York, 1960), p. 422.

([9]) S. H. KOENIG and R. D. BROWN: *Journ. Phys. Chem. Sol.*, **10**, 201 (1959).

([10]) M. P. MADAN, E. I. GORDON, S. J. BUCHSBAUM and S. C. BROWN: *Phys. Rev.*, **106**, 839 (1957).

produce breakdown. The pulse was terminated within a time as short as possible after the required density was attained, usually less than 10 % of the time necessary to obtain the density N. These times were proportionally longer (of the order of 0.3 μs) for pulses shorter than 1 μs. A rapid termination of the breakdown field was particularly important when the longer pulses were used in order to avoid heating of the sample. This became particularly troublesome in samples LL 2 and n-WLB 28-6 for times longer than 100 μs. The reader is referred to ref. [11] for further comments on this point. In our measurements the repetition rate was 60 times per second; changing it to 30 times per second did not alter the result in the reported range of measurements. In the case of samples LL 2 and n-WLB 28-6 the asymptotic value obtained by pulsed breakdown is different from the value obtained in the case of steady state breakdown. The difference might be attributed to heating or, in the case of sample n-WLB 28-6, to the unfavourable geometry as has been discussed in ref. [11].

Contacts were made by soldering with pure tin. Liquid helium filled the cavity insuring good thermal contact to the surface of the sample. The arbitrary density N was much smaller than the density n_∞, the steady state

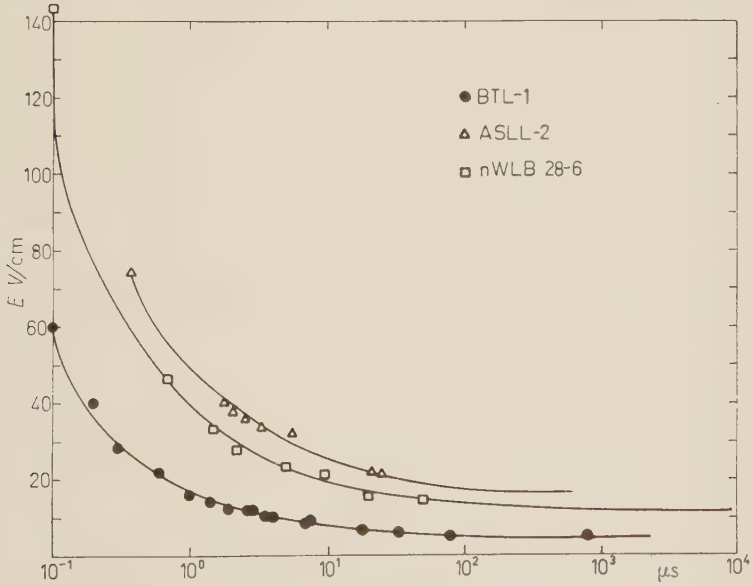

Fig. 1. – Experimental measurement of the time necessary to obtain an arbitrary density N (not necessarily equal for all samples). The time scale is proportional to τ defined by eq. (5). The temperature is 4.2 °K.

[11] G. Ascarelli: *Quarterly Progress Report Research Laboratory of Electronics*, Massachuserts Institute of Technology, **51**, 31 (1958); also *Phys. Rev.*, **120**, 1615 (1960).

density of the broken down sample. The conductivity σ_N (corresponding to the density N) was chosen as that corresponding to the instant the Q of the cavity attained a given arbitrary value, as measured by the microwave power reflected from the cavity. The electron density corresponding to σ_N was about 10^{10} cm^{-3} or 10^{11} cm^{-3}.

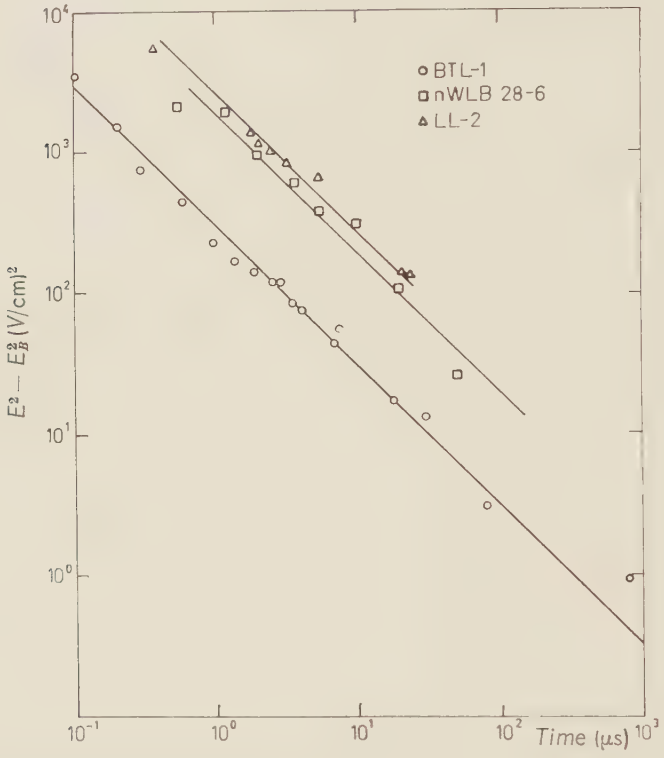

Fig. 2. – The experimental data of Fig. 1 so as to put in evidence the proportionality of τ^{-1} and $(E^2 - E_B^2)$.

The samples used in the experiment are described in Table I. Samples BTL 1 and LL 2 are the same as those used in previous measurements ([11]) while sample n-WLB 28-6 is the same sample that was used by KOENIG ([12]).

The experimental results are given in Fig. 1. It is seen that when the electric field is decreased, the time necessary to obtain a given density N increases continuously; the corresponding electric field approaches asymptotically E_B. No oscillations in the magnitude of the reflected microwave power that would

([12]) S. H. KOENIG: *Phys. Rev.*, **110**, 388 (1958).

TABLE I. – *Characteristics of the samples used in the experiment.*

Sample	Dimensions (mm^3)	Doping element	Photoconductive lifetime	Room temp. resistivity	Evaluations of $N_A(cm^{-3})$
BLT-1	$1.9\times82.03\times22.6$	Sb	$>1\,000\ \mu s$	$31.7\ \Omega cm$	$5\cdot10^{11}$
LL-2	$1.4\times\ 1.4\ \times16.5$	As	$2\,310\ \mu s$	$35\ \ \Omega cm$	10^{12}
n-WLB 28-6 (*)	$1.7\times51.46\times\ 6.96$	Sb	—	$N_D=2\cdot10^{13}\,cm^{-3}$	$5\cdot10^{12}$

The etch pit count on the BTL samples was of the order of 100 mm^2 on the smaller face of the parallelepiped that constituted the samples. No similar data are known for the other samples. The breakdown field in this samples was applied along the (111) direction.

(*) From ref. [12].

correspond to the oscillations of the current through the sample, as reported by SCLAR and BURSTEIN [5], and by REDIKER and MCWHORTER [7], were observed. The results were independent of the polarity of the applied field. The results are replotted in a way which illustrates the proportionality between the time necessary to obtain a given density N and a function of the electric field (Fig. 2). The experimental errors in the measurement of either time or field are not larger than 5%.

3. – Interpretation of the experimental results. Avalanche breakdown.

At helium temperatures, an electron in the conduction band of n-type germanium can either recombine with one of the (N_A+n) ionized donors, or it can have sufficient energy to ionize by impact one of the remaining (N_D-N_A-n) neutral donors. We will call γ the average probability per unit time of impact ionization, α the average probability per unit time of recombination, n the density of electrons in the conduction band, N_D the density of donors, and N_A the density of compensating acceptor impurities.

It has been shown that, in termal equilibrium, for electron densities of the order of 10^{13} electrons/cm^3, impact recombination [11] (*) and diffusion [5] of the electrons to the surface of the sample are not important mechanisms in determining the rate of loss of electrons from the conduction band. Electrons can also be thermally excited from the neutral donors to the conduction band; we will call β the corresponding probability per unit time. This last effect can take place by the absorption of a phonon or by impact ionization of the impurity by another thermal electron.

(*) A mechanism by means of which two electrons collide in the vicinity of an impurity; one of them is trapped in the donor state, while the other removes the excess energy.

Following SCLAR and BURSTEIN [5], the equation governing the change of electron density with time is

$$\frac{\mathrm{d}n}{\mathrm{d}t} = -\alpha n(N_A + n) + \beta(N_D - N_A - n) + \gamma n(N_D - N_A - n)\,. \tag{1}$$

Here we have neglected impact recombination and diffusion. γ can be determined from the steady state solution of the above equation and the density n_∞ corresponding to this condition ($\mathrm{d}n/\mathrm{d}t = 0$) can be calculated

$$\gamma = \frac{\alpha n_\infty(N_A + n_\infty) - \beta(N_D - N_A - n_\infty)}{n_\infty(N_D - N_A - n_\infty)}\,.$$

In the absence of an electric field ($\gamma = 0$), α and β are related by the condition of detailed balance:

$$\beta/\alpha = 2\left(\frac{2\pi m^* kT}{h^2}\right)^{\frac{3}{2}} \exp\left[-(\varepsilon_0/kT)\right]\,; \tag{3}$$

ε_0 is the ionization energy of our donor. Here for the sake of simplicity it is supposed to have only one state.

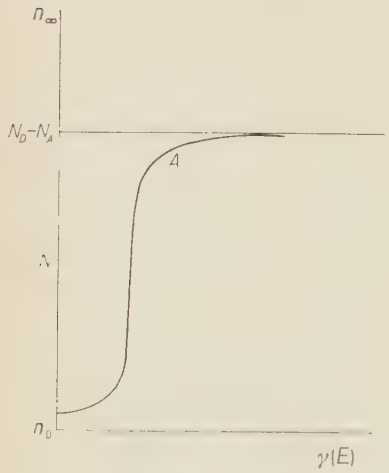

Fig. 3. – Plot of the solution of eq. (2) assuming that the probability of recombination and thermal ionization of a donor are independent of the applied electric field; γ, the probability of impact ionization is a monotonic function of the applied field.

When the variation of γ with n_∞ described by eq. (2) is studied, assuming α and β to be constants, there are no minima or maxima in the γ *vs.* n_∞ curve, only a point of inflection (Fig. 3). Changes in the ratio β/α due to changes in α *e.g.* produced by departures of the distribution from the low field one, or change in β/α produced by ohmic heating of a filament in the sample [9], may be the source of a maximum in the γ *vs.* n_∞ curve. Nome of these effects are taken into account in the above model.

Another approach to the description of breakdown is to solve eq. (1) assuming α, β, and γ to be independent of time, at least up to the moment when most of the impurities have not been ionized. This is different from the assumption, made in the case of the steady state solution, that α and β are independent of the applied field.

It can be shown that after times of the

order of 10^{-9} s the electron distribution has reached an average energy corresponding to equilibrium with the applied field ([11,12]). This energy will, however, be further increased after a large fraction of the donors are ionized.

Based on the above assumptions, the solution of eq. (1) is

$$(4) \qquad (n_\infty - n)^{-1} = (\alpha + \gamma)\tau + [(n_\infty - n_0)^{-1} - (\alpha + \gamma)\tau] \exp[t/\tau] ,$$

$$(5) \qquad \tau^{-1} = \gamma[2n_\infty - (N_D - N_A)] + \alpha(N_A + 2n_\infty) + \beta ,$$

n_∞, the solution of eq. (1) when $\mathrm{d}n/\mathrm{d}t = 0$, acquires here a more evident meaning and is equal to the density n attained after a very long time.

A clear definition of breakdown does not emerge: τ is always positive as can be seen if the value of γ from eq. (2) is substituted in eq. (5); the maximum of τ corresponds to the case when $n_\infty = (\beta/\alpha)\big((N_D - N_A)/N_D\big)$ which is smaller than n_0 for α equal to its value in the absence of an external field. The variation of τ with external field, even if it does not provide a simple definition of breakdown, can give us a tool to investigate the dependence of γ on the applied field.

For values of n_∞ approaching $N_D - N_A$ the influence of the electric field will be principally felt through the variation of τ in the exponential appearing in eq. (4); the time necessary to obtain a given density N is thus very sensitive to the applied field. This is shown in the Appendix. In a case like our experimental one, where we measure the time t necessary to obtain the density N, t will be proportional to τ. Since for relatively large fields n_∞ does not vary very much, and we can expect $\gamma/\alpha \gg 1$, it is reasonable to attribute the large observed variation of τ to changes in the value of γ. Regarding the variation of α with the applied field, the reader is referred to reference ([8]). In the case that impact recombination is the predominant mechanism determining the loss of electrons SCLAR and BURSTEIN ([5]) have shown that τ^{-1} is still proportional to γ.

We can now attempt to explain the observed variation of γ with the applied field as well as the observed temperature dependence of breakdown.

The difficulties connected with the calculation of the hot electron distribution function have already been illustrated in papers by ADAWI ([13]), MORGAN ([14]), YAMASHITA ([15]) in which the interaction between electrons and the scattering mechanism was well known (phonon or impurity scattering). In our case, in which there is yet no theoretical calculation for the energy dependence of the cross-section for impact ionization of the impurities, it seems

([13]) I. ADAWI: *Phys. Rev.*, **115**, 1152 (1959).
([14]) T. N. MORGAN: *Journ. Phys. Chem. Sol.*, **8**, 245 (1959).
([15]) J. YAMASHITA: *Prog. Theor. Phys.*, **24**, 357 (1960).

premature to attempt to calculate the distribution function of the electrons. However, the hot electron calculations (in particular that of YAMASHITA [15]) can furnish many qualitative results applicable to this problem. YAMASHITA compares the results of a calculation of the mobility of hot electrons with the experimental results of GUNN [16] at 77 K. He finds that for low impurity densities (assuming that the only scattering mechanisms are phonon and impurity scattering) the calculation gives a good description of the observed mobilities, but at higher impurity densities (above 10^{15} cm ^{3}) they cannot account for the experimental results. At these higher impurity (and electron) densities, a better description is obtained if one assumes a quasi-Maxwellian distribution of the type

$$f(x) = (1 + px) \exp[-x], \tag{6}$$

where p is a constant proportional to the square of the electric field and where $x = \varepsilon/kT$. In Yamashita's theory $p = (3\pi/16)(\mu_a E/c)^2$, where μ_a is the zero field mobility for acoustical mode scattering and c the velocity of sound. If electron-electron scattering is taken into account, assuming a mobility for electron-electron scattering equal to that for ionized impurity scattering, Yamashita's result is in good agreement with Gunn's experiment for impurity densities (thus also electron densities) varying from 10^{11} to 10^{17} cm^{-3}. This result suggests that if a scattering mechanism that removes energy efficiently is introduced (and electron-electron scattering is such a mechanism), the electron distribution will tend to a function of the type of (6).

According to Yamashita's calculation, at 77 °K, the density above which electron-electron scattering is important is 10^{15} cm^{-3}; at 4 °K this density should be decreased by a factor of the order of 10^4 due to the increase of the lattice mobility and of the cross-section for Rutherford scattering. Such a value is however barely sufficient to ensure a distribution of the type of (6) for our electron densities that are of the order of 10^{10} or 10^{11} cm^{-3}. At 4 °K, another mechanism comes into play, which has not been considered by the authors who have studied hot electrons. This mechanism is impact ionization of electrons bound to excited levels of donor impurities. According to recent calculations [17,18] it is apparent that the recombination of electrons and donors takes place with the capture of the electron in a highly excited state of the donor. The lifetime of the electron in the excited state is relatively long; it will change energy either by emitting a phonon and decaying to the ground state or by being excited back into the conduction band. This last step, in

[16] J. B. GUNN: *Journ. Phys. Chem. Sol.*, **8**, 329 (1959).
[17] M. LAX: *Phys. Rev.*, **119**, 1502 (1961).
[18] S. RODRIGUEZ and G. ASCARELLI: to be published in *Phys. Rev.* (1961).

particular, can easily be accomplished through the collision between an energetic free electron and one which is bound. The probability of such an event is dependent on the density of electrons for which such an impact ionization is energetically possible; consequently the rate of removal of electrons from the conduction band is very much influenced by the application of small fields that will increase the number of high energy electrons. Experimentally this is confirmed by the observations of KOENIG ([8]). Impact ionization of electrons that are in a high excited state of an impurity is thus a very efficient mechanism for depopulating the high energy tail of the electron distribution. The amount by which this tail will be decreased will depend on the number of electrons in such an excited state (the lowest excited state of an electron bound to a donor is $4.5 \cdot 10^{-3}$ eV ([19]); at 4 °K the most important levels for recombination are around 10^{-3} eV ([18]).

We will assume arbitrarily that function (6) describes reasonably well the electron distribution for electrons whose energy is smaller than the ionization energy ε_0 of the ground state of the impurity. For energies larger than ε_0 we will assume that the distribution function $\Phi(x)$ is

$$\Phi(x) = \frac{(1 + px_0) \exp[-x_0]}{\int_0^\infty (1 + px) \exp[-x] x^{\frac{1}{2}} \mathrm{d}x} F(x - x_0)\, x^{\frac{1}{2}} \mathrm{d}x\,. \tag{7}$$

where $F(x - x_0)$ is a function whose value is taken as equal to 1 for $x = x_0$ and such that $F(x - x_0)/F(0)$ is not larger than the corresponding value for the hot electron calculation when impact ionization is not present.

We are now in a condition to make simple assumptions that will allow us to calculate the dependence on temperature and electric field of the parameter γ',

$$\langle \gamma' \rangle = \int_0^\infty \gamma'(x)\, \Phi(x)\, \mathrm{d}x = (kT)^{\frac{1}{2}} \int_0^\infty \sigma_I(x) x^{\frac{1}{2}} \Phi(x)\, \mathrm{d}x\,,$$

where $\gamma'(x)$ is the probability that an electron, whose kinetic energy is ε in a lattice at a temperature T, will ionize by impact a donor; $\sigma_I(x)$ is the corresponding cross-section for impact ionization. We will assume that σ_I has the form

$$\sigma_I = 0\,, \qquad x < x_0\,,$$

$$\sigma_I = \sigma\,, \qquad x > x_0\,.$$

([19]) W. KOHN: *Solid State Physics*, Vol. 5, Ed. by F. SEITZ and D. TURNBULL (New York, 1957), p. 286.

The probability of impact ionization (thermal and that due to the applied field) is then

$$\langle\gamma'\rangle = \frac{(1+px_0)(kT)^{\frac{1}{2}}\sigma \exp[-x_0]}{\int_0^\infty (1+px)x^{\frac{1}{2}}\exp[-x]\,dx}\int_{x_0}^{\infty} F(x-x_0)x\,dx\,. \tag{7a}$$

Making $y = x - x_0$

$$\langle\gamma'\rangle = \frac{\sigma(kT)^{\frac{1}{2}}(1+px_0)\exp[-x_0]}{\Gamma(\frac{3}{2})(1+\frac{3}{2}p)}\int_0^{\infty} F(y)(y+x_0)\,dy\,. \tag{7b}$$

In the case that $F(y)$ has an exponential form, $F(y) = \exp[-y]$, we obtain

$$\langle\gamma'\rangle \simeq \frac{(1+px_0+x_0+px_0^2)(kT)^{\frac{1}{2}}\exp[-x_0]}{(1+\frac{3}{2}p)\Gamma(\frac{3}{2})}\,. \tag{7c}$$

Of the terms appearing in the numerator the largest is that in px_0^2 ($x_0 \sim 30$). Regarding the value of the coefficient p, it probably does not have the same value as in the case of the hot electron theory. If p would be equal to $(3\pi/16)(\mu_a E/c)^2$, where c is the velocity of sound, and μ_a the zero field mobility for acoustical phonon scattering, p would become much larger than 1 for fields of a few volt/cm, and the whole expression for γ' would be nearly field-independent, already for fields of the order of 1 V/cm. This contradicts the experimental results. We are then led to believe that for the range of fields used in this experiment $p \ll 1$.

The term in the expression for γ' that is independent of p represents the probability of impact ionization when no field is applied. It is already contained in the coefficient we previously called β.

We can now attempt to compare (7*c*) with the experimental observations.

a) *Delayed breakdown.* We assume that $p \ll 1$ so that it can be neglected in the denominator. Calling γ_B the value of γ corresponding to E_B we obtain

$$1/\tau - 1/\tau_B \mathrel{\widetilde{\propto}} \gamma - \gamma_B \cong (p-p_B)x_0^2(kT)^{\frac{1}{2}}/\Gamma(3/2)\,.$$

Remembering that $\tau_B = \infty$ and that p is proportional to E^2 we find

$$\tau^{-1} \mathrel{\widetilde{\propto}} E^2 - E_B^2$$

as observed experimentally (*).

(*) *Note added in proof.* – From the fact that the « breakdown field » is proportional to $((N_D/N_A)-1)^{-\frac{1}{2}}$ Bok *et al.* arrived to the conclusion that $\gamma \propto E^2$ (J. Bok, J. C. Sohm and A. Zylberstzejn: *Proc. Int. Conf. Semiconductor Physics* (Prague, 1960), p. 138.

b) Dependence on mobility. SCLAR and BURSTEIN (5) have shown that the breakdown field is inversely proportional to the low field mobility. This would indicate that the coefficient p is proportional to $(\mu_0 E)^2$ where μ_0 is the low field mobility.

c) Steady state breakdown. KOENIG and BROWN (9) measured the field necessary to obtain a certain electron density, as a function of temperature. KOENIG (8) also observed that when an external field is applied to the sample the coefficient α decreases rapidly. This is due to impact ionization of electrons that are bound to the excited states of impurities. If we interpret the published data of KOENIG and BROWN as representing the locus of points of constant γ we should obtain

$$\gamma = C(kT)^{\frac{1}{2}} p x_0^2 \exp[-x_0] = \text{constant}. \tag{8}$$

The experimental data are taken instead as the locus of points of constant electron density, thus (referring to eq. (2)) the locus of points of constant γ/α. If the data can be explained as that describing the locus of points of constant γ it would indicate that in the range of fields and temperature considered α remains constant, due to the fact that the changes produced by the electric field exactly compensate the changes of α produced by changes in temperature.

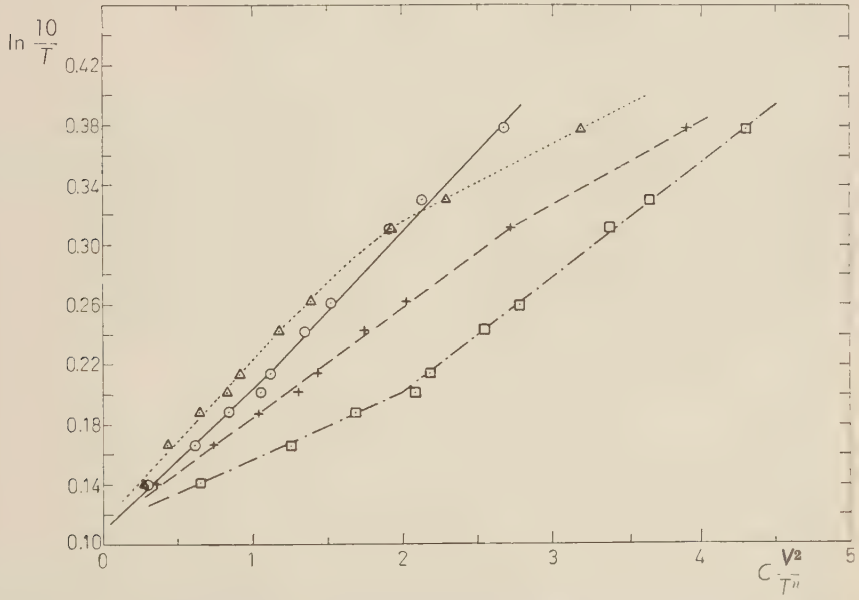

Fig. 4. – Experimental data of KOENIG and BROWN (9) displayed according to what is to be expected from eq. (8). The abscissa scale is $(1/C)V^2/T^n$. □ $n=1$, $C=4$; ○ $n=\frac{3}{2}$, $C=10^{\frac{1}{2}}$; + $n=2$, $C=1$; △ $n=\frac{5}{2}$, $C=2\cdot10^{-\frac{1}{2}}$.

A plot of Koenig's data is shown on Fig. 4, plotted in such a way as to to put in evidence what should be expected from eq. (8). For comparison a plot according to an equation of the type

$$\gamma = CT^{-n}E^2 \exp[-E_B/kT] = \text{constant},$$

with $n = 1, 2$, and $\frac{5}{2}$ is also shown (notice however, the different scales!). It is apparent that the plots with $n = \frac{3}{2}$ and 2 are nearly a straight line; one is slightly convex the other is slightly concave. If our interpretation of the measurements of KOENIG and BROWN is correct, it would indicate that μ_0 is nearly constant between 4 °K and 7.5 °K and that the variation of α due to the applied field and due to the temperature nearly compensate each other.

5. – Conclusions.

Our experiments indicate that the time necessary to obtain a given electron density is proportional to the square of the applied field. Assuming a « quasi-Maxwellian » distribution function for the conduction electrons whose kinetic energy is smaller than the binding energy of the electrons in the ground state of the donor, and a cross-section that is equal to zero for energies smaller than ε_0 and constant for higher energies, we obtain

$$\gamma \tilde{\propto} px_0^2(kT)^{\frac{1}{2}} \exp[-x_0],$$

where $x_0 = \varepsilon_0/kT$ and p is proportional to $(\mu_0 E)^2$ (μ_0 is the low field mobility and E is the applied field). The observed E^{-2}-dependence of the delay time could also be explained with the model proposed by KOENIG ([8]) which, however, would implicate a dependence of the delay on sample dimensions and on the square root of the mobility. It would also have been necessary to make assumptions about the relative times during which impact ionization and space charge limited conduction take place. More experiments are needed to clear these points.

* * *

The author is grateful to Professor S. C. BROWN and W. P. ALLIS for the constant help and encouragement he received. He is also indebted to Drs. S. J. BUCHSBAUM, G. BEKEFI, J. L. HIRSHFIELD, and other members of the microwave gas discharge group of M.I.T. for many fruitful discussions. The help of Dr. L. J. VARNERIN, Jr., of Bell Laboratories, Dr. P. MOODY of Lincoln Laboratory, and Dr. S. H. KOENIG of IBM in providing us with samples is gratefully acknowledged.

Appendix A

In this appendix we will attempt to show that the most important effect determining the variation of the time necessary to obtain a given density is the variation of τ appearing in the exponent of the exponential of eq. (4) rather than the changes in the coefficients.

We must thus calculate the coefficients $(\alpha+\gamma)\tau$ and $(n_\infty - n_0)^{-1} - (\alpha+\gamma)\tau$. We shall consider the case when $\alpha/\gamma \ll 1$. The case when $\alpha/\gamma \gg 1$ can be treated in a very similar way.

Substituting 5 in 4 and taking into account $\alpha/\gamma \ll 1$

$$(n_\infty - n)^{-1} \sim \left[n_\infty \left(2 - \frac{N_D - N_A}{n_\infty} + (\beta/\gamma n_\infty) \right) \right]^{-1} + \\ + \left\{ n^{-1} - [(2n_\infty - (N_D - N_A) + \beta/(\gamma n_\infty) n_\infty)]^{-1} \right\} \times \exp[t/\tau] .$$

Experimentally we have $n_\infty \sim N_D - N_A$. Two simple cases are possible: $\beta/(\gamma n_\infty) \gtrless 1$

Assume $\beta/(\gamma n_\infty) \ll 1$, then

$$(n_\infty - n)^{-1} \simeq n_\infty^{-1} \left\{ 1 + [\beta/(\gamma n_\infty)] \exp[t/\tau] \right\} .$$

If $\beta/(\gamma n_\infty) \gg 1$

$$(n_\infty - n)^{-1} \simeq n_\infty^{-1} [1 + \exp[t/\tau]] .$$

It is accordingly seen that whatever the field-dependence of γ (or α) the changes of τ with electric field, appearing in the exponential of eq. (4), give the principal contribution to the determination of the time t necessary to obtain a field density N. This time will be proportional to τ.

When $\alpha/\gamma \gg 1$ the term that gives the main contribution to the charge of τ with field is that whose coefficient is γ; in case $\gamma/\alpha \ll 1$ it is the term in α. The first represents the case when $n_\infty \simeq N_D - N_A$ (eq. (2)) while the second, that can only take place when $n_\infty \ll N_D - N_A$, represents the case of recombination with a very small applied field.

Appendix B

We will now survey the suggestion of Koenig [8] mentioned in Section 5. According to this model, the free electrons in the bulk of the sample would be swept out being substituted by electrons originating from the contacts. During their travel towards the anode these electrons will ionize donors producing a plasma that grows from the anode towards the cathode. The current originating from the cathode contact is space charge-limited in the case of

ohmic contacts, or it is limited by a depletion layer due to a potential barrier in the case of rectifying contacts. When this plasma moves towards the cathode, most of the potential drop will be between its edge and the « contact cathode »; when the plasma-cathode field attains a certain value E_c, there is field emission from the contact and the large number of extra electrons thus obtained will initiate the multiplication mechanism described previously.

Calculations and experiments have shown that in solids there is a space charge-limited current ([20,21]) whose value in the absence of trapping is

$$J = 10^{-13} \frac{\mu K V^2}{L^3} \text{ A/cm}^2 .$$

K is the dielectric constant of the sample, L the longitudinal dimension of the sample across which the field is applied, μ the mobility of the carriers and V the applied voltage.

Assuming that the plasma grows in volume when it has a constant density N_1 ($N_1 < N$ the density at which breakdown is detected), we can write

(B-1)
$$J = \frac{\mathrm{d}Q}{\mathrm{d}t} \simeq - N_1 e \frac{\mathrm{d}x}{\mathrm{d}t} = 10^{-13} \frac{\mu K V^2}{x^3} ,$$

$$\int_0^{\tau_1} \mathrm{d}t = 10^{13} \frac{N_1 e}{\mu K V^2} \int_{x_c}^{L} x^3 \, \mathrm{d}x ,$$

where $E_c = V/x_c$. The other symbols have their meaning explained in Fig. 5.

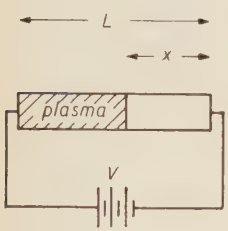

Fig. 5. – Diagrammatic description of the situation envisaged in eq. (B-1).

$$\tau_1 = \frac{10^{13}}{4} \frac{N_1 e}{\mu K V^2} (L^4 - x_c^4) .$$

Calling $E_a = V/L$ and remembering that $L \gg x_c$,

$$\tau_1 = \frac{10^{13} e N_1}{4 \mu K} \frac{L^2}{E_a^2} .$$

After field emission takes place the electron density grows by avalanche from a density N_1 to a density n_∞ in a time small compared with τ_1.

([20]) N. F. Mott and R. W. Gurney: *Electronic Processes in Ionic Crystals*, 2nd. ed. (Oxford, 1957), p. 172.

([21]) R. W. Smith and A. Rose: *Phys. Rev.*, **97**, 1531 (1955); A. Rose: *Phys. Rev.*, **97**, 1538 (1955).

The field E_B is still determined be the condition $n_\infty = N$ so that a dependence of the measured delays on $(E^2 - E_B^2)$ is to be expected. Taking for N_1 a value of the order of 10^9 or 10^{10} cm^{-3} gives a value of τ_1 in good agreement with experiment.

RIASSUNTO

Si sono eseguite misure del tempo necessario a produrre una scarica in germanio di tipo n, in funzione del campo elettrico applicato: questo tempo è risultato proporzionale a E^{-2}. Il risultato sperimentale qui ottenuto, e i risultati ottenuti dalle misure di altri autori con campi statici, possono essere spiegati (sulla base del modello di scarica con moltiplicazione a valanga) se si suppone che la funzione di distribuzione degli elettroni che hanno una energia inferiore alla energia di ionizzazione delle impurità sia data da $f(x) \propto (1+px) \exp[-x]$ (dove p è proporzionale a $(\mu_0 E^2)$ e μ_0 è uguale alla mobilità osservata per i campi bassi, $x = \varepsilon/kT$ dove ε è l'energia dell'elettrone) e che inoltre la sezione d'urto per ionizzazione per urto sia costante per $\varepsilon > \varepsilon_0$ e sia uguale a zero per $\varepsilon < \varepsilon_0$.

Positron Annihilation in Insulators.

A. Bisi, A. Fasana, E. Gatti (*) and L. Zappa

Istituto di Fisica del Politecnico - Milano

(ricevuto il 28 Giugno 1961)

Summary. — The time distribution of the positron annihilation radiation in various plastic insulators has been measured with a time-to-height converter. For each material, the abundance I_2 and the mean life τ_2 of long lived positronium were measured together with the mean life τ_1 of positrons annihilating with shorter lifetime. The obtained values for I_2, τ_2 and τ_1 were found to vary respectively between 10% and 45%, 1.2 and $2.6 \cdot 10^{-9}$ s, 1.5 and $3.0 \cdot 10^{-10}$ s. The bulk of the τ_1 component being made up of the non-positronium decay, from the τ_1 values we deduced the mean life τ_f for the unbound positron annihilation. τ_f was found to vary between 1.5 and $3.0 \cdot 10^{-10}$ s. A rough attempt to correlate the measured lifetimes with the effective electron densities suggested that polarization effects connected with microscopic fields play a significant role.

1. – Introduction.

Several studies of the annihilation rate of positrons in condensed materials have been made until now [1-4]. Their results can be divided into two groups: annihilation lifetimes in metals and annihilation lifetimes in nonmetals. As far as concerns the first group, the positrons display only a short lifetime $\sim 2 \cdot 10^{-10}$ s which in the past few years was found surprisingly constant despite large variations in electron density from one metal to another. However, by

(*) Istituto di Fisica del Politecnico and Laboratori CISE, Milano.

(1) S. Berko and F. L. Hereforrd: *Rev. Mod. Phys.*, **28**, 299 (1956).

(2) R. A. Ferrel: *Rev. Mod. Phys.*, **28**, 308 (1956).

(3) S. Debenedetti: *Suppl. Nuovo Cimento*, **4**, 1209 (1956).

(4) P. R. Wallace: *Solid State Physics*, edited by F. Seitz and D. Turnbull vol. **10** (New York, 1960), p. 1.

adopting quite recently greatly improved techniques it was possible to establish the dependence of the lifetime on the metal ([5,6]).

The second group contains molecular materials, in many of which the positronium formation was ascertained. In this case the decay curve is complex, exhibiting a fast component (τ_1) with a mean life of a few 10^{-10} s and a slow component (τ_2) with a mean life of a few 10^{-9} s. The τ_2 component is due, as it is generally accepted, to the formation of orthopositronium which in these materials decays only by « pick off » annihilation ([7,8]).

The τ_1 component, according to the positronium formation hypothesis, must be in turn a complex one: it partly arises from the annihilation of parapositronium with a mean life τ_s of $1.25 \cdot 10^{-10}$ s ([9]) while a considerable proportion should be due to positrons which survive the process of successive electron capture and loss, and annihilate when free. This picture is actually suggested by the fact that the known values of τ_1 lifetime are longer than those of τ_s; that is what is to be expected if we consider that the actual electron density at free positron in matter does not attain the « electron density » at bound positron in positronium. Unfortunately the slight number of investigated materials and the large errors involved prevent any attempt to deduce more information on the structure of the τ_1 component.

In the present paper we report the results of a set of our measurements on annihilation time spectra accomplished with the same experimental method which proved effective in the investigation on positron lifetime in metals ([5]). The aim was to obtain τ_1 values in some insulators, together with accurate measurements of τ_2 component lifetimes and intensities. This research was claimed also by the opportunity to investigate any possible connection between the general properties of positron annihilation in insulators and the microscopic electric fields in the material. In fact we have recently found that an applied electrostatic field strongly reduces the intensity of the τ_2 component and slightly enhances its annihilation rate in some insulators ([10,11]).

2. – Experimental method.

As positron source we used ^{22}Na which is customary for investigations of this kind; one drop of high specific activity $^{22}NaCl$ in aqueous solution was evaporated on each target of the investigated material, whose thickness was

([5]) A. Bisi, G. Faini, E. Gatti and L. Zappa: *Phys. Rev. Lett.*, **5**, 59 (1960).
([6]) R. E. Bell and M. H. Jørgensen: *Can. Journ. Phys.*, **38**, 652 (1660).
([7]) R. L. Garwin: *Phys. Rev.*, **91**, 157 (1953).
([8]) M. Dresden: *Phys. Rev.*, **93**, 1413 (1954).
([9]) J. Pirenne: *Arch. Sci. Phys. et Mat.*, **29**, 293 (1947).
([10]) A. Bisi, F. Bisi, A. Fasana and L. Zappa: *Phys. Rev.*, **122**, 1709 (1661).
([11]) A. Bisi, A. Fasana and L. Zappa: to be published.

sufficient to stop all β-particles, then covered with an identical target. The sandwich was inserted between two plastic scintillators (Pamelon, $1\frac{1}{2}$ inch diam., 1 inch thick) viewed by RCA 6342A photomultipliers. Of the two counters the first was biased to accept only the Compton edge of the 1.28 MeV γ-ray accompanying each positron from the decay, and the second to accept only the Compton edge of the 0.511 MeV annihilation radiation. The channel widths were regulated in such a manner as to avoid the detection of spurious events resulting from quanta scattered from one scintillator to another. The time distribution of the pulses from the two counters which recorded, respectively, the birth and the death of the positron, was analyzed by means of a time-to-height converter ([12,13]) and a 200-channel pulse height analyzer. The time resolution of the apparatus was checked with the prompt γ-rays from ^{60}Co, without changing the energy channel widths. The prompt resolution curve fits a Gaussian curve with full width at half-height of $8.0 \cdot 10^{-10}$ s.

The time spectra of the annihilation radiation, recorded with channel width of either $4.5 \cdot 10^{-10}$ s, or $2.3 \cdot 10^{-10}$ s were stored in the first hundred channels. In the second hundred channels were stored the prompt pulses from ^{60}Co. As the lifetimes were measured by the centroid shift techniques ([14]), we were particularly interested in minimizing any drift occurring in the whole apparatus. The time-to-height converter is equipped with a pulse generator of artificial coincident pulses, which is able to provide a continuous correction of the intrumental drifts. Moreover we stored the counting runs for the delay spectrum and the prompt curve alternatively with a suitable distribution of recording times. This distribution can be easily obtained as follows. Let us assume that the centroid position can be represented as a function of the time t by the following expansions in a series of positive integral powers of t

$$y(t) = y_0 + \sum_i \alpha_i t^i \qquad i \geqslant 1,$$

$$x(t) = x_0 + \sum_i \alpha_i t^i \qquad i \geqslant 1,$$

y and x refer respectively to the delay spectrum and the prompt curve; obviously y_0 and x_0 are the centroid abscissae when drifts are absent ($\alpha_i = 0$). The mean value of y in the interval from 0 to T is

$$\bar{y} = y_0 + \sum_i \frac{\alpha_i}{i+1} T^i,$$

([12]) C. COTTINI, E. GATTI, V. SVELTO and F. VAGHI: *Proc. of the Second Symposium on Advances in Fast Pulse Techniques for Nuclear Counting*, Lawrence Radiation Laboratory, Berkeley (February 1959), p. 49.

([13]) E. GATTI and V. SVELTO: *Nucl. Instr.*, **4**, 189 (1959).

([14]) Z. BAY: *Phys. Rev.*, **77**, 419 (1950).

T being the whole counting time. By assuming now that the prompt curve is recorded at the times $t_\nu = \beta_\nu T$, $(\beta_\nu < 1)$ with a total counting time $\tau \ll T$ the mean value of x is

$$\bar{x} = x_0 + \sum_i \alpha_i T^i \sum_{\nu=1}^{m} p_\nu \beta_\nu^i ,$$

where p_ν is the weight of the ν-th recording. Clearly the relative position of the centroids

$$\bar{y} - \bar{x} = y_0 - x_0 + \sum_i \frac{\alpha_i}{i+1} T^i - \sum_i \alpha_i T^i \sum_{\nu=1}^{m} p_\nu \beta_\nu^i ,$$

becomes insensitive to drifts when the following conditions are fullfilled

$$\sum_{\nu=1}^{m} p_\nu \beta_\nu^i = \frac{1}{i+1} ,$$

canceling in pairs the terms of the two sums.

For the sake of simplicity we take $p_\nu = 1/m$, so that the unknown β_ν are fixed by the resulting equations

$$\sum_{\nu=1}^{m} \beta_\nu^i = \frac{m}{i+1} .$$

From these equations it appears that it is possible to make the first m drift terms, through m recordings of the prompt curve, equal to zero.

In Table I the β_ν values are reported as a function of m. In the course of our investigation we adopted $m = 3$.

TABLE I.

m	β_ν		
1	$\beta_1 = 0.50$		
2	$\beta_1 = 0.21$	$\beta_2 = 0.79$	
3	$\beta_1 = 0.15$	$\beta_2 = 0.50$	$\beta_3 = 0.85$

The measurement of the τ_2 component lifetime was made in the usual way by reading the logarithmic slope of the delay spectra; its percentage intensity I_2 owing to the complexity of spectrum was obtained by measuring the area I_m under the spectral distribution between the instant of time t_1 for which the τ_1 component contribution is not appreciable and the instant of time t_2 chosen

so as to have a counting rate statistically still significant. Knowing the decay rate λ, I_2 was then deduced with the aid of the equation

$$I_m = I_2(\exp[-\lambda t_1] - \exp[-\lambda t_2]) .$$

As previously mentioned the τ_1 component lifetimes were obtained by measuring the centroid shift t of the whole time spectrum relative to that of the prompt curve. By taking into account the contribution of the τ_2 component we have

$$\tau_1 = \frac{\bar{t} - I_2\tau_2}{(1 - I_2)} . \tag{1}$$

At last, according to the argument reported in the previous section, we can deduce the lifetime τ_f of those positrons which annihilate when free. That is

$$\tau_1 = \frac{I_s\tau_s + I_f\tau_f}{I_s + I_f} , \tag{2}$$

where $\tau_s = 1.25 \cdot 10^{-10}$ s, $I_s = \frac{1}{3}I_2$, $I_f = 1 - \frac{4}{3}I_2$, having assumed that the ortho- and para-positronium are formed in $\frac{3}{4}$ and $\frac{1}{4}$ of the cases.

Eqs. (1) and (2) show that the τ_1 and τ_f values are obtained through the difference of two comparable terms; nevertheless an evaluation of the involved errors shows that the results are still significative.

3. – Results.

Typical time spectra are shown in Fig. 1 and 2, and all the obtained data are collected in Table II together with their experimental errors. We wish to outline that each reported value was obtained by averaging at least four independent measurements made at great intervals of time.

All our measurements were made at room temperature.

A comparison with the results of previous investigations [4] can be made only for a few polymers like polyethylene, Teflon and polystyrene: in any case only the values of the τ_2 component lifetime and intensity can be compared, while this is not possible for the τ_1 component owing to the lack of data. In most cases there is a satisfactory agreement: the slight differences present in some cases must not be attributable only to differences in experimental techniques and procedure but also to the fact that the samples are produced by different manufacturers. This appears to be the case of teflon, though the discrepancies are, for this material, unusually big.

Let us now consider some features of the foregoing results.

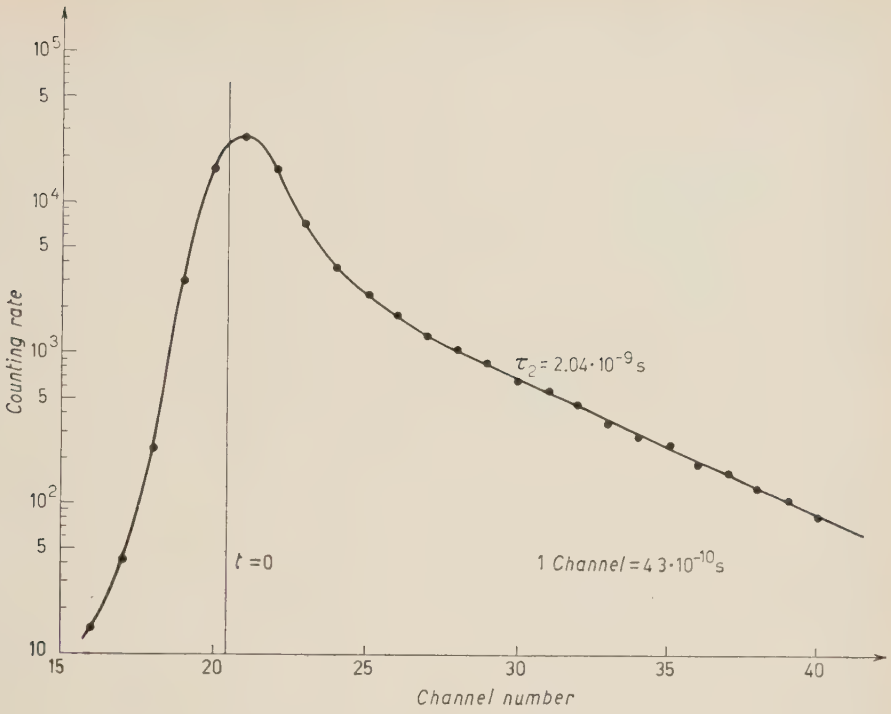

Fig. 1. – Time spectrum of positron annihilation in polyethylene.

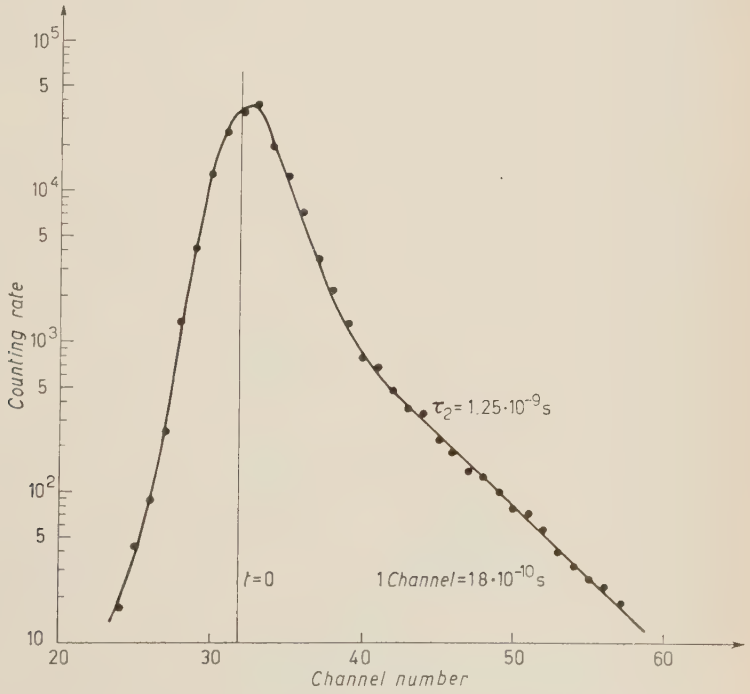

Fig. 2. – Time spectrum of positron annihilation in polyvinylchloride.

TABLE II.

Sample	Formula	$\nu \cdot 10^{-23}$ cm^{-3}	$\tau_2 \cdot 10^{10}$ s	$\tau_1 \cdot 10^{10}$ s	$\tau_f \cdot 10^{10}$ s	I_2 (%)
Paraffin	C_nH_{2n+2}	2.33	21.0±1.0	1.78±0.32	1.84±0.35	21.6±1.3
Polyethylene (*)	$(C_2H_4)_n$	2.34	20.4±0.6	1.93±0.23	2.04±0.27	29.5±0.4
Polystyrene	$[CH_2CHC_6H_5]_n$	2.52	16.0±0.1	1.56±0.05	1.67±0.07	45.2±0.1
Teflon (*)	$(C_2F_4)_n$	4.72	25.8±0.6	1.52±0.22	1.53±0.26	25.1±0.7
Polyisobutylene (*)	$[(CH_3)_2CCH_2]_n$	2.8	17.9±0.2	1.66±0.06	1.75±0.08	35.1±0.5
Polyvinyltoluene	$[CH_2CH(C_6H_7)CH_2]_n$	2.48	17.8±0.5	2.04±0.29	2.23±0.36	35.8±0.5
Polypropylene	$[CH_2CHCH_3]_n$	2.43	18.4±0.3	2.44±0.07	2.56±0.08	22.7±0.8
Cellulose acetate	$C_6H_7O_2(OOCCH_3)_3$	3.01	18.5±0.2	2.30±0.21	2.44±0.23	24.2±0.9
Polyvinyl acetate	$[CH_2CH(OOCCH_3)]_n$	3.0	17.5±0.4	2.38±0.17	2.56±0.20	29.7±0.6
Lucite (**)	$[CH_3CH_2C(OCOCH_3)]_n$	2.84	15.5±0.1	2.27±0.19	2.42±0.22	27.9±1.8
Nylon 66 (**)	$[NH(CH_2)_6NHCO(CH_2)_4CO]_n$	2.79	13.9±0.4	2.47±0.19	2.57±0.22	22.2±1.0
Polyvinyl chloride (**)	$[CH_2CHCl]_n$	2.30	12.5±0.3	2.95±0.26	3.00±0.27	9.5±0.7

(*) Typical non polar polymers.
(**) Typical polar polymers.

1) The relative intensity I_2 shows to be subject to considerable variations from one material to another; its value ranges from 9.5 % in polyvinylchloride to 45.2 % in polystyrene. This spread is quite consistent with what has already resulted from investigations in solid and liquid materials.

2) The τ_2 component lifetime varies between $1.2 \cdot 10^{-9}$ and $2.6 \cdot 10^{-9}$; the lower values pertain to typical polar polymers (polyvinylchloride, Nylon, Lucite), the highest to polymers which are typically non-polar (Teflon, polyethylene and polyisobuthylene) and to paraffin.

3) An opposite behaviour is displayed by the τ_f lifetime whose values are higher in polar than in non-polar polymers. It is interesting to note that at the same average electron density the positron lifetime in metals ([5,6]) lies between these two groups of values.

4. – Discussion.

In order to go forward with the discussion of our results and to attempt an interpretation of the annihilation mechanism, we introduce the average electron density ν evaluated by taking into account only the valence electrons. This parameter will be employed for the discussion of the « pick off » annihilation of positronium and also for that of the free positron annihilation: in fact the strong nuclear repulsion will prevent the positrons from penetrating the atomic core. The choice of this parameter was not made with an aim to getting a correlation between lifetime and electron density, which in general does not appear to occur, but to gain sight of those properties which can differentiate two materials with the same ν, as seen by free or bound positrons.

Polymers can be divided into two general classes ([15]): non-polar polymers, *i.e.* structures in which there are no permanent dipole moments and polar polymers (the vast majority) which have structures containing permanent dipoles. In this last case one should expect large electric fields on microscopic scale. There the positronium will come under a polarization force which will attract it on to the surface of the atoms, this process leading to an actual electron density at positron greater than the average. This picture is consistent with a rough evaluation of the potential energy due to polarization effect, which leads to a value greater than the mean kinetic energy.

On the other hand no similar polarization force acts on positronium in non-polar structures. Hence, two polymers with the same average electron density, will exhibit different lifetimes, of which the greater pertain to non-polar polymers. This is exactly the case of polyethylene (non-polar) and poly-

([15]) F. Würstlin and H. Thurn: *Die Physik der Hochpolymeren*, edited by H. A. Stuart, vol. 4 (Berlin, 1956), p. 525.

vinylchloride (polar) for which τ_2 lifetimes of $2.04 \cdot 10^{-9}$ s and $1.25 \cdot 10^{-9}$ s join with mean electron density of $2.34 \cdot 10^{23}$ cm^{-3} and $2.30 \cdot 10^{23}$ cm^{-3}, respectively. As far as concerns all the other investigated polymeric systems it can be noted that the mean electron densities vary little from one to another, while the values of the lifetimes support the foregoing argument.

As far as regards the positronium formation in various polymers, Ore's analysis ([16]) should be made in order to discuss our I_2 values, but it does not seem feasible for such complicated structures. We should point out only that no connection appears to exist between the dielectric properties of the material and the positronium abundance.

An attempt to schematize the annihilation of positrons when free in polar and non-polar polymers, can be made as follows: in the first group the positron experiences an attractive force due to the microscopic field from permanent dipole moments. So it is attracted on to a definite part of a monomer which will furnish the greater contribution to the actual electron density at the positron. In the non-polar structures, instead, attractive forces between positron and molecules are not determined by pre-existing electric fields which are lacking, but arise from atomic polarization induced by the positrons. Then it is conceivable that in this case each atom surrounding the positron yield about the same contribution to the actual electron density at the positron, which will turn out to be even greater than in the first case.

At the end we wish to emphasize that obviously the discussed polarization effects represent only a particular aspect of the annihilation mechanism and that our picture is certainly rough. However, owing to the fact that all the results on the positron annihilation in solids are very difficult to interpret, we think that it will be useful to propose a simple model while awaiting further experimental and theoretical results.

([16]) A. ORE: *Univ. Bergen Årbok*, no. 9 (1949).

RIASSUNTO

Si riferisce su alcune misure di spettri temporali della radiazione di annichilazione di positroni in vari materiali isolanti, effettuate con un convertitore tempo-ampiezza. Per ogni materiale sono stati misurate l'abbondanza I_2 e la vita media τ_2 del positronio a vita lunga, e la vita media τ_1 dei positroni a vita breve. I valori ottenuti per I_2, τ_2 e τ_1 sono compresi, rispettivamente, tra 10% e 45%, 1.2 e $2.6 \cdot 10^{-9}$ s, 1.5 e $3.0 \cdot 10^{-10}$ s. Poichè la maggior parte della componente τ_1 è costituita da annichilazione di positroni non legati, la vita media τ_f di questi ultimi è stata dedotta dai valori di τ_1. τ_f risulta compreso tra 1.5 e $3.0 \cdot 10^{-10}$ s. Nel tentativo di correlare le vite medie misurate con le densità elettroniche efficaci, viene osservato che fenomeni di polarizzazione dovuti a campi elettrici microscopici giocano un ruolo importante.

IL NUOVO CIMENTO Vol. XXII, N. 2 16 Ottobre 1961

On the Emission of Neutral Hyperons from K^--Interactions at Rest with Emulsion Nuclei.

D. H. Davis

Physics Department, University College - London

M. Csejthey-Barth (*) and J. Sacton (*)

Laboratoire de Physique Nucléaire, Université Libre de Bruxelles - Bruxelles

B. D. Jones, B. Sanjeevaiah (**) and J. Zakrzewski (***)

H. H. Wills Physics Laboratory, University of Bristol - Bristol

(ricevuto il 30 Giugno 1961)

Summary. — A systematic search has been made for decays of Λ^0-hyperons around 5262 interactions of K^--mesons at rest in photographic emulsion. From the 41 decays of correlated Λ^0-hyperons observed in this sample, it has been estimated that $(47\pm7)\%$ of all K^--meson interactions at rest in emulsion nuclei emit neutral hyperons. On consideration of the conservation of strangeness it is suggested that cryptofragments are formed in $(30\pm7)\%$ of all such K^--meson absorptions and that the non-mesonic decays of these cryptofragments give rise to a considerable proportion of the protons of energies greater than 60 MeV emitted from K^--meson captures.

1. – Introduction.

When a K^--meson is absorbed in an emulsion nucleus the emission of a charged Σ-hyperon or hyperfragment indicates negative strangeness amongst the secondary particles of the interaction. However, for the majority of ab-

(*) Chercheur agrégé à l'Institut Interuniversitaire des Sciences Nucléaires, Belgique.
(**) On leave from the University of Mysore, Mysore.
(***) On leave from the University of Warsaw.

sorptions no such evidence is available and it has been concluded that in these cases a neutral hyperon has been emitted or a Λ^0-hyperon has become bound within the struck nucleus and has decayed there.

Occasionally Λ^0-hyperons have been seen to be associated with K^--meson capture stars ([1,2]). BUNIATOV *et al.* ([1]) and CESTER-REGGE *et al.* ([3]) have scanned for Λ^0-hyperons and then attempted to find the parent K^--meson capture star by searching in a cone about the calculated line of flight of the Λ^0-hyperon.

There has, however, been no estimate of the fraction of K^--meson interactions at rest in emulsion nuclei from which neutral hyperons have been emitted.

In this work a systematic attempt has been made to correlate Λ^0-hyperons with particular K^--meson interactions at rest by scanning in a cylinder about each star for Λ^0-hyperon decays, in order to estimate directly the extent of neutral hyperon emission (*).

2. – Experimental procedure.

A stack of Ilford K-5 emulsions exposed to a separated 300 MeV/c K^--meson beam was used for this experiment. The line scanning procedure for finding the K^--meson interactions is described in the K^- European Collaboration work, *Nuovo Cimento*, **19**, 1077 (1961). K^--meson interactions within 50 μm of unprocessed emulsion of either interface were discarded.

In the search for associated Λ^0-hyperons a cylinder of radius 350 μm and of height equal to the thickness of the emulsion sheet was scanned with a low powered objective (10× magnification) about each K^--meson capture at rest in order to find any « V » event or black or grey track originating within this cylinder. Any such origins were scrutinized using an oil immersion objective (~ 50× magnification) to find whether a light track was present. The observational loss of Λ^0-hyperons due to inefficient detection of π^--mesons should be small in this case since the direction of the required π^--meson from the point of origin of the proton is approximately known. However, even then the π^--meson may still escape observation if the Λ^0-hyperon were to decay

([1]) S. A. BUNIATOV, A. WROBLEWSKI, D. K. KOPYLOVA, YU. B. KOROLEVICH, N. J. PETUKOVA, W. M. SIDOROV, E. SKRZYPCZAK and A. FILIPKOWSKI: *Žurn. Èksp. Teor. Fiz.*, **34**, 1028 (1958).

([2]) K^- EUROPEAN COLLABORATION: *Nuovo Cimento*, **13**, 690 (1959), part I.

(*) Preliminary results of this work were reported at the Physical Society Conference, Oxford, April 1959.

([3]) R. CESTER-REGGE, C. DENEY, K. GOTTSTEIN, W. PÜSCHEL, J. TIETGE, A. DEBENEDETTI, C. M. GARELLI, N. MARGEM, G. RINAUDO and M. VIGONE: *Rochester Conference Report* (1960), p. 440.

near an interface of the emulsion. For this reason Λ^0-hyperons which decayed within 50 μm unprocessed of either of the interfaces have been rejected from the analysis.

In order to reduce the observational losses of Λ^0-hyperons the material was scanned a further two times, first in the same manner as before, secondly in a cylinder of radius 210 μm using a higher powered objective (20 × magnification).

Every « V » event was subjected to the following analysis: the coplanarity with the K^--meson interaction was tested. For those « V » events which were possibly associated, both tracks were followed to their end-points (*) and when identified as a proton and π^--meson respectively the Q-value of the assumed Λ^0-hyperon decay was calculated from the dynamics. The momentum components of the proton and π^--meson perpendicular to the line joining the K^--meson interaction with the point of decay of the Λ^0-hyperon were calculated and if found to be equal within the experimental error, the Λ^0-hyperon was taken to be associated.

3. – Results and discussion of experimental bias.

A sample of 5 262 K^--meson interactions at rest, found by line scanning, has been investigated in this work and a total of 41 Λ^0-hyperons has been found in which the Λ^0-hyperon was associated with the K^--meson star. Of these 41 Λ^0-hyperons, 6 were found only upon re-scanning. The energies of the Λ^0-hyperons and the details of the K^--meson interactions at rest with which they are associated are listed in Table I.

Since the observed path length of each Λ^0-hyperon in the scanned cylinder is much less than its decay length then the product

$$\frac{RL}{\tau\beta\gamma c},$$

represents the chance that a Λ^0-hyperon of a particular velocity βc will be seen to decay into a proton and a π^--meson within the scanned cylinder, where:

i) τ is the mean lifetime of the Λ^0-hyperon $= 2.51 \cdot 10^{-10}$ seconds [4].

(*) In 6 cases the π^--meson was not brought to rest and its energy was estimated from extensive ionization measurements.

[4] W. H. Barkas and A. H. Rosenfeld: *Rochester Conference Report* (1960), p. 877.

TABLE I.

Details of Λ^0 hyperon					Parent K^- star characteristics		
Event no.	Q_Λ (MeV)	E_Λ (MeV)	ψ $p\pi^-$	$\frac{\tau\beta\gamma c}{RL}$	Range of stable particles (μm)	E_π (MeV)	B.A.R.
UC 106/32	38.0	35.5	56°	89	—	107^{+15}_{-10}	rec. $1\frac{1}{2}$ μm
139/18	37.9	6.1	142°	37	—	—	A. el.
102/31	37.0	69.4	140°	127	448, 102	—	rec. 2 μm
131/23	37.4	37.	126°	28	2110	—	—
132/22	38.7	48.2	116°	105	2580	—	blob
136/62	38.7	12.5	145°	53	—	139^{+9}_{-6}	—
140/2	38.6	13.6	146°	55	90	—	rec. 2 μm
90/30	(33.6)	57.9	8°	115	4650, 770, 470	—	—
101/22	36.3	7.1	147°	41	—	—	A. el.
136/36	37.8	42.1	81°	99	5	102^{+20}_{-12}	rec. 1.5 μm
135/24	37.8	1.8	148°	20	—	132^{+9}_{-6}	—
138/4	37.6	5.0	173°	34	—	—	—
140/8	38.9	8.3	160°	43	—	—	—
103/30	35.9	17.6	93°	63	840, 182	—	—
96/34	(40.8)	25.0	67°	76	11040	—	blob A. el.
101/28	37.5	23.3	103°	72	84	—	blob
134/20	38.5	19.6	154°	66	9650	π^- 29	A. el.
Bx 2133	40.5	0.6	121°	12	7	electron pair*	—
2192	36.7	14.7	100°	57	6, 7, 7, 470	>40	—
58	37.8	10.6	125°	45	—	—	—
547	33.2	2.9	98°	25	19, 24, 91, 10620, 35500	—	—
579	38.7	1.7	169°	19	340, 390, 680, 860, 700, 730	—	A. el.
3135	38.0	6.4	145°	38	11700	(π^-) 40	blob A. el.
4223	38.8	41.9	61°	99	5, 55, 85	—	—
8081	38.9	13.6	118°	55	—	82 ± 6	—
7138	38.1	7.3	131°	41	35, 20, 530, 400, 2950	—	—
260	(38.7)	23.6	67°	72	—	—	—
620	36.7	1.6	138°	18	213, 3050	—	rec.
1016	(41)	56.0	72°	113	10300, 7000	—	rec. 4 μm
5047	(36.9)	8.6	108°	43	—	—	—
1649	37.5	32.5	114°	85	—	—	—
Br 216/99	(38.3)	4.4	127°	31	57000, 810, 128	—	—
225/56	36.7	15.0	120°	58	80	—	rec. 2 μm, 1 μm
211/42	36.9	20.0	61°	67	637, 237, 192, 5	—	—
177/29	36.3	26.0	61°	76	1510, 582, 29	—	blob
267/28	37.7	15.6	140°	59	12400, 1350	—	—
192/4	37.3	6.4	144°	38	596, 416, 326	—	blob
188/43	38.7	32.0	101°	85	17690	(π^-) 34.5	blob
220/45	36.4	17.4	90°	63	8400, 660, 338, 152, 57	—	rec. 1.5 μm
226/56	36.1	11.0	89°	50	340	—	—
225/49	35.9	32.4	75°	85	327	—	rec. 2.5 μm

Bracketed Q values refer to cases where the π^--meson was not followed to rest.

(*) It is not possible to prove whether or not this complete event represents a Σ^0-hyperon decaying by the Dalitz mode, thus: $\Sigma \rightarrow \Lambda^0 + e^+ + e^-$, as it has been found impossible to obtain a reliable energy estimate for the electron pair.

ii) R is the branching ratio, $R = N(p\pi^-)/(N(p\pi^-) + N(n\pi^0)) = 0.67$, ([5])

iii) L is the mean path length traversed by a Λ^0-hyperon within the scanned cylinder and has been calculated to be 320 μm.

The total number of Σ^0 and Λ^0-hyperons emitted from the sample of 5262 K^--meson interactions has been obtained from the summation of the appropriate correction terms $\tau\beta\gamma c/RL$ listed in Table I. It can be seen that this total is 2457 neutral hyperons, having been derived from 41 observed Λ^0-hyperon decays and leads to a value of $(47 \pm 7)\%$ for the frequency of neutral hyperon emission from the K^--meson interactions at rest.

The Q-value for Λ^0-hyperon decay into a proton and a π^-meson has been found to be (37.53 ± 0.23) MeV (calibration procedure is described elsewhere ([6])). Those events in which the π^--meson was not followed to rest have not been included in the evaluation of Q_Λ.

The corrected energy spectrum, with statistical errors, of the correlated Λ^0-hyperons is given in Fig. 1. Energy spectra of Λ^0-hyperons have also been presented by BOGDANOWICZ *et al.* ([7]), C. J. MASON ([8]) and CESTER-REGGE ([3]), but may include Λ^0-hyperons from other sources (*e.g.* K^--meson interactions in flight) due to the different methods of scanning employed by these authors.

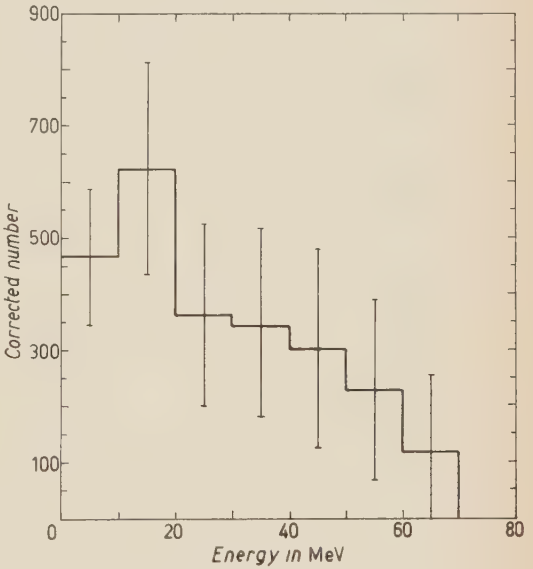

Fig. 1. – Corrected energy distribution of Λ^0-hyperons.

It is likely that there may still be some loss of higher energy Λ^0-hyperons due to the failure to observe the tracks of fast π^--mesons and also to the fact that those Λ^0-hyperon decay events which resemble small angle elastic scatterings of charged particles might escape observation. However, the losses arising from

([5]) D. GLASER: *Kiev Conference Report* (1959).

([6]) D. EVANS, B. D. JONES and J. ZAKRZEWSKI: *Phil. Mag.*, **4**, 1255 (1959).

([7]) J. BOGDANOWICZ, A. FILIPKOWSKI, A. KRZYWICKI, E. MARQUIT, E. SKRZYPCZAK, A. WROBLEWSKI and J. ZAKRZEWSKI: unpublished report no. 107/VI of Institute for Nuclear Research, Warsaw.

([8]) C. J. MASON: UCRL 9297.

both of these causes should be small, since the detection efficiency of light tracks is high in this stack ([9a]) and then umber of Λ^0-hyperon decays in which the velocities of the proton and π^--meson are comparable and the angle between them is close to 180°, is small ($\leqslant 2\,\%$).

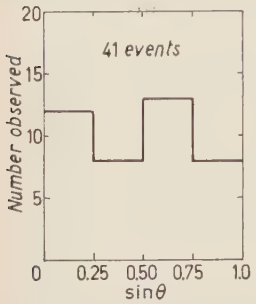

Fig. 2. – Dip distribution of Λ^0-hyperons.

Since the ability to observe a decay of a Λ^0-hyperon may depend upon the following:

i) dip angle of the Λ^0-hyperon,

ii) dip angle of the π^--meson,

iii) dip angle of the proton;

these dip angle distributions have been compiled and are given in Figs. 2, 3 and 4. They are seen to be isotropic within statistical error and it is concluded that no preferential loss arises from these sources.

It might also be expected that Λ^0-hyperons decays which occur near the boundary of the scanned field of view might be more easily lost to observation. Therefore the percentage of neutral hyperon emission has also been evaluated for a cylinder of radius 210 μm, for which the value of L is 225 μm, and was found to be $(46 \pm 10)\,\%$. This is in good agreement with the result given above.

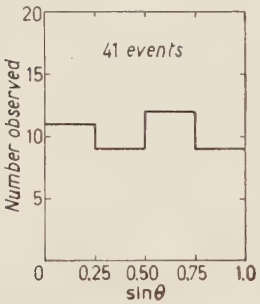

Fig. 3. – Dip distribution of π^--mesons emitted in the decays of Λ^0-hyperons.

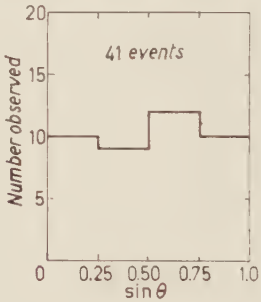

Fig. 4. – Dip distribution of protons emitted in the decays of Λ^0-hyperons.

The distribution of the angle of decay of the π^--meson in the centre of mass system of the Λ^0-hy-

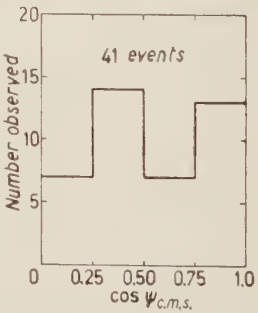

Fig. 5. – Distribution in the centre of mass of the decay angle of π^--mesons emitted in the decays of Λ^0-hyperons.

([9a]) K$^-$ European Collaboration: *Nuovo Cimento*, **12**, 91 (1959).

peron is given in Fig. 5 and there is forward-backward symmetry ([9b]). If there were a significant loss of Λ^0-hyperons due to the inability to observe the track of the decay π^--meson when it is lightly ionizing one would expect a backward peaking in this distribution.

4. – Discussion.

From the above it is concluded that the lower limit of the frequency of emission of neutral hyperons from K^--meson absorptions at rest in emulsion nuclei is $(47 \pm 7)\%$.

It has been established previously ([2]) that $(18 \pm 1)\%$ of such absorptions emit charged Σ-hyperons and $(5 \pm 1)\%$ emit hyperfragments. Thus the products of K^--meson captures exhibit negative strangeness in $(70 \pm 7)\%$ of the cases. If the Λ^0-hyperon observational loss is indeed small then the remaining $(30 \pm 7)\%$ must be ascribed to the formation and decay of cryptofragments, (*i.e.* hyperfragments which decay within the nuclei in which they are produced or so close to them as to be indistinguishable from them) ([9c,10,11]). Although this percentage of cryptofragment formation appears high (cf. WEBB *et al.* ([12]) and KOCH *et al.* ([13])) it is not so surprising if the binding energy of the Λ^0-hyperon in a heavy nucleus is as large as $(25 \div 35)$ MeV ([14]).

It is suggested that the decays of these cryptofragments frequently lead to the emission of energetic protons from K^--meson stars.

TABLE II. – *Number of* K^- *stars* = 2 450.

Fast proton	Fast Σ	Slow Σ	HF + π	HF no π	no HF π	Stable particles only	Total
Corrected number	16	3	8	9	27	285	348
Corrected percentage	0.7 ± 0.2	0.13 ± 0.07	0.3 ± 0.1	0.4 ± 0.1	1.1 ± 0.2	11.6 ± 0.7	14.2 ± 0.8

([9b]) THE HELIUM BUBBLE CHAMBER COLLABORATION GROUP: *Rochester Conference Report* (1960), p. 423.

([9c]) M. W. FRIEDLANDER, Y. FUJIMOTO, D. KEEFE and M. G. K. MENON: *Nuovo Cimento*, **2**, 90 (1955).

([10]) C. C. DILWORTH: *Rochester Conference Report* (1957), p. IV-19.

([11]) A. BONETTI: *Padua-Venice Conference Report* (1957), p. II-79.

([12]) F. W. WEBB, E. L. ILOFF, F. H. FEATHERSTONE, W. W. CHUPP, C. GOLDHABER and S. GOLDHABER: *Padua-Venice Conference Report* (1957), p. II-69; *Nuovo Cimento*, **8**, 899 (1958).

([13]) W. KOCH, Y. EISENBERG, M. NIKOLIĆ, M. SCHNEEBERGER and H. WINZELER: *Helv. Phys. Acta*, **33**, 237 (1960).

([14]) R. H. DALITZ and B. W. DOWNS: *Phys. Rev.*, **111**, 967 (1958); see also T. TATI and H. TATI: *Nuovo Cimento*, **3**, 1136 (1956); Y. POC KWON, J. OBA and G. GOTÔ: *Nuovo Cimento*, **6**, 832 (1957); R. GATTO: *Nuovo Cimento*, **3**, 99 (1956).

Table II summarizes the data concerning the emission of protons of energies greater than 60 MeV from K -meson interactions at rest in emulsion nuclei.

The table shows the percentage of all K^--meson absorptions in which a fast proton (*) is emitted accompanied by a fast Σ-hyperon, etc. If these protons arise directly from multinucleon K^--meson capture processes, their energy spectrum would be expected to peak above 100 MeV whereas the observed spectrum shows a continuous increase towards lower energies. It seems, therefore, that a major contribution to the fast proton spectrum must come from other sources such as Σ^+ and Σ^0 absorption, π-meson scattering and absorption and cryptofragment decays. However, the absorption of Σ^- and Σ^0-hyperons resulting from one-nucleon capture processes will not often produce protons of energies exceeding 60 MeV [2] and the absorptions of fast Σ-hyperons arising from multinucleon captures will contribute little to the number of fast protons (of the order of 1 % of all K^--meson captures). The inelastic scattering of π^--mesons does not contribute much to the emission of fast protons [15] and also the absorption probability of π^--mesons is known to be small (~ 0.1, see K European Collaboration, Part II). Little is known about the absorption probability of π^0-mesons created by K^--meson interactions. However, even if the high value of (0.8 ± 0.1) [16] is accepted it seems that no more than 3 % of all K -meson stars emit fast protons as a result of π^0-meson absorption.

One is led, therefore, to the conclusion that a substantial proportion of fast protons are not produced directly in K^--meson multinucleon capture processes but result from other sources, mainly the stimulated decays of Λ^0-hyperons bound within cryptofragments. The stimulated decays of Λ^0-hyperons bound within light hypernuclei and the energy distribution of the resultant protons have been studied by BALDO-CEOLIN *et al.* [17], SILVERSTEIN [18], SACTON [19] and GORGE *et al.* [20]. They find that (24 ± 4) % of non-mesonic decays of light hyperfragments emit protons of energies greater than 60 MeV. If it is assumed that cryptofragments decay non-mesonically and that the above

(*) A recent work of the K^- European Collaboration (*Nuovo Cimento*, **21**, 741 (1961)) has shown that 10 % of these so-called fast protons are in fact deuterons and tritons.

[15] See *e.g.*, G. BERNARDINI and F. LÉVY: *Phys. Rev.*, **84**, 610 (1951) and Bologna Group quoted by K^- European Collaboration, part I.

[16] K^- EUROPEAN COLLABORATION: *Nuovo Cimento*, **14**, 315 (1959), part II.

[17] M. BALDO-CEOLIN, C. C. DILWORTH, W. F. FRY, W. D. B. GREENING, H. HUZITA, S. LIMENTANI and A. E. SICHIROLLO: *Padua-Venice Conference Report* (1957), p. II-99; *Nuovo Cimento*, **7**, 328 (1958).

[18] E. M. SILVERSTEIN: *Suppl. Nuovo Cimento*, **10**, 41 (1958).

[19] J. SACTON: *Nuovo Cimento*, **18**, 266 (1960).

[20] V. GORGE, W. KOCH, W. LINDT, M. NIKOLIĆ, S. SUBOTIC-NIKOLIĆ and H. WINZELER: *Nucl. Phys.*, **21**, 599 (1960).

result is applicable in this case, then the $(30 \pm 7)\%$ of cryptofragment decays should give rise to the emission of protons of energies exceeding 60 MeV in $(7 \pm 3)\%$ of all K⁻-meson absorptions in emulsion nuclei. Also the shape of the fast proton spectrun ([21]) is better understood on this basis since the mean kinetic energy of the above sample—the majority of fast protons—should be of the order of 70 MeV.

Whereas the trapping of a Λ^0-hyperon in a light nucleus of the emulsion frequently leads to the emission of a hyperfragment ([22]) it is to be expected that if the trapping occurs in silver or bromine the hyperfragments so formed would not often be emitted from the parent nucleus. The Λ^0-hyperons so trapped would undergo stimulated decay. Therefore, since formation of cryptofragments and indeed other secondary absorption processes such as $\Sigma \to \Lambda^0$ will preferentially occur upon the heavy nuclei of the emulsion, these fast protons should be emitted more often from heavy nuclei.

5. – Conclusions.

i) The lower limit of the frequency of emission of neutral hyperons from K⁻-meson interactions at rest with emulsion nuclei is $(47 \pm 7)\%$.

ii) If the observational loss of Λ^0-hyperon decays is small, then from strangeness conservation it is concluded that $(30 \pm 7)\%$ of K⁻-meson interactions lead to cryptofragment formation.

iii) It is suggested that the non-mesonic decays of these cryptofragments give rise to the emission of protons of energies greater than 60 MeV in $(7 \pm 3)\%$ of all K⁻-meson absorptions.

* * *

We wish to thank Professor E. J. Lofgren and the Bevatron team for the exposure. We are greatly indebted to Professor E. H. S. Burhop, Dr. P. H. Fowler and Dr. W. M. Gibson for many stimulating discussions. The Bristol group are grateful to Professor C. F. Powell for his encouragement.

Acknowledgment is made to D.S.I.R. for a special development grant to University College London Emulsion Group and for research scholarships to

([21]) K⁻ European Collaboration: *Nuovo Cimento*, **19**, 1077 (1961).

([22]) See *e.g.* C. F. Powell, P. H. Fowler and D. H. Perkins: *The Study of Elementary Particles by the Photographic Method* (1959), p. 392; P. E. Schlein and W. E. Slater: *Nuovo Cimento* **21**, 213 (1961); J. Sacton: *Thesis*, unpublished (1961).

B.D.J. and J.Z., and to the Indian Ministry of Education and the University of Mysore for an overseas scholarship to B.S.

We wish to thank our scanners, Mrs. F. JOHNSON, Miss J. LEONARD and Miss B. WOODMAN for their assistance.

RIASSUNTO (*)

Si è condotta una ricerca sistematica dei decadimenti degli iperoni Λ^0 nei pressi di 5262 interazioni di mesoni K a riposo in emulsione fotografica. Dei 41 decadimenti di iperoni Λ^0 correlati osservati in questo campione si è stimato che il $(47\pm7)\%$ di tutte le interazioni di K^- a riposo nei nuclei dell'emulsione emettono iperoni neutri. In considerazione della conservazione della stranezza si fa l'ipotesi che si formino criptoframmenti nel $(30\pm7)\%$ di questi assorbimenti di mesoni K^- e che i decadimenti non mesonici di tali criptoframmenti diano luogo a una considerevole proporzione di protoni di energie maggiori di 60 MeV emessi nelle catture di mesoni K^-.

(*) *Traduzione a cura della Redazione.*

Cosmic Ray Observations at 42 m w.e. Underground at Hobart, Tasmania

A. G. Fenton, R. M. Jacklyn (*) and R. B. Taylor (**)

Physics Department, University of Tasmania - Hobart

(ricevuto il 3 Luglio 1961)

Summary. — A cosmic ray observatory and associated recording equipment located at 42 m water equivalent underground are described. The average primary proton energy corresponding to this depth is about 300 GeV. Data from two large vertical meson telescopes have been used to determine the atmospheric correction coefficients, and the results are compared with calculated values. The observed coefficients are:

Total barometer coefficient (95% fiducial limits).	$= -(0.655 \pm 0.042)\%$/cm
Partial barometer coefficient	$= -(0.591 \pm 0.044)\%$/cm
Negative temperature coefficient	$= -(0.459 \pm 0.250)\%$/km
Positive temperature coefficient	$= +(0.020 \pm 0.010)\%$/°C
Positive 3-fold temperature coefficient	$= +(0.028 \pm 0.009)\%$/°C

The low value for the positive temperature coefficient suggests that the attenuation length for π-mesons in the upper atmosphere is at least 125 g cm^{-2}. The effect on the underground intensity of a large change in the water content of the soil above the recorder is discussed.

1. – Introduction.

For the investigation of cosmic ray intensity variations of primary origin, it is desirable to determine the magnitude of the variations as a function of primary particle energy. For this purpose use is often made of data obtained

(*) Research Officer, Antarctic Division, Department of External Affairs, stationed at Hobart.

(**) Present address: School of Physical Sciences, Australian National University, Canberra, A.C.T.

at various latitudes, involving vertical primary cut-off energies in the geomagnetic field ranging up to about 15 GeV. In order to extend the observations to higher mean energies, it is convenient to locate the detecting equipment below ground so that the less penetrating secondary particles are filtered out. Results obtained in this way are particularly suitable for comparison with those from nearby ground level stations, because the particles detected in each case have traversed practically the same regions of the exosphere and atmosphere. On the other hand, recorders located at different latitudes detect particles that have traversed substantially different regions of the earth's environment; this may lead to undesirable influences of a local nature when the energy dependence of transient cosmic ray intensity changes is being studied.

With the above points in mind, a small cosmic ray observatory was installed in a disused railway tunnel about 6 miles from the main cosmic ray station at Hobart.

In this paper we shall present a brief description of the underground observatory and the meson telescopes, together with the results of a correlation analysis carried out in order to obtain atmospheric correction coefficients. Transient intensity variations have been observed on a number of occasions since the telescopes commenced operation in 1957; discussion of these will be deferred until later papers.

2. – Location of observatory and description of equipment.

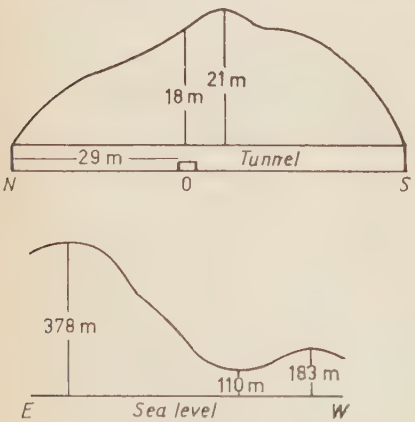

Fig. 1. – Vertical sections through the tunnel at Hobart, Tasmania, in the N-S and E-W directions. The surface of the land above *O*, the cosmic ray observatory, is 110 m above sea level.

The observatory is located in a disused railway tunnel approximately 6 miles north-east from Hobart; the geographic co-ordinates are 42.8° S latitude, 147.5° E longitude. The tunnel runs in a north-south direction below a saddle joining two hills, as shown in Fig. 1. The equipment is at an altitude of 110 metres above sea level. The absorber vertically above the equipment amounts to approximately 4 200 g cm^{-2} of shale and clay, or 42 metres water equivalent (m w.e.). It is not possible at present to give accurate values for the amount of absorber as a function of zenith and azimuth angles, but we have ascertained that this is a minimum in the vertical direction.

The cosmic ray equipment consists of two vertically directed triple coincidence Geiger counter telescopes, together with recording apparatus. The counter trays are each of 1 m^2 sensitive area and the distance between the top and bottom trays is 50 cm. In detail, the telescopes and electronic circuits are similar to those operated elsewhere by the Hobart cosmic ray group, as described by PARSONS [1]. The counting rate of each telescope is about 34 000 counts per hour, data from the two telescopes together having a statistical standard deviation of $\pm 0.38\%$ for hourly values and $\pm 0.07\%$ for daily mean values. Hourly totals are recorded photographically, while for short-term data a chart recorder is used. Mains voltage stabilisers are used to provide a constant AC supply to the equipment. The temperature inside the underground observatory remains within about five degrees of 13 C throughout the year without thermostatic control. Intermittent operation of the telescopes began in May 1957, and practically continuous records are available from October 1957.

3. – Energy of particles detected.

The particles detected by the telescopes are predominantly muons of high energy. In order to penetrate the atmosphere followed by 42 m w.e. of absorber, these must have an energy at production in excess of 15 GeV (GEORGE [2]); however, due to the multiplicity of production in the upper atmosphere, the corresponding primary particle energies are much higher. DORMAN [3] states that from available evidence, the muon energy at production is about one tenth of the primary proton energy. Assuming a differential energy spectrum of the form $E^{-2.7}$ for the protons concerned, this leads to the conclusion that the average energy of the primary particles responsible for the counting rate observed at 42 m w.e. is about 350 GeV. The low energy cut-off of 150 GeV suggested by Dorman's factor of 10 will in practice not be sharp due to fluctuations in the meson production multiplicity. This may lower the average energy somewhat, so that the above figure should probably be reduced to 300 GeV. For comparison, the average primary proton energy corresponding to particles detected by standard I.G.Y. neutron monitors and

---

(1) N. R. PARSONS: *The Design and Operation of ANARE Cosmic Ray Recorder « C »*, Australian Nat. Antarctic Res. Expeditions Interim Report no. 17, Melbourne (March 1957).

(2) E. P. GEORGE: *Progress in Cosmic Ray Physics*, J. G. WILSON (Ed.), chap. 7 (Amsterdam, 1952).

(3) L. I. DORMAN: *Cosmic Ray Variations*, State Publishing House for Technical and Theoretical Literature (Moscow, 1957). Translation Tech. Doc. Liason Office, Wright-Patterson Air Force Base (Washington, 1958).

meson telescopes operated near sea level at high geomagnetic latitudes is about 7 and 30 GeV respectively.

Thus, in the underground measurements, we are concerned with effects due to primary protons of energy about an order of magnitude above the minimum energy required to enter the earth's atmosphere vertically at the equator. About 10% of the cosmic ray muons near sea level arise from this portion of the primary spectrum and are capable of penetrating to 42 m w.e.

4. – Variations of atmospheric origin.

We have followed the usual practice of assuming that the meteorological effect on the cosmic ray meson intensity is adequately described for most purposes by the relation

$$\frac{\mathrm{d}I}{I} = \beta_{IB.HT}\mathrm{d}B + \beta_{IH.BT}\mathrm{d}H + \beta_{IT.BH}\mathrm{d}T\,,$$

where B is the barometric pressure at sea level, H is the height of the assumed mean pressure level for production (the 100 mb level is used here) and T is the temperature in the neighbourhood of the production level (we have taken this as the mean temperature in the pressure interval (100÷200) mb). Accordingly, $\beta_{IB.HT}$ is the partial barometer coefficient, $\beta_{IH.BT}$ the negative temperature coefficient and $B_{IT.BH}$ is the positive temperature coefficient. The total barometer coefficient will be referred to as β.

The various coefficients were found experimentally in two series of 4-fold correlation analyses, using selected data from the years 1958 and 1959. Daily mean values of cosmic ray intensity were correlated with daily mean values of barometric pressure and the values of H and T extracted from radiosonde data, supplied by the Hobart Bureau of Meteorology. All days on which it was known that pronounced anomalous variations of the primary cosmic ray intensity had occurred were rejected. In the analysis for 1958, the cosmic ray results from a single telescope were used and a total of 202 selected days of data was available. By comparison, the accuracy of the coefficients for 1959 was considerably greater since the combined data from both telescopes were available for most of the 230 days selected. A large secular change of cosmic ray intensity that was clearly not correlated with secular changes of B, H or T, (evidently part of the 11-year cycle of intensity variation) was eliminated before using the data.

In a recent criticism of the use of the least squares method of regression analysis, TREFALL and NORDÖ [4] have pointed out that errors of measure-

[4] H. TREFALL and J. NORDÖ: *Tellus*, **11**, 4, 467 (1959).

ment of the radiosonde data may influence the regression coefficients considerably. We have therefore used the estimated error variances and covariances (extracted from Table II and Table III of their paper) of the height H and the temperature T at the 100 mb level to take account of the systematic errors of measurement of the height of the 100 mb level and the temperature in the (100÷200) mb interval at Hobart. The ratios between the total variances and estimated error variances are shown in Table I. All the observed values of

TABLE I. *The ratios of the total variances to the estimated error variances for H and T at Hobart.*

	T ((100÷200) mb)	H (100 mb)
1958	5.87	5.77
1959	6.21	9.15

the regression coefficients involving H and T have been corrected for these errors. The partial barometer coefficient was practically unaffected, the negative temperature coefficient was increased by 15%, the positive temperature coefficient $\beta_{IT.HB}$ by 33% and $\beta_{IT.B}$ by 20%. Only the corrected values are quoted below, under the headings for the various coefficients, and, unless otherwise stated, the observed values of the coefficients are the weighted means of the 1958 and 1959 values.

4·1. *The total barometer effect.* – The coefficient β was found to have a weighted mean value of $\beta = (-0.651 \pm 0.041)\%$/cm Hg (95% fiducial limits). TREFALL [5] has obtained the total barometer coefficient as a function of cut-off energy at sea level for energies up to about 11 GeV. As well as considering the effect of pure mass absorption, he has taken into account the contribution from μ-e decay arising from the dependence of the mean life of the μ-meson on the distribution of energy loss in traversing the atmosphere. It appears that the latter contribution is the dominant one at low cut-off energies (less than about 500 MeV), but at 12 GeV (equivalent to 15 GeV at production) the barometer coefficient is due almost entirely to the effect of mass absorption. Extrapolation of Trefall's curve to 12 GeV gives a theoretical value of -0.57%/cm Hg. Our observed value is significantly greater than this. However, the result has been obtained from a wide angle recorder and no account has been taken of the dependence of the barometer coefficient on zenith angle.

[5] H. TREFALL: *International Conference on Cosmic Radiation*. National Institute for Scientific Investigation (Mexico, 1958).

BARNOTHY and FORRO (6) have investigated this problem with a telescope at sea level using different thicknesses of lead absorber and there is an indication from their work that at high cut-off energies the barometer coefficient increases with zenith angle.

4·2. *The partial barometer effect.* – The following value for $\beta_{IB.HT}$ was found:

$$\beta_{IB.HT} = (-0.591 \pm 0.044)\,\%/\text{cm Hg} \quad (95\,\%\ \text{fiducial limits}).$$

The usual day to day range of pressure at Hobart is about 1.5 cm Hg and the seasonal range is about 1 cm, so that the partial barometric effect contributes appreciably to variations of the underground intensity.

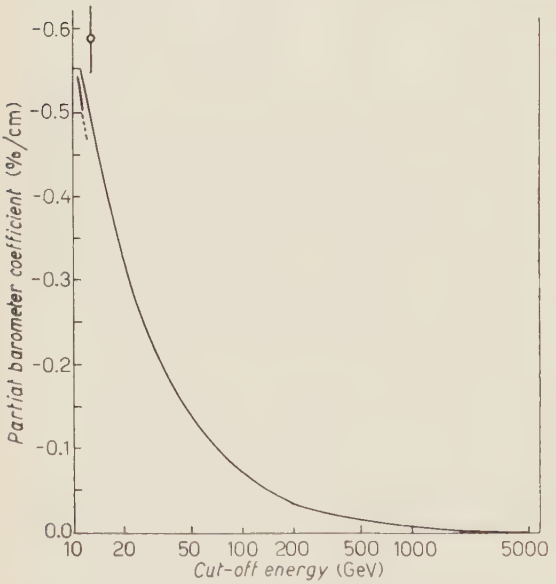

Fig. 2. – The calculated partial barometer coefficient as a function of cut-off energy at sea level. The overlap with a similar curve calculated by Trefall for lower energies is also shown. The error tails on the value observed underground at Hobart are the 95% fiducial limits.

Once again, as TREFALL has shown, the effect of μ-e decay must be taken into account when calculating $\beta_{IB.HT}$ for low cut-off energies, but in our case it appears that the contribution from this process can be neglected (*e.g.* see Trefall's Fig. 2 (5)). Using an expression that is identical with that used by TREFALL, but for a slightly different μ-meson spectrum at production, the partial barometer coefficient has been calculated as a function of cut-off energy at sea level in the range $(10 \div 5) \cdot 10^3$ GeV. In Fig. 2 the difference between our calculated values and Trefall's, where they overlap, is seen to be very small. On the other hand, the observed value is significantly greater than either estimate. Bearing in mind that the barometer coefficient may increase with zenith angle at high energies, our result indicates that the theoretical values of $\beta_{IB.HT}$ for vertical incidence are probably not greatly in error.

(6) J. BARNOTHY and M. FORRO: *Zeits. f. Phys.*, **100**, 742 (1936).

4·3. *The negative temperature effect.* – The value of the negative temperature coefficient was found to be

$$\beta_{IH.BT} = (-0.459 \pm 0.250)\,\%/\mathrm{km} \quad (95\,\%\ \text{fiducial limits}) .$$

The range of H (100 mb) from day today is usually about 0.3 km and the seasonal range is about 0.5 km. Therefore, fluctuations of H (100 mb) have very little influence on the underground intensity and, for most purposes for which daily mean values of intensity are used, may be neglected.

The negative temperature coefficient is thought to be due solely to the effect of variations in the path length on the probability of μ-meson decay.

One has to be careful, when calculating a theoretical coefficient, to choose a model atmosphere which conforms to the regression equation from which observed values are obtained. TREFALL has demonstrated this clearly in his theories of the meteorological effects. He has calculated the dependence of the negative temperature effect on cut-off energy for two cases:

i) in which the model conforms to the equation

$$\frac{\mathrm{d}I}{I} = \beta_{IB.H}\,\mathrm{d}B + \beta_{IH.B}\,\mathrm{d}H .$$

Accordingly, temperature variations are assumed to be uniform through the atmosphere;

ii) in which the model conforms to eq. (1). In this case the stratospheric temperature T is constant. The marked difference between the calculated case i) and case ii) values at low energies comes from a different distribution of energy losses along the path of the μ-meson for each case. The distinction becomes relatively unimportant at high energies.

As seen in Fig. 3, our observed value of $\beta_{IH.BT}$ is considerably less than our estimate. The curve shows the calculated value of the coefficient as a function of sea-level cut-off energy in the range $(10 \div 5)\cdot 10^3$ GeV. It has been obtained by partial dif-

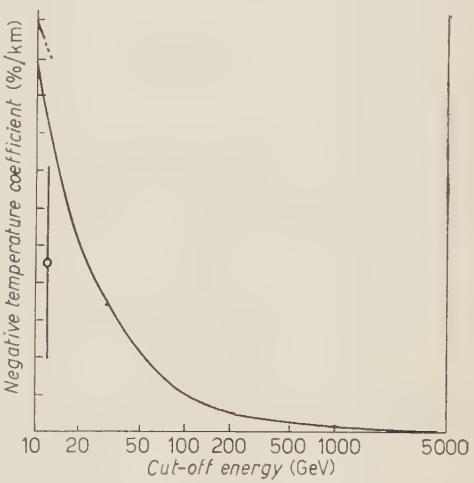

Fig. 3. The calculated negative temperature coefficient as a function of cut-off energy at sea level. Also shown is the overlap with a similar curve calculated by Trefall for lower energies. The error tails on the weighted mean value observed underground at Hobart are the 95% fiducial limits.

ferentiation of the integral momentum spectrum at sea level with respect to H. In deriving the integral momentum spectrum the expression $F(\varepsilon) = f(E)\exp[-k]$ has been used, relating the differential energy spectrum at sea-level, $F(\varepsilon)$, to the differential energy spectrum at production, $f(E)$, where E is the energy at production of a μ-meson which has the energy ε on arrival at sea-level. In the evaluation of $k = (Hm_{\mu}c/\tau_0 E')$ the loss of meson energy in traversing the atmosphere is neglected, and consequently E' has been given the value E. Here H is the meson production height, c the velocity of light, m_{μ} the μ-meson rest mass, τ_0 its mean lifetime at rest, and $\varepsilon < E' < E$. It can be seen that our curve and that for Trefall's case ii) differ only slightly where they overlap.

For the energies we are concerned with, the mean level of production of mesons is probably higher that the 100 mb level (Barton (7)). It may be that the choice of the reference level and of T (100 ÷ 200) mb as the stratospheric temperature in the neighbourhood of production are the main reasons why the coefficient $B_{IH.BT}$ is so much lower than the theoretical estimate. The question of the effect of choice of reference levels and stratospheric temperatures on the negative temperature coefficient at Hobart is at present being investigated.

4·4. *The positive temperature effect.* – The weighted mean value of $\beta_{IT.BH}$ was found to be

$$\beta_{IT.BH} = (0.020\,2 \pm 0.010)\,\%/^{\circ}\mathrm{C} \quad (95\,\%\ \text{fiducial limits}) .$$

The day to day range of temperature of the (100 ÷ 200) mb level is approximately 8 °C and the seasonal range is about the same. Therefore variations of stratospheric temperature have only a slight influence on the underground intensity. The magnitude of the effect is about the same as that due to variations in height of the 100 mb level.

In his theoretical treatment of the positive temperature effect due to π-μ decay Trefall (8) has used a model atmosphere in which temperature variations are independent of atmospheric depth. Therefore the temperature coefficient appropriate to this model is assumed to be the partial 3-fold coefficient $\beta_{IT.B}$ obtained from the regression equation

$$\mathrm{d}I = \beta_{IB.T}\,\mathrm{d}B + \beta_{IT.B}\,\mathrm{d}T . \tag{2}$$

For such a model Trefall shows that there are three contributions to the tem-

(7) J. Barton: *Proc. Phys. Soc.*, A **67**, 637 (1954).
(8) H. Trefall: *Proc. Phys. Soc.*, A **68**, 625 (1955).

perature coefficient. The first is a negative effect of μ-e decay due to the change in survival probability which accompanies the change in height of an assumed reference level in the vicinity of the mean level of production of mesons. The second is a smaller second-order effect of μ-e decay depending on the displacement of the mean level of production relative to the reference level. The third contribution is Duperier's positive temperature effect of π-μ decay caused by competition between absorption and decay of π-mesons. The total contribution from μ-e decay as a function of cut-off energy for the equipment may be calculated from Trefall's eq. (5) and used as a correction so that the net positive temperature effect of π-μ decay can be obtained from observed values of $\beta_{IT.B}$.

The positive temperature effect of π-μ decay is a function of λ_π, the attenuation length of π-mesons. Trefall's calculated values of the effect as a function of cut-off momentum (Fig. 2 ([5])) are rather insensitive to the value of λ_π for the low cut-off energies applicable to cosmic ray intensity measurements at sea level, and also for the very high cut-off energies which apply to measurements at extreme depths underground. However, as he points out, his calculations show that measurements at moderate depths underground should enable us to determine from the positive temperature effect whether the value of λ_π is comparable with the collision mean free path for π-mesons, or with the attenuation length, λ_p, of the primary proton component. The curves in Trefall's Fig. 2 for each of these cases and for the case where $\lambda_\pi \simeq 2\lambda_p$ have been redrawn in our Fig. 3 (where the positive temperature effect is expressed as a function of cut-off energy instead of momentum). Also reproduced from his figure is Trefall's estimated value of the π-μ effect using the positive temperature coefficient obtained by MacAnuff ([9]) at a depth of 60 m w.e. underground. MacAnuff found a positive temperature coefficient $\beta_{IT.B}=-(+0.055 \pm 0.005)\%/°C$, where T was the temperature of the (100 ÷ 300) mb layer. A total correction for μ-e decay of $+0.054\%/°C$ gave the net positive temperature effect of π-μ decay as $+0.109\%/°C$.

Our data were re-analysed in conformity with eq. (2) and annual values of $\beta_{IT.B}$ of $(+0.049\,7 \pm 0.022)\%/°C$ and $(+0.024\,3 \pm 0.010)\%/°C$, were obtained for the years 1958 and 1959 respectively. The errors given are the 95% fiducial limits. The weighted mean value was $(+0.028\,6 \pm 0.009)\%/°C$. The correction for the principal μ-e decay effect calculated from Trefall's eq. (5), where the cut-off energy at production was taken as $E_0 = 142\,mc^2$, was found to be so close to the value Trefall quoted for $E_0 = 155\,mc^2$ that the same total correction of $+0.054\%/°C$ has been used. This finally gave a weighted mean value of $(+0.082\,6 \pm 0.009)\%/°C$ for the net positive temperature effect of π-μ decay at 42 m w.e. underground, as shown in Fig. 3.

([9]) J. W. MacAnuff: *Thesis* (University of London, 1951).

BARTON (7) has criticized MacAnuff's choice of the temperature of the (100 : 300) mb layer as the temperature variable T in the regression analysis. Since there are contributions to the positive temperature effect at all levels of the atmosphere a weighted mean temperature, such as the T_{eff} used by some investigators (see TREFALL (5)), is possibly the best one to use. BARTON has pointed out that the use of $T_{(100 \div 300)\,mb}$ as the temperature variable leads to an under-estimation of the atmospheric temperature variation and would make MacAnuff's coefficient too large by a factor of ~ 2. Since the temperature variations tend to be greater at the higher levels of the atmosphere our use of $T_{(100 \div 200)\,mb}$ as the temperature variable should also tend to make our estimate of the positive temperature effect too large but might give a better estimate of the effect than if we had used $T_{(100 \div 300)\,mb}$.

It would seem from our results and those of MACANUFF that the attenuation length λ_π, of π-mesons is at least 125 g cm^{-2}, and may be considerably larger.

In addition to the meteorological influences we have described we have evidence that variations in the amount of water in the soil above the tunnel can produce significant changes of cosmic ray intensity underground. A striking example of this occurred at the end of April 1960 when phenomenal rains caused severe flooding in Southern Tasmania, following several months of very dry weather. The total rainfall recorded near the tunnel from February 1st to April 21st was 3.1 in., whereas 9.5 in. fell during the 22nd, 23rd and 24th of April. Between the 21st and 23rd of April the pressure-corrected underground intensity showed a gradual decrease of 0.8% ($\pm$0.07% standard error) and remained at this reduced level until the end of April. Over the same period the vertical meson intensity at sea level in the Hobart laboratory remained at a constant level after the usual corrections for atmospheric

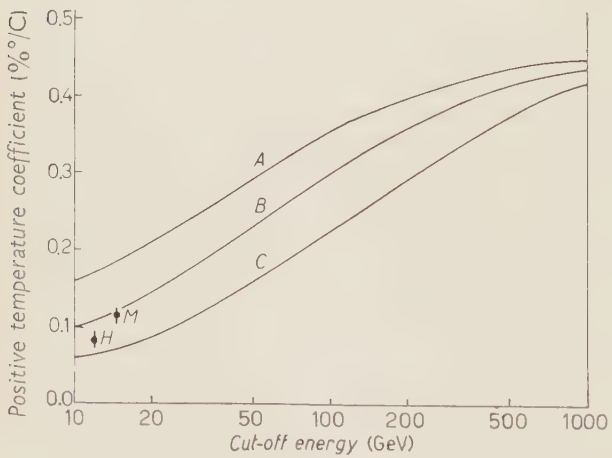

Fig. 4. – The positive temperature effect due to π-μ decay calculated by Trefall for A: $\lambda_\pi = 62.8$ g cm^{-2}; B: $\lambda_\pi = 125$ g cm^{-2} and C: $\lambda_\pi = 250$ g cm^{-2}. The value M has been derived by TREFALL from the positive temperature coefficient $\beta_{IT.B}$ observed by MACANUFF, corrections having been made for 1st and 2nd order effects of μ-e decay. The value H from Hobart has been derived in the same way. The error tails on the Hobart value are the 95% fiducial limits.

changes had been applied. Using an intensity-depth relationship published by CLAY [10] it was found that a reduction of the counting rate by 0.8% at 42 m w.e. underground would indeed correspond to an increase of the absorber by approximately 10 in. water equivalent.

Variations in the moisture content of the material above the tunnel are naturally rather difficult to assess. They must, in particular, seriously complicate the observed seasonal changes of the daily mean underground intensity. However, apart from rare occasions such as the one quoted, day to day changes of the absorber due to rainfall would generally not produce intensity variations greater than the standard error of observation ($\pm 0.07\%$).

We conclude from the foregoing that the variations in atmospheric structure have a very small influence on the underground cosmic ray intensity. In this respect underground observations have an advantage over ground level meson intensity measurements which are often considerably influenced by changes in atmospheric structure. However the mass absorption effect is appreciable and in many cases the data must be corrected for this effect.

* * *

Financial assistance for this project was received from the Commonwealth Scientific and Industrial Research Organization and the Australian Academy of Science.

---

(10) J. CLAY: *Rev. Mod. Phys.*, **11**, 128 (1939).

RIASSUNTO (*)

Descriviamo un osservatorio per raggi cosmici e le relative apparecchiature di registrazione collocati sottoterra a 42 m a. e. L'energia media dei protoni primari in corrispondenza di questa profondità è circa 300 GeV. Abbiamo usato due grandi telescopi verticali per mesoni per determinare i coefficienti di correzione atmosferica, ed abbiamo confrontato i risultati con i valori calcolati. I coefficienti osservati sono:

Coefficiente barometrico totale (limiti di fiducia 95%)	$= -(0.655 \pm 0.042)\%$/cm
Coefficiente barometrico parziale	$= -(0.591 \pm 0.044)\%$/cm
Coefficiente di temperatura negativo	$= -(0.459 \pm 0.250)\%$/km
Coefficiente di temperatura positivo	$= +(0.020 \pm 0.010)\%/°C$
Coefficiente triplo di temperatura positivo	$= +(0.028 \pm 0.009)\%/°C$

Il basso valore del coefficiente di temperatura positivo suggerisce che la lunghezza di attenuazione per i mesoni π nella parte superiore dell'atmosfera è almeno 125 g cm^{-2}. Discutiamo l'effetto sull'intensità sotterranea di una forte variazione del contenuto di acqua nel suolo al di sopra degli apparecchi di registrazione.

(*) *Traduzione a cura della Redazione.*

The Mass of the Λ^0-Hyperon.

B. Bhowmik, D. P. Goyal and N. K. Yamdagni (*)

Department of Physics, University of Delhi - Delhi

(ricevuto il 10 Luglio 1961)

Summary. — An accurate determination of the Λ^0-mass has been made using nuclear emulsion. From an analysis of 101 Λ^0-decays, we obtain for the mass of the Λ^0-hyperon, $M_\Lambda = (1115.46 \pm 0.15)$ MeV and $Q_\Lambda = (37.62 \pm 0.14)$ MeV.

1. – Introduction.

The need for an accurate estimation of the Λ^0-mass has been felt in recent years. The Q-value in the decay $\Lambda^0 \to p + \pi$ has a special significance in the study of the binding energy of the Λ^0-hyperon in hypernuclei. Early determinations of the Λ^0-mass were made in cloud chambers using cosmic rays, but the accuracy in these measurements was limited as the momenta of the secondaries were uncertain by about 10%. The latest cloud chamber value of Q_Λ by Armenteros *et al.* [1] is

$$Q_\Lambda = (37.90 \pm 0.40) \text{ MeV}.$$

In nuclear emulsion the Λ^0-mass can be determined with much higher accuracy. Here the secondaries can be brought to rest and their momenta determined by an accurate range-energy relation. The first accurate mass

(*) On leave of absence from Education Dept., M. P. Govt., Bhopal.

(1) C. D'Andlau, R. Armenteros, A. Astier, H. C. DeStaebler, B. P. Gregory, L. Leprince-Ringuet, F. Muller, C. Peyrou and J. H. Tinlot: *Nuovo Cimento*, **6**, 1135 (1957).

determination was made by FRIEDLANDER *et al.* [2] in nuclear emulsion exposed to cosmic rays. The Q_Λ obtained in this experiment for 9 events was

$$Q_\Lambda = (36.84 \pm 0.21) \text{ MeV} .$$

With the availability of the K^--meson beam at the Berkeley Bevatron BARKAS [3] using nuclear emulsion exposed to this beam obtained Q_Λ on the basis of 18 events as

$$Q_\Lambda = (37.45 \pm 0.17) \text{ MeV} .$$

Another accurate mass determination was made by BOGDANOWICZ *et al.* [4]. Their value for 53 events was

$$Q_\Lambda = (37.58 \pm 0.18) \text{ MeV} .$$

The wide dispersion in the above mentioned Q-values alone justified another accurate determination of Λ^0-mass. Besides this, it is significant to observe that, though the $^3H_\Lambda$ hyperfragment had been observed, the B_Λ of the Λ^0-hyperon in the $^3H_\Lambda$ hyperfragment was negative, if Q_Λ was taken as the weighted mean of these three values. This suggested that the mass of the Λ^0-hyperon may be higher than the value given by these groups. In the present experiment Q_Λ on the basis of 101 events is

$$Q_\Lambda = (37.62 \pm 0.14) \text{ MeV} .$$

Since the design of the present experiment two more accurate estimations of the Λ^0-mass have been made by LODGE *et al.* [5] and BARKAS *et al.* [6]. These values are consistent with our value.

The present experiment was carried out in a stack (K_2^-) of 100 pellicles (60 Ilford G-5 and 40 Ilford K-5 emulsions) exposed to the Berkeley K^--beam. The details of the exposure are described elsewhere [7].

---

[2] M. W. FRIEDLANDER, D. KEEFE, M. G. K. MENON and M. MERLIN: *Phil. Mag.*, **45**, 533 (1954).

[3] W. H. BARKAS: *Padua-Venice Conference* (1957).

[4] J. BOGDANOWICZ, M. DANYSZ, A. FILLIPOWSKI, G. MARQUIT, E. SKRZYPCZAK, A. WROBLEWSKI and J. ZAKRZEWSKI: *Nuovo Cimento*, **11**, 727 (1959).

[5] J. LODGE, F. ANDERSON, E. B. BRUCKER, A. PEVSNER and R. STRAND: *Nuovo Cimento*, **18**, 147 (1960). Also, L. ALVAREZ: *Ninth International Conference on High Energy Physics* (Kiev, 1959), p. 477.

[6] C. J. MASON, W. H. BARKAS, J. N. DYER, H. H. HECKMAN, N. A. NICKOLS and F. M. M. SMITH: *Bull. Am. Phys. Soc.*, **5**, 224 (1960).

[7] B. BHOWMIK, P. C. JAIN and P. C. MATHUR: *Nuovo Cimento*, **20**, 857 (1961)

2. – Scanning procedure.

The following methods are in use for finding the Λ^0-decay-like events.

1) Back following σ_{π^-} stars to a distance of $\simeq 25$ mm to get a decay-like event.

2) Area scanning under low magnification for protons which appear to have been produced within the pellicles (« hanging protons ») and then to observe under higher magnification any possible light particle associated with the proton.

3) Area scanning for V-events.

Although, for determining the Λ^0-mass any of the above mentioned methods, could be used, for the energy spectrum of Λ^0 and angular distribution of its secondaries an unbiassed sample is necessary. The later two problems will be discussed separately. While the first and third methods pick up events with slow pion secondary, the second method selects preferentially faster pions. Following the second method we obtained two examples of electronic decay of the Λ^0-hyperon to be published elsewhere.

A combination of the second and third methods was used in the present experiment. However, few events initially found by the first method were also included in the sample. It was observed that the majority of Λ^0 having kinetic energy ~ 50 MeV had such geometry, projected angle and ionization of the secondaries, that they were likely to be missed by an average observer. In this work 90 % of the scanning was done by the physicists. Our sample is characterized by Λ^0 of energy as high as 100 MeV and events having projected angles $< 1°$ have been recorded.

A major problem in this work is the elimination of background stars simulating decay-like events. It was observed that many events of the type $\pi^- + p \to \pi^- + p$ looked like Λ^0-decays, if the high energy primary π^--track was missed from observation. Many such events with a clear primary π^--meson gave on analysis Q_Λ (35 ± 10) MeV. Owing to a high minimum ionization (blob density $\sim 25/100\ \mu$m) and flat π -beam in our experiment, only in events close to either of the surfaces of the pellicles ($\sim 5\ \mu$m) a flat primary may not be observed. In our sample no event was recorded in this region.

Another source of background may be due to neutron produced stars via the reaction,

$$\Lambda^0 + \Lambda^0 \to \Lambda^0 + p + \pi^- .$$

The frequency of such events should be very small. However, they can be easily excluded from Q-value considerations.

3. – Measurements and sources of error.

The mass of the Λ^0-hyperon, M_Λ was determined from the equation,

$$M_\Lambda^2 = M_p^2 + M_\pi^2 + 2E_p E_\pi - 2p_p\, p_\pi \cos\varphi\,,$$

where E_p, E_π, p_p, p_π, M_p, M_π are the total energies, the momenta, and the masses of the proton and the pion respectively, and φ is the opening angle between the directions of emission of these secondary particles.

The errors were then calculated by using the equation given below:

$$\mathrm{d}M_\Lambda = \frac{1}{M_\Lambda}\left(M_p + E_\pi - T_p\frac{p_\pi}{p_p}\cos\varphi\right)\mathrm{d}M_p + \frac{1}{M_\Lambda}\left(M_\pi + E_p - T_\pi\frac{p_p}{p_\pi}\cos\varphi\right)\mathrm{d}M_\pi +$$

$$+\frac{1}{M_\Lambda}\left(E_\pi - E_p\frac{p_\pi}{p_p}\cos\varphi\right)\mathrm{d}T_p + \frac{1}{M_\Lambda}\left(E_p - E_\pi\frac{p_p}{p_\pi}\cos\varphi\right)\mathrm{d}T + \frac{p_p p_\pi}{M_\Lambda}\sin\varphi\,\mathrm{d}\varphi\,,$$

$$\sin\varphi\,\mathrm{d}\varphi = \sin\theta\cos\delta_p\cos\delta_\pi\,\mathrm{d}\theta + (\cos\delta_p\sin\delta_\pi - \cos\theta\cos\delta_\pi\sin\delta_p)\,\mathrm{d}\delta_p +$$

$$+(\cos\delta_\pi\sin\delta_p - \cos\theta\cos\delta_p\sin\delta_\pi)\,\mathrm{d}\delta_\pi\,,$$

where T_p, T_π, δ_p, δ_π are the kinetic energies and the dip angles of the proton and pion respectively, and θ is the plane angle between them.

The sources and magnitude of errors are as follows:

Random errors.

1) Range measurement and straggling: All ranges were determined by two observers independently. It was found that the measurements did not differ by more than 0.5 %. The measurement error in range was taken as 0.5 %.

The straggling error was estimated by using the data of BARKAS and YOUNG [8].

2) Measurement of angles:

a) Projected angles were measured a number of times by the same observer and then by a second observer. The maximum difference in these measurements was 0.3°. So an error of 0.3° was taken.

b) For dip angles the measurements of Δz was found to be consistent within 1 μm. The magnitude of error in dip angles varied from 0.3° to 2.0°. The error in space angles varied from 0.3° to 2.1°.

---

[8] W. H. BARKAS and D. M. YOUNG: UCRL 2549.

Systematic errors.

1) Shrinkage factor: The thicknesses of individual pellicles were determined at a particular location before the exposure. By measuring thicknesses at the same location at the time of measurements the shrinkage factor was evaluated with an accuracy of 1%.

2) Stopping power: The stopping power of the emulsion was determined by measuring the range of 111 flat μ-mesons from $\pi \to \mu \to e$ decay events. The mean range of the μ-meson in our experiment was (597.4 ± 1.7) μm as against (602.2 ± 1.5) μm for standard emulsion. The error in the Λ^0-mass due to this source was evaluated to be 0.07 MeV.

3) Range-energy relation: The kinetic energies were calculated by using the data of BARKAS (9). Taking an uncertainty of 0.5% in Barkas' range-energy relation, the average error was 0.11 MeV, and cannot be reduced by a larger number of events.

4) Error in secondary masses: The mass values of proton and pion used in this work are

$$M_p = (938.213 \pm 0.01)\ \text{MeV}\,,$$

$$M_\pi = (139.63 \pm 0.06)\ \text{MeV}\,.$$

and the errors indicated were used for calculating M_Λ. For Q_Λ consideration of this error is not necessary.

Besides the above mentioned errors, two additional sources of error must be considered: the influence of distortion and the possibility of some undetected inelastic scattering of the secondary pion. Since all the events were situated in a distortion-free region, the effect due to the former source of error should be negligible. This is further demonstrated by the agreement between the internal and external standard deviations. As regards inelastic scattering of pions, only those cases will remain undetected for which the energy loss is $\simeq 2$ MeV. The probability for such an energy loss is very small. However, an event whose mass value is one standard deviation away from the mean changes the mean mass value by only 0.01 MeV.

4. – Results and discussion.

A total of 109 Λ-like events were found out of which in 102 cases both the secondaries came to rest. In the remaining 7 events, in one case the pion suffered inelastic scattering, in two cases it disappeared in flight, in one case

(9) W. H. BARKAS: *Nuovo Cimento*, **8**, 201 (1958).

the pion interacted in flight, while in the remaining 3 cases the pion could not be stopped within the stack. The mass distribution for the 102 events is shown in Fig. 1. The distribution shows that but for one event all others are concentrated in the region 1113.5 MeV to 1117.0 MeV with a pronounced peak at about 1 115.5 MeV. A constant area histogram for the mass of 101 Λ^0-events where the random errors were taken into account is shown in Fig. 2. The weighted mean mass of this distribution is

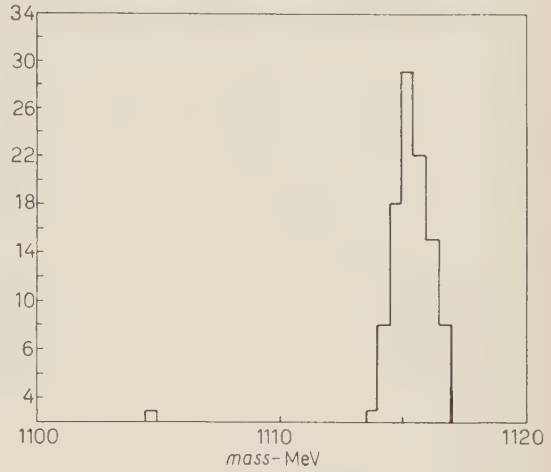

Fig. 1. – Histogram for the mass of 102 Λ-like events.

$$M_\Lambda = (1115.46 \pm 0.06)\ \text{MeV},$$

and

$$Q_\Lambda = (\ 37.62 \pm 0.06)\ \text{MeV}.$$

The error quoted here is only the random error. The external standard deviation of the distribution, 0.72 MeV, is in good agreement with the internal standard deviation, 0.69 MeV, computed from the distribution of events. All the 101 Λ^0-events lie within 2.5 standard deviations from the mean.

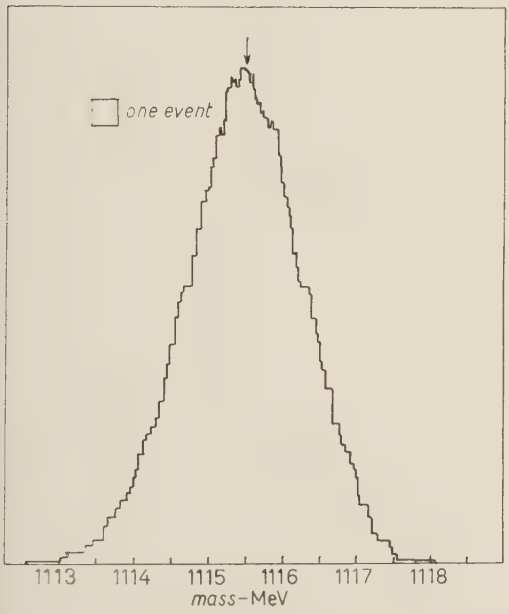

Fig. 2. – Constant area histogram for the mass of 101 Λ^0-events.

The systematic error in the Λ^0-mass was 0.14 MeV which when combined with the random error gives the final error in M_Λ as $= = 0.15$ MeV.

The Q_Λ-values obtained by various emulsion groups using K^--beams is shown in Table I.

A glance at the table shows that in most of the cases the systematic error is greater than the random error. The systematic error from an uncertainty in range-energy relation alone is $\simeq 0.11$ MeV. It may be noted that by combining the world statistics

to date, the random error reduces to 0.04 MeV, while the systematic error remains at 0.12 MeV. Thus, in order to improve further the accuracy in the Λ^0-mass it is necessary to improve the accuracy of the range-energy relation.

TABLE I.

	No. of events	Q_Λ (MeV)	Random error (MeV)	Systematic error (MeV)	Total error (MeV)
BOGDANOWICZ *et al.*	53	37.58	0.08	0.15	0.18
LODGE *et al.*	25	37.71	0.12	0.11	0.16
BARKAS *et al.* (*)	116	37.56	0.07	0.11	0.13
BHOWMIK *et al.*	101	37.62	0.06	0.13	0.14

(*) This includes the previously published data with $Q_\Lambda = (37.45 \pm 0.17)$ MeV see C. J. MASON, UCRL - 9297.

The weighted mean Q_Λ-value from the table given above is

$$(37.60 \pm 0.13) \text{ MeV}.$$

If we take the recent value of the pion mass, $m_\pi = (139.59 \pm 0.05)$ MeV [10] we obtain for the mass of the Λ^0-hyperon

$$M = (1115.42 \pm 0.15) \text{ MeV},$$

while Q_Λ remains at (37.62 ± 0.14) MeV.

* * *

Thanks are due to Dr. E. J. LOFGREN for exposure facilities at the Bevatron and to Prof. D. J. PROWSE for making the exposure. We are grateful to Prof. C. F. POWELL for extending to us the facility of processing the stack at Bristol. One of us (N.K.Y.) thanks C.S.I.R. for the award of a Research

[10] W. H. BARKAS and A. H. ROSENFELD: *Proc. of the 1960 Annual International Conference on High Energy Physics at Rochester* (New York, 1960), p. 878.

fellowship and the M.P. Government for the grant of study leave. This work is financially supported by the Department of Atomic Energy, Government of India. Our indebtedness to the department is gratefully acknowledged.

RIASSUNTO (*)

Abbiamo eseguito un'accurata determinazione della massa del Λ^0, usando emulsioni nucleari. Dall'analisi di 101 decadimenti Λ^0 otteniamo per la massa dell'iperone Λ^0: $M_\Lambda = (1115.46 \pm 0.15)$ MeV e $Q_\Lambda = (37.62 \pm 0.14)$ MeV.

(*) *Traduzione a cura della Redazione.*

IL NUOVO CIMENTO Vol. XXII, N. 2 16 Ottobre 1961

Extraordinary High-Energy Nuclear Interactions of μ-Mesons.

S. Higashi, T. Kitamura, Y. Mishima, S. Miyamoto,
T. Oshio, H. Shibata and Y. Watase

Osaka City University - Osaka

(ricevuto il 12 Luglio 1961)

Summary. — An observation on penetrating showers produced by high-energy μ-mesons was done at 50 m w.e. underground by the use of two large multiplate cloud chambers. In the course of the analysis, we found out one large nuclear shower whose energy transferred from μ-meson seems to be larger than 300 GeV. The occurrence of this event would be very large compared with the conventionally expected one.

Nuclear interactions of μ-mesons have been well interpreted [1] in terms of nuclear interactions of virtual photons associated with the μ-mesons expressed by the Williams-Weizsäcker method. The lowest energies for triggering them so far observed by the use of hodoscoped counters [2] or cloud chamber [3,4] were estimated to be several GeV according to the condition of the triggering and most of their transferred energies were assumed to be less than a few tens of GeV because of the sharply decreasing energy spectrum of μ-mesons below ground and of the associated virtual photons. It is therefore very important to survey the characteristics of nuclear showers of μ-mesons with

[1] For example: G. N. Fowler and A. W. Wolfendale: *Progress in Elementary Particles and Comic Ray Physics*, Vol. **4**, (Amsterdam, 1958) p. 123.

[2] P. E. Argan, A. Gigli and S. Sciuti: *Nuovo Cimento*, **11**, 530 (1954); P. H. Barrett, L. M. Bollinger, G. Cocconi, Y. Eisenberg and K. Greisen: *Rev. Mod. Phys.*, **24**, 133 (1952); S. Higashi, I. Higashino, M. Oda, T. Oshio, H. Shibata, K. Watanabe and Y. Watase: *Journ. Phys. Soc. Japan*, **11**, 1021 (1956).

[3] D. Kessler and R. Maze: *Nuovo Cimento*, **5**, 1540 (1957).

[4] S. Higashi, S. Mitani, T. Oshio, H. Shibata, K. Watanabe and Y. Watase: *Nuovo Cimento*, **13**, 265 (1959).

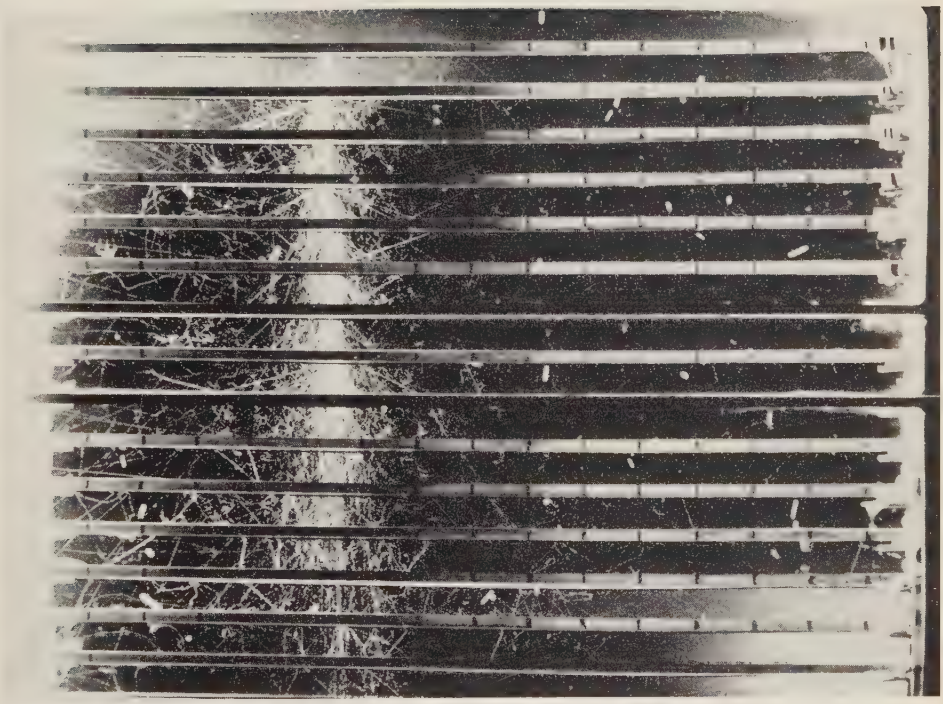

Plate I. – Nuclear interaction produced by a μ-meson in a lead plate. The transferred energy is estimated to be larger than 130 GeV.

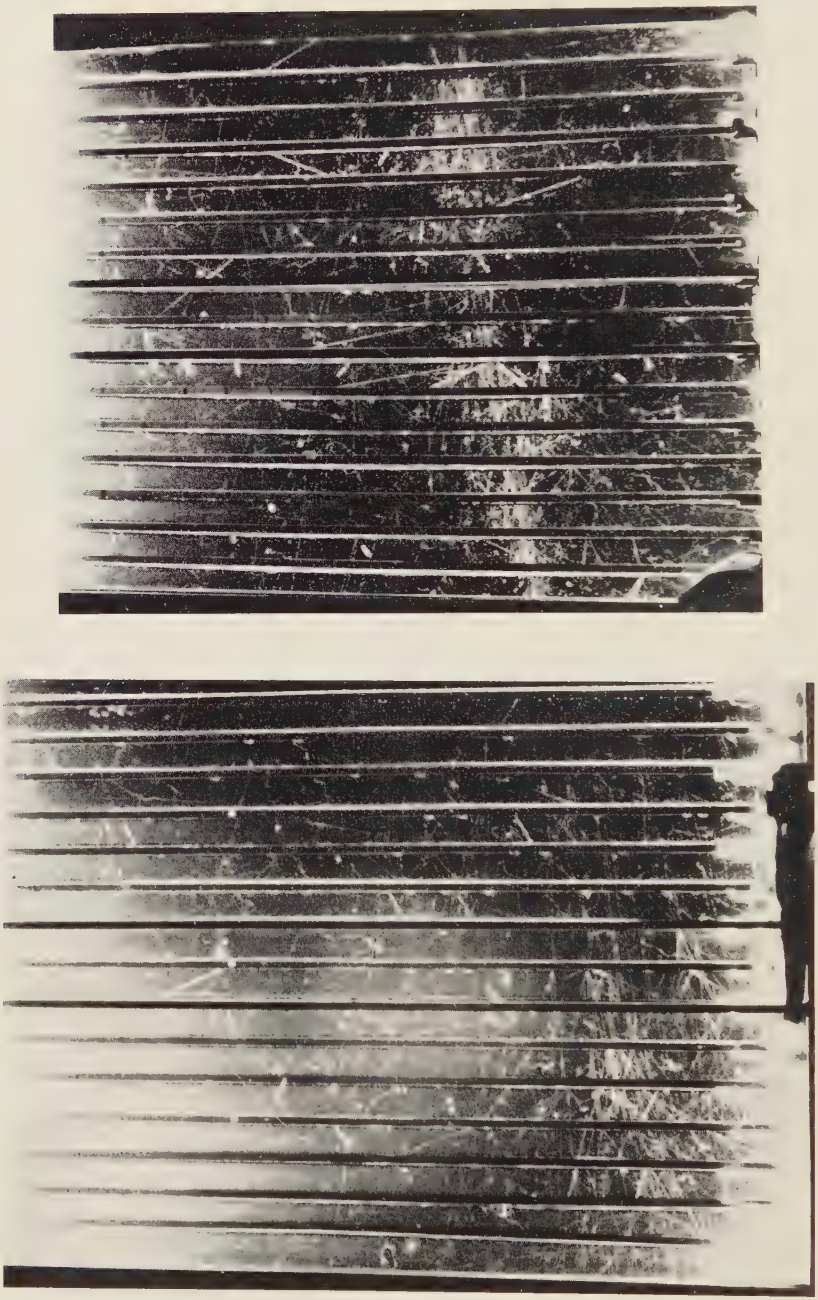

Plate II. – Nuclear interaction occured in the rock over the cloud chamber. The transferred energy is estimated to be larger 300 GeV.

transferred energies of more than hundred GeV. There might be some anomalies in the dynamic property of μ-mesons which would reveal the mass difference between μ-meson and electron.

A large multiplate cloud chamber containing in its effective volume of $(80\times70\times40)$ cm^3 15 lead plates one cm thick and associated hodoscoped counters were operated at a depth of 250 m w.e. underground. In the observing time of 3603.1 hours, 12 nuclear showers occurred in the lead plates of the cloud chamber. Two showers among them were of extremely high energy. (The larger one is shown in Plate I.) Their transferred energies were estimated to be larger than 90 GeV and 130 GeV, respectively, from the size of the cascade showers generated as decay products of secondary π^0-mesons by the use of the track-length method (5) and also, independently, from the angular distribution of secondary penetrating particles. The occurrence of nuclear showers produced by μ-mesons is estimated, the W-W method being used. The photonuclear cross-section was taken as $1.4\cdot10^{-28}$ cm^2/nucleon because SHIBATA (6) showed that the frequencies of the showers are well interpreted with this constant cross-section at various depths down

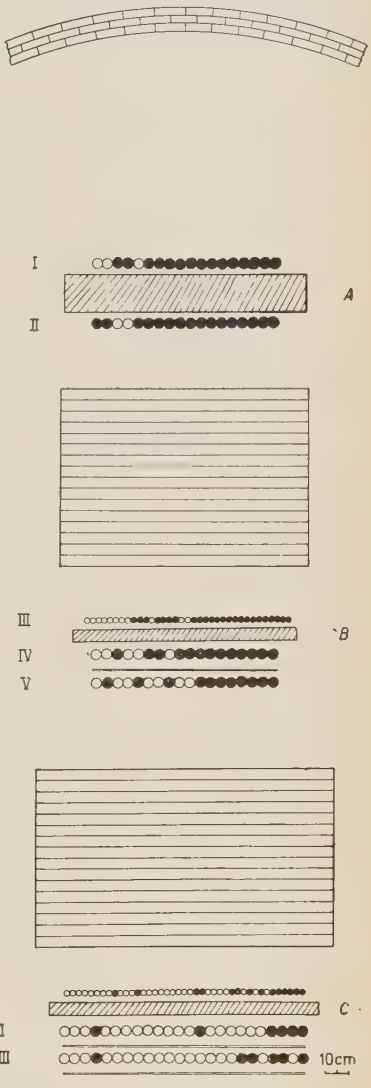

Fig. 1. – Experimental arrangement and the map of discharged counters corresponding to the high energy nuclear interaction which is shown in Plate II (●: discharged counters).

(5) There are some confusions in the literatures about the value by which the track length should be multiplied in order to obtain the visible energy of the cascades. We used the value of 25 MeV per cm of lead according to HINOTANI *et al.* and DANILOVA *et al.* because their value leads to a cascade energy lower than the others do. K. HINOTANI, K. SUGA and T. TANAKA: *Journ. Phys. Soc. Japan*, **9**, 883 (1954) T. V. DANILOVA, O. I. DONZHENKO, S. I. NIKOLSKI and T. V. RAHABOLSKAYA: *Žurn. Éksp. Teor, Fiz.*, **34**, 541 (1958).

(6) H. SHIBATA: *Journ. Phys. Soc. Japan*, **16**, 372 (1961).

to 1600 m w.e. and HIGASHI (7) showed that this value also could apply to the transferred energies up to several tens of GeV. The value of 0.25 was obtained as the expected number of showers with an energy larger than 90 GeV. The possibility that the difference between the estimated 0.25 event and the observed 2 events would occur as the result of statistical chance factors alone is excluded with the significance level of 3%.

For the purpose of making this discrepancy more clear, a further observation was carried out at 50 m w.e. underground. A larger multiplate cloud chamber with an effective volume of $(100 \times 60 \times 70)$ cm^3 containing 15 iron plates one cm thick was set under the previously mentioned one. In the course of the analysis of the observed photographs, we found out one extraordinary high-energy shower for an observing time of 1950 hours, the origin of the shower being assumed to be in the rock over the upper chamber. The experimental arrangement is shown in Fig. 1 together with the discharge map of hodoscoped counters corresponding to the present event and its cloud chamber photographs are shown in Plate II. The number of the secondary penetrating particles and the energies of the electronic cascades observed in this event are listed in the Table. The energy transfer of the nuclear shower was estimated by means of the energies of cascades and the angular distribution of secondary particles. Although various modes of analysis gave values of the energy transfer of this event somewhat different from one another, all the values were within the region of 300 to 600 GeV. The rate of this event is in much better agreement with that of the observed two events in the previous experiment than with that expected from the same method as the previous one (15 cm lead producer +10 cm lead in c.c.+three times collision m.f.p. of rock were used as the producer). It may, thus, be expected that this result is ascribed either to the fact that

TABLE – *The behaviour of the extraordinary high-energy nuclear μ-meson shower.*

	Produced in rock	Produced in lead producer	
	penetrating particles	penetrating particles	cascade showers
Upper-chamber	$\geqslant 2$ their angular spread: 0.07 rad	$\geqslant 8$ their angular spread: 0.7 rad	3 { 1 GeV 8 GeV 13 GeV
Lower-chamber	$\geqslant 5$ their angular spread: 0.1 rad	$\geqslant 10$	a few small ones

(7) S. HIGASHI: to be published.

the photo-nuclear cross-section shows a great increase in the corresponding energy region or that μ-mesons have some unusual behaviour in the interaction with matter at very high energies (say, larger than thousand GeV).

RIASSUNTO (*)

Con l'uso di due grandi camere a nebbia con molte piastre abbiamo eseguito osservazioni sotterranee a 50 m a.e. di due sciami penetranti prodotti da mesoni μ di energia elevata. Nel corso dell'analisi abbiamo trovato un grande sciame nucleare la cui energia trasferita dai mesoni μ sembra maggiore di 300 GeV. La frequenza di questo evento sembrerebbe molto grande in confronto con quella convenzionalmente attesa.

(*) *Traduzione a cura della Redazione.*

IL NUOVO CIMENTO Vol. XXII, N. 2 16 Ottobre 1961

Multiple Scattering Measurements in Nuclear Emulsions Exposed to Momentum-Analysed Particle Beams from the CERN Proton Synchrotron.

A. Hossain (*), M. F. Votruba (**) and A. Wataghin (***)

CERN - Geneva

(ricevuto il 14 Luglio 1961)

Summary. — Results of multiple Coulomb scattering measurements on the tracks of high momentum particles in nuclear emulsion are described. It is shown that the method can be used to give reliable momentum estimates, for particles whose tracks are essentially flat in the emulsion, up to 25 GeV/c. Possible deviations from theoretical multiple Coulomb scattering expectations for high cell-sizes are presented.

1. – Introduction.

The aim of the work was to study the reliability of the multiple scattering method for estimating values of the momentum, p, of high energy particles in nuclear emulsions. One stack of Ilford G-5 pellicles of size 29 cm × 14 cm × 600 μm was exposed to a negative pion beam of momentum (16.2 ± 0.6) GeV/c, while a second stack of size 19 cm × 9.5 cm × 500 μm was exposed to a proton beam of momentum (24.0 ± 0.4) GeV/c. Great care was taken to align the stacks so that the pellicles were accurately horizontal at the time of exposure. In this

(*) On leave from Pakistan Atomic Energy Commission, Ford Foundation Fellow, CERN.

(**) On leave from Physical Institute of Czechoslovak Acad. of Science, Prague; IAEA Fellow, Vienna.

(***) On leave from Centro Brasileiro de Pesquisas Fisicas, Rio de Janeiro, Ford Foundation Fellow, CERN, Geneva.

way the average track length of the primary particles in both stacks was in excess of 15 cm. The microscope used for the measurements was a Koristka type R4 which has an X movement of 10 cm. This feature of the microscope enabled us to take measurements over this length on every particle track that was studied. The emulsions were processed by the usual CERN routine (1).

The specific objects of study were to investigate:

a) the effect of different cut-off procedures and scattering constants on the values of the momentum obtained,

b) the magnitude of spurious scattering effects in the two emulsion stacks, and

c) scattering measurements in the region of very high cell-sizes (from 12 to 24 mm), where the ratio of signal to noise varied from 15 to 40.

2. – Experimental procedure.

A singly charged particle of momentum p and velocity β undergoes multiple Coulomb scattering in a condensed material. It is convenient to express the magnitude of the scattering in terms of the average second difference $\bar{D}_c$ of the y co-ordinate readings taken at regular intervals, t, along the direction of motion of the particle (usually taken as the x axis). The values of $p\beta$ and $\bar{D}_c$ are related by the formula

$$p\beta = \frac{Kt^{\frac{3}{2}}}{\bar{D}_c \cdot 0.57 \cdot 10^3}, \tag{1}$$

where K is the scattering constant for the medium in question, the cell size t is in units of 100 μm, $\bar{D}_c$ is in microns and $p\beta$ is in GeV/c.

Now $\bar{D}_c$ is the average second difference due to Coulomb scattering only. In practice the measured second difference, $\bar{D}_{\text{meas}}$, contains contributions from effects other than those of Coulomb scattering. We have taken the relation suggested by DAHL-JENSEN *et al.* (2), *viz.*

$$\bar{D}^2_{\text{meas}} = \bar{D}^2_c + \bar{D}^2_\varepsilon + \bar{D}^2_\gamma + \bar{D}^2_{ss}, \tag{2}$$

(1) *Report on the Problems of Distortion in Nuclear Emulsions and Spurious Scattering Measurements at High Energies* (Copenhagen, Oct. 1960).

(2) E. DAHL-JENSEN, M. GAILLOUD, W. O. LOCK and G. VANDERHAEGHE (1961), *Il Nuovo Cimento*, in press.

where: $\bar{D}_{\text{meas}}$ = arithmetic mean of the absolute values of measured second differences;

$\bar{D}_c$ = mean second difference due to multiple Coulomb scattering, obtained from the known momentum of the incident particles;

$\bar{D}_\varepsilon$ = mean second difference due to reading, grain noise and the irreproducible part of the stage noise;

$\bar{D}_\gamma$ = mean second difference due to the reproducible part of the stage noise (stage profile); (*)

$\bar{D}_{ss}$ = mean second difference due to spurious scattering.

We also define:

$$\bar{\delta} \equiv \sqrt{\bar{D}_\varepsilon^2 + \bar{D}_\gamma^2} = \text{total noise}, \tag{3}$$

and

$$\bar{D} \equiv \sqrt{\bar{D}_{\text{meas}}^2 - \bar{\delta}^2} = \sqrt{\bar{D}_c^2 + \bar{D}_{ss}^2}. \tag{4}$$

The majority of the experimental results presented in this paper will be given in terms of $\bar{D}$. The statistical errors are given as $\bar{D}/\sqrt{n}$ or $p\beta/\sqrt{n}$, respectively, where n is the number of (independent) measured second differences. To obtain values of momentum, we have used eq. (1), with $\bar{D}_c$ replaced by $\bar{D}$ (see eq. (4) above), and where $\beta = 1$ for the range of momenta we have investigated.

The tracks were aligned so that they stayed within the eyepiece scale (50 μm) over the entire 10 cm movement of the stage. Out of 64 tracks taken in the stack exposed to pions only 3 had to be rejected because they did not fulfil this condition; none of the tracks in the stack exposed in the proton beam had to be rejected. Each track was measured over a distance of 10 cm in a central region of each plate using a Leitz filar eyepiece (12.5×) and a Koristka objective ×55. The filar movement was connected to an automatic device for calculating second differences (**). The co-ordinate method of Fowler [3] was employed. In order to obtain a high signal to noise ratio (> 4), measurements were taken using basic non-overlapping cell-sizes, t, of 4 and 6 mm.

(*) We have assumed that the individual values of D_γ follow a gaussian distribution. This assumption, however, cannot influence our results on account of the high signal to noise ratio.

(**) The construction of this device was initiated by Dr. W. M. Gibson, following the approach of Castagnoli *et al.* (1958), and it was built by Mr. M. A. Roberts in this laboratory [C. Castagnoli, M. Ferro-Luzzi and M. Muchnik: *Nuovo Cimento*, **8**, 936 (1958)].

[3] P. H. Fowler: *Phil. Mag.*, **41**, 169 (1950).

3. – Results.

a) *Noise.* – We have measured the total noise $\bar{\delta}$, using 100 μm cell-size across the whole stage movement. It was found to be ~ 0.2 μm and its dependence on cell-size is shown in Fig. 1. We have also measured the total

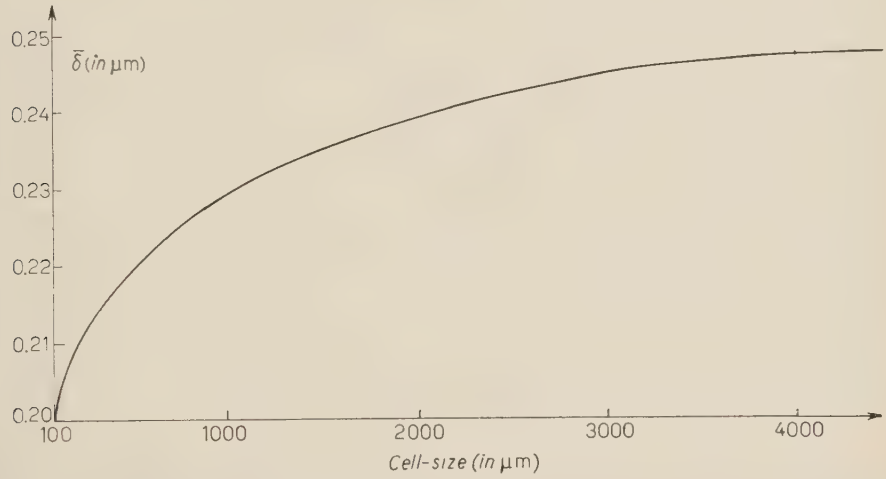

Fig. 1. – Variation of total noise, $\bar{\delta}$, with cell-size for CERN Koristka R4 microscope.

noise with the Boggild and Scharff ([4]) diamond line method. We obtained again the value 0.2 μm, which shows that grain noise is small in relation to stage plus reading noise. The total noise, $\bar{\delta}$, is negligible in comparison with the signal for the range of cell-sizes employed.

b) *Cut-off procedures* (*pion stack*). – In order to study the effect of different cut-off procedures and of the choice of scattering constant, we applied to the experimental data for $t = 4$ mm three different cut-off procedures, with the corresponding three different scattering constants:

i) no cut-off; scattering constant, K, (for $\beta = 1$) given by reference ([5]) and Fig. 2 of this paper;

ii) cut-off at $4\bar{D}_{\text{meas}}$ with replacement; K values 0.8 units less than those of Fig. 2 (according to the recommendation of reference ([5]));

([4]) J. K. Bøggild and M. Scharff: *Suppl. Nuovo Cimento*, **12**, 374 (1954).
([5]) C. F. Powell, P. H. Fowler and D. H. Perkins: *The Study of Elementary Particles by the Photographic Method* (London, 1959), p. 114.

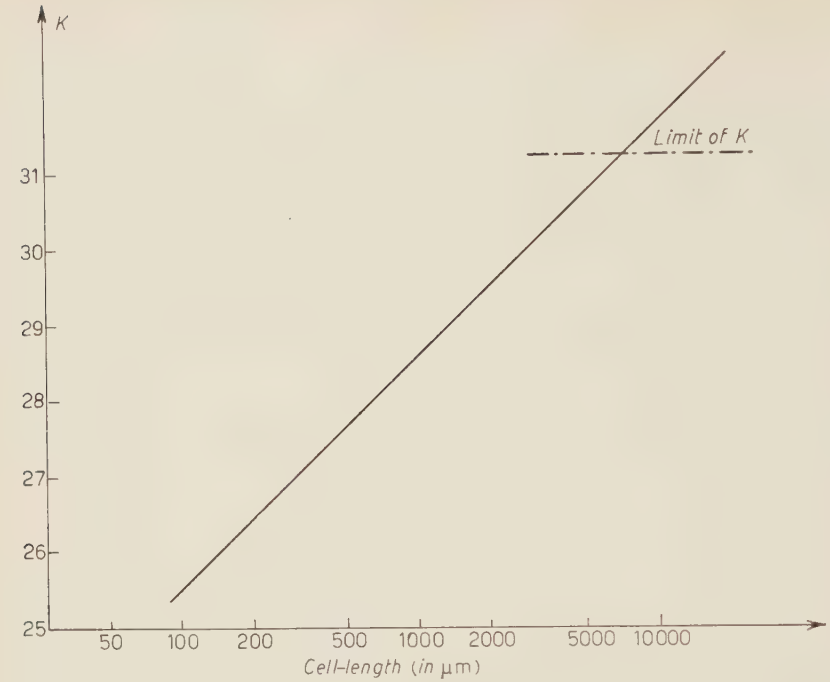

Fig. 2. – Theoretical curve of K (without cut-off) *vs.* cell-size ([5]).

iii) cut-off at $4\bar{D}_{\text{meas}}$ without replacement; K as given by VOYVODIC and PICKUP ([6]).

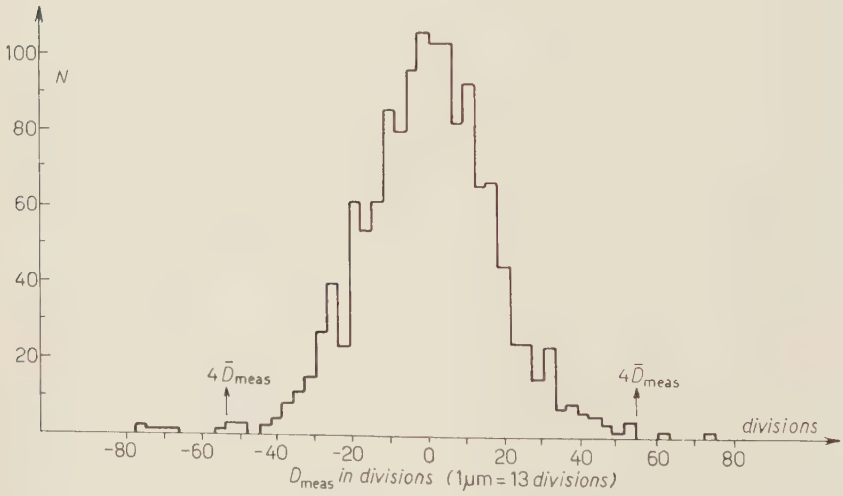

Fig. 3*a*. – Distribution in the values of D_{meas} for cell-size of 4 mm; π^- beam tracks.

([6]) L. VOYVODIC and E. PICKUP: *Phys. Rev.*, **85**, 91 (1952).

The distribution of 1454 values of D_{meas} for $t = 4$ mm is plotted in Fig. 3*a* and 3*b*, which show that the distribution is effectively gaussian. The values

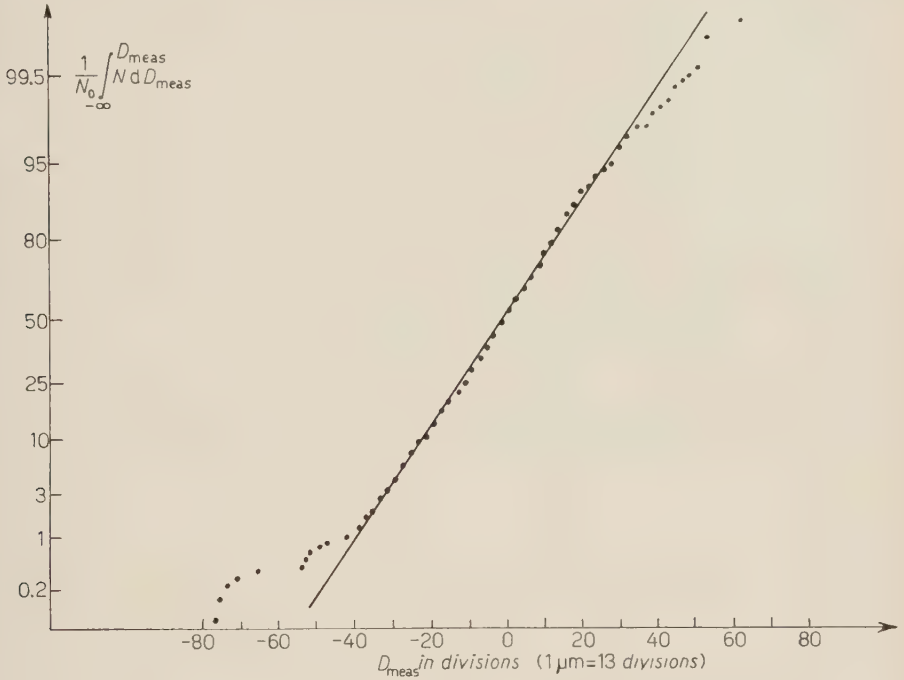

Fig. 3*b*. – Integral plot of $(1/N_0)\int_{-\infty}^{D_{\text{meas}}} N\,dD_{\text{meas}}$ against D_{meas} (4 mm cell) on a Gaussian paper; π^- beam tracks.

of $\bar{D}$ and of $p\beta$ obtained are given in Table I. It can be seen that the three procedures give the same results, within statistical errors, as is expected for a large sample. For the results presented in the remainder of this paper we

TABLE I. – *Values of $p\beta$ for pions of* 16.2 GeV/c *momentum, calculated from measurements taken at* 4 mm *cell-length using three different cut-off procedures, together with the appropriate scattering constants.*

	No cut-off	Cut-off $4\bar{D}_{\text{meas}}$ with replacement	Cut-off $4D_{\text{meas}}$ without replacement
$\bar{D}$ (μm)	0.99±0.03	0.98±0.03	0.96±0.03
K used	30.5	29.7	29.0
$p\beta$ (GeV/c)	13.6 ±0.4	13.4 ±0.4	13.3 ±0.4

have used the no cut-off procedure. The values of $p\beta$ in Table I are lower than the known beam momentum, presumably due to the presence of spurious scattering.

c) Presence of spurious scattering. – The expected magnitude of $\bar{D}_c$ can be calculated from eq. (1). Thus any difference between $\bar{D}_{\text{meas}}$ and $\bar{D}_c$ at 4 mm cell can be attributed to $\bar{D}_{ss}$, using eq. (4).

For the pion stack we find $\bar{D}_{ss} = (0.54 \pm 0.05)$ μm for $t = 4$ mm and $\bar{D}_{ss} = (0 \pm 0.3)$ μm for $t = 8$ mm. The average cotangent of the dip angle for the tracks measured was 600.

For the proton stack $\bar{D}_{ss} = (0.23 \pm 0.1)$ μm for $t = 4$ mm, $\bar{D}_{ss} = (0.185 \pm 0.35)$ μm for $t = 6$ mm and $\bar{D}_{ss} = (0.37 \pm 0.6)$ μm for $t = 8$ mm. For cell-sizes of 6 mm up to 1 cm the signal obtained is much greater than $\bar{D}_{ss}$ so that a good estimate of the momentum of the track measured is obtained.

d) Variation of $\bar{D}$ with cell-size. – As we have a large sample of values of D_{meas} we have investigated the variation of $\bar{D}$ with cell-size. For the pion stack the results are summarized in Fig. 4. In the figure the full line shows

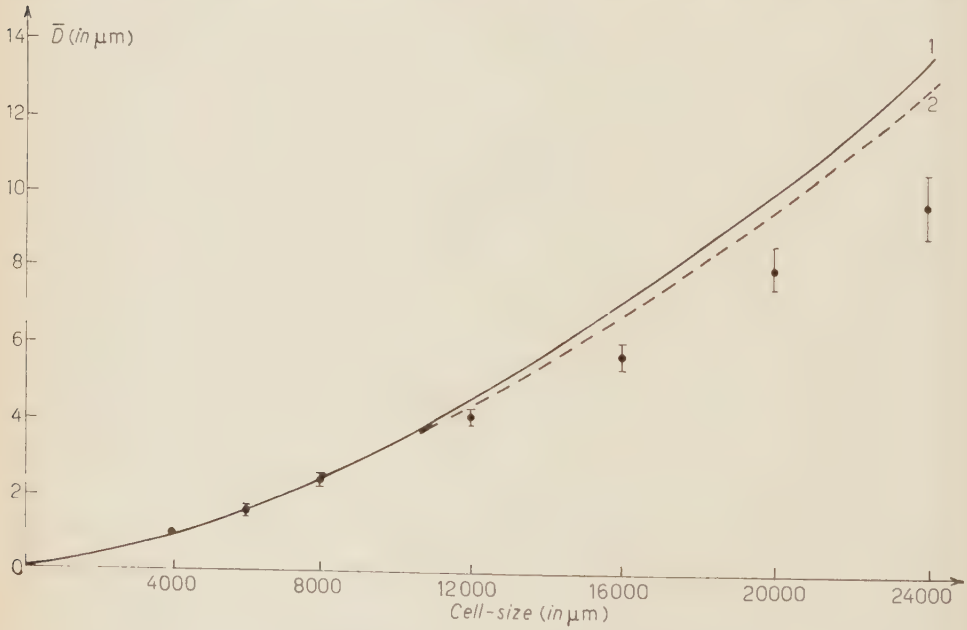

Fig. 4. – Variation of $\bar{D}$ with cell-size: π^- meson tracks. Theoretical curve 1 for $p\beta = 16.2$ GeV/c, using values of scattering constant K according to reference [5]. Curve 2 takes into account the finite size of nucleus as given by [6].

the theoretical variation of $\bar{D}_c$ with t, while the dotted line shows the effect of correcting this curve for the finite size of nucleus [6]. The experimental

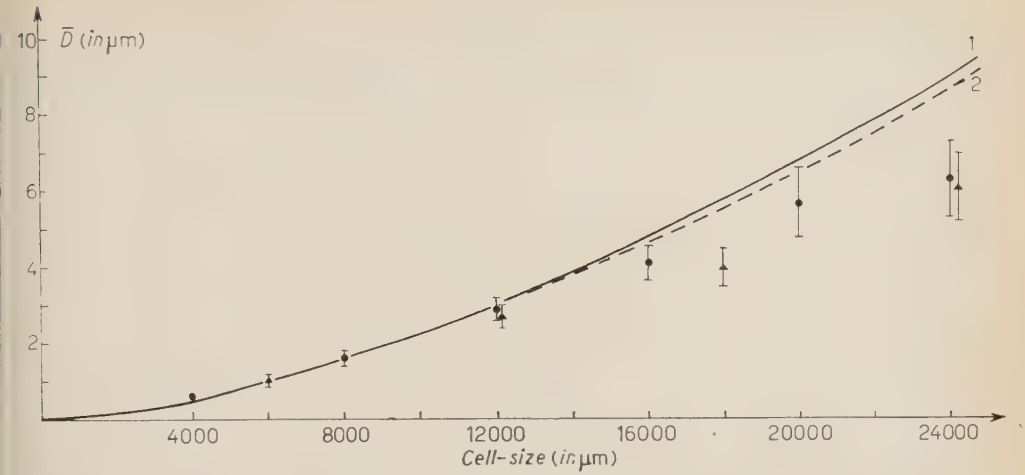

Fig. 5. – Variation of $\bar{D}$ with cell-size; proton tracks. Experimental points: ⊥ for 4 mm basic cell-size; ▲ for 6 mm basic cell-size. Theoretical curves 1, 2 show $\bar{D}_c$ (calculated for $p\beta = 24$ GeV/c) similarly as in Fig. 4.

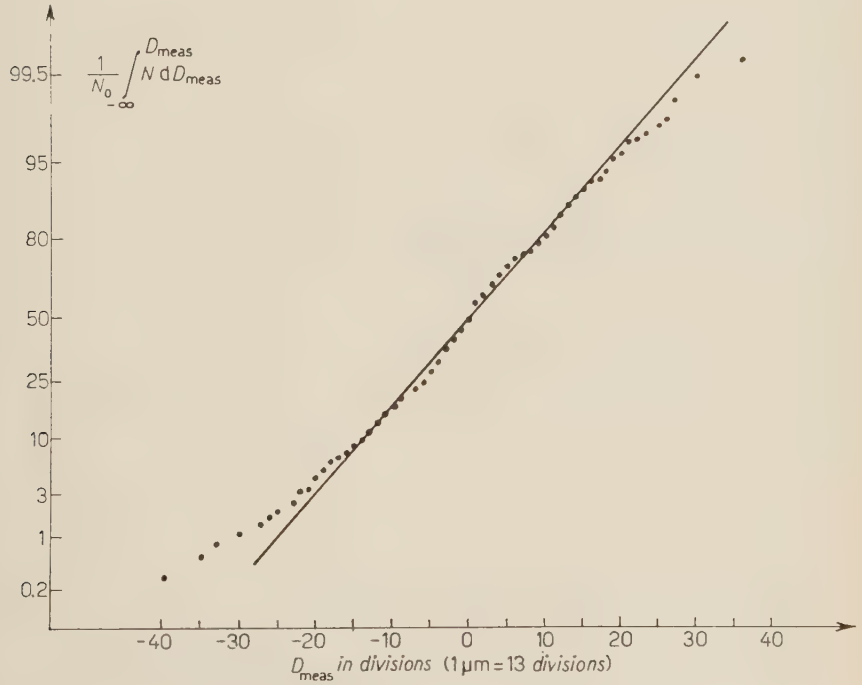

Fig. 6. – Integral plot of $(1/N_0)\int_{-\infty}^{D_{meas}} N\,dD_{meas}$ against D_{meas} for 4 mm cell-size; proton beam tracks.

points seem to fall systematically below the theoretical curves for $t \geq 1$ cm. The same effect was found for the tracks in the proton stack as is shown in Fig. 5. In both cases the distribution of the values of D_{meas} is gaussian (Fig. 6 and 7).

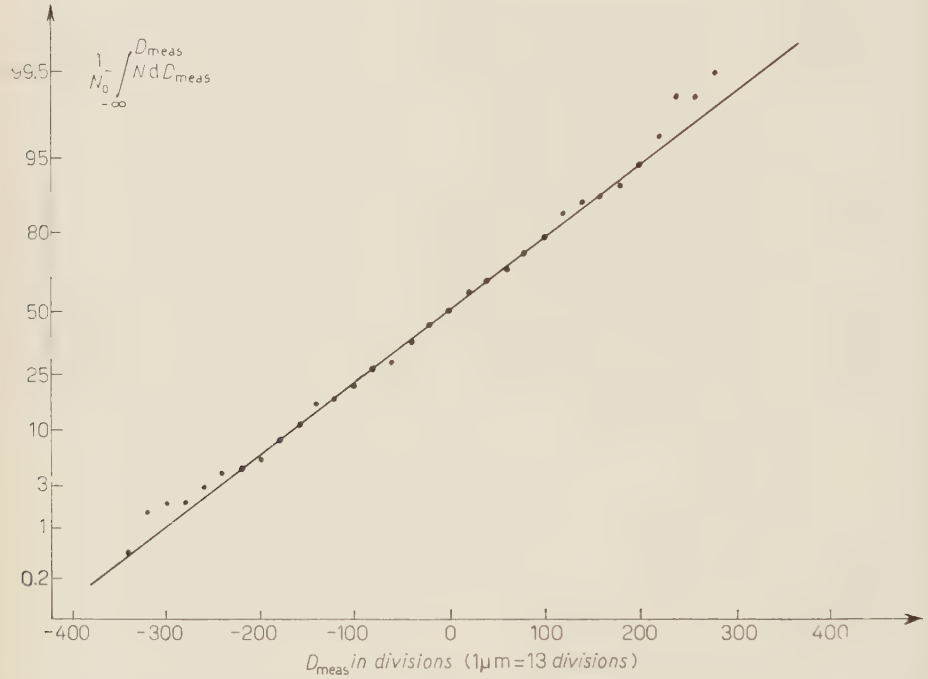

Fig. 7. - Integral plot of $(1/N_0)\int_{-\infty}^{D_{\text{meas}}} N D_{\text{meas}}$ against D_{meas} for 20 mm cell-size; π^- beam tracks.

If further investigation should confirm the result mentioned in this paragraph, some modification of the statistical theory of multiple Coulomb scattering for high cell-sizes ($t \geq 1$ cm) may be necessary.

4. – Conclusions.

1) Spurious scattering effects in the two emulsion stacks investigated are small enough so that for cell-sizes of 6 mm and greater ($p\beta \sim 16$ GeV/c) the contribution to $\overline{D}_{\text{meas}}$ from the true multiple Coulomb scattering is much greater than that from spurious scattering and from noise.

2) For large samples of D_{meas}, the three usual alternatives for cut-off procedure are equivalent.

3) Our experimental data suggest that in the region of cell-sizes greater than 1 cm $\bar{D}$ is smaller that expected theoretically, even with the correction due to the finite size of the nucleus ([6]).

* * *

We wish to thank Dr. W. O. Lock and Dr. J. Combe for their continued interest and support of this work.

We also wish to thank Dr. Lock, Dr. G. Vanderhaeghe and Dr. D. Evans for useful discussions.

Dr. G. Vanderhaeghe, Mr. M. A. Roberts and Mr. R. Sterchi were responsible for the excellent processing.

The exposures were carried out in the beams set up at the CERN Proton synchrotron by the G. Cocconi Group (for the proton beam) and by H. Bingham, B. de Raad and R. G. P. Voss (for the pion beam). We thank them whole-heartedly.

RIASSUNTO (*)

Si descrivono i risultati delle misure dello scattering di Coulomb multiplo eseguite sulle tracce di particelle di elevato impulso in emulsioni nucleari. Si mostra che il metodo può essere usato per avere valutazioni attendibili dell'impulso, per particelle le cui tracce sono sostanzialmente diritte nell'emulsione, sino a 25 GeV/c. Si presentano le possibili deviazioni dalle previsioni teoriche del scattering di Coulomb multiplo per grandi ampiezze di cella.

(*) *Traduzione a cura della Redazione.*

Magnetic Deflection of Positive Ions in Liquid Helium at 0.2 °K (*).

G. Careri (**), F. Duprè (**) and I. Modena (***)

Istituto di Fisica dell'Università - Padova
Istituto Nazionale di Fisica Nucleare - Sezione di Padova

(ricevuto il 22 Luglio 1961)

Summary. — The mobility of positive ions in liquid helium at a temperature of about 0.2 °K has been measured by the magnetic deflection of an ionic beam. The mobilities are surprisingly low, well below the extrapolated values that one would have predicted from the higher temperature behaviour.

1. – Introduction.

So far the mobility of positive ions in liquid Helium II has been measured by various authors with different methods, but all measurements have been confined to the temperature region above 0.6 °K [1-4].

The mobility of an ion in « low » electric fields (that is, when the energy acquired by the ions in the field is negligible compared to kT) is limited by the scattering centers existing in the superfluid « bath », namely the excitations and the ^{3}He impurities. As well-known, these can be treated as a dilute gas, at least at low enough temperatures (see ref. [3]) [5].

(*) This work has been partly supported by the U. S. Army, under Contract P.C.F. 60 199.

(**) Present permanent address: Istituto di Fisica dell'Università, Roma.
(***) Present permanent address: Laboratori Nazionali del CNEN, Frascati (Roma).

[1] R. L. Williams: *Can. Journ. Phys.*, **35**, 134 (1957).
[2] G. Careri, F. Scaramuzzi and J. O. Thomson: *Nuovo Cimento*, **13**, 186 (1959).
[3] F. Reif and L. Meyer: *Phys. Rev.*, **119**, 1164 (1960).
[4] G. Careri, S. Cunsolo and P. Mazzoldi: *Phys. Rev. Lett.*, **7**, 151 (1961).
[5] G. Careri: *Progress in Low Temp. Phys.*, vol. **3** (Amsterdam, 1961), p. 58.

At sufficiently high electric fields, however, the ions should be able to gain enough extra energy and momentum between collisions, and thus create new excitations out of the background fluid. When this process becomes predominant, in the limit of very high fields one would expect that the velocity of the ions might reach a constant value, that is, a « critical velocity » ([3]).

Measurements ([3]) made with « high » electric fields in the region above 0.6 °K cannot give an easy insight into the creation processes of excitations by the ions, as these processes are in competition with the scattering against the pre-existing excitations, which may disturb the creation of new ones. Therefore we have measured the mobility of ions at temperatures of about 0.2 °K, where new excitations may be created, unhindered by the very few still existing in the liquid, so that one may search for the critical velocity arising from such a mechanism.

2. – Method and experimental devices.

For these measurements the magnetic deflection method has been used. This technique was first employed by TOWNSEND in 1913 to measure the mobility in gases, and was afterwards refined by several authors ([6]). Our apparatus is quite similar to that used for gases by HUXLEY and ZAAZOU ([7]).

The principle is quite simple: when a small ion beam, accelerated by an electric field, goes through a magnetic field at right angles to the electric one, it is deflected by the Lorenz force, and its path is a straight line which forms an angle ϑ with the direction of the electric field; one can easily derive how $\operatorname{tg}\vartheta$ is related to μ, the mobility expressed in $\mathrm{cm^2/V \cdot s}$, and B, the magnetic field expressed in gauss, being

$$\operatorname{tg}\theta = \frac{\mu B}{10^8}. \tag{1}$$

(The derivation is identical to that for the Hall angle.)

One should notice that this expression is independent of E, the electric field. Having a magnetic field of the order of $\sim 10^4$ gauss, it is therefore possible to measure with this method mobilities

$$\mu \gtrsim 10^2 \ \mathrm{cm^2/V\ s}.$$

([6]) An extensive bibliography can be found on LOEB: *Basic Processes of Gaseous Electronics* (1955), p. 180 (9).

([7]) L. H. G. HUXLEY and A. A. ZAAZOU: *Proc. Roy. Soc.*, A **196**, 402 (1949).

In order to be sure that the electric field is uniform, a cylindrical geometry with a guard ring has been used (Fig. 1). The receiving electrodes can be connected in pairs, in order to obtain (see Fig. 1*a*):

A) connecting *C*-*C* and *M*-*M*, a circular electrode surrounded by a ring electrode,

B) connecting *C*-*M*, *C*-*M* two symmetric semicircular electrodes.

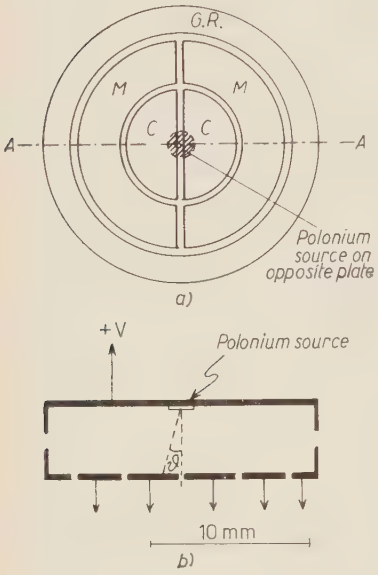

Fig. 1. – Schematic wiew of the deflection cell: *a*) top view; *b*) side view.

In position *A*) one can measure the ratio of the currents received by the central and by the ring electrode, giving a measure of the spreading of the beam. The position *B*) instead shows the deflection of the beam, permitting the measurement of the ratio of the currents on the two halves into which the receiving surface is divided. A fifth receiving electrode is a guard ring, which is needed to obtain a uniform electric field, and serves also to control that the beam does not suffer too much spreading or deflection. The gaps between the electrodes are 0.2 mm, and give rise to no distorsion of the field.

The ions are obtained by α-ionization, caused by a small circular ^{210}Po source, 1.5 mm in diameter (α-particles have a range < 0.3 mm in liquid helium).

Both emitting electrode and receiving guard ring extend with a short cylinder (see fig. 1*b*) in order that the source and the ions may not « see » the plexiglass wall, so avoiding charge collection and polarization effects which would disturb the electric field. All electrodes are in silver, supported on plexiglass. The whole is enclosed in a vacuum-tight brass cylinder, from which the wires come out through araldite seals.

A copper tube serves to fill the system with helium, and to make a good thermal contact with the paramagnetic salt cylinder, which contains 23 g of iron-metyl-ammonium-sulphate ([8]), soaked with tholuene to make a good thermal contact. Having a heat leak of about 70 erg/s, we could stay for about 1 hour between 0.2 and 0.3 °K.

([8]) Studied by A. H. COOKE, H. MEYER and W. P. WOLF: *Proc. Roy. Soc.*, A **237**, 404 (1956).

Five insulated leads were brought out of the Dewar corresponding to the five electrodes (besides one for the application of voltage to the disk with the source, and three others for the temperature measurements). An external switch allowed us to make the two alternative connections already described. Currents where then measured by three vibrating reed electrometers and recorded.

The same magnet was first used to perform the demagnetization on the salt, and afterwards to deflect the beam of ions in the cell, while the salt was protected by a magnetic shield mounted outside the Dewars.

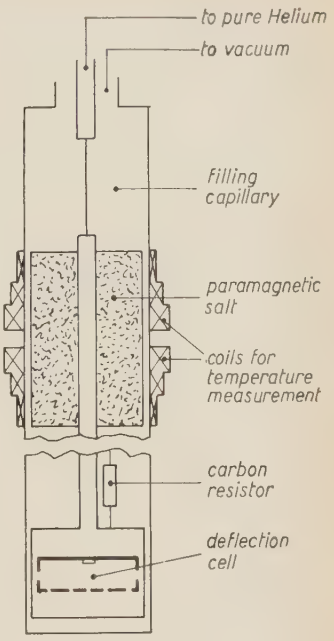

Fig. 2. – Schematic drawing of the low-temperature part of the cryostat. The magnetic field is perpendicular to the paper.

3. – Analysis of data.

Unfortunately the surface of the source was not quite clean and perfectly conducting, and this gave rise to a fairly large spreading of the beam, due to charge collection, especially at low electric fields (see Appendix).

In order to find $\operatorname{tg}\vartheta$ from the current measurements made in position B) one has to know the current density distribution on the receiving electrode. We make the *a priori* assumption, that this distribution is a two parameter Gaussian:

$$i = H \exp\left[-\left(\frac{r}{r_0}\right)^2\right],$$

where i = current density,

r = distance from the central axis,

H, r_0 = parameters to be determined by the measurements with A) connections.

Several controls showed that this assumption seems fairly consistent, but it is evidently a weak point in the analysis.

The errors given for the single points on Fig. 3 have been simply calculated from the sensitivity of our apparatus; they should therefore be maximum errors. But all the data suffer from the systematic error introduced by the already described assumption, the error of which is difficult to evaluate, even if it seems reasonable to think it should not be large (less than 30 %, see Appendix).

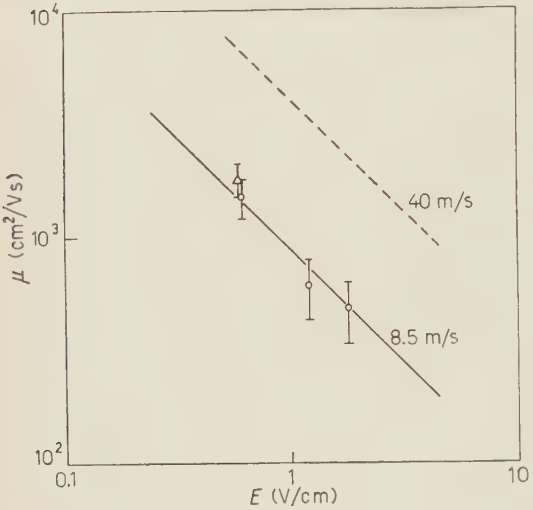

Fig. 3. – Graph of the results. All points have been measured with a B of 17 kG. The point marked with a triangle has been obtained with a reversed magnetic field. The dotted line is the limiting velocity as quoted by Reif and Meyer. (ref. 3).

4. – Results.

On Fig. 3 we report only the results of one good experiment, obtained deflecting the beam in a magnetic field of 17 kG. Other experiments, giving measurements which are consistent with these, but which have larger errors, are not reported. Especially some values measured applying a low magnetic field (~ 4 kG) show a very good agreement with these (but have obviously a much larger error), indicating that the mobility is insensitive to the magnetic field, in this field range. The point marked with a triangle has been obtained applying a reversed magnetic field. It may furthermore be noticed that the total current underwent no appreciable variation when the magnetic field was turned on. The temperature was approximately 0.2 °K, slowly rising at a rate of 0.002 °K/min.

The rather large errors are due to the fact that the apparatus is almost at the limit of its sensitivity, having been planned for much higher values of μ, which unexpectedly could not be reached. For this reason we felt it inconvenient to push further the measurements with this apparatus.

5. – Discussion.

We note that our mobilities are well below the values Meyer and Reif measured at « low » fields at about 0.5 °K [9]. Moreover a reasonable extra-

[9] L. Meyer and F. Reif: *Phys. Rev. Lett.*, **5**, 1 (1960).

polation after their line of reasoning (which considers as the only scattering agents at these temperatures the phonons and the ^{3}He impurity), gives a $\mu \sim 1.3 \cdot 10^5$ cm^2/V s at 0.2 °K.

The low values we find for the mobility are quite understandable, because at our temperature, due to the scarcity of scattering centers, (*i.e.* the long mean free path of the ions), the electric fields we have used are certainly « high ». That this is so can also be seen from the experimental fact that the mobility depends strongly on the field. Therefore our results should be compared with the behaviour found by MEYER and REIF at « high » fields ([3]). They report, in this case, a limiting velocity of about 40 m/s, which is of the order of magnitude predicted by LANDAU for the creation of rotons. Our results are similar in that we find a constant drift velocity; however, in our case, the value is 8.5 m/s, which seems to call for some different creation process, of lower energy.

The possibility of creation of vortical rings of atomic size suggests itself, because some unpublished calculations by VINEN ([10]) indicate 7.5 m/s as the most likely critical velocity for creation of these lines from the superfluid. On the other hand the scarcity of our data, and the approximations made, make it premature to draw such a conclusion. Anyhow our unexpected results call attention to the problem of ionic motion in superfluid helium at such low temperatures, and show that at the present we are still far from any satisfactory understanding of the processes.

* * *

Thanks are due to E. MENDOZA, for helpful advice and assistance in setting up the technique of adiabatic cooling.

APPENDIX

The weakest point in our measurements is given by an unexpectedly large spreading of the beam, not justified either by space charge repulsion or by diffusion.

We think it due to a charge collection on the not perfectly clean surface of the source, which gives rise to a local distorsion of the electric field. This supposition suggests by itself, as on different runs, with the source in different conditions of polishing, we obtained various spreadings. But we were not able to calculate it, in order to deduce what the current density distribution would be on the receiving electrodes. Therefore we had to postulate a distribution, which we took to be « gaussian », and verified that it satisfied fairly well the experimental data.

([10]) W. F. VINEN: *Progress in Low Temp. Phys.*, vol. 3 (Amsterdam, 1961), p. 40.

Of course the whole holds only if the distribution is cilindrically symmetrical. This seems to be confirmed by measurements made with reversed magnetic field (= reversed deflection), which fairly agree with the other ones.

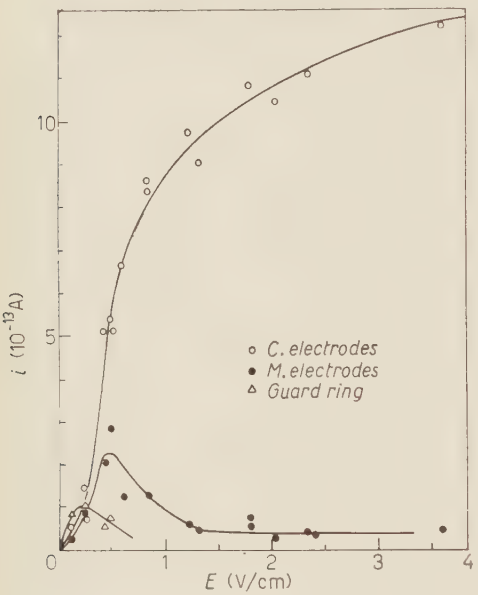

Fig. 4. – A typical plot of i *vs.* E on the three separate electrodes when they are connected in circular symmetry (A-connection).

On Fig. 4 we show one typical curve in the A-connection; from curves of this kind, at every value of the voltage, the two parameters H and r_0 of the gaussian were calculated, with the two conditions,

$$\int_0^\infty i\,\mathrm{d}r - I_C + I_M \frac{\int_0^{r_c} i\,\mathrm{d}r}{\int_{r_c}^\infty i\,\mathrm{d}r} = \frac{I_C}{I_M},$$

I_C = current on the C-electrodes;

I_M = current on the M-electrodes;

r_c = radius of the first gap.

Once the spreading of the impinging beam (depending only on r_0) is known, it is possible to deduce the displacement d of the center of the beam, relative to the central slit, measuring the ratio R of the currents to the two halves of the apparatus, while connected in the B-position. On Fig. 5 we report the curve used for this, which has been calculated solving the appropriate geometrical problem. Then $\mathrm{tg}\,\vartheta = d/h$, where h is the distance of the receiving plane from the source.

Anyhow, while the assumption of a « gaussian » distribution (which was chosen only because it was physically reasonable and mathematically easy to handle), is a weakness in the cal-

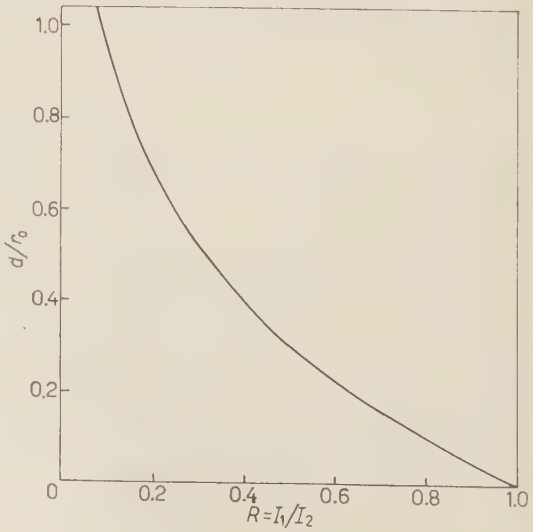

Fig. 5. – Calculated curve to obtain the deflection d of the beam, knowing the ratio R of the currents on the two halves of the receiver, and the spreading r_0 of the beam. A « gaussian » distribution for the current density has been assumed.

culation of mobility, it may be shown that the values for the mobility depend but little upon the exact form chosen.

If we take, for example, a cone shaped current density distribution

$$i = A(r - r_0)\,, \qquad r < r_0,$$

$$i = 0\,, \qquad r > r_0,$$

the new values one calculates coincide, within the experimental errors, with those obtained using the gaussian distribution.

Thus, even if we are left with an uncertainty in the absolute value of μ, we can estimate that it will surely not exceed 30 % of the value, which leaves unaffected the conclusions drawn before in the discussion.

RIASSUNTO

Si è misurata la mobilità degli ioni positivi nell'elio liquido a una temperatura di circa 0.2 K, per mezzo della deflessione magnetica di un fascetto di ioni. Le mobilità sono inaspettatamente basse, rispetto a quelle che ci si era atteso da una ragionevole estrapolazione dei valori noti a temperature più alte.

IL NUOVO CIMENTO Vol. XXII, N. 2 16 Ottobre 1961

Analytic Properties of Off-Energy Shell Potential Scattering Amplitudes.

D. I. Fivel (*) (**)

University of Pennsylvania - Philadelphia, Penna.

(ricevuto il 27 Luglio 1961)

Summary. — A proof is given that a double dispersion relation in the momentum transfer and outgoing energy holds for off-energy shell scattering by a Yukawa potential in which the incoming energy is held fixed and real. It is shown that unitarity then determines the off-shell in terms of the on-shell amplitude. The analytic properties of the off-shell amplitude on unphysical Riemann sheets are described and some results on the domain of holomorphy in both energy variables are also included.

1. – Introduction.

The purpose of this paper is to investigate the question of the equivalence of the Mandelstam representation and the Schrödinger equation for Yukawa potentials. It was shown by Blankenbecler *et al.* [1] that the Mandelstam representation plus unitarity provides an iterative scheme for calculation of the scattering amplitude from the first Born approximation. The question then naturally arises as to whether one can obtain the wave function itself or equivalently the off-energy shell scattering amplitude in a similar fashion. It would in fact be very useful if one could employ the dispersion relations to compute off-shell amplitudes from phenomenologically or theoretically given on-shell amplitudes.

(*) Supported in part by the U. S. Atomic Energy Commission.

(**) Address as of September 1, 1961: Laboratorio Sincrotrone - Frascati (Roma).

(1) R. Blankenbecler, M. L. Goldberger, M. N. Khuri and S. B. Treiman: *Ann. of Phys.*, **10**, 62 (1960).

To establish the desired connection between on- and off-shell amplitudes it is only necessary to show that when one of the energies involved in the off-shell scattering is fixed and real, a double dispersion relation in the energy and the momentum transfer is obeyed. The unitarity condition will then yield a linear integral equation for determination of the off-shell amplitude with the on-shell amplitude as the kernel. The proof of the double dispersion relation is divided into a proof of analyticity in the energy for restricted momentum transfer and a proof of analyticity in the momentum transfer for positive energy. The first proof, which is taken up in Section **3**, consists of obvious generalizations of the proof in ref. [2] for the on-shell case and is included merely for completeness. The second proof, given in Section **4**, is based on the method of complex angular momenta introduced by REGGE [3]. For this proof it was necessary to modify some of the techniques of ref. [3] due principally to the failure of the WKB method in the off-shell case.

The use of the unitarity condition in obtaining the off-shell amplitude iteratively is discussed in Section **5** using the conical wave formalism discussed in ref [4].

In Section **6** we discuss the analytic properties of off-shell amplitudes on unphysical Riemann sheets and in the second energy variable. Part of the domain of holomorphy in the second energy variable is obtained rigorously and a possible method of extending this result is suggested. The complete domain of holomorphy in both energies of the off-shell partial wave amplitudes is also included.

2. – Notation.

We write the Schrödinger equation

$$(1) \qquad \left(\nabla^2 + k^2 - \Lambda V(r)\right)\psi(\boldsymbol{r}) = 0$$

for energy k^2 and study the usual scattering solution

$$(2) \qquad \psi(\boldsymbol{r}; k, \Lambda) = \exp\left[i\boldsymbol{k}\cdot\boldsymbol{r}\right] + \Lambda\int G_0(\boldsymbol{r}, \boldsymbol{r}', k)\, V(r')\,\psi(\boldsymbol{r}', k, \Lambda)\,\mathrm{d}^3 r',$$

(2) A. KLEIN and C. ZEMACH: *Ann. of Phys.*, **7**, 440 (1959).
(3) T. REGGE: *Nuovo Cimento*, **14**, 951 (1959).
(4) D. FIVEL: *New formulation of dispersion relations, etc.*, to be published.

with the unperturbed Green's function

$$G_0(\boldsymbol{r}, \boldsymbol{r}', k) = -(4\pi|\boldsymbol{r}-\boldsymbol{r}'|)^{-1}\exp[ik|\boldsymbol{r}-\boldsymbol{r}'|]\,. \tag{3}$$

The scattering amplitude for incoming wave $\boldsymbol{k}'$ and outgoing wave $\boldsymbol{k}$ is

$$F(k, k', \Delta) = -(4\pi)^{-1}\Delta\int\exp[-i\boldsymbol{k}'\cdot\boldsymbol{r}]\,V(r)\,\psi(\boldsymbol{r};\,\boldsymbol{k}, \Delta)\,\mathrm{d}^3r = \tag{4}$$

$$= u(\Delta) - (4\pi)^{-1}\Delta^2\int\exp[-\tfrac{1}{2}\boldsymbol{\Delta}\cdot(\boldsymbol{r}+\boldsymbol{r}')]\cdot$$

$$\cdot\exp[iB\boldsymbol{n}\cdot(\boldsymbol{r}-\boldsymbol{r}')]\,V(r')\,G(\boldsymbol{r}', \boldsymbol{r}, k)\,V(r)\,\mathrm{d}^3r\,\mathrm{d}^3r',$$

where

$$\boldsymbol{\Delta} = \boldsymbol{k}'-\boldsymbol{k}\,; \qquad \boldsymbol{B} = \tfrac{1}{2}(\boldsymbol{k}'-\boldsymbol{k}) = B\boldsymbol{n} = \left(\frac{k^2+k'^2}{2} - \frac{\Delta^2}{4}\right)^{\frac{1}{2}}\boldsymbol{n}\,; \tag{5}$$

and $G(\boldsymbol{r}', \boldsymbol{r}, k)$ is the exact Green's function satisfying

$$G(\boldsymbol{r}', \boldsymbol{r}, k) = G_0(\boldsymbol{r}', \boldsymbol{r}, k) + \Delta\int G_0(\boldsymbol{r}', \boldsymbol{r}'', k)\,V(r'')\,G(\boldsymbol{r}'', \boldsymbol{r}, k)\,\mathrm{d}^3r'', \tag{6}$$

and $u(\Delta)$ is the Born approximation

$$u(\Delta) = -(4\pi)^{-1}\Delta\int\exp[-i\boldsymbol{\Delta}\cdot\boldsymbol{r}]\,V(r)\,\mathrm{d}^3r\,. \tag{7}$$

The scattering amplitude on the energy shell is characterized by $\boldsymbol{k} = \boldsymbol{k}'$ or $\boldsymbol{n}\cdot\boldsymbol{\Delta} = 0$ and is written

$$F(k, \Delta) \equiv F(k, k, \Delta)\,. \tag{8}$$

From time-reversal invariance and the hermiticity of the Hamiltonian it follows that

$$G(\boldsymbol{r}, \boldsymbol{r}', k) = G(\boldsymbol{r}', \boldsymbol{r}, k)\,. \tag{9}$$

This together with space reflection invariance implies that eq. (4) may be written

$$F(k, k', \Delta) = u(\Delta) - (4\pi)^{-1}\Delta^2\int\cos[\tfrac{1}{2}\boldsymbol{\Delta}\cdot(\boldsymbol{r}+\boldsymbol{r}')]\cdot \tag{10}$$

$$\cdot\cos\left[\left(\frac{k^2+k'^2}{2} - \frac{\Delta^2}{4}\right)^{\frac{1}{2}}\boldsymbol{n}\cdot(\boldsymbol{r}-\boldsymbol{r}')\right]V(r')\,G(\boldsymbol{r}', \boldsymbol{r}, k)\,V(r)\,\mathrm{d}^3r\,\mathrm{d}^3r'\,.$$

A consequence of the several invariance properties is thus that the apparent branch cuts due to the square roots are absent in view of the evenness of the cosine.

While the conclusions obtained in this work will be valid for arbitrary superpositions of Yukawa potentials, it is convenient to assume that $V(r)$ has the simple Yukawa form with range μ^{-1}

$$V(r) = r^{-1} \exp[-\mu r] . \tag{11}$$

3. – Analyticity in k.

Following ref. (2) we prove the following

Theorem 1. – For Δ, k' fixed and real and $|\Delta| < 2\mu$:

a) $F(k, k', \Delta)$ is analytic in k in $\operatorname{Im} k > 0$ except for a finite set of poles on $\operatorname{Re} k = 0$ corresponding to the bound states;

b) $F(k, k', \Delta) \to u(\Delta)$, $|k| \to \infty$ in any manner in $\operatorname{Im} k \geqslant 0$.

We define

$$4\pi \langle \boldsymbol{r}' | T(k, k', \Delta) | \boldsymbol{r} \rangle = \tag{12}$$

$$= -\Delta^2 \cos[\tfrac{1}{2} \Delta \cdot (\boldsymbol{r} + \boldsymbol{r}')] \cos[B \cdot \boldsymbol{n}(\boldsymbol{r} - \boldsymbol{r}')] V(r') G(\boldsymbol{r}', \boldsymbol{r}, k) V(r),$$

whence

$$F_1(k, k', \Delta) \equiv F(k, k', \Delta) - u(\Delta) = \iint \langle \boldsymbol{r}' | T(k, k', \Delta) | \boldsymbol{r} \rangle \, \mathrm{d}^3 r \, \mathrm{d}^3 r' . \tag{13}$$

Since $G(\boldsymbol{r}', \boldsymbol{r}, k)$ is the resolvent of the self-adjoint Hamiltonian, by Stone's theorem it is analytic in k except on the spectrum, *i.e.* at the points $k = iK_i$, $K_i > 0$ corresponding to the bound state energies $E_i = -K_i^2$. For potentials of the assumed type these are finite in number. If in fact we decompose the Green's function into bound state and continuum parts:

$$G(\boldsymbol{r}', \boldsymbol{r}, k) = G_B(\boldsymbol{r}', \boldsymbol{r}, k) + G_c(\boldsymbol{r}', \boldsymbol{r}, k) . \tag{14}$$

Then the contribution of the spectrum may be made explicit by writing G_B in the bilinear form:

$$G_B(\boldsymbol{r}', \boldsymbol{r}, k) = \sum_{i=1}^{N} \frac{\psi_i(\boldsymbol{r}) \psi_i(\boldsymbol{r}')}{k^2 + K_i^2} . \tag{15}$$

The bound state wave functions $\psi_i(\boldsymbol{r})$ have the form

$$\psi_i(\boldsymbol{r}) = \psi_i(r)\, Y_{l_i}(\theta, \varphi); \qquad \psi_i(\boldsymbol{r}) \to \exp[-K_i r], \qquad r \to \infty \tag{16}$$

where l_i is the angular momentum of the i-th bound state.

The above considerations permit us to apply Cauchy's theorem to $\langle \boldsymbol{r}' | T(k, k', \Delta) | \boldsymbol{r} \rangle$ which we do for contour Γ consisting of that part of the real k axis and a semi-circle bounding the region $|k| < C$; $C > \max_i K_i$; $\operatorname{Im} k > 0$. Integrating both sides of the resulting equation with respect to r and r' and introducing (13) one obtains

$$F_1(k, k', \Delta) = \sum_{i=1}^{N} \frac{R_i(k', \Delta)}{k^2 + K_i^2} + \frac{1}{\pi i} \iint \mathrm{d}^3 r\, \mathrm{d}^3 r' \int \frac{k''\, \mathrm{d}k'' \langle \boldsymbol{r}' | T(k'', k', \Delta) | \boldsymbol{r} \rangle}{k''^2 - k^2}, \tag{17}$$

where

$$R_i(k', \Delta) = -(4\pi)^{-1} \Delta^2 \iint \cos[\tfrac{1}{2}\boldsymbol{\Delta} \cdot (\boldsymbol{r} + \boldsymbol{r}')] \cos[B\boldsymbol{n} \cdot (\boldsymbol{r} - \boldsymbol{r}')] \cdot \cdot V(r')\, V(r)\, \psi_i(r')\, \psi_i(r)\, \mathrm{d}^3 r'\, \mathrm{d}^3 r\,. \tag{18}$$

For real k' the imaginary part of

$$B \equiv \left(\frac{k'^2 - K_i^2}{2} - \frac{\Delta^2}{4} \right)^{\frac{1}{2}},$$

is majorized by $K_i + \Delta/2$. The assumption $|\Delta| < 2\mu$ and the asymptotic form of $\psi_i(\boldsymbol{r})$ (eq. 16) then insure the convergence of (18). Thus $R_i(k', \Delta)$ is bounded and in fact uniformly in k'.

Next we must show that it is permissible to exchange orders of integration in (17) when the constant C defining Γ is permitted to become infinite. To do so it suffices to establish the convergence of (13) when k lies on any finite part of Γ (*i.e.* k real and bounded) and the uniform convergence of (13) with respect to k on the infinite portions of Γ.

For k real and bounded the existence of (13) is insured by the existence of the scattering amplitude only in the physical region $\Delta^2/4 \leqslant (k^2 - k'^2)/2$. That (13) converges for all real k can be established under the assumption $|\Delta| < 2\mu$. Thus from eqs. (3), (5) it is evident that for potentials of the Yukawa type, the Born series solution for $G(\boldsymbol{r}', \boldsymbol{r}, k)$ converges to $G_0(\boldsymbol{r}', \boldsymbol{r}, k)$ when either r or r' are sufficiently large compared to the range of the potential and k is an arbitrary real number. Examination of (12) then shows that $V(r)V(r')$ provide sufficient damping for convergence if $|\Delta| < 2\mu$.

For k on the unbounded portions of Γ we use the result of ref (²), namely:

$$|G(\boldsymbol{r}', \boldsymbol{r}, k) - G_0(\boldsymbol{r}', \boldsymbol{r}, k)| \leqslant \delta(k)\, |\boldsymbol{r}' - \boldsymbol{r}|^{-1} \exp[-\operatorname{Im} k\, |\boldsymbol{r}' - \boldsymbol{r}|] \tag{19}$$

where $\delta(k) \to 0$ as $|k| \to \infty$ in any manner in $\operatorname{Im} k \geqslant 0$.

Now when $|k| \to \infty$ it is clear that the divergence produced by

$$\cos\left(\left(\frac{k^2 + k'^2}{2} - \frac{\Delta^2}{4}\right)^{\frac{1}{2}} \boldsymbol{n} \cdot (\boldsymbol{r} - \boldsymbol{r}')\right),$$

is determined by $\operatorname{Im} k/\sqrt{2}$. However, from (3) and (19) we see that in $\operatorname{Im} k \geqslant 0$ the Green's function factors must compensate. In fact if $|k| \to \infty$ on any ray in $\operatorname{Im} k \geqslant 0$ other than the real axis the integral vanishes. If $|k| \to \infty$ on $\operatorname{Im} k = 0$ the contribution to the double integral vanishes in virtue of the Riemann-Lebesgue lemma except on a set of relative measure zero ($\boldsymbol{r} = \boldsymbol{r}'$). Thus not only may the orders of integration be exchanged but in fact the contour Γ may be replaced by the real k-axis. We may then employ (13) and the unitarity condition

$$F(-k, k', \Delta) = F^*(k, k', \Delta) \tag{20}$$

to write the dispersion relation

$$F(k, k', \Delta) = \sum_{i=1}^{N} \frac{R_i(k', \Delta)}{k^2 + K_i^2} + \frac{2}{\pi} \int_0^\infty \frac{k'' \, \mathrm{d}k'' \operatorname{Im} F(k'', k', \Delta)}{k''^2 - k^2} + u(\Delta), \tag{21}$$

which is equivalent to Theorem 1.

Finally we observe that the restriction Δ real and $|\Delta| < 2\mu$ can be removed when $|k|$ is sufficiently large. This follows from (12), (13), (19), and the finiteness of the number of poles of $G(\boldsymbol{r}', \boldsymbol{r}, k)$. Thus:

Theorem 2. – For arbitrary k' and Δ there exists a number $C(k', \Delta)$ such that $F(k, k', \Delta)$ is analytic in k provided $\operatorname{Im} k \geqslant 0$ and $|k| > C(k', \Delta)$. Further $F(k, k', \Delta) \to u(\Delta)$ as $|k| \to \infty$.

4. – Analyticity in $\cos\theta$ and Δ.

In the present section we examine the analytic properties of $F(k, k', \Delta)$ when k and k' are fixed real numbers. Since $F(k, -k', \Delta) = F(k, k', \Delta)$ (eq. (10)) we may consider k and k' as relatively positive. We define

$$\mathscr{F}(k, \zeta, \cos\theta) \equiv F(k, k', \Delta) \tag{22}$$

$$\zeta = k'/k \geqslant 0 . \tag{23}$$

The partial wave series is

$$\mathscr{F}(k,\zeta,z)=\sum_{l=0}^{\infty}(2l+1)A_l(k,\zeta)P_l(z)\,, \tag{24}$$

$$A_l(k,\zeta)=-A(2l+1)^{-2}\int_0^{\infty}\psi_0^{(-)}(\zeta kr)\,V(r)\,\psi_l^{(+)}(k,r)\,\mathrm{d}r\,, \tag{25}$$

where

$$\psi_{0l}^{(-)}(\zeta kr)=(-i)kr^l\mathscr{J}_l(\zeta kr)(2l+1)\,, \tag{26}$$

and $\psi^{(+)}(k,r)$ is the outgoing scattering solution of the l-th radial Schrödinger equation.

It is convenient to introduce the following notation:

$$\begin{cases}(a)\ \lambda=l+\frac{1}{2}; & (b)\ x=kr; & (c)\ \psi^{(\pm)}(\lambda;x)=k\psi_l^{(\pm)}(k,r);\\ (d)\ U(x)=Ak^{-2}V(r); & (e)\ \mathscr{T}_\zeta(\lambda)=kA_{\lambda-\frac{1}{2}}(k,\zeta); & (f)\ \mathscr{T}_1(\lambda)=\mathscr{T}(\lambda)\,.\end{cases} \tag{27}$$

Note that the dependence of these expressions on k has been suppressed for convenience. Eq. (25) may now be written

$$\mathscr{T}_\zeta(\lambda)=-(4\lambda^2)^{-1}\int_0^{\infty}\psi_0^{(-)}(\lambda;\zeta x)\,U(x)\,\psi^{(+)}(\lambda;x)\,\mathrm{d}x\,. \tag{28}$$

$\psi^{(+)}(\lambda;x)$ satisfies the radial equation

$$\left\{\frac{\mathrm{d}^2}{\mathrm{d}x^2}+1-U(x)-\frac{\lambda^2-\frac{1}{4}}{x^2}\right\}\psi^{(+)}(\lambda;x)=0\,. \tag{29}$$

The behavior of $\psi^{(+)}(\lambda;x)$ as $x\to\infty$ is

$$\begin{cases}(a)\quad \psi^{(+)}(\lambda;x)\to\psi_0^{(+)}(\lambda;x)+2\lambda\mathscr{T}(\lambda)\exp[ix]\,,\\ \qquad\text{or}\qquad\qquad \to A^{(+)}(\lambda)\sin\left(x-\dfrac{\pi\lambda}{2}+\dfrac{\pi}{4}+\delta(\lambda)\right),\end{cases} \tag{30}$$

where

$$A^{(+)}(\lambda)=2\lambda i^{\lambda-\frac{1}{2}}\exp[i\delta(\lambda)]\,,$$

$$\exp[2i\delta(\lambda)]=1+2i\mathscr{T}(\lambda)\,.$$

Near $x=0$

$$\psi^{(+)}(\lambda;x)\sim k^{(+)}(\lambda)\chi^{\lambda+\frac{1}{2}}\,, \tag{31}$$

where $k^{(+)}(\lambda)$ is independent of x.

Following ref. [3] we introduce solutions of (29) satisfying other boundary conditions:

$$\text{(32)}\qquad \left\{\begin{array}{ll} (a) & C(\lambda;x)\to\cos(x-\pi/4) \\ (b) & S(\lambda;x)\to\sin(x-\pi/4) \end{array}\right\} x\to\infty\,,$$
$$(c)\quad \Phi(\lambda;x)\sim x^{\lambda+\frac{1}{2}}\,,\qquad x\to 0\,.$$

From the invariance of the Wronskians one then obtains

$$\text{(33)}\qquad \left\{\begin{array}{l} (a)\ \ \Phi(\lambda;x)=2\lambda[C(\lambda)S(\lambda;x)-S(\lambda)C(\lambda;x)]\,, \\ (b)\ \ C(\lambda;x)=C(\lambda)\Phi(-\lambda;x)+C(-\lambda)\Phi(\lambda;x)\,, \\ (c)\ \ S(\lambda;x)=S(\lambda)\Phi(-\lambda;x)+S(-\lambda)\Phi(\lambda;x)\,, \end{array}\right.$$

where

$$\text{(34)}\qquad \big(C(\lambda);S(\lambda)\big)=\lim_{x\to 0}x^{\lambda-\frac{1}{2}}\big(C(\lambda;x);S(\lambda;x)\big)\,.$$

The unperturbed values of these quantities are

$$\text{(35)}\qquad \left\{\begin{array}{ll} (a) & \Phi_0(\lambda;x)=x^{\frac{1}{2}}\Gamma(\lambda+\tfrac{1}{2})\,2^{\lambda}J_\lambda(x)\,, \\ (b) & \big(C_0(\lambda;x);S_0(\lambda;x)\big)=(\pi x/8)^{\frac{1}{2}}\Big(\cos\frac{\pi\lambda}{2};\sin\frac{\pi\lambda}{2}\Big)^{-1}\big(J_\lambda(x)\pm J_{-\lambda}(x)\big)\,, \\ (c) & \big(C_0(\lambda);S_0(\lambda)\big)=\pm(2\pi)^{-\frac{1}{2}}2^{\lambda}\Gamma(\lambda)\Big(\sin\frac{\pi\lambda}{2};\cos\frac{\pi\lambda}{2}\Big)\,, \end{array}\right.$$

$C(\lambda;x)$ and $S(\lambda;x)$ satisfy Volterra's integral equations which are given in the Appendix A.

The asymptotic from of $\Phi(\lambda;x)$ is determined by $C(\lambda)$ and $S(\lambda)$. $\psi^{(+)}(\lambda;x)$ and $\Phi(\lambda;x)$ are proportional for all x in view of the boundary conditions and hence have the same asymptotic phase. This phase determines $A^{(+)}(\lambda)$ and hence the proportionality factor $k^{(+)}(\lambda)$. It is then easy to show using the integral eq. (A.1)

$$\text{(36)}\qquad \mathscr{T}_\zeta(\lambda)=\frac{S_0(\lambda)C(\zeta:\lambda)-C_0(\lambda)S(\zeta:\lambda)}{\big(C_0(\lambda)-iS(\lambda)\big)\big(C(\lambda)+iS(\lambda)\big)}\,,$$

where

$$\text{(37)}\qquad \big(C(\zeta:\lambda);S(\zeta:\lambda)\big)=\big(C_0(\lambda);S_0(\lambda)\big)+$$
$$+(2\lambda)^{-1}\int_0^\infty U(x)\big(C_0(\lambda;\zeta x);S_0(\lambda;\zeta x)\big)\,\Phi(\lambda;x)\,\mathrm{d}x\,,$$

and

$$\text{(38)}\qquad \big(C(1:\lambda);S(1:\lambda)\big)=\big(C(\lambda);S(\lambda)\big)\,.$$

It is convenient to define functions

$$F^{(\pm)}(\zeta;\lambda) = \frac{C(\zeta:\lambda) \pm iS(\zeta:\lambda)}{C_0(\lambda) \pm iS_0(\lambda)}\,, \tag{39}$$

and write

$$\mathscr{T}_\zeta(\lambda) = \frac{F^{(-)}(\zeta:\lambda) - F^{(+)}(\zeta:\lambda)}{2iF^{(+)}(1:\lambda)}\,. \tag{40}$$

From (29), (32), (34) and (37) it is evident that

$$\big(F^{(-)}(\zeta:\lambda)\big)^* = F^{(+)}(\zeta:\lambda^*)\,, \tag{41}$$

so that $\mathscr{T}_\zeta(\lambda)$ reduces to the familiar form (30*b*) when $\zeta = 1$ and λ is real. In fact since ζ occurs only in the unperturbed function $\psi_0^{(-)}(\lambda;\zeta x)$ (see (28)), the phase of $\mathscr{T}_\zeta(\lambda)$ is independent of ζ when λ, ζ are real and we may conclude that

$$\arg F^{(-)}(\zeta:\lambda) = \delta(\lambda)\,, \tag{42}$$

and

$$\operatorname{Im}\mathscr{T}_\zeta(\lambda) = \mathscr{T}_\zeta(\lambda)\,\mathscr{T}^*(\lambda)\,. \tag{43}$$

Eq. (43) is the statement of unitarity off the energy shell.

We now outline the method to be followed [3] in determining the domain of analyticity of the amplitude in $z = \cos\theta$ for fixed k and ζ.

The series (24) is now written

$$\mathscr{F}(k,\zeta,z) = k^{-1}\sum_\lambda 2\lambda\,\mathscr{T}_\zeta(\lambda)\,P_{\lambda-\frac{1}{2}}(z) \qquad \lambda = \tfrac{1}{2}, \tfrac{3}{2}, \ldots\,, \tag{44}$$

and we carry out the following steps:

A) By examining the behavior of $\mathscr{T}_\zeta(\lambda)$ as $\lambda \to \infty$ and employing the known behavior of Legendre functions in the same limit we ascertain the domain of z for which (44) converges uniformly in z.

B) To analytically continue beyond this region we study the analytic properties of $\mathscr{T}_\zeta(\lambda)$ as a function of the *complex* variable λ and conclude from these properties that (44) may be replaced by a Sommerfeld integral [4]

$$\mathscr{F}(k,\zeta,z) = (2ik)^{-1}\int_C \lambda\,\mathrm{d}\lambda\,\mathscr{T}_\zeta(\lambda)(\cos\pi\lambda)^{-1}\,P_{\lambda-\frac{1}{2}}(-z)\,, \tag{45}$$

where C is a contour in the right-half λ-plane enclosing the points $\lambda = \frac{1}{2}, \frac{3}{2} \ldots$ In fact it will be shown that for potentials of the Yukawa type $\mathscr{T}_\zeta(\lambda)$ is such as to allow a deformation of C into a pair of rays defined by $\arg \lambda = \pi/2 - \varepsilon$ and $\arg \lambda = -(\pi/2 - \varepsilon)$ with ε arbitrarily small. It will be shown that in the course of this deformation we will encounter only poles of $\mathscr{T}_\zeta(\lambda)$ and the latter for Yukawa potentials will yield a function of z analytic in the plane cut from $z = +1$ to $z = +\infty$ while the deformed integral will converge uniformly in the same domain.

It might at first glance seem natural to investigate the properties of $\mathscr{T}_\zeta(\lambda)$ by means of the functions $F^{(\pm)}(\zeta : \lambda)$ (cf. (39) and (40)) in analogy to ref. [3] for $\zeta = 1$. Unfortunately, complications arise when $\zeta \neq 1$ which prevent this approach and it is easier to deal with the numerator of (40) as a whole. Thus we write

$$\mathscr{T}_\zeta(\lambda) = \Omega(\zeta : \lambda)/F^{(+)}(1 : \lambda)\,, \tag{46}$$

where from the definitions and the relations (33) one obtains

$$\Omega(\zeta : \lambda) = (2i)^{-1}\big(F^{(-)}(\zeta : \lambda) - F^{(+)}(\zeta : \lambda)\big) = \tag{47}$$

$$= -\big[(4\lambda^2)\big(C_0^2(\lambda) + S_0^2(\lambda)\big)\big]^{-1}\int_0^\infty \Phi_0(\lambda; \zeta x)\, U(x)\, \varphi(\lambda; x)\, \mathrm{d}x\,.$$

As in ref. [3] the analysis is carried out by obtaining a rough estimate of the fuctions Ω and $F^{(+)}$ for arbitrary $\lambda \varepsilon$ Re $\lambda > 0$ and a more precise estimate on Re $\lambda = 0$ and Im $\lambda = 0$. One then obtains an improved estimate for arbitrary $\lambda \in$ Re $\lambda > 0$ by means of Montel's theorem. The methods of ref. [3] are unsatisfactory for $\Omega(\zeta : \lambda)$ if $\zeta \neq 1$* although the conclusions have a similar form.

We begin by stating the results from ref. [3], for $F^{(+)}(1 : \lambda)$ which will be required. A brief outline of the proofs is included in Appendix A as a number of them are required in the discussion of $\Omega(\zeta : \lambda)$

$$\begin{cases} (a)\ C(\lambda) \text{ is an entire function in Re } \lambda > 0 \text{ and for some } K > 0 \\ \quad |C(\lambda)| < |(K\lambda)^\lambda|\,. \\ (b)\ C(\lambda) \to C_0(\lambda) + o(1)\big(C_0^2(\lambda) + S_0^2(\lambda)\big)^{\frac{1}{2}},\ \lambda \to \infty \text{ and similarly for } S(\lambda). \\ (c)\ C(\lambda) \to C_0(\lambda)\big(1 + o(1)\big)\,, \qquad \lambda \to \pm i\,\infty\,. \end{cases} \tag{48}$$

(*) For the boundary Im $\lambda = 0$ the methods of ref. [3] can be and are used for ζ finite. The rough estimate for arbitrary $\lambda \in$ Re $\lambda > 0$ presents no special difficulty For the boundary Re $\lambda = 0$ the WKB method of ref. [3] fails and the iteration solution of (47) must be examined. See Appendix B.

From (48), (35 c) and (39) it follows that

$$(49)\quad \begin{cases} (a)\ F^{(\pm)}(1:\lambda) \text{ are entire functions in } \operatorname{Re}\lambda > 0 \text{ and for some } K > 0;\ |F^{(\pm)}(1:\lambda)| < |K^{\lambda}|. \\ (b)\ F^{(\pm)}(1:\lambda) \to 1 + o(1), & \lambda \to \infty, \\ (c)\ F^{(+)}(1:\lambda) \to 1 + o(1), & \lambda \to -i\infty, \\ (d)\ F^{(-)}(1:\lambda) \to 1 + o(1), & \lambda \to +i\infty. \end{cases}$$

It is further shown that for $\operatorname{Re}\lambda > 0$

$$(50)\qquad F^{(+)}(1:\lambda) \neq 0, \quad \operatorname{Im}\lambda \leqslant 0, \quad F^{(-)}(1:\lambda) \neq 0, \quad \operatorname{Im}\lambda \geqslant 0.$$

The following properties of $\Omega(\zeta:\lambda)$ are proved in Appendix B:

$$(51)\quad \begin{cases} (a)\ \Omega(\zeta:\lambda) \text{ is an entire function of } \lambda \text{ in } \operatorname{Re}\lambda > 0 \text{ for arbitrary } \zeta \in 0 \leqslant \zeta \leqslant \infty \text{ and for some } K > 0: |\Omega(\zeta:\lambda)| < |K^{\lambda}| \text{ where } K \text{ is independent of } \zeta \text{ and } \lambda. \\ (b)\ \Omega(\zeta:\lambda) = O(\exp[-\varrho\lambda]),\ \lambda \to \infty \text{ where } \varrho = \varrho(\mu,\zeta) \geqslant \varepsilon > 0 \text{ for all } \zeta: 0 \leqslant \zeta \leqslant \infty \text{ provided that the range } \mu^{-1} \text{ of the potential is bounded.} \\ (c)\ |\Omega(\zeta:\lambda)| = O(|\lambda|^{-\frac{1}{2}}),\ \lambda \to \pm i\infty \text{ for arbitrary } \zeta \in 0 \leqslant \zeta \leqslant \infty \text{ provided that } \mu^{-1} < \infty. \end{cases}$$

From eq. (49), (50), (51) and Montel's theorem we arrive at the following conclusions for $\mathscr{T}_{\zeta}(\lambda)$.

$$(52)\quad \begin{cases} (a)\ \mathscr{T}_{\zeta}(\lambda) \text{ is analytic in } \operatorname{Re}\lambda > 0 \text{ except for a finite set of poles lying in } \operatorname{Im}\lambda > 0. \\ (b)\ \mathscr{T}_{\zeta}(\lambda) = O(\exp[-\varrho\lambda]) \text{ as } |\lambda| \to \infty \text{ along any ray in } \operatorname{Re}\lambda \geqslant 0. \text{ [See (51}b\text{) for properties of } \varrho\text{].} \end{cases}$$

The asymptotic expansion of the Legendre functions for large order begins

$$(53)\qquad P_{\lambda-\frac{1}{2}}(\cos\theta) \sim (2\pi\lambda \sin\theta)^{-\frac{1}{2}} \exp[\pm i\lambda(\theta - \pi)].$$

Thus we see that (44) converges only for $\operatorname{Im}\theta < \varrho$. Now from (52) we see that, except for the contribution of the poles, the contour C in (45) may be deformed into the imaginary λ-axis and that the resulting integral converges for arbitrary $\operatorname{Im}\theta$ provided only that $\operatorname{Re}\theta \neq 0, 2\pi$. That is to say, the deformed integral represents an analytic function of z in the entire complex z plane except

for a branch cut on the real z axis from $z=+1$ to $z=+\infty$. Further, from the Riemann-Lebesgue lemma, the integral vanishes as $|z|\to\infty$ along any ray. Now the i-th pole of $\mathscr{F}_\zeta(\lambda)$ contributes a term of the form $P_{\lambda_i-\frac{1}{2}}(-z)$ which is an entire function of z in the plane cut from $z=+1$ to $z=+\infty$.

We may now summarize the results of this section, expressing them in terms of Δ^2 rather than z. We note that since

$$\Delta^2 = k^2 + k'^2 - 2kk'z\,, \tag{54}$$

we have obtained analyticity in t for fixed k and k' except possibly for a cut when $z>1$, *i.e.* when

$$\Delta^2 < (k-k')^2\,.$$

Now it is apparent from (10) that $F(k, k', \Delta) - u(\Delta)$ is also analytic in Δ^2 in some neighborhood of the real axis between $-4\mu^2$ and $2(k^2+k'^2)$. Since $2(k^2+k'^2)\geqslant(k-k')^2$ for all real k and k' we may strengthen the above results as follows:

Theorem 3. – For arbitrary real k and k', $F(k, k', \Delta) - u(\Delta)$ is analytic in the entire Δ^2-plane cut from $\Delta^2=-4\mu^2$ to $\Delta^2=-\infty$. ($u(\Delta)$ is evidently analytic in Δ^2 except for the cut $(-\infty, -\mu^2)$.)

The usual arguments from the theory of several complex variables may now be applied using Theorems 1, 2 and 3 with the result:

Theorem 4. – For arbitrary real k', $F(k, k', \Delta)$ is analytic in $s=k^2$ and in $t=\Delta^2$ except for the following cuts: in s for $0<s<\infty$; in t for $-\infty<t<-\mu^2$ (the $-\mu^2$ being replaceable by $-4\mu^2$ except for the first Born term). Further for any finite t, $F\to u(\Delta)$ as $|s|\to\infty$ with $\operatorname{Im}\sqrt{s}>0$.

In order to write a dispersion relation in t we must know how $F(k, k', \Delta)$ behaves as $|\Delta|\to\infty$. As we have seen this will be determined by the functions $P_{\lambda_i-\frac{1}{2}}(-z)$ where λ_i is a point in $\operatorname{Im}\lambda>0$ for which $F^{(+)}(1:\lambda)=0$. From the results concerning $F^{(-)}(1:\lambda)$ and $\Omega(\zeta:\lambda)=2i(F^{(-)}-F^{(+)})$ for $\zeta=1$ we were able to conclude that the number of such points is finite and hence there exists a positive number γ such that $0\leqslant\operatorname{Re}\lambda_i\leqslant\gamma$ for all i. Hence, the divergence at $z\to\infty$ is majorized by $|z|^\gamma$. Of course the number γ here depends on the energy which was suppressed in the discussion of λ dependence. From (29), $k\to\infty$ can be treated as $k=1$ but Δ and $\mu\to 0$. From (52*b*) one may then easily show that the poles $\lambda_i(k)$ and hence γ must be bounded in k [5]. It is interesting that the number γ is also bounded below [1] as a consequence

[5] T. Regge: *Nuovo Cimento*, **18**, 947 (1960).

of unitarity, the bound being the largest angular momentum admitting a bound state.

The results of Sect. 3 and 4 now enable one to write a Mandelstam representation for off-energy-shell amplitudes as follows:

$$f(\bar{s}, s, t) = f_B(t) + \sum_{i=1}^{r} \frac{\Gamma_i(\bar{s}, t)}{s + s_i} + \tag{55}$$

$$+ t^\gamma \int_0^\infty \frac{\mathrm{d}s'}{\pi} \int_0^\infty \frac{\mathrm{d}t'}{\pi} \frac{\varrho(\bar{s}, s, t)}{t'^\gamma (t' + t)(s' - s - i\varepsilon)} + \sum_{j=0}^{\gamma} t^j \int_0^\infty \mathrm{d}s' \frac{g_j(\bar{s}, s')}{s' - s - i\varepsilon} ,$$

where

$$f(\bar{s}, s, t) = F(k, k', \Delta) , \qquad s = k^2 , \qquad \bar{s} = k'^2 , \qquad t = \Delta^2 ,$$

and $\Gamma_i(\bar{s}, t)$ is the residue at the i-th bound state. The dependence of Γ_i on $\cos(\boldsymbol{k}, \boldsymbol{k}')$ is that of the Legendre function $P_{l_i}(\cos \boldsymbol{k}, \boldsymbol{k}')$, l_i being the angular momentum of the bound state.

5. – The unitary condition—closure of the system.

As we have pointed out elsewhere [4] the integral representation (45) after deformation into the imaginary axis permits one to write the Mandelstam representation in a simpler form. One introduces the so-called conical amplitude

$$A(ip, s, s') = is^{-\frac{1}{2}} \left(\mathscr{T}_\zeta(ip, s) - \mathscr{T}_\zeta(-ip, s) \right) , \qquad 0 \leqslant p \leqslant \infty , \; \zeta = \left(\frac{s'}{s} \right)^{\frac{1}{2}} , \tag{56}$$

where we have restored the previously suppressed energy-dependence. In the absence of bound states and subtractions, (45), (56) and the properties of the Legendre functions $P_{ip-\frac{1}{2}}(z)$ (conical functions) imply the relations

$$A(ip, s, s') - A_B(ip, s, s') = \int_0^\infty \frac{\operatorname{Im} A(ip, s'', s')}{s - s - i\varepsilon} \frac{\mathrm{d}s''}{\pi} - \int_0^\infty \frac{\operatorname{Im} A(ip, -s'', s')}{s'' + s + i\varepsilon} \frac{\mathrm{d}s''}{\pi} , \tag{57}$$

with the Born term

$$A_B(ip, s, s') = \frac{A\pi \operatorname{tgh} \pi p}{2\sqrt{ss'}} P_{ip-\frac{1}{2}} \left(\frac{s + s' + \mu^2}{2\sqrt{ss'}} \right) , \tag{58}$$

$$\operatorname{Im} A(ip, -s, s') = \frac{-\sinh \pi p}{2\pi} \int_0^\infty q \, \mathrm{d}q \int_0^\infty \frac{\mathrm{d}u}{u + 1} \xi(p, q, u) \operatorname{Im} A(iq, su, s') , \tag{59}$$

where

$$\xi(p, q, u) = \int_1^\infty P_{ip-\frac{1}{2}}(y) P_{iq-\frac{1}{2}}\left(1 + \frac{1+y}{u}\right) \mathrm{d}y \,. \tag{60}$$

From the unitarity condition one obtains for $s \geqslant 0$

$$\operatorname{Im} A(ip, s, s') = \frac{1}{2}\sqrt{s}\,\operatorname{Re}\left\{A^*(ip, s, s')\frac{\boldsymbol{P}}{\pi}\int_0^\infty \frac{2q\,\mathrm{d}q}{q^2 - p^2} A(iq, s) + \right. \tag{61}$$

$$\left. - A^*(ip, s)\frac{\boldsymbol{P}}{\pi}\int_0^\infty \frac{2q\,\mathrm{d}q}{q^2 - p^2} A(iq, s, s')\right\} .$$

Substitution of (61) into (59) and into (57) leads to a pair of coupled linear integral equations for the real and imaginary parts of $A(ip, s, s')$ of the form

$$A^{(j)}(ip, s, s') = A_B^{(j)}(ip, s, s') + \sum_{i=1}^{2} \int_0^\infty \mathrm{d}s'' \int_0^\infty \mathrm{d}q\, K_{ji}(p, s; q, s'') A^{(i)}(iq, s'', s') \,, \tag{62}$$

where real and imaginary parts are indicated by superscripts 1 and 2 and the kernels $K_{ji}(p, s; q, s'')$ are determined by the on-shell amplitude $A(ip, s)$. Application of (62) to the calculation of particular off-shell amplitudes will be discussed in a subsequent paper.

6. – Unphysical sheets and analyticity in the second energy.

Up to now we have restricted ourselves to a study of analytic properties in one energy (s) and the momentum transfer (t) with the second energy (s') fixed and real. Further we have obtained results only in the first Riemann sheet for $s(\operatorname{Im}\sqrt{s} > 0)$. We now wish to study the possibility of removing these restrictions.

If in (10) we introduce new variables

$$\alpha = (k + k')/2; \qquad \beta = (k - k')/2 \,, \tag{63}$$

$$F(\alpha + \beta, \alpha - \beta, \Delta) = u(\Delta) - (4\pi)^{-1}\Delta^2 \int \cos\left(\tfrac{1}{2}\boldsymbol{\Delta}\cdot(\boldsymbol{r} + \boldsymbol{r}')\right) \cdot \tag{64}$$

$$\cdot \cos\left((\alpha^2 + \beta^2 - \Delta^2/4)^{\frac{1}{2}}\boldsymbol{n}\cdot(\boldsymbol{r} - \boldsymbol{r}')\right) V(r') G(\boldsymbol{r}', \boldsymbol{r}, \alpha + \beta) V(r)\, \mathrm{d}^3r\, \mathrm{d}^3r' ,$$

we see that the methods of Sect. 3 and 4 may be applied replacing k by α with β fixed >0, or by β with α fixed >0. One then obtains analyticity in α, β, and t in the cut t-plane and the upper half α and β planes except for bound state poles.

The restriction $\operatorname{Im}\alpha,\ \operatorname{Im}\beta > 0$ means $0 \leqslant |\operatorname{Im} k'| \leqslant \operatorname{Im} k$. For fixed z in $-1 < z < +1$ the restriction $\operatorname{Im} k > 0$ can be removed. The method is to analytically continue in k to $\operatorname{Im} k < 0$ by means of an integral equation expressing the symmetry of the S-matrix (6) namely the relation

$$\mathscr{F}^{\mathrm{II}}(s, s', z) = \mathscr{F}^{\mathrm{I}}(s, s', z) + \frac{\sqrt{s}}{2\pi i}\int_{-1}^{+1} \mathrm{d}z'\, K(s, z, z')\, \mathscr{F}^{\mathrm{II}}(s, s', z')\,. \tag{65}$$

Here I and II denote functions on the two Riemann sheets $\operatorname{Im}\sqrt{s} > 0$ and $\operatorname{Im}\sqrt{s} < 0$ respectively and

$$K(s, z, z') = \int_0^{2\pi} \mathscr{F}^{\mathrm{I}}\big(s,\ zz' + (1 - z^2)^{\frac{1}{2}}(1 - z'^2)^{\frac{1}{2}}\cos\varphi\big)\,\mathrm{d}\varphi\,. \tag{66}$$

(65) is equivalent to the property

$$S_l(k, k') = S_l^{-1}(-k, k')\,, \tag{67}$$

of the partial wave S-matrices.

The analytic continuation is carried out by means of a generalization of the Fredholm theory due to Tamarkin (6). This result concerns the analytic properties of solutions of Fredholm equations in some parameter on which the kernel and the inhomogeneous term have a given simple analytic dependence. If $\mathscr{F}^{\mathrm{I}}$ is considered known, (65) is a Fredholm equation for $\mathscr{F}^{\mathrm{II}}$ with a symmetric kernel. By the Mandelstam representation $\mathscr{F}^{\mathrm{I}}(s, z)$ is meromorphic in s when $-1 \leqslant z \leqslant +1$ except for cuts on $\operatorname{Im} s = 0$ and clearly $K(s, z, z')$ has the same property. At a pole s_i in the angular momentum state l_i the residue of $K(s, z, z')$ is proportional to

$$\int_0^{\pi} P_{l_i}\big(zz' + (1 - z^2)^{\frac{1}{2}}(1 - z'^2)^{\frac{1}{2}}\cos\varphi\big)\,\mathrm{d}\varphi = 2\pi P_{l_i}(z)\,P_{l_i}(z')\,, \tag{68}$$

thus becoming separable.

(6) J. Tamarkin: *Ann. of Math.*, **28**, 127 (1926).

The Tamarkin's theorem then states that the resolvent of $K(s, z, z')$ is meromorphic in the same domain as K itself if it exists at all. From (10) it follows that for Yukawa potentials there is some strip $0 > \mathrm{Im}\,\sqrt{s} > -\varepsilon$ in which $\mathscr{F}(s, z)$ exists and hence for which $K(s, z, z')$ has a resolvent. It now follows from the properties of $\mathscr{F}^{\mathrm{I}}(s, s', z)$ discussed previously that for $s' > 0$ and $-1 \leqslant z \leqslant +1$ $\mathscr{F}^{\mathrm{II}}(s, s', z)$ is meromorphic in s except for cuts on $\mathrm{Im}\,s = 0$. That the poles in the second sheet are just the resonances may be seen by substituting the Mandelstam representation for $\mathscr{F}^{\mathrm{I}}$ into (65) and performing the φ-integration (7). One then finds that for arbitrary fixed s not on $s < 0$ there is an ellipse with foci ± 1 within which $\mathscr{F}^{\mathrm{II}}$ is analytic in z and hence has a Legendre expansion.

The extension of the above conclusion to arbitrary complex z is made difficult by the presence of complex branch points in s when z is not on $-1 \leqslant z \leqslant +1$. We have shown however (4) that complex branch points in the second sheet for on-shell scattering arise from complex poles in the conical amplitudes (56). It is clear from (40) that no additional poles can arise from going off the energy shell.

In order to study the analytic properties of $\mathscr{F}(s, s', z)$ when $|\mathrm{Im}\,\sqrt{s'}| > |\mathrm{Im}\,\sqrt{s}|$ it is necessary to find some functional relation connecting the behaviour of the amplitude in this region with that in $|\mathrm{Im}\,\sqrt{s'}| < |\mathrm{Im}\,\sqrt{s}|$ discussed above. The natural candidate is the Low equation which may be written

$$\mathscr{F}(s, s', z) = \mathscr{F}_{\mathrm{Born}}(s, s', z) + \int_0^\infty \mathrm{d}s'' \int_{-1}^{+1} \mathrm{d}z'\, E(s, z, s'', z')\mathscr{F}(s'', s', z')\,, \tag{69}$$

where

$$E(s, z, s'', z') = 2\pi(s'' - s - i\varepsilon)^{-1} \int_0^{2\pi} \mathscr{F}^*\big(s, s'', zz' + (1-z^2)^{\frac{1}{2}}(1-z'^2)^{\frac{1}{2}}\cos\varphi\big)\,\mathrm{d}\varphi\,. \tag{70}$$

Since $E(s, z, s'', z')$ is independent of s' it is tempting to employ Tamarkin's theorem as above to arrive at the analytic properties of $\mathscr{F}(s, s', z)$ for $-1 \leqslant z \leqslant +1$. Here, however, the Fredholm's equation involves an infinite interval and we are not entirely certain that the theorem is then valid. It is very interesting to observe that the result obtained by blithely applying Tamarkin's theorem to the Low's equation for the off-shell partial wave amplitudes in spite of the infinite interval, does yield the correct result. This may be shown by employing the methods of ref. (8) to obtain the representation

(7) R. Blankenbecler: *Proc. Rochester Conf.* (1960), p. 247.
(8) D. Fivel and A. Klein: *Journ. Math. Phys.* **1**, 274 (1960).

for the partial wave amplitude (25)

$$A_l(k,\zeta) = (2ik)^{-1}\zeta^l\{\tau_l(k,\zeta) - S_l(k)\tau_l(-k,\zeta)\}\,, \tag{71}$$

in which $S_l(k)$ is the partial wave S-matrix

$$S_l(k) = (1+\tau_l(k,1))(1+\tau_l(-k,1))^{-1}\,, \tag{72}$$

and for the potential (11)

$$\tau_l(k,\zeta) = A\varkappa_l(-k\,\mathrm{d}/\mathrm{d}\mu_1)_{\mu_1=\mu}\left\{\int_{\mu_1}^{\infty}\frac{\mathrm{d}\alpha}{(\alpha+ik(1+\zeta))(\alpha+ik(1-\zeta))}\cdot\right. \tag{73}$$

$$\cdot\left[\frac{(\mu_1+ik(1+\zeta))(\mu_1+ik(1-\zeta))}{(\alpha+ik(1+\zeta))(\alpha+ik(1-\zeta))}\right]^l + A\int_{\mu_1}^{\infty}\frac{\mathrm{d}\alpha}{\alpha(\alpha+2ik)}\left[\frac{\mu_1(\mu_1-2ik)}{\alpha(\alpha+2ik)}\right]^l\cdot$$

$$\left.\cdot\int_{\alpha+\mu}^{\infty}\frac{\mathrm{d}\beta}{(\beta+ik(1+\zeta))(\beta-ik(1-\zeta))}\left[\frac{(\alpha-\mu-ik(1-\zeta))(\alpha-\mu-ik(1-\zeta))}{(\beta-ik(1-\zeta))(\beta-ik(1-\zeta))}\right]^l - \ldots\right\},$$

where

$$\varkappa_l(\varrho) = \sum_{m=0}^{l}\frac{(2l-m)!\,l!}{(2l)!\,m!\,(l-m)!}(2i\varrho)^m\,.$$

It can now be seen that the on-shell branch cuts

$$\frac{n\mu}{2} < \pm k < \infty\,, \qquad n = 1, 2, 3, \ldots$$

split into pairs of cuts in the off-shell case:

$$\frac{n\mu}{1+\zeta} < \pm k < \infty \quad \text{and} \quad \frac{n\mu}{1-\zeta} < \pm k < \infty\,, \quad n = 1, 2, 3, \ldots,$$

so that again the branch cuts «recede» as one proceeds through the Born series. The result is thus that the partial wave amplitudes are meromorphic in the k (or k') planes cut along the first Born approximation branch cut. Since this conclusion can be arrived at directly and for any (!) potential if Tamarkin's theorem can be applied to the Low's equation, we hope to discuss the validity of this procedure in a subsequent paper.

7. – Conclusion.

We have proven that a Mandelstam representation with a finite number of subtractions holds in potential scattering of the Yukawa type for off-shell energy processes. We have further indicated how off-shell amplitudes can be obtained from on-shell amplitudes by means of a linear integral equation. Finally we have given some information as to the behavior of off-shell amplitudes on unphysical energy sheets and as a function of the second energy.

It is not at all clear to what extent these relations continue to hold in field theory or how successful the method here suggested for computing off-shell quantities may be in practice.

* * *

I wish to express my appreciation to Drs. R. Amado, C. Fronsdal, A. Klein, B. Lee and M. Vaughn for many helpful conversations.

Appendix A

Some properties of solutions of the radial equation.

The several solutions of (29) defined by the boundary conditions (32) may be shown to obey the integral equations:

$$\text{(A.1}a\text{)} \qquad \Phi(\lambda; x) = x^{\lambda+\frac{1}{2}} + (2\lambda)^{-1}\int_0^x (xy)^{\frac{1}{2}}\big(U(y)-1\big)\big[(xy^{-1})^{\lambda} - (x^{-1}y)^{\lambda}\big]\,\Phi(\lambda; y)\,\mathrm{d}y\,,$$

or

$$\text{(A.1}b\text{)} \qquad \Phi(\lambda; x) = \varphi_0(\lambda; x) + (2\lambda)^{-1}\int_0^x G_a(\lambda; x, y)\,U(y)\,\Phi(\lambda; y)\,\mathrm{d}y\,,$$

where

$$G_a(\lambda; x, y) = \Phi_0(\lambda; x)\,\Phi_0(-\lambda; y) - \Phi_0(-\lambda; x)\,\Phi_0(\lambda; y) =$$

$$= 2\lambda\,\Phi_0(\lambda; x)\,\Phi_0(\lambda; y)\int_y^x \mathrm{d}z\big(\Phi_0(\lambda; z)\big)^{-2},$$

$$\text{(A.1}c\text{)} \qquad C(\lambda; x) = \cos(x - \pi/4) + \int_x^{\infty}\left(\frac{\lambda^2 - \frac{1}{4}}{y^2} + U(y)\right)\sin(y - x)\,C(\lambda; y)\,\mathrm{d}y\,,$$

or

$$C(\lambda; x) = C_0(\lambda; x) + \int_x^\infty G_b(\lambda; x, y)\, U(y)\, C(\lambda; y)\, \mathrm{d}y\,, \tag{A.1d}$$

where

$$G_b(\lambda; x, y) = C_0(\lambda; x)\, S_0(\lambda; y) - C_0(\lambda; y)\, S_0(\lambda; x)\,.$$

The basic properties of $\Phi(\lambda; x)$ and $C(\lambda; x)$ can be extracted from (A.1) by means of the fundamental iteration inequality for Volterra's equations with bounded kernels [9]. Thus from (A.1a) and (A.1c):

$$\Phi(\lambda; x) \text{ is analytic in } \operatorname{Re}\lambda > \tfrac{1}{2} \text{ and as } |\lambda| \to \infty\,, \tag{A.2a}$$

$$\Phi(\lambda; x) = x^{\lambda+\frac{1}{2}}\left(1 + \exp\frac{Q(x)x^2}{|\lambda|}\right), \qquad |Q(x)| \leqslant C < \infty;$$

$C(\lambda; x)$ is an entire function of λ for all $x \neq 0$ and as $|\lambda| \to \infty$ [*]: (A.2b)

$$|C(\lambda; x)| < K \exp\left|\frac{|\lambda|^2}{x}\right|, \quad \text{for some } K > 0.$$

Similar bounds may be obtained for $S(\lambda; x)$, $\Phi'(\lambda; x)$, $C'(\lambda; x)$, etc.

The invariance of the Wronskians of two solutions yields

$$W\big(C(\lambda; x),\, \Phi(\lambda; x)\big) = W\big(C(\lambda; 0),\, \Phi(\lambda; 0)\big) = W\big(C(\lambda; \lambda),\, \Phi(\lambda; \lambda)\big)\,.$$

From (34) the second member is just $2\lambda C'(\lambda)$ so that substitution of (A.2a) and (A.2b) into the third member gives

$$|C(\lambda)| < |(K\lambda)^\lambda|. \qquad \text{for some } K > 0. \tag{A.3}$$

Next we consider the case $\lambda \to \infty$. From the differential equation satisfied by the function $x^m \Phi_0(\lambda; x)$ for an arbitrarily fixed $m > 0$, it is easy to show that $x^m \Phi_0(\lambda; x)$ is non-decreasing for all x in $0 < x < \lambda$ when λ is sufficiently large. It then follows that the Green's function of (A.1b) satisfies for λ sufficiently large

$$|G_a(\lambda; x, y)| < |(m - \tfrac{1}{2})^{-1} y\, \Phi_0(\lambda; x)\big(\Phi_0(\lambda; y)\big)^{-1}|.$$

Since m is arbitrary the Volterra's inequality then implies

$$\Phi(\lambda; x) \to \Phi_0(\lambda; x) O(1) \text{ uniformly in } 0 \leqslant x \leqslant \lambda,\ \lambda \to \infty. \tag{A.4}$$

[9] F. Riesz and B. Sz. Nagy: *Functional Analysis* (New York, 1956), p. 147.

[*] Since its boundary conditions are independent of λ the entirety also follows by the well-known theorem of Poincaré.

From the integral representations of Bessel functions [10] one finds that $|C_0(\lambda; x)| < K\sqrt{x}$ for some K when $x \geqslant \lambda$ and similarly for $S_0(\lambda; x)$. Then from (A.1*d*) and the Volterra's inequality:

$$|C(\lambda; x)| < K\sqrt{x}\,, \tag{A.5}$$

for some K for $x \geqslant \lambda$ and similarly for $S(\lambda; x)$.

Now $C(\lambda)$ satisfies the relation

$$C(\lambda) = C_0(\lambda) + (2\lambda)^{-1} \int_0^\infty U(x)\, C_0(\lambda; x)\, \Phi(\lambda; x)\, \mathrm{d}x\,. \tag{A.6}$$

Use of (A.4) on the interval $(0, \lambda)$ of the range together with the asymptotic expansion of Bessel functions (*) and (33*a*) with (A.5) in (λ, ∞) one obtains the result (48*b*).

Finally consider the case $\lambda \to i\infty$. From the properties of Bessel functions (**) it follows that

$$|C_0(\lambda; x)|,\ |S_0(\lambda; x)| < K\sqrt{x}; \qquad |\Phi_0(\lambda; x)| < K|\lambda|^{\frac{1}{2}}\sqrt{x}\,, \tag{A.7}$$

for some K, arbitrary x, $\lambda = ia$, a real.

From (A.6), (A.1*b*) and (A.1*d*) and the Volterra's inequality

$$|C(\lambda; x)|,\ |S(\lambda; x)| < K\sqrt{x}; \qquad |\Phi(\lambda; x)| < K|\lambda|^{\frac{1}{2}}\sqrt{x}\,, \tag{A.8}$$

for some K, arbitrary x, $\lambda = ia$, a real.

Use of (A.8) on the range $(|\lambda|^{\frac{1}{2}}, \infty)$ of (A.6), and (A.8) with (33*b*) and (A.2*a*) in $(0, |\lambda|^{\frac{1}{2}})$ then yields (48*c*).

Finally one proves the following property of $C(\lambda)$ and $S(\lambda)$ required for eq. (50).

$$C(\lambda) = -iS(\lambda) \text{ for } \operatorname{Re}\lambda > 0 \text{ can hold only in } \operatorname{Im}\lambda > 0\,. \tag{A.9}$$

Suppose $\operatorname{Im}\lambda \neq 0$. From (29) and (32)

$$\Phi(\lambda; x) = \Phi^*(\lambda^*, x),\ C(\lambda; x) = C^*(\lambda^*, x)\,, \quad \text{etc.}$$

$$\Phi(\lambda; x)\, \Phi''(\lambda^*, x) - \Phi''(\lambda; x)\, \Phi(\lambda^*, x) = -\frac{4i}{x^2} \operatorname{Re}\lambda \operatorname{Im}\lambda\, |\Phi(\lambda; x)|^2\,.$$

Integration of both sides of the last equation from 0 to ∞ and use of (32)

([10]) G. W. WATSON: *Theory of Bessel functions*, 2nd ed. (Cambridge, 1958), p. 176 (4). p. 178 (1).

(*) Ref. ([10]), p. 243 (3) and (4).

(**) Ref. ([10]), p. 47.

and (33) to evaluate the limits gives

$$|\lambda|^2\{C^*(\lambda)S(\lambda) - S^*(\lambda)C(\lambda)\} = i\,\mathrm{Re}\,\lambda\,\mathrm{Im}\,\lambda\int_0^\infty \frac{\mathrm{d}x}{x^2}|\Phi(\lambda;x)|^2 .$$

From this (A.9) follows. If $\mathrm{Im}\,\lambda = 0$, $\Phi(\lambda;x)$ is real and $S(\lambda)$ and $C(\lambda)$ must be real hence $C(\lambda) \neq -iS(\lambda)$. Now $F^{(+)}(1:\lambda) = 0$ holds only if $C(\lambda) = -iS(\lambda)$, $C(\lambda) = S(\lambda) = 0$ or $C_0(\lambda) + iS_0(\lambda) = 0$. The second case implies $\Phi(\lambda;x) \equiv 0$ which is impossible while from (35) third case cannot occur for finite $|\lambda|$ in $\mathrm{Re}\,\lambda > 0$. Eq. (50) then follows.

Appendix B

Some properties of the function $\Omega(\zeta:\lambda)$.

We first obtain a rough estimate for $\Omega(\zeta:\lambda)$ for arbitrary λ in $\mathrm{Re}\,\lambda > 0$ For $\zeta < 1$ one divides the interval of integration in (47) into $(0, |\lambda|)$, $(|\lambda|, \zeta^{-1}|\lambda|)$ and $(\zeta^{-1}|\lambda|, \infty)$ so that in each interval $\Phi(\lambda;x)$ and $\Phi_0(\lambda;x)$ may be bounded by (A.2*a*) or (A.2*b*); similarly for $\zeta \geqslant 1$ with the divisions $(0, \zeta^{-1}|\lambda|)$, $(\zeta^{-1}|\lambda|, |\lambda|)$, $(|\lambda|, \infty)$. From (A.3) and application of Stirling's formula to $C_0^2(\lambda) + S_0^2(\lambda)$ the result (51*a*) follows.

Next we consider the case $\lambda \to \infty$. We treat separately the situation for bounded ζ, *i.e.* $0 \leqslant \zeta \leqslant \zeta_0 < \infty$ and that for $\zeta \to \infty$. For bounded ζ the situation is particularly simple. Application of Schwartz' inequality to (47) (noting that Φ and Φ_0 are real for real λ) we obtain

$$(\mathrm{B.1}) \qquad |\Omega(\zeta:\lambda)| \leqslant (4\lambda^2)^{-1}\big(C_0^2(\lambda) + S_0^2(\lambda)\big)^{-1} \cdot \left\{\int_0^\infty \Phi_0^2(\lambda;\zeta x)\,U(x)\,\mathrm{d}x + \int_0^\infty \Phi^2(\lambda;x)\,U(x)\,\mathrm{d}x\right\}.$$

Since ζ is finite the first integral is just

$$\int_0^\infty \Phi_0^2(\lambda;x)\,U_\zeta(x)\,\mathrm{d}x\,,$$

where $U_\zeta(x)$ has range $\zeta\mu^{-1} \leqslant \zeta_0\mu^{-1} < \infty$.

Thus we need only discuss the second integral for potentials of arbitrary ranges with uniform bounds determined by ζ_0. This is accomplished as in ref. [3] by division of the range of integration into $(0, \lambda)$ and (λ, ∞). On the

first interval by (A.4):

$$\int_0^\lambda \Phi^2(\lambda; x)\, U(x)\, \mathrm{d}x = O(1) \int_0^\lambda \Phi_0^2(\lambda; x)\, U(x)\, \mathrm{d}x$$

$$\leqslant O(1) \left\{ \left| \int_0^\infty \Phi_0^2(\lambda; x)\, U(x) \mathrm{d}x \right| + \left| \int_\lambda^\infty \Phi_0^2(\lambda; x)\, U(x) \mathrm{d}x \right| \right\}.$$

The first term may be evaluated exactly (*) while a strong bound may be imposed on the second by means of the asymptotic expansion of Bessel functions (**). The result is (51*b*).

Now we consider the situation $\zeta \to \infty$ in which case the estimate above gives a vanishing coefficient of λ in (51*b*) and is therefore useless. We begin by dividing the range of integration in (47) into four parts, $(0, \zeta^{-1}\lambda)$, $(\zeta^{-1}\lambda, 2\zeta^{-1}\lambda)$, $(2\zeta^{-1}\lambda, \lambda)$ and (λ, ∞) with the corresponding integrals denoted $I_1, \ldots, I_4$, resp. Here we assume $\zeta \gg 2$ so that the intervals have natural order. In the first interval we have by change of variables and denoting $U_\zeta(x) = \zeta^{-1} U(\zeta^{-1}x)$

$$|I_1| = \int_0^\lambda U_\zeta(y)\, \Phi_0(\lambda; y)\, \Phi(\lambda; \zeta^{-1}y)\, \mathrm{d}y \leqslant O(1) \int_0^\lambda U_\zeta(y) |\Phi_0(\lambda; y)|\, |\Phi_0(\lambda; \zeta^{-1}y)|\, \mathrm{d}y$$

by (A.4).

The absolute values are not needed as the functions are positive in the range of integration. In fact using the properties of the function $x^{-m}\Phi_0(\lambda; x)$ (see the remarks following [A.3]) one can show that for arbitrary K in $0 < K < 1$, $\gamma_0(\lambda; x) x^{-\lambda\sqrt{1-x^2}}$ is non-decreasing in $0 \leqslant x \leqslant K\lambda$ for all $\lambda > 0$. Choosing $K = \zeta^{-1}$ the above inequality becomes

$$|I_1| \leqslant O(1) \zeta^{-\lambda\sqrt{1-\zeta^{-2}}} \int_0^\lambda U_\zeta(x)\, \Phi_0^2(\lambda; x)\, \mathrm{d}x\,.$$

The integral here may be treated as in the case for bounded ζ and while as $\zeta \to \infty$ it then tends to a constant, the factor $\zeta^{-\lambda\sqrt{1-\zeta^{-2}}}$ provides the exponential decay required in (51*b*).

For $I_2 + I_3$ we may still use (A.4) for $\Phi(\lambda; x)$ and in addition use the asymptotic expansion of the Bessel functions for $\Phi_0(\lambda; \zeta x)$ for order less than

(*) See WATSON: op. cit. and also BATEMAN: *Higher Transcendental Functions*, vol. **1**, p. 137 (44).

(**) See WATSON: op. cit., p. 243 (3).

argument (*). Thus

$$|I_2| \leqslant O(1)\, 2^\lambda \Gamma(\lambda+1)\zeta^{\frac{1}{2}} \int_{\zeta^{-1}\lambda}^{2\zeta^{-1}\lambda} \sqrt{x}\, U(x)\, \Phi_0(\lambda; x)[(\zeta x)^2 - \lambda^2]^{-\frac{1}{4}}\, \mathrm{d}x\,,$$

and similarly for $|I_3|$ with the range $(2\zeta^{-1}\lambda, \lambda)$. For the $\Phi_0(\lambda; x)$ in I_2, $x \ll \lambda$ for $\zeta \gg 1$ so that (*)

$$|\Phi_0(\lambda; x)| < \text{const}\, \sqrt{x}\, 2^\lambda \Gamma(\lambda+1)\lambda^{-\frac{1}{3}}\zeta^{-\lambda}\,.$$

The factor $\zeta^{-\lambda}$ provides the damping required in (51*b*) while obvious bounds apply to the other factors in the integral. For $|I_3|$ we observe that

$$\int_{2\zeta^{-1}\lambda}^{\lambda} x\, U(x) J_\lambda(x)[(\zeta x)^2 - \lambda^2]^{-\frac{1}{4}}\, \mathrm{d}x \leqslant$$

$$\leqslant \text{const}\, \lambda^{-\frac{1}{3}} \int_0^{\lambda} x\, U(x) J_\lambda(x)\, \mathrm{d}x \leqslant \text{const}\, \lambda^{\frac{1}{3}} \int_0^{\lambda} U(x) J_\lambda(x)\, \mathrm{d}x \leqslant$$

$$\leqslant \text{const}\, \lambda^{\frac{1}{3}} \left\{ \left| \int_0^{\infty} U(x) J_\lambda(x)\, \mathrm{d}x \right| + \left| \int_{\lambda}^{\infty} U(x)\, J_\lambda(x)\, \mathrm{d}x \right| \right\}.$$

The first integral may be explicitly evaluated (11) and with the obvious bound in the second integral the result is in accordance with (51*b*). Finally for I_4 we may use (33*a*) with (A.5) and (48*b*) for $q(\lambda; x)$ together with the asymptotic expansion of Bessel functions for $\Phi_0(\lambda; \zeta x)$ with (51*b*) as the result.

Lastly we investigate $\Omega(\zeta; \lambda)$ for $\lambda \to \pm i\infty$ in which case we have been unable to avoid some rather laborious calculation. We first rewrite (47) as

$$\Omega(\zeta; \lambda) = -\frac{\pi}{2} A \zeta^{\frac{1}{3}} \int_0^{\infty} J^\lambda(\zeta x) \xi(\lambda, x) \exp[-\mu x]\, \mathrm{d}x\,, \tag{B.2}$$

with $\xi(\lambda, x)$ defined by the integral equation

$$\xi(\lambda, x) = J_\lambda(x) + \tfrac{1}{2}\beta(\lambda) \int_0^{x} \xi(\lambda, y) \exp[-\mu y][J_\lambda(x) J_{-\lambda}(y) - J_\lambda(y) J_{-\lambda}(x)]\, \mathrm{d}y\,, \tag{B.3}$$

(*) Ref. (10), p. 241.

(11) P. M. Morse and H. Feshbach: *Methods of Mathematical Physics*, (New York, 1953) vol. 2, p. 1329.

where

$$\beta(\lambda) = \pi(2 \sin \pi\lambda)^{-1} \to \mp i\pi \exp[-\pi a], \qquad \lambda = ia \to \pm i\infty .$$

The first iteration term is easily calculated and is

$$\Omega_1(\zeta : \lambda) = -\tfrac{1}{2}\Lambda Q_{\lambda-\frac{1}{2}}(Z) , \tag{B.4}$$

where $Z = (\mu^2+\zeta^2+1)/2\zeta$. (Note that $Z>1$ for $\mu>0$.)
As $\lambda = ia \to \mp i\infty$ one obtains

$$|\Omega_1(\zeta : \lambda)| \to \frac{\pi}{2}\Lambda(Z^2-1)^{-\frac{1}{4}}(2\pi a)^{-\frac{1}{2}} . \tag{B.5}$$

We now consider the remaining part of the iteration series which cannot be treated exactly. Our method is based on the following heuristic which will be justified at the end of this appendix: the general iteration term contains as its innermost integral

$$\int_0^x J_\lambda(y) \exp[-\mu y][J_\lambda(x)J_{-\lambda}(y) - J_{-\lambda}(x)J_\lambda(y)]\,dy , \tag{B.6}$$

where x is the preceding variable of integration. The Bessel functions for imaginary order will oscillate rapidly when the order becomes large. However the function $J_\lambda(x)J_{-\lambda}(y) - J_\lambda(y)J_{-\lambda}(x)$ (which vanishes at $y=x$) has as its derivative at $y=x$ the Wronskian which does not contain the oscillation. Thus we suspect that the principal contribution at large imaginary order will be obtained by approximating the integral (B.6) by the contribution of that part of the range for which $|y-x|<|\lambda|^{-1}x$. Thus we replace (B.6) by

$$\int_{(1-\delta)x}^{x} J_\lambda(y) \exp[-\mu y][J_\lambda(x)J_{-\lambda}(y) - J_{-\lambda}(x)J_\lambda(y)]\,dy \simeq \tag{B.7}$$

$$\simeq (\beta(\lambda))^{-1}\tfrac{1}{2}\delta^2 x J_\lambda(x) \exp[-\mu x], \qquad \delta = O(|\lambda|^{-1}) .$$

Thus the preceding integral will be of the form

$$\sim \int_0^x x J_\lambda(x)[J_\lambda(x')J_{-\lambda}(x) - J_{-\lambda}(x')J_\lambda(x)] \exp[-2\mu x]\,dx ,$$

which may then be treated according to the same approximation. In this

fashion we obtain the contribution for the entire series with the result:

$$\text{(B.8)} \qquad \Omega(\zeta:\lambda) \xrightarrow{\lambda\to\pm i\infty} \int_0^\infty \exp[-\mu x] J_\lambda(\zeta x) J_\lambda(x) \left[1 + \frac{\Lambda\delta^2}{2} x \exp[-\mu x]\right]^{-1} \mathrm{d}x\,.$$

While one is inclined then to write $\Omega(\zeta:\lambda) \to \Omega_1(\zeta:\lambda)$, $\lambda \to \pm i\infty$ if $\delta \to 0$ as $|\lambda| \to \infty$ it may be seen from an examination of the general term (*) that this is the case only if $\delta \to 0$ as $|\lambda| \to \infty$ faster than $|\lambda|^{-\frac{1}{2}}$.

We conclude now with a justification of our approximation. We shall indicate the proof only in the second iteration term but it will be obviously generalizable. Consider the integral (**)

$$\int_0^\infty \exp[-\mu x] J_\lambda(\zeta x) J_{-\lambda}(x)\,\mathrm{d}x \int_0^x \exp[-\mu y]\, J_\lambda(y) J_\lambda(y)\,\mathrm{d}y =$$

$$= \int_0^1 \mathrm{d}t \int_0^\infty x \exp[-\mu(1+t)x]\,\mathrm{d}x J_\lambda^2(tx)\, J_\lambda(\zeta x) J_{-\lambda}(x) =$$

$$= \int_0^1 \mathrm{d}t\, \frac{\zeta^\lambda}{\Gamma(\lambda+1)} \sum_{m=0}^\infty \frac{(-4)^{-m} F_1(-m,\ \lambda-m,\ \lambda+1, \zeta^2)}{m!\,\Gamma(-\lambda+m+1)} \int_0^\infty x^{2m+1} \exp[-\mu(1-t)x] J_\lambda^2(tx)\,\mathrm{d}x\,.$$

But (***)

$$\int_0^\infty x^{2m+1} \exp[-\mu(1+t)x] J_\lambda^2(tx)\,\mathrm{d}x = \left(-\frac{\mathrm{d}}{\mathrm{d}\varrho}\right)_{\varrho=0}^{m+1} \frac{1}{\pi t} Q_{\lambda-\frac{1}{2}}\left(1 + \frac{(\varrho+\mu(1-t))^2}{2t^2}\right) \to$$

$$\xrightarrow{\lambda\to i\infty} \left(-\frac{\mathrm{d}}{\mathrm{d}\varrho}\right)_{\varrho=0}^{m+1} (\pi t)^{-1} \left(\frac{\pi}{2\lambda}\right)^{\frac{1}{2}} (Z^2-1)^{-\frac{1}{4}} \left(Z - (Z^2-1)^{\frac{1}{2}}\right)^\lambda,$$

where

$$Z = 1 + \frac{(\varrho+\mu(1-t))^2}{2t^2}\,.$$

Applying the method of steepest descent to the oscillating factor $\left(Z - (Z^2-1)^{\frac{1}{2}}\right)^\lambda$ we conclude that the principal contribution arises from the neighborhood

(*) Replacing powers of x by differentiations with respect to μ and using (B.4).
(**) Ref. ([10]), p. 148.
(***) See (B.4).

of $t=1$ of length $|\lambda|^{-1}$. Next consider the integral

$$\int_0^\infty \exp[-\mu x] J_\lambda(\zeta x)\, J_\lambda(x)\, \mathrm{d}x \int_0^x \exp[-\mu y]\, J_\lambda(y) J_{-\lambda}(y)\, \mathrm{d}y =$$

$$= \int_0^1 \mathrm{d}t\, \frac{1}{\Gamma(\lambda+1)} \sum_{m=0}^{\infty} \frac{(-4)^{-m} F_1(-m,\, \lambda-m,\, \lambda+1,\, 1)}{m!\, \Gamma(-\lambda+m+1)}\, t^{2m} \cdot$$

$$\cdot \left(-\frac{\mathrm{d}}{\mathrm{d}\varrho}\right)_{\varrho=0}^{m+1} \frac{1}{\pi \zeta^{\frac{1}{2}}}\, Q_{\lambda-\frac{1}{2}}\left(\frac{1+\zeta^2+(\mu(1+t)+\varrho)^2}{2\zeta}\right).$$

Proceeding as above we obtain the stated result. The same techniques can be applied in every iteration term with the same result (*).

(*) For $\zeta \geqslant 1$ it is possible to obtain these results more elegantly by means of the addition theorems (ref. [10], p. 367).

RIASSUNTO

Si dimostra la validità di una doppia regola di dispersione sull'impulso trasferito e sulla energia uscente per lo scattering da un potenziale di Yukawa fuori dall'energy shell, quando si mantenga fissa e reale l'energia entrante. Si mostra che l'unitarietà determina in questo caso l'ampiezza fuori dall'energy shell in termini dell'ampiezza sull'energy shell. Si descrivono le proprietà analitiche dell'ampiezza fuori dall'energy shell sui foglietti non fisici della superficie di Riemann, e si espongono alcuni risultati sul dominio di analiticità nelle due variabili energetiche.

IL NUOVO CIMENTO Vol. XXII, N. 2 16 Ottobre 1961

Mass Anisotropy and Planetary Motion (*).

E. V. Ivash and R. F. Sweet

University of Texas - Austin, Tex.

(ricevuto il 28 Luglio 1961)

Summary. — The consequences of mass anisotropy for planetary motion are investigated. A precession of the perihelion in the plane of the orbit is predicted. Application of the theory to Mercury establishes an upper limit for the mass anisotropy ratio of $1.57 \cdot 10^{-10}$ for planetary systems.

1. – Introduction.

It has been suggested by Cocconi and Salpeter [1] that, as a consequence of Mach's principle, which postulates that the inertia of a test body is a function of the total mass of the universe as well as its distribution, inertial mass may be anisotropic. Several investigations [2] have attempted to detect and measure such an anisotropy for atomic and nuclear systems.

The main purpose of this article is to report an investigation on the effect of a possible anisotropy of inertia on planetary motion. It may be anticipated here that precession of the perhelion of a planet is predicted by the theory. The results obtained are applied in particular to the motion of Mercury. Other implications of anisotropy of mass for planetary motion are also examined.

It must be admitted that none of the experimental investigations reported

(*) Part of a thesis submitted by one of us (R.F.S.) in partial fulfillment of the requirements for the M. S. degree, Department of Physics, University of Texas.

(1) G. Cocconi and E. Salpeter: *Nuovo Cimento*, **10**, 646 (1958).

(2) R. V. Pound and G. A. Rebka, Jr.: *Phys. Rev. Lett.*, **3**, 554 (1959); C. W. Sherwin, H. Frauenfelder, E. L. Garwin, E. Lüscher, S. Margulies and R. N. Peacock: *Phys. Rev. Lett.*, **4**, 399 (1960); V. W. Hughes, H. G. Robinson and V. Beltran Lopez: *Phys. Rev. Lett.*, **4**, 342 (1960).

thus far have detected an observable mass anisotropy. In fact, the nuclear magnetic resonance experiments of HUGHES *et al.* [2] have yielded the very small value of 10^{-20} for the upper limit of the mass anisotropy ratio. In view of this minute figure it is appropriate to justify the *raison d'être* of the present theoretical investigation which, as shall be seen, yields a considerably greater upper limit of about 10^{-10}. It is evident, of course, that only by actually performing the pertinent calculations for a particular experimental situation is it possible to obtain an estimate which can be compared with previous results. However, the chief significance of the present investigation does not rest alone with this consideration.

We should like to emphasize, therefore, that the problem of planetary motion is the first yet considered dealing with the effect of mass anisotropy on a system which is neither atomic nor nuclear. It is entirely conceivable that the effect might be detectable on a macroscopic level but not on a microscopic level, just as, for example, the precession predicted by the general theory of relativity has been observed for a planetary system, but, as yet, there is no evidence of such an effect for atomic and nuclear systems. In addition, mass anisotropy possibly may be accompanied by a corresponding charge anisotropy in which the Coulomb force between two charges is a function of the direction of the relative acceleration. Such an effect, having the proper magnitude and functional dependence, might account for the negative results obtained thus far for nuclear and atomic systems. Planetary motion, depending only on a gravitational field, would, of course, not be subject to such a possible compensation.

2. – Basic relations.

The most obvious anisotropy in the distribution of matter with respect to the solar system is, as has been pointed out by COCCONI and SALPETER [1], that of the galaxy itself. It may be assumed [1] that the contribution to the inertial mass of a test body by a mass M is proportional to

$$\frac{M|\cos\theta|}{|\boldsymbol{r}|^{\nu}},$$

here $\boldsymbol{r}$ is the position vector of M, ν is a constant whose value remains to be determined, and θ is the angle between $\boldsymbol{r}$ and the direction of acceleration of the test body. As a consequence of this assumption the inertial mass of a test body should be greatest for acceleration toward or away from the galactic center.

For a non-isotropic mass distribution the generalization of Newton's second

law of motion is

$$F_i = \sum_j m_{ij} a_j \,, \tag{1}$$

where F_i and a_j are the components of force and acceleration, respectively, and m_{ij} are the components of the mass tensor (1). It is evident that, in general, $\boldsymbol{F}$ and $\boldsymbol{a}$ are not mutually parallel. The present calculations are based on this fundamental equation.

The mass tensor can be diagonalized by taking the line to the center of the galaxy as one of the principal axes. It may readily be shown that the mass tensor then has the diagonal elements $m+\Delta m$ and $m-\frac{1}{2}\Delta m$, corresponding to this principal axis and to the other two principal axes, respectively, where m is the isotropic contribution to the mass and $\Delta m/m \ll 1$. Assuming that the anisotropy is due entirely to the galaxy, COCCONI and SALPETER (1) have derived for the mass anisotropy ratio $\Delta m/m$ the expression

$$\frac{\Delta m}{m} = \frac{M}{r^\nu} \frac{3-\nu}{4\pi\varrho R^{3-\nu}} \,,$$

where ϱ is the average mass density of the universe, R is its radius, and r is the distance to the galactic center

3. – The effect of mass anisotropy on simple harmonic motion.

We begin by considering the effect of mass anisotropy on simple harmonic motion. The reason for this is, as will be shown in Section **4**, that for an almost circular planetary orbit, which is of greatest present interest, the equations of motion can be approximated by the simple harmonic equations of motion in three dimensions. In particular, the rate of precession of an almost circular planetary orbit is given by the appropriate simple harmonic expression modified in a trivial way.

We consider first the two-dimensional motion of a particle in the x-y plane under the action of an isotropic, simple harmonic restoring force, the plane of motion containing the galactic line. By «galactic line» we mean the position vector from the center of the given orbit to the center of the galaxy. Choosing the x-axis along the galactic line, we have from eq. (1)

$$\begin{cases} F_x = m_x \ddot{x} = -kx \,, \\ F_y = m_y \ddot{y} = -ky \,, \end{cases} \tag{2}$$

where k is the isotropic force constant, $m_x = m_{xx}$, $m_y = m_{yy}$, and all other components of the mass tensor are zero. Since $F_z = 0$ it is clear that the motion of the particle will be confined in the x-y plane in the absence of an initial velocity perpendicular to that plane.

The solutions of eq. (2) are

$$(3) \qquad \begin{cases} x = A \sin(\omega_x t + \alpha), \\ y = B \sin(\omega_y t + \beta), \end{cases}$$

where

$$(4) \qquad \omega_x = \sqrt{\frac{k}{m_x}}, \qquad \omega_y = \sqrt{\frac{k}{m_y}},$$

A and B are amplitudes, and α and β are the phase factors.

Eliminating the time t between these two relations, the equation of the orbit may be written

$$(5) \qquad y = B \sin\left(\beta - \alpha\frac{\omega_y}{\omega_x} + \frac{\omega_y}{\omega_x}\sin^{-1}\frac{x}{A}\right).$$

For $m_x = m_y$, or for $\omega_x = \omega_y$, eq. (5) becomes,

$$(6) \qquad y = B \sin\left(\varphi_0 + \sin^{-1}\frac{x}{A}\right),$$

or

$$(Ay - Bx\cos\varphi_0)^2 = B^2(A^2 - x^2)\sin^2\varphi_0,$$

where

$$\varphi_0 = \beta - \alpha,$$

an equation of an ellipse. Introducing polar co-ordinates in eq. (6), one obtains

$$(7) \qquad r\sin\theta = \frac{B}{A} r\cos\varphi_0\cos\theta + \frac{B}{A}\sqrt{A^2 - r^2\cos^2\theta}\sin\varphi_0.$$

The perihelion angle θ_0 for $m_x = m_y$ is determined from the condition $dr/d\theta = 0$. Squaring eq. (7), and differentiating with respect to θ yields

$$(8) \qquad \operatorname{tg} 2\theta_0 = \frac{2AB}{A^2 - B^2}\cos\varphi_0,$$

which expresses the perihelion angle of the elliptical orbit as a function of the amplitudes A and B and the phase difference φ_0.

Next, we consider the case for which $m_x \neq m_y$ with $\delta m = m_y - m_x$, and $|\delta m| \ll m_x$. The angular frequencies are now given by

$$\omega_x = \sqrt{\frac{k}{m_x}}, \qquad \omega_y = \sqrt{\frac{k}{m_x + \delta m}}. \tag{9}$$

Defining

$$\delta\omega = \omega_y - \omega_x \simeq -\frac{\omega_x}{2}\frac{\delta m}{m_x}, \tag{10}$$

and substituring into eq. (5) one obtains

$$y = B \sin\left|\varphi_0 + \delta\omega t + \sin^{-1}\frac{x}{A}\right|. \tag{11}$$

It is plausible (and may be justified [3]) that for $|\delta m| \ll m_x$ the aphelion angle is given to a very good approximation by eq. (8) with the phase difference φ_0 on the right hand side replaced by $\varphi = \varphi_0 + \delta\omega t$. Then,

$$\operatorname{tg} 2\theta_0 = \frac{2AB}{A^2 - B^2}\cos\varphi\,. \tag{12}$$

Differentiating with respect to t, one gets for the rate of precession of the perihelion, Ω, the expression

$$\Omega = -\frac{S\,\delta\omega\sin\varphi}{4S^2\cos^2\varphi + 1}, \tag{13}$$

where

$$S = \frac{AB}{A^2 - B^2}. \tag{14}$$

The average precessional velocity may readily be shown to be

$$\Omega_{av} = \frac{\delta\omega}{\pi}\operatorname{tg}^{-1} 2S\,.$$

---

[3] R. F. SWEET: *M. S. Thesis*, University of Texas (1961), unpublished.

As might be expected, the precessional velocity, average or instantaneous, is directly proportional to the mass anisotropy ratio through the $\delta\omega$ term.

If the orbit were perpendicular to the galactic line, then m_x and m_y would be equal, and there would be no precession of the orbit. For the general situation in which the galactic line is oriented in an arbitrary direction with respect to the orbit it is clear that the motion of the particle is not confined to a plane.

For the general case we define the z-axis to be along the galactic line. Application of eq. (1) now results in three harmonic equations with masses m_x, m_y, and m_z. However, for our particular choice of the z-axis, $m_x = m_y$, and it is clear that as a consequence the projection of the orbit onto the x-y plane exhibits no precession. The precessional velocities, Ω_x and Ω_y, about the x and y axes, respectively, may be obtained by application of eq. (13) for the two-dimensional case. The results are

$$\Omega_x = -\frac{S_x \delta\omega_x \sin\varphi_x}{4S_x^2\cos^2\varphi_x + 1}\,, \tag{15a}$$

$$\Omega_y = -\frac{S_y \delta\omega_y \sin\varphi_y}{4S_y^2\cos^2\varphi_y + 1}\,, \tag{15b}$$

where

$$S_x = \frac{BC}{B^2 - C^2}\,, \qquad S_y = \frac{CA}{C^2 - A^2}\,, \tag{16a, b}$$

$$\delta\omega_x = \omega_z - \omega_y\,, \qquad \delta\omega_y = \omega_x - \omega_z\,, \tag{17a, b}$$

and

$$\operatorname{tg} 2\theta_{0x} = 2S_x\cos\varphi_x\,, \tag{18a}$$

$$\operatorname{tg} 2\theta_{0y} = 2S_y\cos\varphi_y\,. \tag{18b}$$

4. – The effect of mass anisotropy on planetary motion.

In this section we consider the effect of mass anisotropy for a body moving under the action of an inverse-square gravitational force. Suppose first that the galactic line is in the plane of the orbit with the x-axis along the galactic line. Application of eq. (1) yields (disregarding reduced mass corrections)

$$\begin{cases} F_x = m_x\ddot{x} = -\dfrac{Gm_xM_xx}{r^3}\,, \\ F_y = m_y\ddot{y} = -\dfrac{Gm_yM_yy}{r^3}\,, \end{cases} \tag{19}$$

where $m_x = m_{xx}$, $m_y = m_{yy}$, are the mass components of the moving body, and $M_x = M_{xx}$, $M_y = M_{yy}$ are the mass components of the central mass. Newton's Law of Universal Gravitation has been utilized, assuming equivalence of inertial and gravitational mass, G being the constant of universal gravitation.

Some sort of approximation appears necessary to solve eq. (19). Since it is our intention to apply the results of the theory to solar planetary motions it is appropriate to restrict the present discussion to orbits which are nearly circular. One may then write

$$r = R + s \,, \tag{20}$$

where R is a constant, and $|s| \ll R$. Substituting eq. (20) into eq. (19), and expanding in powers of s, one obtains

$$\ddot{x} + \frac{GM_x}{R^3}\left(1 - \frac{3s}{R}\right)x = 0 \,,$$

$$\ddot{y} + \frac{GM_y}{R^3}\left(1 - \frac{3s}{R}\right)y = 0 \,,$$

where terms of higher order in s have been neglected. It may, in fact, be shown [3] that the zeroth order equations, obtained by neglecting terms proportional to s, give an excellent approximation to the rate of precession for a nearly circular orbit. The zeroth order equations are then

$$\left\{\begin{aligned} &\ddot{x} + \frac{GM_x}{R^3}x = 0 \,, \\ &\ddot{y} + \frac{GM_y}{R^3}y = 0 \,, \end{aligned}\right. \tag{21}$$

which are identical in form to eq. (2) for the simple harmonic oscillator. Hence, the solutions can again be written in the form

$$\left\{\begin{aligned} &x = A \sin(\omega_x t + \alpha) \,, \\ &y = B \sin(\omega_y t + \beta) \,, \end{aligned}\right. \tag{22}$$

where

$$\omega_x = \sqrt{\frac{GM_x}{R^3}} \,, \qquad \omega_y = \sqrt{\frac{GM_y}{R^3}} \,. \tag{23}$$

It follows immediately that, to the zeroth order of approximation, the equation

for the precessional velocity of the perihelion of a planetary orbit is identical in form to the equation for a simple harmonic orbit.

5. – The effect of mass anisotropy on the motion of Mercury.

It is our intention in this section to apply the results of the preceding sections to the determination of the rate of precession of Mercury's orbit due to mass anisotropy. Using standard astronomical data [4] extrapolated to the year 1961 one finds that the orientation of Mercury's orbit with respect to the galactic line may be specified by the following angles:

$$\chi = 170^\circ 59' , \qquad \psi = 91^\circ 14' ,$$

where χ and ψ are the angles between the galactic line and the perihelion line and the perpendicular to Mercury's orbit, respectively. It is to be noted that the galactic line is almost in the plane of the orbit of Mercury, so that any anisotropy effect should very nearly be maximum.

Choosing the z-axis coincident with the galactic line with the y-axis in the plane of the orbit, it is clear that $\Omega_z = 0$. Since the y-axis by definition is in the plane of the orbit, the projection of the orbit onto the x-z plane is a straight line. From eq. (11) (expressed in terms of x and z) the phase angle φ_y must then be a multiple of π. Consequently, $\Omega_y = 0$, and there is no precession about the y-axis. The precession is entirely about the x-axis.

Using the above values for the angles χ and ψ, and other necessary astronomical data [4] for the orbit of Mercury, a somewhat lengthy, though straightforward calculation based on eqs. (15a), (16a), (17a), and (18a) yields the result

$$\Omega_x = (5.98 \cdot 10^9) \frac{\delta m}{m} \text{ seconds of arc per century} , \tag{24}$$

for the rate of precession about the x-axis. Resolving Ω_x into a component Ω_x' perpendicular to the plane of Mercury, and a component Ω_x'' in the plane of Mercury, one obtains

$$\Omega_x' = (5.98 \cdot 10^9) \frac{\delta m}{m} \text{ seconds of arc per century} , \tag{25a}$$

$$\Omega_x'' = (1.29 \cdot 10^8) \frac{\delta m}{m} \text{ seconds of arc per century} . \tag{25b}$$

[4] C. W. ALLEN: *Astrophysical Quantities* (London, 1955).

Ω'_x is the usual precessional velocity of the perihelion, while Ω''_x is the precessional velocity of the perihelion about an axis lying in the plane of the orbit. For the case of Mercury the latter angular velocity is nearly two orders of magnitude smaller than the former, corresponding to the fact that the galactic line is nearly in the plane of the orbit.

The direction of motion of the perihelion of Mercury with respect to the motion of the planet may be determined by an inspection of eq. (15*a*) for the precessional velocity. The denominator, of course, is always positive. The parameters specifying the orbit of Mercury are such that S_x is negative. From eq. (17*a*) $\delta\omega_x$ is positive. Thus, the sign of Ω_x is the same as the sign of $\sin\varphi_x$. However, an examination of the simple harmonic equations of motion shows that a positive $\sin\varphi_x$ corresponds to negative, or clockwise rotation around the x-axis, so that the precession and rotation are in opposite directions to each other. For a negative $\sin\varphi_x$ the orbital motion is reversed, but so is the precessional velocity, so that in all cases the two motions are in opposite directions.

It is well known that within experimental error general relativity can account for that portion of the precession of Mercury's orbit not explainable by classical mechanics. Recent experimental and theoretical values [5] for this precession are:

Experimental:	$42.56 \pm .94$	seconds of arc per century,
Theoretical:	$43.03 \pm .03$	seconds of arc per century.

The difference between these two values is $.47 \pm .94$ seconds of arc per century, so that they are substantially in agreement. A possible discrepancy has a probable upper limit of 1.41 seconds of arc per century. It is to be noted that the effect of mass anisotropy is to produce a retrograde motion of the perihelion, which thus can compensate for the slight relativistic overestimate for the advance of the perihelion of Mercury. Substitution of the upper limit, $\Omega'_x \leqslant 1.41$ seconds of arc per century into eq. (25*a*) yields the relation

$$\frac{\delta m}{m} \leqslant 2.35 \cdot 10^{-10}. \tag{26}$$

The mass difference, Δm, introduced in Section 2, and generally used by other investigators, is related to δm by the equation $\Delta m = \frac{2}{3}\,\delta m$. In comparing the present results with the previous ones one must therefore use

$$\frac{\Delta m}{m} \quad 1.57 \cdot 10^{-10}. \tag{27}$$

[5] G. M. Clemence: *Rev. Mod. Phys.*, **19**, 361 (1947).

Though small, this value is large compared with the figure 10^{-20} obtained by HUGHES *et al.* [2] from nuclear magnetic resonance experiments.

A further item of interest with cosmological implications is the long-term effect of a small anisotropy on planetary and galactic motion. For example, the plane of a planetary orbit would tend to « wobble » with respect to the galactic line over a long period of time in a manner roughly similar to that in which a top precesses about the vertical axis. The cumulative effects of a possible anisotropy of mass might become quite noticeable over long periods of time, even for very small mass anisotropy ratios.

6. – Conclusion.

The existence of mass anisotropy, if it could be established with certainty, would be far from mere academic interest, even though such an effect appears to be very small. The basic theoretical structure in nearly all fields would be affected, since the mass of a body nearly always enters directly or indirectly into a physical theory, even though observable effects in most cases would be negligible. The philosophical implications in science would be profound. From the time of Newton there have raged controversies concerning the nature of mass, whether mass is an intrinsic property of matter having, so to say, an independent existence of its own, or whether, as formulated in Mach's principle, it depends in some manner on all other matter in the universe, on the so-called « fixed stars » that serve to define the primary inertial system for the universe [6]. These differences are as yet unresolved. The existence of mass anisotropy would clearly favor the latter point of view, and thus would be certain to be of fundamental importance in the formulation of a future sophisticated cosmological description of the universe.

---

[6] D. W. SCIAMA: *The Unity of the Universe* (New York, 1959).

RIASSUNTO (*)

Si esaminano le conseguenze della anisotropia della massa sul moto dei pianeti. Si prevede una precessione del perielio nel piano dell'orbita. L'applicazione della teoria a Mercurio pone per i sistemi planetari per il rapporto di anisotropia della massa un limite massimo di $1.57 \cdot 10^{-10}$.

(*) *Traduzione a cura della Redazione.*

The Isoscalar Amplitudes for Meson Photoproduction.

A. E. A. Warburton (*) and M. Gourdin

Laboratoire de Physique Théorique et Hautes Energies - Orsay (S.-et-O.)

(ricevuto il 2 Agosto 1961)

Summary. — A detailed investigation is made into the form of the isoscalar amplitudes for meson photoproduction from nucleons, using the Mandelstam technique, for energies up to 250 MeV. The « bipion » approximation to the pion-pion interaction is used, and, in the photoproduction channel, an intermediate $I=\frac{1}{2}=J$ pion-nucleon state is considered. The results are used to obtain satisfactory agreement with the experimental values of $d\sigma^-/d\sigma^+$, giving strong evidence for the existence of the pion-pion resonance. An estimate of the « coupling constant » for the process $\gamma+\pi\to\pi+\pi$ is hence obtained.

1. – Introduction.

A long-standing puzzle (1) in the theory of the photoproduction of π-mesons has been the disagreement between the theoretical predictions, based on the dispersion relations of Chew, Goldberger, Low and Nambu (2), and the experimentally measured cross-sections for the production of charged mesons. In particular, the ratio $d\sigma^-/d\sigma^+$ in the energy range $(170\div250)$ MeV differs significantly from the theoretical predictions.

Recently, the suggestion has been made (3) that the discrepancy may be resolved by a consideration of the pion-pion interaction, in the approximation of a narrow resonance in the $I=1=J$ state. This model has been used to

(*) Permanent address: Pembroke College, Cambridge, U.K.

(1) M. Beneventano, G. Bernardini, G. Stoppini and L. Tau: *Nuovo Cimento*, **10**, 1109 (1958).

(2) G. F. Chew, M. L. Goldberger, F. E. Low and Y. Nambu: *Phys. Rev.*, **106**, 1345 (1957).

(3) M. Gourdin, D. Lurié and A. Martin: *Nuovo Cimento*, **18**, 933 (1960).

explain the isovector part of the nucleon electromagnetic form factors ([4,5]), via the process $\pi+\pi \to N'+\overline{N'}$, and to obtain a theoretical understanding of the process $\gamma+\pi \to \pi+\pi$ ([6]).

Both these latter processes enter into a consideration of meson photoproduction from nucleons, and in ref. ([3]) these results were used to determine the effect of such a resonance on the isoscalar amplitudes for meson photoproduction. Neglecting intermediate pion-nucleon states in the photoproduction channel, it was shown that the results were reproduced by the Born contribution of the « bipion », an isovector vector boson. The ratio $d\sigma^-/d\sigma^+$ is insensitive to small charges in the isovector amplitudes, and the effect on these may be neglected. The solution contains an unknown constant, A, the « coupling constant » for the process $\gamma+\pi \to \pi+\pi$, which may be determined by fitting the experimental data.

The fitting of the data will, however, be extremely sensitive to small corrections to the isoscalar amplitudes, and for this reason we calculate the effect of an intermediate pion-nucleon state $(I=\frac{1}{2}, J)$, in the photoproduction channel.

Comparison of theoretical and experimental values of $d\sigma^-/d\sigma^+$, at various energies and angles, will then give a critical test of the theory, and a reasonably reliable value of A, which can be applied to the theory of Compton scattering on nucleons.

2. – Outline of procedure.

In ref. ([3]) the isoscalar amplitudes were written as the sum of Born and « bipion » contributions. In Sect. **3** to **6** we consider the corrections to this approximation due to the effects of the indeterminate $I=\frac{1}{2}=J$ pion-nucleon state. This affects only the electric dipole amplitude, E_{0+}.

In Sect. **3**, the kinematics of the process are recalled. The effect of the $J=\frac{1}{2}=J$ state on the invariant amplitudes A, B, C, D is considered in Sect. **4**, with a view to determining the kinematical factor by which E_{0+} must be multiplied in writing a dispersion relation.

The dispersion relation for E_{0+} takes the form of an inhomogeneous Mushkelishvili-Omnès integral equation, and the solution may be written down directly in terms of the singularities of the Born and bipion contributions (Sect. **5**).

([4]) W. Frazer and J. Fulco: *Phys. Rev.*, **117**, 1609 (1960).
([5]) J. Bowcock, N. Cottingham and D. Lurié: *Nuovo Cimento*, **16**, 918 (1960).
([6]) M. Gourdin and A. Martin: *Nuovo Cimento*, **16**, 78 (1960).

The experimental values of the pion-nucleon phase shift δ_l are then used to perform a numerical evaluation of the correction to E_{0+}, and hence of those to the $\mathscr{F}_i$, in terms of which the ratio $d\sigma/d\sigma^+$ are evaluated, using the CGLN form of the isovector amplitudes (Sect. 6). Hence an estimate is obtained for the « coupling constant », A, for the process $\gamma+\pi\to\pi+\pi$.

3. – Kinematics.

We first summarize the relevant formulae pertaining to the kinematics of the process of Fig. 1, following the notation of CGLN.

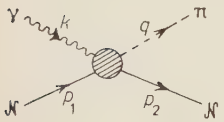

Fig. 1.

The transition matrix element may be written in the form

$$(1)\qquad T_{fi}=\bar{u}_f(p_2)\{\delta_{3\alpha}H^+ + \tfrac{1}{2}[\tau_\alpha,\tau_3]H^- + \tau_\alpha H^0\}u_i(p_1)\,,$$

where α denotes the isospin of the π-meson and $u(p)$ is a Dirac spinor, normalized according to $\bar{u}u=1$.

Each function H may be decomposed in the form

$$(2)\qquad H = AM_A + BM_B + CM_C + DM_D\,,$$

where A, B, C, D are functions of $W^2=-(p_1+k)^2$ and $t=-(p_1-p_2)^2$, and

$$(3)\qquad \begin{cases} M_A = i\gamma_5(\gamma\cdot\varepsilon)(\gamma\cdot k)\,,\\ M_B = 2i\gamma_5[(P\cdot\varepsilon)(q\cdot k)-(P\cdot k)(q\cdot\varepsilon)]\,,\\ M_C = \gamma_5[(\gamma\cdot\varepsilon)(q\cdot k)-(\gamma\cdot k)(q\cdot\varepsilon)]\,,\\ M_D = 2\gamma_5[(\gamma\cdot\varepsilon)(P\cdot k)-(\gamma\cdot k)(P\cdot\varepsilon)-iM(\gamma\cdot\varepsilon)(\gamma\cdot k)]\,, \end{cases}$$

ε being the photon polarization, and $P=\frac{1}{2}(p_1+p_2)$. We take the pion mass as unity throughout.

In the centre of mass system for the photoproduction channel we set $k=(k,\boldsymbol{k})$; $p_1=(E_1,-\boldsymbol{k})$; $q=(\omega,\boldsymbol{q})$; $p_2=(E_2,-\boldsymbol{q})$, so that

$$(4)\qquad \begin{cases} E_1=\dfrac{W^2+M^2}{2W}\,, & E_2=\dfrac{W^2+M^2-1}{2W}\,,\\ \omega=\dfrac{W^2-M^2+1}{2W}\,, & k=\dfrac{W^2-M^2}{2W}\,. \end{cases}$$

Then the differential cross-section for meson production is

$$\frac{\mathrm{d}\sigma}{\mathrm{d}\Omega} = \frac{q}{k} |\langle 2 | \mathscr{F} | 1 \rangle|^2 , \tag{5}$$

where $|i\rangle$ is a Pauli spinor, and, for a given isotopic spin configuration, $\mathscr{F}$ may be written

$$\mathscr{F} = i\boldsymbol{\sigma}\cdot\boldsymbol{\epsilon}\mathscr{F}_1 + \frac{(\boldsymbol{\sigma}\cdot\boldsymbol{q})\boldsymbol{\sigma}\cdot(\boldsymbol{k}\times\boldsymbol{\epsilon})}{qk}\mathscr{F}_2 + \frac{i(\boldsymbol{\sigma}\cdot\boldsymbol{k})(\boldsymbol{q}\cdot\boldsymbol{\epsilon})}{qk}\mathscr{F}_3 + \frac{i(\boldsymbol{\sigma}\cdot\boldsymbol{q})(\boldsymbol{q},\boldsymbol{\epsilon})}{q^2}\mathscr{F}_4 . \tag{6}$$

The multipole amplitudes may be projected from the $\mathscr{F}_i$, we shall only need the electric dipole amplitude, E_{0+}, given by

$$E_{0+} = \frac{1}{2}\int_{-1}^{1} \mathrm{d}x \left[\mathscr{F}_1 - x\mathscr{F}_2 + \frac{1-x^2}{2}\mathscr{F}_4\right], \tag{7}$$

where x is the cosine of the angle of emission in the barycentric system. The functions $\mathscr{F}_i$ are related to A, B, C, D by

$$\begin{cases} F_1 = \dfrac{1}{N}\mathscr{F}_1 = A + (W-M)D - \dfrac{(k\cdot q)}{W-M}(C-D) , \\ F_2 = \dfrac{M+E_2}{qN}\mathscr{F}_2 = -A + (W+M)D - \dfrac{(k\cdot q)}{W+M}(C-D) , \\ F_3 = \dfrac{1}{qN}\mathscr{F}_3 = (W-M)B + (C-D) , \\ F_4 = \dfrac{M+E_2}{q^2N}\mathscr{F}_4 = -(W+M)B + (C-D) , \end{cases} \tag{8}$$

where

$$N = \frac{W-M}{8\pi W}[(M+E_1)(M+E_2)]^{\frac{1}{2}} . \tag{9}$$

4. – Unitarity and choice of amplitude.

The Born and bipion terms indicate that we should assume Mandelstam representations for the isoscalar amplitudes A, B, C, D; then the analytic properties of the multipole amplitudes may be deduced. We make the following approximations to the unitarity condition in the various channels:

(i) In the photoproduction channel, we consider only the $I = \frac{1}{2} = J$ pion-nucleon state, since the phases of the multipole amplitudes are given

by the corresponding pion-nucleon phase shifts in the $I = \frac{1}{2}$ state, which are all very small except δ_1, in the considered energy range (0 ÷ 300) MeV.

(ii) In the crossed photoproduction channel ($\gamma + \overline{\mathcal{N}} \to \pi + \overline{\mathcal{N}}$) we neglect the absorptive parts, since these will give a small contribution compared with (i) which is already a small correction.

(iii) In the channel $\gamma + \pi \to \mathcal{N} + \overline{\mathcal{N}}$ we replace the effect of the two-pion intermediate state by the Born contribution of the bipion, an isovector vector boson.

Thus, only the amplitude E_{0+} has an absorptive part, the other amplitudes are given as the sum of Born and bipion parts. Writing $F_i = F_i^{\text{Born}} + F_i^{\text{bipion}} + \delta F_i$, etc., we see that $\delta F_2 = \delta F_3 = \delta F_4 = 0$, or, in terms of the amplitudes A, B, C, D:

$$\text{(10)} \qquad \begin{cases} \delta A = \dfrac{W + M}{2W} \delta F_1 , \\ \delta B = 0 , \\ \delta C = \dfrac{1}{2W} \delta F_1 = \delta D . \end{cases}$$

From (7), (8), (10) and the fact that A, B, C, D have Mandelstam representations, we see that $(1/N)E_{0+}$ has only the physical cut in addition to the singularities of its Born and bipion terms.

5. – Integral equation for E_{0+}.

The results of the last section show that if we set

$$\text{(11)} \qquad \bar{E}_{0+} = \frac{1}{N} E_{0+} ,$$

we may write a dipersion relation for $\bar{E}_{0+}$, viz.

$$\text{(12)} \qquad \bar{E}_{0+}(W) = \bar{E}_{0+}^{\text{Born}}(W) + \bar{E}_{0+}^{\text{bipion}}(W) + \frac{1}{\pi} \int_{M+1}^{\infty} \frac{E_{0+}(W') \exp\left[-i\delta_1(W_1)\right] \sin \delta_1(W')}{W' - W - i\varepsilon} \, \mathrm{d}W' ,$$

using the fact that the phase of E_{0+} on the physical cut is δ_1 and assuming that the integrand vanishes sufficiently fast at infinity so that the integral converges.

Since $\bar{E}_{0+}^{\text{Born}}$ and $\bar{E}_{0+}^{\text{bipion}}$ are known functions of W, (12) is an inhomogeneous Mushkelishvili-Omnès integral equation [7], whose solution may be written down directly in terms of the singularities of $\bar{E}_{0+}^{\text{Born}}$ and $\bar{E}_{0+}^{\text{bipion}}$.

5·1. *Singularities of* $\bar{E}_{0+}^{\text{Born}}$. – The Born terms of A, B, C, D are given in CGLN, whence (8) and (7) give

$$(13)\quad \bar{E}_{0+}^{\text{Born}} = \frac{-4M\alpha}{W^2-M^2} - \frac{2M^2\alpha}{(W-M)^2(W+M)} + \frac{4M^2\beta}{W^2-M^2} - \frac{M\beta}{W-M} - \frac{M\beta}{W+M} + \\ + \left(\alpha - M\beta + \frac{M\alpha}{W-M}\right)\frac{4MW^2}{[(W-M)^2-1](W^2-M^2)}\left(1+\frac{M}{2q}\log\frac{E_2+q}{E_2-q}\right),$$

where we have set $\alpha = -\frac{1}{2}e_r f_r$; $\beta = \frac{1}{2}f_r(\mu_{Pr}+\mu_{Nr})$ with

$$(14)\qquad \mu_{Pr} = 1.79\,\frac{e_r}{2M}\,; \qquad \mu_{Nr} = -1.91\,\frac{e_r}{2M}\,; \quad \frac{e_r^2}{4\pi} = \frac{1}{137}\,; \quad \frac{f_r^2}{4\pi} = .08\,.$$

Note that $\bar{E}_{0+}^{\text{Born}}$ has no singularities at $W = -M \pm 1$, nor has it kinematical singularities due to the factor $\sqrt{q^2}$. The singularities it has are:

(i) A double pole at $W = M$. The behaviour near here is as

$$(15)\qquad \frac{R_0}{(W-M)^2} + \frac{R_1}{W-M}\,,$$

where

$$(16)\qquad R_0 = (1+A_M)\frac{2M^3\alpha}{4M^2-1} - M\alpha\,,$$

$$(17)\qquad R_1 = -\frac{3}{2}\alpha + M\beta + \frac{2M^2}{4M^2-1}(1+A_M)(3\alpha - M\beta) - \\ - (1+A_M)\frac{M^3\alpha}{4M^2-1}\left(\frac{2B_M}{1+A_M} + \frac{12M^2-1}{4M^3-M}\right),$$

with

$$A_M = P\left\{\frac{M^2}{i\sqrt{4M^2-1}}\log\frac{2M^2-1+i\sqrt{4M^2-1}}{2M^2-1-i\sqrt{4M^2-1}}\right\},$$

$$B_M = \frac{M}{4M^2-1}\left(2 - \frac{2M^2-1}{M^2}A_M\right).$$

(ii) A simple pole at $W = -M$ with residue R_2, where

$$(18)\qquad R_2 = (\alpha - 2M\beta)[\tfrac{3}{2} + M^2(1-A_M)]\,.$$

(7) R. Omnès: *Nuovo Cimento*, **8**, 316 (1958).

(iii) A cut along the whole imaginary axis due to the logarithm. In calculating the discontinuity, the sign of q is specified by the requirement that Im $q \geqslant 0$ for Im $W > 0$, Im $q \leqslant 0$ for Im $W < 0$. The sense of the discontinuity is indicated in Fig. 2.

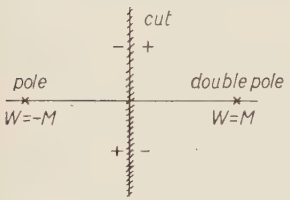

Fig. 2. – The singularities of $\bar{E}_{0+}^{\text{Born}}$.

5·2. *Singularities of* $\bar{E}_{0+}^{\text{bipion}}$. – The bipion contribution to H^0 is given explicitly in ref. [3], it is

$$(19) \qquad H_0^{\text{bipion}} = \lambda \left[\frac{\mathscr{C}_2}{t - t_R} (tM_A - M_B) - \frac{\mathscr{C}_1}{t - t_R} M_D \right],$$

where the values of t_R and $\mathscr{C}_1/\mathscr{C}_2$ may be obtained from ref. [3]. Using (7) and (8), we see that

$$(20) \qquad \bar{E}_{0+}^{\text{bipion}} = \lambda B + \frac{\lambda C}{2kq} \log \frac{1 - 2k\omega - t_R + 2kq}{1 - 2k\omega - t_R - 2kq},$$

with

$$(21) \qquad B = \mathscr{C}_2 - \frac{\frac{1}{2}\mathscr{C}_1}{W - M} + \frac{1}{2k(M + E_2)} \left[\mathscr{C}_2 t_R + (W + M)\mathscr{C}_1 + \frac{1}{2} \frac{t_R - 1}{W + M} \mathscr{C}_1 \right] + \\ + \frac{(W + M)\mathscr{C}_2 + \mathscr{C}_1}{8k^2(M + E_2)} (1 - 2\omega k - t_R),$$

and

$$(22) \qquad C = \frac{1}{2(W - M)} \left[\mathscr{C}_2 t_R (W - M) - (W - M)^2 \mathscr{C}_1 - \frac{1}{2}(t_R - 1)\mathscr{C}_1 \right] + \\ + \frac{1 - 2k\omega - t_R}{4k(M + E_2)} \left[- \mathscr{C}_2 t_R - (W + M)\mathscr{C}_1 - \frac{1}{2} \frac{t_R - 1}{W + M} \mathscr{C}_1 \right] - \\ - \frac{(W + M)\mathscr{C}_2 + \mathscr{C}_1}{4(M + E_2)} \left[\left(\frac{1 - 2k\omega - t_R}{2k} \right)^2 - q^2 \right].$$

Note that $C/2kq$ behaves as W^3 at $W = 0$ and as $1/W^2$ at $W = \infty$. We see that $\bar{E}_{0+}^{\text{bipion}}$ has no poles, nor has it kinematical singularities of the form $\sqrt{q^2}$, the only singularities coming from the logarithm. The branch points (P_i) are given by

$$(23) \qquad W^2 = 0\,, \qquad W^2 = \infty \qquad \text{and} \qquad W^2 = M^2 + (t_R - 1)y\,,$$

where

$$y^2 + y + \frac{M^2}{t_R} = 0\,.$$

The cuts (L_i) defined by taking the principal value of the logarithm are difficult to find. Instead, we note that they enter the solution of (12) in the form

$$\int_{L_i}\left(\frac{\lambda C}{2kq}\right)_{W'}\frac{\exp\left[-\varrho(W')\right]}{W'-W}\,\mathrm{d}W'\,.$$

where ϱ has only the physical cut. We may thus deform the contours of integration (L_i) to new contours (L_i') provided that we avoid the singularities of ϱ and $\lambda C/2kq$, which are

(i) the physical cut,

(ii) poles at $W=\pm M$ and $W=\pm M\pm 1$ (none at $W=0$), and

(iii) cuts from $-M-1$ to $-M+1$ and from $M-1$ to $M+1$ due to the factor q.

Noting that $\sum L_i$ is invariant under $W\to -W$, cannot intersect the physical cut, nor the cuts (iii), we see that we may take L_i' as in Fig. 3, where the sense of the discontinuity is indicated.

With our assumption about the behaviour of the integrand in (12) at infinity, we see that $\bar{E}_{0+}^{\text{bipion}}\sim\lambda\mathscr{C}_2$ at infinity, and so the solution of (12) may be written (uniquely) as

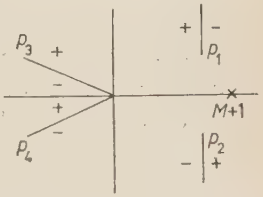

Fig. 3. – The cuts of $\bar{E}_{0+}^{\text{bipion}}$.

$$(24)\quad \bar{E}_{0+}(W)=\exp\left[\varrho(W)+i\delta_1(W)\right]\left\{\lambda\mathscr{C}_2+\exp\left[-\varrho(M)\right]\left(\frac{R_0}{(W-M)^2}+\frac{R_1}{W-M}\right)+\right.$$

$$+\exp\left[-\varrho(-M)\right]\frac{R_2}{W+M}-\int_{\infty}^{0}\mathrm{d}K\,\frac{2KM}{\left[(M^2-1)^2+2K^2(M^2+1)+K^4\right]^{\frac{1}{2}}}\cdot$$

$$\cdot\,\mathrm{Re}\left[\frac{\exp\left[-\varrho(iK)\right]\cdot 4MK^2(\alpha-M\beta+M\alpha/(iK-M))}{(iK-W)(K^2+M^2)[(M+iK)^2-1]}\right]+$$

$$\left.+\sum_i\int_{L_i}\mathrm{d}W'\left(\frac{\pm C}{2kq}\right)_{W'}\frac{\exp\left[-\varrho(W')\right]}{W'-W}\right\},$$

where

$$(25)\qquad \varrho(W)=\frac{P}{\pi}\int_{M+1}^{\infty}\frac{\delta_1(W')}{W'-W}\,\mathrm{d}W'.$$

6. – Numerical evaluation.

Setting $\delta = 0 = \varrho$ in (24) will, of course, give us back $\bar{E}_{0+}^{\text{Born}} + \bar{E}_{0+}^{\text{bipion}}$, hence $\delta F_1 = \delta \bar{E}_{0+}$ may be obtained directly from (24) by replacing $\exp[\varrho(W) - \varrho(M) + i\delta(W)]$ by $[\exp[(\quad) - 1]]$, etc. The residues R_i given by (16), (17), (18) may be expanded in powers of $1/M$ giving

$$(26) \qquad \begin{cases} R_0 = \dfrac{\alpha}{3M} + \dfrac{\alpha}{10M^3} + \dots, \\ R_1 = \dfrac{\alpha - 2M\beta}{6M^2} - \dfrac{\alpha + 2M\beta}{20M^4} + \dots, \\ R_2 = \dfrac{4}{3}(\alpha - 2M\beta) - \dfrac{\alpha - 2M\beta}{30M^2} - \dots. \end{cases}$$

From ref. ([5]), we take the values $t_R = 22.4$; $\mathscr{C}_2/\mathscr{C}_1 = 1.83/M$.

The phase shift δ_1 is determined ([8]) sufficiently accurately for our purposes up to about 100 MeV (laboratory system for pion-nucleon scattering), though above this energy several possible sets of values have been proposed. In order to estimate the high-energy contribution to ϱ we follow the procedure of ref. ([9]), setting $\delta_1 = .13q$. We apply a cut-off at $W = M + 4$, corresponding to a pion energy of about 560 MeV (laboratory system for pion-nucleon scattering). ϱ is best calculated in subtracted form:

$$(27) \qquad \varrho(W) - \varrho(M) = \frac{W - M}{\pi} \int_{M+1}^{M+4} \left(\frac{\delta_1(W')}{W' - M} - \frac{\delta_1(W)}{W - M} \right) \frac{\mathrm{d}W'}{W' - W} - \\ + \frac{\delta_1(W)}{\pi} \log \frac{M + 4 - W}{W - M - 1},$$

since the function $\delta_1(W)/(W - M)$ is approximately constant over much of the range. Note that, apart from the bipion constant term, ϱ only enters the solution in subtracted form.

Values of δ_1 and ϱ for photon energies up to about 250 MeV (laboratory system) are shown in Table I, while the ratios $\delta\mathscr{F}_1^{\text{Born}}/\mathscr{F}_1^{\text{Born}}$ and $\delta\mathscr{F}_1^{\text{b.plou}}/\mathscr{F}_1^{\text{bipion}}$ are shown in Table II. Since the amplitudes to which the corrections are being applied have only small imaginary parts, we need consider only the real parts of the corrections.

([8]) J. Hamilton and W. S. Woolcock: *Phys. Rev.*, **118**, 291 (1960).
([9]) J. Hamilton and T. D. Spearman: *Ann. of Phys.*, **12**, 172 (1961).

TABLE I. – *Values of* δ_1 *and* ϱ *(unsubtracted).*

$W-M$	E_γ (MeV)	δ_1	ϱ
1.0	147	0	.24
1.1	163	.075	.23
1.2	179	.105	.22
1.3	195	.126	.20
1.4	211	.140	.19
1.5	228	.148	.18
1.6	245	.152	.17

In order to calculate the cross-sections, and hence $d\sigma^-/d\sigma^+$, we need values for the isovector amplitudes $\mathscr{F}_i^{(-)}$. It is known ([10]) that approximate agreement with the S-wave coefficients $a_0^\pm$ may be obtained from the CGLN results on

TABLE II. – *Corrections to* $\mathscr{F}_1^{\text{Born}}$ *and* $\mathscr{F}_1^{\text{bipion}}$, *and to* R *due to* $\delta\mathscr{F}_1^{\text{Born}}$. *All at* 90° *(c.m.).*

$W-M$	$\text{Re}\,(\delta\mathscr{F}_1^{\text{Born}}/\mathscr{F}_1^{\text{Born}})$	$\text{Re}\,(\delta\mathscr{F}_1^{\text{bip}}/\mathscr{F}_1^{\text{bip}})$	δR^{Born}
1.0	.21	1.14	.07
1.1	.19	.84	.06
1.2	.17	.66	.05
1.3	.15	.54	.04
1.4	.13	.45	.04
1.5	.12	.37	.03
1.6	.11	.29	.03

the basis of the predominance of the $(\frac{3}{2}, \frac{3}{2})$ pion-nucleon interaction and with $N^{(-)}=0$. This agreement breaks down above 200 MeV. However, since a

TABLE III. – *Values of* $R=d\sigma^-/d\sigma^+$ *for various values of* $K=\lambda\mathscr{C}_1/ef$ *(at* 90°*).*
(Corresponding to $\Lambda=1.5$, 2.2, 3.0, *respectively.)*

$W-M$	$d\sigma^-/d\sigma^+$ $(K=4)$	$d\sigma^-/d\sigma^+$ $(K=6)$	$d\sigma^-/d\sigma^+$ $(K=8)$
1.0	1.30	1.28	1.25
1.1	1.29	1.26	1.23
1.2	1.28	1.25	1.21
1.3	1.27	1.23	1.20
1.4	1.25	1.22	1.18
1.5	1.25	1.21	1.17
1.6	1.24	1.20	1.17

([10]) *Proc. of the 1959 Annual International Conference on High Energy Physics.*

change in the $\mathscr{F}_i^{(-)}$ sufficient to increase a_0^+ by 10% only decreases $R = \mathrm{d}\sigma^-/\mathrm{d}\sigma^+$ by .02, we may safely use these values. On the basis of the discrepancy between the theoretical and experimental values of $a_0^\pm$ above 200 MeV, we may expect our results (at 90°) to over-estimate R slightly above 200 MeV. The correction δR^{Born} due to $\delta\mathscr{F}^{\mathrm{Born}}$ is also shown in Table I.

In Table III we show sets of values of $\mathrm{d}\sigma^-/\mathrm{d}\sigma^+$ at 90°, using corrected values of both Born and bipion terms, for values of $\lambda\mathscr{C}_1/ef = 4, 6, 8$.

7. – Conclusion.

We have thus applied three significant corrections to the theoretical curves given by BENEVENTANO *et al.*, viz.:

(i) the use of the exact expressions for the isoscalar amplitudes, rather than the approximation to order $1/M$ of CGLN,

(ii) the corrections due to the intermediate $I = \frac{1}{2} = J$ pion-nucleon state, which are small enough to indicate that the higher angular-momentum states are safely ignored,

(iii) The bipion approximation to the pion-pion interaction, corrected as under (ii).

We see that a reasonable fit to the data at 90° is obtained with $K = \lambda\mathscr{C}_1/ef \approx 6$, corresponding to $A \approx 2$ in ref. (3). This tends to over-estimate R slightly above 200 MeV, but this is as expected, due to our lack of understanding of the isovector amplitudes. At other angles we get similar agreement; it turns out that R is most sensitive to the bipion contribution at large center-of-mass production angles. At 160°, with $K = 6.0$, we find that R should increase slowly, from 1.36 to 1.39, in the energy range (170 ÷ 250) MeV, in good agreement with the experimental values. In comparison, at 245 MeV, $K = 4.5$ gives $R = 1.50$, $K = 7.5$ gives $R = 1.29$. Thus we have a reasonably reliable estimation of A, despite the large uncertainties in the experimental values of R.

It is important to note that the resultant threshold ratio, 1.28, has hardly been altered by our considerations, and we thus have no difficulty with the well-known connection with the Panofsky ratio (see, for example, ref. (8)). This is due to a cancellation, at threshold, between the bipion and rescattering contributions.

We have thus achieved satisfactory agreement with the experimental values of $\mathrm{d}\sigma^-/\mathrm{d}\sigma^+$ up to 250 MeV, and this may be considered to be strong evidence for the existence of the pion-pion resonance.

It has recently been suggested [11] that the value $t_R = 22.4\mu^2$ may be too large, however, at the momentum transfers we consider ($t/t_R \sim 0(\frac{1}{10})$) a change in t_R would merely cause a corresponding change in K for a satisfactory fit to the data to be reobtained. Thus our method cannot be used to estimate t_R, unless Δ be determined by some other method, or the experimental data greatly improved.

* * *

One of us (A.E.A.W.) wishes to thank Prof. M. LÉVY for hospitality extended to him during his stay at Orsay, where this work was carried out, and also the D.S.I.R. for a maintenance grant.

(11) J. HAMILTON, P. MENOTTI, T. D. SPEARMAN and W. S. WOOLCOCK: *Nuovo Cimento*, **20**, 519 (1961).

RIASSUNTO (*)

Si esamina minutamente la forma delle ampiezze isoscalari per la fotoproduzione di mesoni dai nucleoni, usando la tecnica di Mandelstam per energie fino a 250 MeV. Si usa l'approssimazione dei « bipione » all'interazione pione-pione e si considera nel canale di fotoproduzione uno stato pione-nucleone intermedio $I = \frac{1}{2}$, J. I risultati sono impiegati per ottenere un accordo soddisfacente coi valori sperimentali di $d\sigma^+/d\sigma^-$ che è una prova importante dell'esistenza della risonanza pione-pione. Se ne deduce un valore della « costante d'accoppiamento » per il processo $\gamma + \pi \to \pi + \pi$.

(*) *Traduzione a cura della Redazione.*

IL NUOVO CIMENTO Vol. XXII, N. 2 16 Ottobre 1961

On the Structure of Liquid ^{4}He from the Elastic Scattering of Neutrons.

S. Franchetti

Istituto di Fisica dell'Università - Firenze

(ricevuto il 3 Agosto 1961)

Summary. — The experimentally known angular dependence of the scattering of cold neutrons from liquid ^{4}He has been compared with that calculated for an assembly of very small randomly oriented crystals. The result of this analysis, which constitutes in fact an evaluation of the amount of randomness, has been utilized together with the value of the zero point energy, to determine the two basic parameters appearing in a model proposed for the liquid. This model is equivalent to a statistical description of the fundamental state eigenfunction for the atoms of the liquid and as such it allows the radial distribution function to be calculated, thus permitting a check of the theory by comparison with the experimental radial distribution (from neutron scattering). The agreement is found to be satisfactory.

1. – Introduction.

Liquid ^{4}He is well known to be a quantum liquid, that is a liquid in which the quantum indetermination in the position of the atoms is of the same order as their distance apart. However X-ray and neutron diffraction patterns of liquid helium are strikingly similar to those of « ordinary » monoatomic liquids, suggesting that the structures must be, at least formally, closely related. It seems worth-while investigating this fact, since from its analysis one may hope to gather information about the kind of eigenfunctions appropriate for describing the liquid, at least in the simplest case of its fundamental state.

In previous papers by the Author (1) on liquid helium, use has been made

(1) S. Franchetti: *Nuovo Cimento*, **12**, 743 (1954); *Proc. V International Conference on Low Temperature Physics and Chemistry* (Madison, 1958), p. 128; *Suppl. Nuovo Cimento*, **9**, 286 (1958).

of one-particle eigenfunctions based on the idea that a spherically symmetric « wave packet » — which will be called a φ-function for short — repeats itself throughout the space occupied by the liquid, that is eigenfunctions of the form

$$\psi(\boldsymbol{\rho}) = \sum_n c_n \varphi(|\boldsymbol{\rho} - \boldsymbol{r}_n|) , \tag{1}$$

with the $\boldsymbol{r}_n$ given vectors.

For instance, the fundamental eigenfunction of an assembly of N atoms would obtain as a product of such like eigenfunctions with $c_n = \text{const}$, that is — with Q_N a normalization factor

$$\psi(\boldsymbol{\rho}_1, \boldsymbol{\rho}_2 \cdots \boldsymbol{\rho}_N) = Q_N \prod_{\alpha=1}^{N} \sum_{n=1}^{N-1} \varphi(|\boldsymbol{\rho}_\alpha - \boldsymbol{r}_n|) . \tag{2}$$

An element of arbitrariness, probably inessential, is inherent in the above formulae and this is their giving definite positions to the centers (characterized by the end points of the vectors $\boldsymbol{r}_n$) of the φ-functions. These centers are obviously not fixed. Speaking « classically » one can think of them as being localized at any specified instant, while moving slowly about as time goes on, so as to sweep with statistical uniformity the whole space occupied by the liquid. There is probably some way of embodying such a notion in a rigorous quantum description, but it is doubtful whether the increase of accuracy would compensate for the increase of intricacy. We shall therefore not worry about this kind of arbitrariness.

A second and more important element of arbitrariness, not inherent to the above formulae, was introduced — for the sake of simplicity — in previous work, and this is the assumption that the end points of the r_n vectors form a *perfect lattice*. It was found on this basis, by comparing the radial distribution which follows from (2) with that deduced from neutron scattering by HURST and HENSHAW ([2]), that the most suitable type of lattice is a f.c.c. or hexagonal close packing. (See Fig. 1.)

Now, one should evidently expect the lattice of the $\boldsymbol{r}_n$ not to be rigorously regular and this can be assumed without abandoning neither the idea of the local φ-eigenfunctions, nor the formulae (1), (2) themselves.

The present work is essentially an attempt to evaluate the degree of departure of the $\boldsymbol{r}_n$ lattice from absolute regularity through a more detailed analysis of the neutron scattering data. Of course an additional source of randomness could arise if the local φ-functions themselves were thought to vary from site to site. This possibility cannot be ruled out a priori. It will however not be

([2]) D. G. HURST and D. G. HENSHAW: *Phys. Rev.*, **100**, 994 (1955).

considered, again for simplicity's sake, or at least we shall admit that we can work with an « average » φ-function.

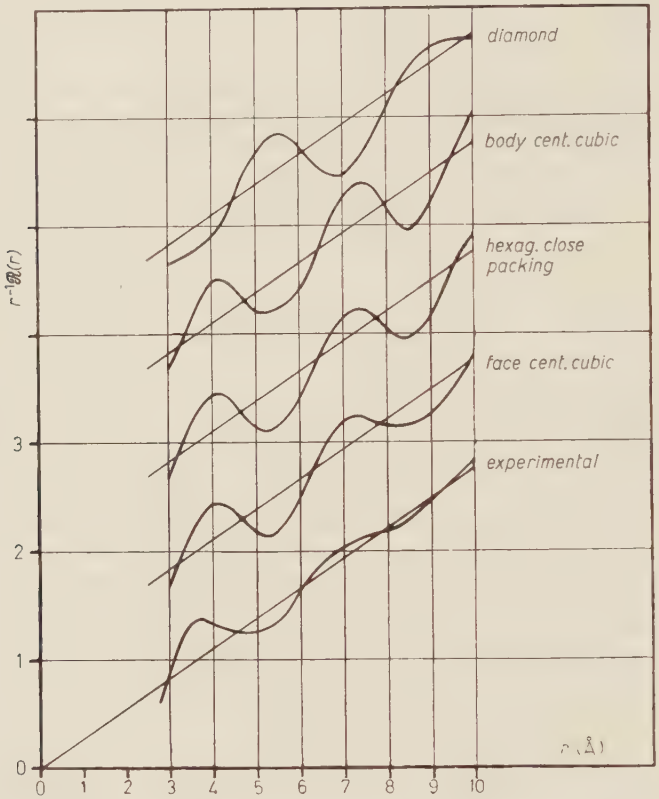

Fig. 1. – Earlier radial distributions calculated in the schematic assumption of an ideally regular lattice of wave packets. The lowest curve is true to scale. The other have been shifted upwards by one unit each. The degree of agreement can be evaluated numerically and it decreases from bottom to top. (Indeed the top curve has been added only as an example of a completely unrelated structure.) Note the excess of order (indicated by wider oscillations) and the drift toward the right shown by the three intermediate curves in comparison to the experimental one.

Imperfections in a lattice are well known from solid state theory; however, except for vacancies, *i.e.* missing lattice points, they cannot be expected to be the same in the liquid state. Instead, we propose describing the departure of a liquid from a perfect lattice in the following way.

In trying to identify the best fitting lattice one will have to start from a minimum of three initial nodes (not collinear), one of which is assumed as origin. With the right choice of the lattice type, three atoms — or better three centers of φ-functions — will be found that lie very near to the initial nodes,

if these are — as we suppose — next-neighbouring ones. The same will be true for the nearest neighbours of these atoms. However, the farther we go from the origin, the larger will be the displacement to be expected (in any direction) for the real positions with respect to the ideal ones. In other words, with increasing distance from the origin we shall have an increasingly broader distribution of the centers of the φ-functions about the nodes of a perfect lattice, reflecting the fact that small distortions accumulate statistically to give ever increasing ones.

We shall assume these « structural » distributions to be gaussian and their mean square deviation $\sigma^2(r)$ to increase linearly with the distance r from the origin, starting from a minimum value σ_0^2 at the origin (3).

We shall call such an arrangement of the φ-function centers a « statistical lattice » for short.

The model of liquid resulting from the above assumptions (though arrived at independently by the Author) is similar to that proposed long ago for ordinary liquids by PRINS and PETERSEN (4). It differs however from that model for having split — so to speak — the disorder of the liquid in two components, a « local » one, expressed by the finite width of the φ-function, and a « structural » one (the one increasing with distance) which alone was considered by PRINS and PETERSEN. Moreover, even on this point, the present treatment differs because of the introduction of the minimal dispersion σ_0^2. (On the importance of considering both components see end of Sect. **4**.)

2. – The liquid compared to a random assembly of very small crystals.

In the elastic scattering of neutrons, the fact that each atom is distributed about a central position according to the square of the local eigenfunction $|\varphi|^2$ results in a factor in the expression of the scattered intensity similar to the atomic scattering factor in X-ray diffraction. (See further on.) The effect of random vacancies is presumably that of flattening somewhat the scattering pattern without altering it essentially.

As for the effect of the *imperfect regularity* in the positions of the local φ-functions, it will result in an average incertitude $\pm\Delta l$ in the path difference between the waves scattered by any two atoms. All other conditions being equal, this quantity Δl will increase with increasing distance of the atoms until at some average distance L it will reach the value $\pm(\lambda/2)$, with λ the

(3) This minimum is imposed by the impossibility of setting with arbitrary exactitude the starting elements (*e.g.* three non-collinear neighbouring nodes) of the lattice that form the basis of the description.

(4) See J. FRENKEL: *Kinetic Theory of Liquids* (Oxford, 1946), p. 114.

wavelength of the scattered radiation. From this distance on, the atoms will scatter mostly *incoherently*, while coherence prevails for smaller distances. (A more detailed discussion of this point is given at the end of the next section.) We shall call L the *coherence distance* (obviously a function of the wavelength).

The above considerations suggest that the scattering by the liquid should be similar to that from an assembly of randomly oriented crystals of linear size L. Since it is possible to predict the scattering from such an assembly, it should be possible to evaluate L by determining the value of this parameter for which the predicted scattering is most similar to the actual one. For instance, by determining the value of L that gives the right width for the main peak in the scattering curve $I = I(\theta)$. In turn, the knowledge of L will render possible an evaluation of the structural randomness parameter σ_0^2.

We have first to calculate the elastically scattered intensity $I(\theta)$ as a function of the scattering angle θ for a distribution of scattering centers whose density is given by the squared modulus of (2), with the $\boldsymbol{r}_n$ appropriate for a small crystal (5). A standard procedure gives

$$I(s) = |A(s)^2| \sum_n \exp[i\boldsymbol{s}\cdot\boldsymbol{r}_n]|^2 , \tag{3}$$

where $\boldsymbol{s}$ is given by

$$\boldsymbol{s} = \frac{2\pi}{\lambda}(\boldsymbol{u} - \boldsymbol{u}_0) , \qquad s = \frac{4\pi}{\lambda}\sin(\theta/2) , \tag{4}$$

with $\boldsymbol{u}_0$ and $\boldsymbol{u}$ unit vectors indicating the direction of the incident and scattered waves, while

$$A(s) = \int |q(r)|^2 \exp[i\boldsymbol{s}\cdot\boldsymbol{r}]\,\mathrm{d}\boldsymbol{r} . \tag{5}$$

This factor $A(s)$ is the already mentioned analogue of the atomic scattering factor.

The squared sum in (3) can be factored by usual methods into a product of a « structure factor » and three Laue functions, with the result

$$\sum|^2 = |\sum_{\nu=1}^{p} \exp[i\boldsymbol{s}\cdot\boldsymbol{r}_\nu]|^2 \frac{\sin^2(\nu_1/2)(\boldsymbol{s}\cdot\boldsymbol{a}_1)}{\sin^2\frac{1}{2}(\boldsymbol{s}\cdot\boldsymbol{a}_1)} \cdot \frac{\sin^2(\nu_2/2)(\boldsymbol{s}\cdot\boldsymbol{a}_2)}{\sin^2\frac{1}{2}(\boldsymbol{s}\cdot\boldsymbol{a}_2)} \cdot \frac{\sin^2(\nu_3/2)(\boldsymbol{s}\cdot\boldsymbol{a}_3)}{\sin^2\frac{1}{2}(\boldsymbol{s}\cdot\boldsymbol{a}_3)} . \tag{6}$$

(5) Formula (2) is justified only for $T = 0\,^\circ\mathrm{K}$, but there is no experimental evidence of important changes in the scattering when the temperature varies, at least up to some degrees above $0\,^\circ\mathrm{K}$.

Here the $\boldsymbol{r}_\nu$'s give the positions of the p atoms in the unit cell; ν_1, ν_2, ν_3 are the number of cells comprised in the edges of the crystal, assuming it to be a parallelepiped with edges parallel to the basic vectors $\boldsymbol{a}_1, \boldsymbol{a}_2, \boldsymbol{a}_3$ of the lattice.

The next step is to average the above expression over all the orientations of the crystal, by constant scattering angle θ, or, what amounts to the same, over all the directions of $\boldsymbol{s}$, by constant modulus s. (The « atomic » factor need not be included in the averaging since it already depends only on the modulus of $\boldsymbol{s}$.)

The task is easier for a cubic close-packing. In this case and with $\nu_1 = \nu_2 = \nu_3 = \nu_0$ (crystals of cubic shape), the average of (6) is given by the integral

$$(7) \qquad \frac{1}{4\pi}\int_0^{\pi} \sin\theta\, d\theta \int_0^{2\pi} d\varphi \, \frac{\sin^2 \nu_0 \pi \varrho_x}{\sin^2 \pi \varrho_x} \cdot \frac{\sin^2 \nu_0 \pi \varrho_y}{\sin^2 \pi \varrho_y} \cdot \frac{\sin^2 \nu_0 \pi \varrho_z}{\sin^2 \pi \varrho_z} \cdot$$

$$\cdot\, 4(1 + \cos \pi\varrho_y \cdot \cos \pi\varrho_z + \cos \pi\varrho_x \cdot \cos \pi\varrho_z + \cos \pi\varrho_x \cdot \cos \pi\varrho_y) \,,$$

with

$$(8) \qquad \boldsymbol{\rho} = \frac{a}{2\pi}\, \boldsymbol{s} \,,$$

where a is the edge of the fundamental cell ($a = a_1 = a_2 = a_3$).

Note that the quantity ν_0 is related to the number N_c of atoms in each crystal by

$$(7') \qquad N_c = 4\nu_0^3 \,.$$

The first three factors in the integrand of (7) are periodic functions of their arguments having maxima at

$$x = u \,, \qquad y = v \,, \qquad z = w \,,$$

with u, v, w integers (positive or negative). The factor into parentheses (structure factor) behaves similarly, except that it vanishes when u, v, w are of different parities. The whole integrand is a function which is a maximum whenever the dimensionless vector $\boldsymbol{\rho}$ has components which are integers (+ or —) of the same parity. In the vicinity of these maxima this function behaves very much like the product of three gaussian functions

$$(9) \qquad \exp[-h[(\varrho_x - u)^2 + (\varrho_y - v)^2 + (\varrho_z - w)^2]] \,, \qquad h = \frac{\pi^2}{3}\left(\nu_0^2 + \frac{1}{2}\right) .$$

This « gaussian » approximation allows the integration to be performed elementarily. The result (valid for non-vanishing ϱ) is

$$(10) \qquad \overline{|\sum_n \exp[i\boldsymbol{s}\cdot\boldsymbol{r}_n]|^2} = \frac{4\nu_0^6}{h}\frac{1}{\varrho}\sum_{[u}\sum_{v}\sum_{w]} U^{-1}\exp[-h(\varrho-U)^2],$$

with $U=(u^2+v^2+w^2)^{\frac{1}{2}}$ and where the brackets are to remind that the sum must be extended only to integers (+ or —) of the same parity.

An alternative way to calculate integral (7) is to resort to numerical computation.

Curves have been calculated by means of (10) for $\nu_0=3$ and $\nu_0=5$ and several points have been calculated numerically from (7) for the case $\nu_0=3$, with the aid of an I.B.M. digital computer. Fig. 2 shows the results.

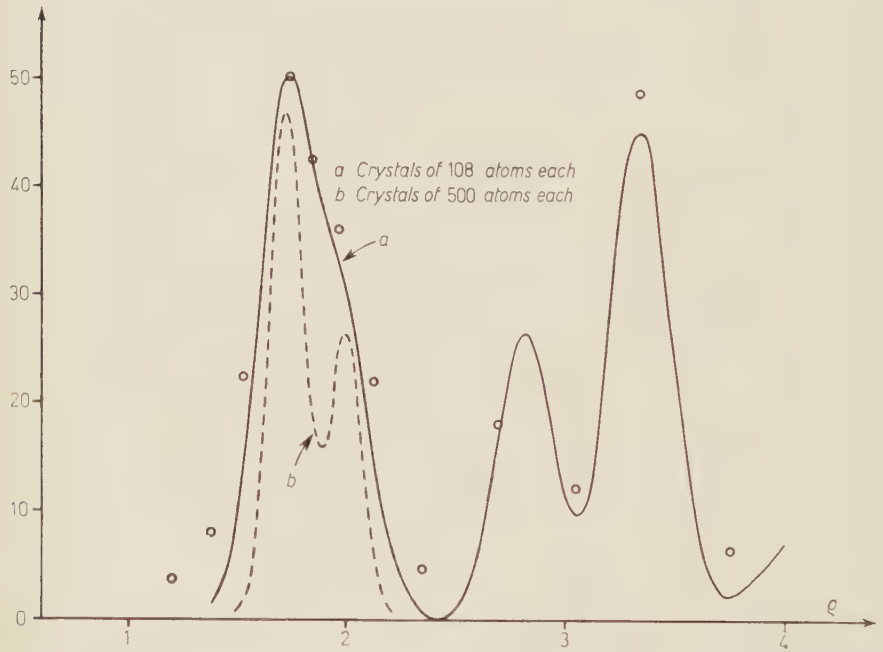

Fig. 2. – The average of $|\sum \exp[i\boldsymbol{s}\cdot\boldsymbol{r}_n]|^2$ over all directions of $\boldsymbol{s}$, as a function of $\varrho=(a/2\pi)s$, for f.c.c. crystals of cubic form and size as specified. The *curves* are obtained from the approximate formula (10). The *circles* are numerically computed values for crystals of 108 atoms each.

These results refer to the average of the second factor in expression (3). As for the other factor $|A(s)|^2$ (which — as said — need not be averaged). use of eqs. (5) and (8) shows that, if the q-function is approximated by a gaus-

sian such that

$$\varphi^2(r) = \exp\left[-\frac{3}{2\tau_0^2} r^2\right], \tag{11}$$

(omitting an obvious normalization factor), $|A(s)|^2$ is given by

$$|A(s)|^2 = \text{const} \exp\left[-\frac{4\pi^2\tau_0^2}{3a^2} \varrho^2\right]. \tag{11'}$$

The precise value of τ_0 is quite immaterial at this stage. Indeed, within any reasonable range it has almost no influence on the width of the main peak in the calculated $I(\varrho)$ curve, which is the quantity of interest. Its order of magnitude can be evaluated from the φ-function introduced in earlier work ([6]) — which is approximately gaussian — or from the rate of decrease of the maxima in the experimental $I(\varrho)$ curve itself. The result is that τ_0 is of the order of unity (in Å). A more accurate value will be deduced in the next Section.

When the $|A|^2$ factor is inserted, the calculated curve for the elastically scattered intensity, case $\nu_0 = 3$, that is for a random mosaic of cubic crystals of edge $3a$, takes the aspect of curve a, Fig. 4.

To compare it with the experimental results of ref. ([2]) which refer to *total* scattering, one needs to separate the inelastic contribution. Following a suggestion by HURST and HENSHAW (ref. ([2])) this has been done by subtracting from the intensity normalized to unity at large angles, a « best fitting » term of the form $1 - \exp[-\alpha\varrho^2]$. There is of course some uncertainty about the value of α, but this — again — affects but little the width of the peak of $I(\varrho)$. Fig. 3 shows a typical result.

In Fig. 4 two experimental curves, b and c, are plotted together with the calculated curve a for $\nu_0 = 3$. Visibly, the latter is somewhat narrower than the experimental ones, by an amount of 17 % for curve b at the lowest temperature (7 % for the other) ([7]). Since an approximate inverse proportionality can be assumed between the width of the peak and the linear dimensions of the crystals ([8]), one can guess that $\nu_0 \approx 2.6$ would give the correct width for the lower temperature curve.

([6]) A closer comparison is not allowed since the former φ-function was employed in connection with an ideally perfect lattice and therefore its width had to take account of both the width of the local function itself and the incertitude in the location of is center.

([7]) The disagreement at larger ϱ values (secondary maxima) is presumably due to the assumption of an exact regularity of the elementary crystals.

([8]) This is at least the behaviour of X-ray diffraction peaks in crystals.

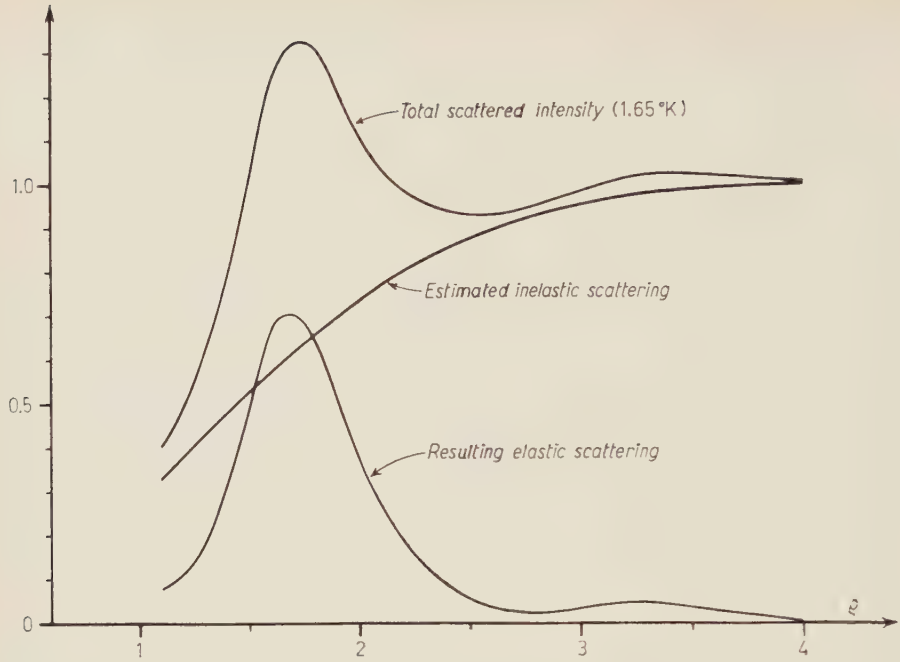

Fig. 3. – Evaluation of the intensity of elastically scattered neutrons from the total scattered intensity (see text, Sect. 2).

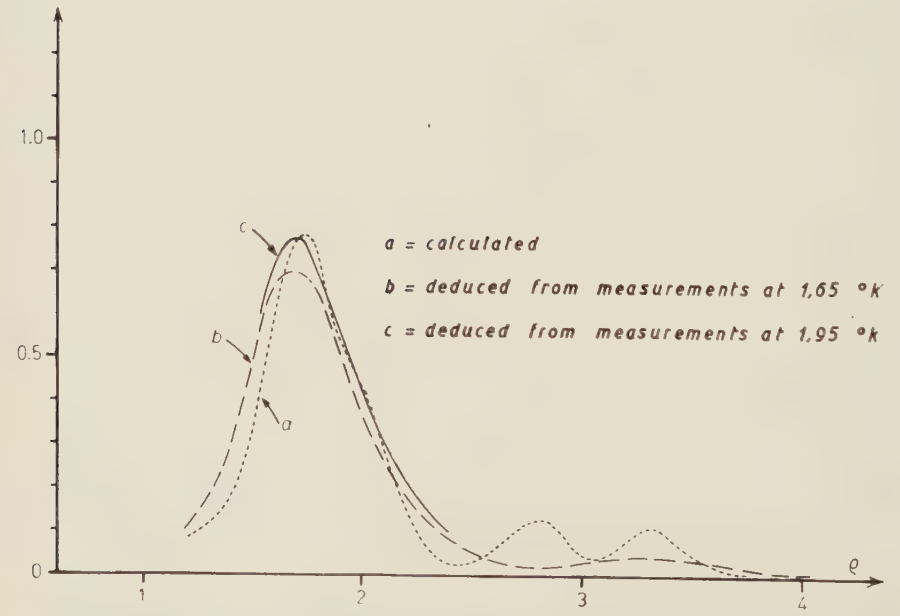

Fig. 4. – Comparison of the calculated elastically scattered intensity with the experimental results.

We come therefore to the approximate value

$$L \approx 2.6\, a\,, \tag{12}$$

for the coherence distance for the scattering of neutrons with $\lambda = 1.04$ Å.

We can get a figure for a from the angle θ_{max} of maximum scattered intensity which is found to be 19.6° for neutrons of the said wavelength (ref. [2]). The maxima of $I(s)$, eq. (3), are but little affected by the first factor and are therefore determined essentially by the second factor, that is by expression (6). Independently from the size of the crystals (which affects only the width of the maximum) the first maximum of expression (6) takes place when

$$\varrho_x = \varrho_y = \varrho_z = 1\,,$$

(eq. (8)), that is when $\varrho = \sqrt{3}$, or else (eq. (4)) when

$$\frac{2a}{\lambda} \sin\frac{\theta_{max}}{2} = \sqrt{3}\,, \tag{13}$$

from which, inserting numerical values, one obtains

$$a = 5.29\ \text{Å}\,. \tag{14}$$

One can calculate the density corresponding to an ideal f.c.c. lattice with the above value (14) for the edge of the fundamental cell. Since there are 4 atoms in it, one gets

$$\frac{4m}{a^3} = 0.173\ \text{g cm}^{-3}\,. \tag{15}$$

The actual value is only 0.146 that is 84 % of the calculated one. It looks improbable that the distortion of the lattice can cause such a substantial change of the density. A more likely explanation is that about one node in six is *empty*, that is the fraction η of vacant sites in the statistical lattice is

$$\eta = 0.16\,. \tag{15'}$$

The value of a which would obtain from the real density of the liquid assuming a close packed structure without vacancies is

$$a = 5.67\ \text{Å}\ [9]\,. \tag{14'}$$

[9] This is the value which was adopted in earlier work when calculating the curves in Fig. 1, and here is the reason why even the best ones show a noticeable displacement toward the right.

From (12) and (14) we get

$$L = 13.7 \text{ Å} \qquad \text{for} \qquad \lambda = 1.04 \text{ Å} . \tag{16}$$

The interpretation of this result requires some discussion.

If O_1 and O_2 are two scattering centers and $\boldsymbol{u}_0$, $\boldsymbol{u}$ are unit vectors in the directions of the incident and scattered waves, one has $(\boldsymbol{u}_0 - \boldsymbol{u})\cdot(O_2 - O_1)$ for the difference of path. If the scattering centers are displaced from their positions by the amounts $\boldsymbol{\delta}_1$ and $\boldsymbol{\delta}_2$, the path difference is altered by an amount $\Delta l = (\boldsymbol{u}_0 - \boldsymbol{u})\cdot(\boldsymbol{\delta}_2 - \boldsymbol{\delta}_1)$. If $\boldsymbol{\delta}_1$, $\boldsymbol{\delta}_2$ are fluctuating, we shall have

$$\overline{(\Delta l)^2} = (\boldsymbol{u}_0 - \boldsymbol{u})^2 \overline{(\boldsymbol{\delta}_2 - \boldsymbol{\delta}_1)^2 \cos^2\psi} ,$$

with ψ the angle between $\boldsymbol{\delta}_2 - \boldsymbol{\delta}_1$ and $\boldsymbol{u}_0 - \boldsymbol{u}$. In absence of correlations one has $\overline{\cos^2\psi} = \frac{1}{3}$, while $(\boldsymbol{u}_0 - \boldsymbol{u})^2 = 4\sin^2(\theta/2)$, with θ the scattering angle. One has therefore

$$\overline{(\Delta l)^2} = \frac{4}{3}(\overline{\delta_1^2} + \overline{\delta_1^2})\sin^2\frac{\theta}{2} . \tag{*}$$

According to the scheme put forward in Sect. **1**, $\overline{\delta_1^2} = \overline{\delta_2^2}$ will increase with the distance $O_1O_2 = r$ as $\sigma_0^2 + \sigma^2(r)$, where

$$\sigma^2(r) = \sigma_0^2 \varkappa r . \tag{17}$$

We shall put

$$\varkappa = \frac{1}{R_1} = 0.267 \text{ Å}^{-1} , \tag{17'}$$

where R_1 is the next neighbours distance (3.74 Å). This means assuming no correlations between the motion of the atoms and would be a rigorous value (in the same assumption) for a one-dimensional case.

We therefore get from (*)

$$\overline{(\Delta l)^2} = \frac{4}{3}\sigma_0^2\left(1 + \frac{r}{R_1}\right)\sin^2\frac{\theta}{2} . \tag{18}$$

It is natural to assume that incoherence prevails when $|\Delta l| \geqslant \lambda/2$. Therefore the above equation means that, for a given r, the radiation is scattered mostly coherently only if θ is smaller than a value θ_0 such that

$$\left(\frac{\lambda}{2}\right)^2 = \frac{4}{3}\sigma_0^2\left(1 + \frac{r}{R_1}\right)\sin^2\frac{\theta_0}{2} .$$

As we have found that the liquid scatters more or less like an assembly of independently scattering regions of linear size $L \sim 13.7$ Å, this can only mean that inserting L for r in the above equation, the angle θ_0 represents the boundary between « strong » and « weak » interference. Indeed the $I(\varrho)$ curve for the elastically scattered intensity (Fig. 3) shows a very pronounced maximum followed by a very flat one. It looks reasonable to take $\varrho_0 = (2a/\lambda) \sin(\theta_0/2)$ to lie somewhere between the two. Choosing the point where the two peaks give presumably equal contributions to $I(\varrho)$, one finds $\sin^2(\theta_0/2) \approx 0.070$. Inserting this figure, together with $\lambda = 1.04$ Å in the foregoing equation the value

$$\sigma_0^2 = 0.62 \text{ Å}^2 , \tag{19}$$

results, which of course should be considered as an indicative rather than an exact value.

At first sight, a coherence distance of ~ 14 Å looks small indeed. It must however be remembered that the gauge itself — the neutron half wavelength — is also small. A more significant measure for the degree of order is the distance D at which the width $\sigma(D)$ of the structural distribution is so large that an atom in that region can be assigned indifferently either to a node of the ideal lattice or to one of its neighbours. This means $\sigma_0^2(D/R_1) \approx R_1^2$, from which it follows that D is about 84 Å.

3. – Connection with the zero point energy.

It is fairly evident that as far as the overlapping of the local distributions can be neglected, as most likely it can in this connection, the zero point energy E_0 will be determined by the width of the spatial distribution of the single atoms. In the approximation employed here, this spatial distribution is a gaussian $\exp[-3r^2/2(\sigma_0^2 + \tau_0^2)]$ resulting from the combination of the gaussian $\exp[-3r^2/2\tau_0^2]$ approximating φ^2 and the gaussian $\exp[-3r^2/2\sigma_0^2]$ representing the minimal incertitude in the position of the center of the φ-function itself. Interpreting this distribution as pertaining to the fundamental state of an oscillator, we get the corresponding energy as

$$E_0 = \frac{9\hbar^2}{4m} \frac{1}{\sigma_0^2 + \tau_0^2} . \tag{20}$$

Information about E_0 is not very accurate. From their radial distribution HENSHAW and HURST ([10]) were able to derive figures for the kinetic energy

([10]) D. G. HENSHAW and D. G. HURST: *Can. Journ. of Phys.*, **33**, 797 (1955).

per atom in the liquid at 2 °K ranging from 18.4 to $24.2 \cdot 10^{-16}$ erg, according to the various potentials choosen to represent the He-He interaction. However, to get E_0 one has to extrapolate down to 0 °K and to guess the right amount of potential energy to be added. Taking $\partial E_{\text{kin}}/\partial T = 0.513\, \frac{3}{2} k$ (ideal, fully degenerate, Bose-Einstein gas of non-relativistic particles) and taking $\bar{E}_{\text{pot}} = \bar{E}_{\text{kin}}$ (harmonic approximation) one finds values for E_0 between the limits

$$E_0 = 32.6 \cdot 10^{-16} \text{ erg}\,, \qquad E_0 = 44.2 \cdot 10^{-16} \text{ erg}\,. \tag{21}$$

There is also some uncertainty in the result that can be deduced from the T^3-law of the phononic specific heat (or, equivalently, from the velocity of sound). Here the uncertainty comes from the fact that phonons utilize one third of the degrees of freedom of the liquid and one does not know whether a factor 3 is the proper correction for the zero point energy so deduced. Anyway, one has for C_{phon}, theoretically

$$C_{\text{phon}} = 12\, \Gamma(4)\, \zeta(4)\, N k \left(\frac{T}{\Theta}\right)^3, \tag{22}$$

and on inserting the experimental value for the coefficient of T^3, that is ([11]) $C_{\text{phon}} T^{-3} = 0.0235$ joule g^{-1} °K^{-1}, one finds

$$\Theta = 19.0 \text{ °K}\,, \tag{22'}$$

for the Debye temperature ([12]). From this follows

$$E_0 \approx 3(E_0)_{\text{phon}} = \tfrac{9}{8} k\Theta = 29.5 \cdot 10^{-16} \text{ erg/atom}\,. \tag{21'}$$

As there is some sort of agreement between this figure and the lowest one among (21), it looks as the best choice. Indeed, this will be confirmed by the analysis of the radial distribution. (See next Section.) Inserting (21') in (20) the result is

$$\sigma_0^2 + \tau_0^2 = 1.28 \text{ Å}^2\,, \tag{23}$$

([11]) H. C. KRAMERS, J. D. WASSCHER and C. J. GORTER: *Physica*, **18**, 329 (1952).

([12]) Sometimes a value $3^{\frac{1}{3}} = 1.442$ times larger is quoted. This comes from employing in place of (22) the corresponding formula for a monoatomic solid, disregarding the fact that in a solid the contribution to the specific heat comes from all the degrees of freedom of the body and not as here from one third only.

from which follows, recalling (19),

$$\tau_0^2 = 0.66\ \text{Å}^2\ , \tag{23'}$$

again, an indicative value only.

4. – The radial distribution. Conclusions.

The results of the preceding Sections allow a « statistical description » of the (one-particle) fundamental state eigenfunction to be given, in that they allow to depict it as an assembly of q-functions whose centers are distributed according to a f.c.c. « statistical lattice » (with vacancies) as defined in Sect. 1.

The fundamental state eigenfunction for the liquid can in turn be derived (eq. (2)) and from this the radial distribution $\mathscr{R}(r)$ can be obtained by standard methods. The details of the procedure are given in the Appendix. The result is expressed by the formula

$$\mathscr{R}(r) = \omega r \sum_i \frac{G_i}{R_i} (\alpha + \beta R_i)^{-\frac{1}{2}} \exp\left[- \frac{(r - R_i)^2}{\alpha + \beta R_i} \right]. \tag{24}$$

Here ω is a normalization factor, R_i and G_i are the radius of and the number of lattice points in the i-th shell surrounding anyone lattice point and α, β are given by

$$\alpha = \frac{4}{3}\tau_0^2 + \frac{2}{3}\sigma_0^2\ , \qquad \beta = \frac{2}{3}\frac{\sigma_0^2}{R_1}\ . \tag{24'}$$

With the values for R_i and G_i appropriate for a f.c.c. lattice, and with the value (23') for τ_0, corresponding tot he value (21') for the zero point energy E_0, curve c in Fig. 5 is obtained. It is in good agreement with the experimental curve for, say, $r \geqslant 4.5$ Å, while being somewhat too flat in the region of the first maximum. A likely cause of this is the assumption of uncorrelated displacements (implicit in eq. (17)) which is certainly not correct for next neighbours and will lead to an exaggerated spreading of their distance.

All in all, the agreement can be considered satisfactory and this is the more significant as no parameter has been adjusted to fit the experimental curve, except for the normalization factor ω ([13]). Another point to note is that the

([13]) That is imposed by the existence of an unknown amount of random vacancies in the liquid. Were it not for these, one would have $\omega = \pi^{-\frac{1}{2}}$ (Appendix, eq. (A.10')) We should expect the same ratio between $\pi^{-\frac{1}{2}}$ and ω as between the « calculated » (eq. (15)) and real densities. Indeed the agreement is within $(1 \div 2)\%$. Which of course constitutes a consistency test only.

calculated radial distribution does not seem to be affected by the « wandering about » of the q-function centers, which has been neglected at the start (see Introduction). This appears to confirm the secondary character of that feature.

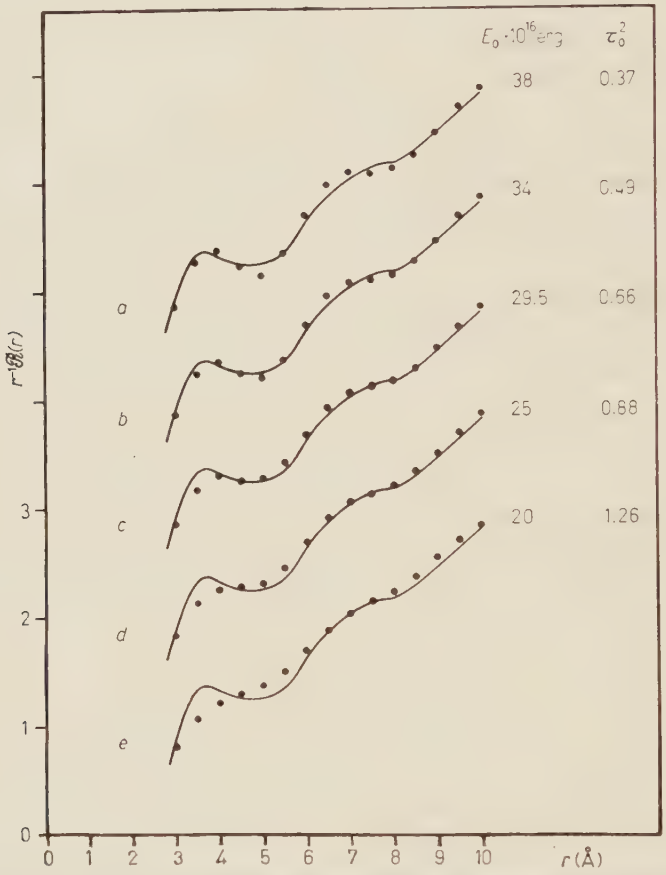

Fig. 5. *Full curves*: experimental radial distribution (Hurst and Henshaw, ref (2)) *Circles*: calculated values for a statistical f.c.c. lattice on various assumptions, concerning the zero point energy E_0. The parameter τ_0 is the resulting width of the local φ-function (eq. (20)). The most reliable experimental value for E_0 is that corresponding to curve c which is also the best fitting one (see Fig. 6).

Since, as we have seen, the value of E_0 is somewhat uncertain, some different values have been tried. The results are plotted in Fig. 5 together with the corresponding values of E_0 and of τ_0^2 (from eq. (20)). Fig. 6 presents a rough evaluation of

$$\Delta = \int_{4.5}^{10} (\mathcal{R}_{\text{calc}} - \mathcal{R}_{\text{exp}})^2 \, \mathrm{d}r \, .$$

This is a measure of the disagreement between $\mathscr{R}_{calc}$ and $\mathscr{R}_{exp}$ outside the correlation sensitive region. The plot shows that the best value for the zero point energy per atom should lie in the vicinity of $30 \cdot 10^{-16}$ erg, thus lending support to the phonon deduced value (21′).

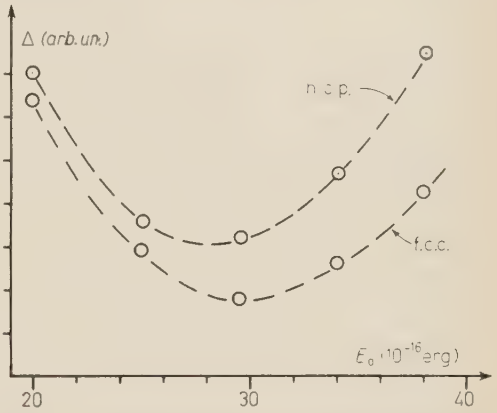

Fig. 6. – The ordinates express the degree of departure of the calculated curves in Fig. 5 from the experimental curve, in the region $4.5\ \text{Å} < r < 10\ \text{Å}$ (where correlations between atom positions are unimportant). The graph shows that E_0 must be $\sim 30 \cdot 10^{-16}$ erg per atom, in agreement with the value obtained by tripling the zero point *phonon* energy.

Similar results can be obtained by using an exagonal close packing as the base lattice. They are however somewhat more laborious to obtain and the agreement with experiment is slightly but definitely less satisfactory.

As a final conclusion it is worth noting that, should the assumption of a local q-function be unwarranted, its width τ_0 should have turned out to be very small against the parameter of structural disorder σ_0. On the contrary, comparison with experiment has shown that τ_0 and σ_0 are of the same order of magnitude. On the other hand, consideration of the local disorder alone, in a measure suited to give the appropriate zero point energy, leads just to the old curves of Fig. 1 showing an excess order. It can therefore be concluded that both kinds of disorder, local and structural, are needed for a proper description of the liquid ([14]).

* * *

The Author is particularly grateful to Professor G. Puppi of the University of Bologna for having included the electronic computation of integral (7) in the program of computational work of the Istituto Nazionale di Fisica Nucleare and to the staff of the Centro di Calcolo dell'Istituto di Fisica (University of Bologna) for the performance of the task.

A grant from the Consiglio Nazionale delle Ricerche for numerical work is also acknowledged.

Thanks are also due to G. De Fazio for many numerical calculations and to G. Tortorici for the drawing of the graphs.

([14]) It is evidently quite conceivable that analogous conclusions with the changes imposed by the non-quantum character of the distributions might hold for « ordinary » liquids as well. This point however has not been explored for the moment.

Appendix

Calculation of the radial distribution function.

Given an assembly of N atoms described by an eigenfunction $\Psi(\boldsymbol{\rho}_1, \boldsymbol{\rho}_2 \dots \boldsymbol{\rho}_N)$, the probability $\mathscr{R}(r)\,\mathrm{d}r$ for two of them, say 1 and 2, to be found at a distance between r and $r+\mathrm{d}r$ is

$$\mathscr{R}(r)\,\mathrm{d}r = \int_{r'=r}^{r'=r+\mathrm{d}r} \mathrm{d}\boldsymbol{r}' \int \dots \int |\Psi|^2 \delta(\boldsymbol{\rho}_1 - \boldsymbol{\rho}_2 - \boldsymbol{r}')\,\mathrm{d}\boldsymbol{\rho}_1\,\mathrm{d}\boldsymbol{\rho}_2 \dots \mathrm{d}\boldsymbol{\rho}_N . \tag{A.1}$$

On putting $\boldsymbol{\rho}_1 - \boldsymbol{\rho}_2 = \boldsymbol{\rho}$ this formula becomes

$$\mathscr{R}(r)\,\mathrm{d}r = \int_{r'=r}^{r'=r+\mathrm{d}r} \mathrm{d}\boldsymbol{r}' \int \dots \int |\Psi(\varrho + \varrho_2, \varrho_2 \dots \varrho_N)|^2 \delta(\boldsymbol{\rho} - \boldsymbol{r}')\,\mathrm{d}\boldsymbol{\rho}\,\mathrm{d}\boldsymbol{\rho}_2 \dots \mathrm{d}\boldsymbol{\rho}_N ,$$

from which we get

$$\mathscr{R}(r)\,\mathrm{d}r = \int_{r'=r}^{r'=r+\mathrm{d}r} \mathrm{d}\boldsymbol{r}' \int \dots \int |\Psi(\boldsymbol{r}' + \boldsymbol{\rho}_2,\ \boldsymbol{\rho}_2 \dots \boldsymbol{\rho}_N|^2\,\mathrm{d}\boldsymbol{\rho}_2\,\mathrm{d}\boldsymbol{\rho}_3 \dots \mathrm{d}\boldsymbol{\rho}_N . \tag{A.2}$$

The radial distribution at 0 °K will follow from this formula inserting in it expression (2) for Ψ. One must however remember that the φ-function on which Ψ, eq. (2) is built, represents the behaviour of an atom in the *average* field of the others. It cannot therefore be expected that a formula based on it will give correctly the distribution at *small* distances, when the potential energy of the colliding atoms becomes substantially higher than average. However, as we are interested here in medium and long range order in the liquid this limitation is not important. Indeed, the average kinetic energy per atom in liquid helium being in the range of $(15 \div 20)\cdot 10^{-16}$ erg it equals the repulsive potential energy at a distance of (2.5 ; 2.6) Å from another atom, according to the various potentials calculated for the He-He interaction. In this range of distances the effect of binary collisions becomes certainly important. It should however be negligible around and above the average distance between next neighbours (3.74 Å). Restricting our considerations to the range $r \lesssim 3.5$ Å, we may therefore replace Ψ in (A.2) by its expression (2), getting

$$\mathscr{R}(r)\,\mathrm{d}r = |Q_N|^2 \int_{r'=r}^{r'=r+\mathrm{d}r} \mathrm{d}\boldsymbol{r}' \int \dots \int \Big[\sum_{m=0}^{N-1} \varphi(|\boldsymbol{r}' + \boldsymbol{\rho}_2 - \boldsymbol{r}_m|) \sum_{n=0}^{N-1} \varphi(|\boldsymbol{\rho}_2 - \boldsymbol{r}_n|) \cdot \prod_{\alpha=3}^{N-1} \sum_{p=0}^{N-1} \varphi(|\boldsymbol{\rho}_\alpha - \boldsymbol{r}_p|)\Big]^2 \mathrm{d}\boldsymbol{\rho}_2\,\mathrm{d}\boldsymbol{\rho}_3 \dots \mathrm{d}\boldsymbol{\rho}_N .$$

Here the subscripts m, n, p are intended to run through all the centers of the q-functions starting from an initial one which is assumed as origin for the vectors $\boldsymbol{r}_n$. It is therefore $r_0 = 0$.

By separating the two $\boldsymbol{\rho}_2$-dependent factors one obtains

$$\mathscr{R}(r)\,\mathrm{d}r = c \int_{r'=r}^{r'=r+\mathrm{d}r} \mathrm{d}\boldsymbol{r}' \int \sum_{m=0}^{N-1} \sum_{m'=0}^{N-1} q(\boldsymbol{r}' - \boldsymbol{\rho}_2 - \boldsymbol{r}_m)\, q(|\boldsymbol{r}' - \boldsymbol{\rho}_2 - \boldsymbol{r}_{m'}|) \cdot$$

$$\cdot \sum_{n=0}^{N-1} \sum_{n'=0}^{N-1} q(|\boldsymbol{\rho}_2 - \boldsymbol{r}_n|)\, q(|\boldsymbol{\rho}_2 - \boldsymbol{r}_{n'}|)\, \mathrm{d}\boldsymbol{\rho}_2 ,$$

where c, which is independent of $\boldsymbol{r}'$ and hence of $\boldsymbol{r}$, is most conveniently determined through a normalization condition.

The main contribution to the above expression comes from the diagonal terms in the double sums, that is those with $m = m'$, $n = n'$. The main non-diagonal ones are those containing a factor

$$\int \varphi(|\boldsymbol{\rho}_2 - O|)\, \varphi(|\boldsymbol{\rho}_2 - O'|)\, \mathrm{d}\boldsymbol{\rho}_2 ,$$

with O, O' neighbouring nodes. These terms however are much smaller, owing to the rather small overlapping of the q-functions (*). Moreover, the earlier calculations with the « ideal-lattice » model have shown that these terms are rather similar to the main ones in their dependence on r. We therefore drop them altogether, writing (the φ's are real)

$$\mathscr{R}(r)\,\mathrm{d}r = c \int_{r'=r}^{r'=r+\mathrm{d}r} \mathrm{d}\boldsymbol{r}' \sum_{m=0}^{N-1} \sum_{n=0}^{N-1} \varphi^2(|\boldsymbol{r} + \boldsymbol{\rho}_2 - \boldsymbol{r}_m|)\, \varphi^2(|\boldsymbol{\rho}_2 - \boldsymbol{r}_n|)\, \mathrm{d}\boldsymbol{\rho}_2 .$$

Neglecting size and surface effects, one of the sums can be replaced by a factor N. Doing this for the m-sum and putting $\boldsymbol{r}_m = \boldsymbol{r}_0 = 0$, one finally has

$$\mathscr{R}(r)\,\mathrm{d}r = C \int_{r'=r}^{r'=r+\mathrm{d}r} \mathrm{d}\boldsymbol{r}' \sum_{n=0}^{N-1} \int \varphi^2(|\boldsymbol{r} + \boldsymbol{\rho}_2|)\, \varphi^2(|\boldsymbol{\rho}_2 - \boldsymbol{r}_n|)\, \mathrm{d}\boldsymbol{\rho}_2 .$$

Here the contribution of the term $n = 0$ can be neglected as it is restricted to values of r comparable to the width of the q-function (< 1 Å). The sum is therefore to be extended to all nodes except the central one: we shall write it as $\sum_n$ without specifying limits.

(*) Implying that effects connected with the kind of statistics, such as superfluidity, however striking they may be, are in a certain sense secondary, and in particular they affect but very little the structure of the liquid. (As evidenced indeed by the smallness of the density anomaly at the λ-point).

Putting

$$\boldsymbol{\rho}_2 - \boldsymbol{r}_n = \boldsymbol{k} ,$$

one has

$$\mathscr{R}(r)\,\mathrm{d}r = C \sum_n \int \varphi^2(k)\,\mathrm{d}\boldsymbol{k} \int_{r'=r}^{r'=r+\mathrm{d}r} \varphi^2\big(|\boldsymbol{r}' + \boldsymbol{r}_n + \boldsymbol{k}|\big)\,\mathrm{d}\boldsymbol{r}' .$$

By introducing spherical co-ordinates with the direction of $\boldsymbol{k} - \boldsymbol{r}_n$ as the polar axis, the integral over $\mathrm{d}r'$ can easily be transformed giving

$$\mathscr{R}(r)\,\mathrm{d}r = 2\pi C r\,\mathrm{d}r \sum_n \int \varphi^2(k)\,\mathrm{d}\boldsymbol{k}\,\frac{1}{K} \int_{|r-K|}^{r+K} \varphi^2(u) u\,\mathrm{d}u ,$$

where

$$K = |\boldsymbol{k} + \boldsymbol{r}_n| .$$

And putting

$$I(y) = \int_0^y \varphi^2(u) u\,\mathrm{d}u , \tag{A.3}$$

one obtains

$$\mathscr{R}(r) = 2\pi C r \sum_n \int \varphi^2(k)\,\mathrm{d}\boldsymbol{k}\,\frac{1}{K}\,\big[I(r+K) - I\big(|r-K|\big)\big] .$$

Introducing again spherical co-ordinates with $\boldsymbol{r}_n$ as polar axis one finally gets after some transformations and obvious simplifications

$$\mathscr{R}(r) = 4\pi^2 C r \sum_n \frac{1}{r_n} \int_0^\infty \big[I(\infty) - I\big(|r-K|\big)\big]\big[I(\infty) - I\big(|r_n - K|\big)\big]\,\mathrm{d}K . \tag{A.4}$$

The integral in this expression is a function $\mathscr{F}\big(|r-r_n|\big)$ of $|r-r_n|$ only, and it can be evaluated without difficulty if φ^2 is assumed to be a gaussian, as in (11). One finds

$$I(y) = \frac{3^{\frac{1}{2}}}{(2\pi)^{\frac{3}{2}}}\,\frac{1}{\tau_0}\left[1 - \exp\left(-\frac{3}{2\tau_0^2}\,y^2\right)\right], \tag{A.5}$$

$$\mathscr{F}\big(|r-r_n|\big) = \frac{(3/2)^{\frac{1}{2}}}{(2\pi)^{\frac{5}{2}}}\,\frac{1}{\tau_0} \exp\left[-\frac{3}{4\tau_0^2}\,(r-r_n)^2\right] . \tag{A.5'}$$

We therefore have

$$\mathscr{R}(r) = \text{const}\, r \sum_n \frac{1}{r_n} \exp\left|-\frac{3}{4\tau_0^2}(r-r_n)^2\right|. \tag{A.6}$$

Up to this point no assumption has been made about the $\boldsymbol{r}_n$. Assuming they form an ideal lattice, the above formula can be evaluated immediately. Indeed, for each type of lattice one knows the possible values R_i for the r_n's and the number G_i of nodes surrounding a central one at a distance R_i. One has therefore

$$\mathscr{R}(r) = \text{const}\, r \sum_{i=1}^{\infty} \frac{G_i}{R_i} \exp\left|-\frac{3}{4\tau_0^2}(r-R_i)^2\right|. \tag{A.7}$$

This sum converges rapidly for any value of interest for r. For $r \to \infty$ the discontinuous character of R_i can be disregarded and the above formula becomes

$$\lim_{r\to\infty} \mathscr{R}(r) = \text{const}\, r \int_0^{\infty} \frac{1}{R} \exp\left|-\frac{3}{4\tau_0^2}(r-R)^2\right| 4\pi n R^2 \mathrm{d}R,$$

with n the number of atoms per unit volume. This transforms easily into

$$\lim \mathscr{R}(r) = \text{const}\, \frac{8}{3^{\frac{1}{2}}} \pi^{\frac{3}{2}} n \tau_0 r^2, \tag{A.8}$$

from which one deduces

$$\text{const} = \frac{1}{2\tau_0}\left(\frac{3}{\pi}\right)^{\frac{1}{2}}. \tag{A.8'}$$

(The procedure employed in calculating the curves in Fig. 1 was actually a little more involved, as the φ-function of ref. [1]) (1951) was employed which is not exactly a gaussian.)

If we now turn from an ideal to a statistical lattice, any node will be distributed around its ideal position $\boldsymbol{r}_{n_0}$ according to a gaussian

$$\exp\left|-\frac{3}{2\sigma_n^2}(\boldsymbol{r}_n - \boldsymbol{r}_{n_0})^2\right|,$$

with $\sigma_n = \sigma(r_n)$ given by (17), (17'), (19). As σ_n is small in comparison with r_{n_0} the distribution for r_n is again a gaussian

$$\prod(r_n)\,\mathrm{d}r_n = \left(\frac{3}{2\pi\Sigma_n^2}\right)^{\frac{1}{2}} \exp\left|-\frac{3}{2\Sigma_n^2}(r_n - r_{n_0})^2\right|,$$

with

$$\Sigma_n^2 = \sigma_n^2 + \sigma_n^2.$$

In each term of the sum in (A.6) the denominator may be safely taken to be r_{n_0}, while the exponential has to be replaced by

$$\int_{-\infty}^{\infty} \exp\left[-\frac{3}{4\tau_0^2}(r-r_n)^2\right] \prod(r_n)\,\mathrm{d}r_n\,.$$

The result is a gaussian

$$\mathrm{Const}\left(\frac{4}{3}\tau_0^2+\frac{2}{3}\Sigma_n^2\right)^{-\frac{1}{2}} \exp\left[-\left(\frac{4}{3}\tau_0^2+\frac{2}{3}\Sigma_n^2\right)^{-1}(r-r_n)^2\right],$$

Thus $\mathscr{R}(r)$ turns out to be (making the same changes as from (A.6) to (A.7))

$$\mathscr{R}(r) = \mathrm{Const}\, r \sum_i \frac{G_i}{R_i}\left(\frac{4}{3}\tau_0^2+\frac{2}{3}\Sigma_n^2\right)^{-\frac{1}{2}} \exp\left[-\left(\frac{4}{3}\tau_0^2+\frac{2}{3}\Sigma_n^2\right)^{-1}(r \quad R_i)^2\right], \tag{A.9}$$

where

$$\Sigma_n^2 = \sigma_0^2\left(1+\frac{R_i}{R_1}\right). \tag{A.9'}$$

For $r\to\infty$ this formula gives, in analogy to (A.8)

$$\lim_{r\to\infty}\mathscr{R}(r) = \mathrm{Const}\,\pi^{\frac{1}{2}}\,4\pi n r^2\,, \tag{A.10}$$

from which follows

$$\mathrm{Const} = \pi^{-\frac{1}{2}}\,. \tag{A.10'}$$

RIASSUNTO

La dipendenza angolare — nota sperimentalmente — dell'intensità dei neutroni diffusi dall'elio liquido viene confrontata con quella calcolata per un mosaico di cristalli molto piccoli orientati a caso. Il risultato di questa analisi — che è in sostanza una valutazione del grado di disordine — viene utilizzato, insieme col valore della energia allo zero assoluto, per determinare i due parametri fondamentali che compaiono in un modello proposto per il liquido. Questo modello equivale a una descrizione statistica dell'autofunzione fondamentale per gli atomi del liquido e come tale permette di ricavare la distribuzione radiale delle distanze, rendendo così possibile un controllo della teoria per mezzo del confronto con la distribuzione sperimentale (ricavata dalla diffusione dei neutroni). Si trova che l'accordo è soddisfacente.

IL NUOVO CIMENTO Vol. XXII, N. 2 16 Ottobre 1961

Simplification of the Two-Body Unitarity Relation (*).

M. Froissart (**)

Department of Physics, University of California - Berkeley, Cal.

(ricevuto l'8 Agosto 1961)

Summary. — A reduction is obtained in the number of integrations needed to compute the scattering amplitude from a potential by dispersion-theoretical methods.

It has recently been proposed by Chew and Frautschi [1] to solve the relativistic two-body problem by a method very close to that proposed by Blanckenbecler *et al.* [2] for the Schrödinger equation with a central potential. This method is essentially a perturbative expansion yielding all but the lowest partial waves, which may be found in turn by solving an integral equation (so called N/D method [2]). This procedure might be performed by digital computers. The computation of each successive term in the perturbation series involves however a single integration and a double integration, and the latter may demand a prohibitive computation time. We want to propose here a way of reducing this double integration to a single integration, without modifying the single integration.

This reduction is done in the following way: we use an integral transformation of the amplitude. Under such a transformation, the equation involving a double integration simplifies and requires only one integration. The procedure thus is: transform the data (potential) by this integral transformation

(*) This work was supported by the U.S. Air Force under contract no. AF 49(638)-327 monitored by the AF Office of Scientific Research of the Air Research and Development Command.

(**) On leave of absence from C.E.N., Saclay.

(1) G. F. Chew and S. C. Frautschi: Report UCRL-9685.

(2) R. Blankenbecler, M. L. Goldberger, N. N. Khuri and S. B. Treiman: *Ann. of Phys.*, **10**, 62 (1960).

then compute all successive terms in the new representation, add them up and transform back the sum to the original representation by means of the inverse integral transformation. It is also possible to compute the partial waves directly in the new representation.

We use throughout the notations of reference [2] except for the definition of t, which we take as $t = 2s(\cos\theta - 1)$. The basic equations are given by eq. (3.1) and (3.8) of ref. [2]. We write them as

$$f(s, t) = \frac{1}{\pi}\int_0^\infty \frac{g(s, t')\,\mathrm{d}t'}{t' - t}\,, \tag{1}$$

$$g(s, t) = \frac{1}{\pi}\int_0^\infty \frac{\zeta(s', t')\,\mathrm{d}t'}{(s' - s - i\varepsilon)} - \frac{\pi}{2\sqrt{t}}\,\sigma(\sqrt{t})\,, \tag{2}$$

$$\zeta(s, t) = \frac{1}{\pi^2}\int_0^\infty \mathrm{d}t_1 \int_0^\infty \mathrm{d}t_2\, g(s, t_1) g^*(s, t_2) K(s, t; t_1, t_2)\,\mathrm{d}t_1\,\mathrm{d}t_2\,, \tag{3}$$

$$K(s, t; t_1, t_2) = \frac{\pi}{2}\frac{\theta\left[2s(t - t_1 - t_2) - t_1 t_2 - \{t_1 t_2(16s^2 + 4st_1 + 4st_2 + t_1 t_2)\}^{\frac{1}{2}}\right]}{[s(t^2 + t_1^2 + t_2^2 - 2t_1 t_2 - 2t_1 t - 2t_2 t) - t t_1 t_2]^{\frac{1}{2}}}\,. \tag{4}$$

These equations in general need subtractions, but this is a trivial matter, and we shall assume for simplicity that no subtractions are needed.

We seek a transformation leaving the form of (1) and (2) invariant, and which transforms K into a δ-function, in order to reduce the number of integrations in (3). The first condition is easily satisfied by a transformation involving the t variable, and being independent of s.

To fulfill the second condition, let us look closer to the meaning of eq. (3). By introducing the partial wave expansion

$$f(s, t) = \frac{1}{\sqrt{s}}\sum_{l=0}^{\infty}(2l + 1) a_l(s) P_l\left(1 + \frac{t}{2s}\right),$$

we see that eq. (3), which expresses unitarity, must be equivalent to

$$\mathrm{Im}\, a_l(s) = |a_l(s)|^2\,. \tag{5}$$

We have the following expression for $a_l(s)$, derived from (2):

$$a_l(s) = \frac{\sqrt{s}}{\pi}\int_0^\infty Q_l\left(1 + \frac{t}{2s}\right) g(s, t)\,\mathrm{d}t\,, \tag{6}$$

where Q_l is the Legendre function of second kind. Taking the imaginary part of it, we find

$$\text{Im}\, a_l(s) = \frac{\sqrt{s}}{\pi} \int_0^\infty Q_l\left(1 + \frac{t}{2s}\right) \zeta(s, t)\, \mathrm{d}t \,. \tag{7}$$

If we substitute these expressions into (5), we find

$$\int_0^\infty Q_l\left(1 + \frac{t}{2s}\right) \zeta(s, t)\, \mathrm{d}t = \frac{\sqrt{s}}{\pi} \iint_0^\infty Q_l\left(1 + \frac{t_1}{2s}\right) Q_l\left(1 + \frac{t_2}{2s}\right) g(s, t_1) g^*(s, t_2)\, \mathrm{d}t_1\, \mathrm{d}t_2 \,.$$

Using (3), we find

$$\iiint_0^\infty Q_l\left(1 + \frac{t}{2s}\right) K(s, t; t_1, t_2) g(s, t_1) g^*(s, t_2)\, \mathrm{d}t_1\, \mathrm{d}t_2 =$$

$$= \pi\sqrt{s} \iint_0^\infty Q_l\left(1 + \frac{t_1}{2s}\right) Q_l\left(1 + \frac{t_2}{2s}\right) g(s, t_1) g^*(s, t_2)\, \mathrm{d}t_1\, \mathrm{d}t_2 \,,$$

which is an identity, as

$$\int_0^\infty Q_l\left(1 + \frac{t}{2s}\right) K(s, t; t_1, t_2)\, \mathrm{d}t = \pi\sqrt{s}\, Q_l\left(1 + \frac{t_1}{2s}\right) Q_l\left(1 + \frac{t_2}{2s}\right) . \tag{8}$$

This last equation shows clearly why K is complicated: it has to express the product of two Q functions as a linear superposition of Q's, independent of the order l.

Let us introduce the unknown kernel of our transformation $\chi(t, t')$, and label the transformed quantities with a tilde, *e.g.*:

$$\tilde{f}(s, t) = \int f(s, t')\, \chi(t, t')\, \mathrm{d}t' , \qquad \frac{\tilde{\sigma}(\sqrt{t})}{\sqrt{t}} = \int \frac{\sigma(\sqrt{t'})}{\sqrt{t'}}\, \chi(t, t')\, \mathrm{d}t' \,,$$

and so on. In any case, we will get equations analogous to (6) and (8):

$$a_l(s) = \frac{1}{\pi} \int_0^\infty \alpha(l, s, t)\, \tilde{g}(s, t)\, \mathrm{d}t \tag{9}$$

$$\int_0^\infty \alpha(l, s, t) \tilde{K}(s, t; t_1, t_2)\, \mathrm{d}t = \pi\alpha(l, s, t_1)\alpha(l, s, t_2) \,.$$

This has to be satisfied for every l, and the kernel $\tilde{K}$ has to be of the form $\delta[t - F(s, t_1, t_2)]$, in order that our goal be achieved.

A trivial solution of this problem is to take

$$\alpha(l, s, t) = [\alpha(s, t)]^l ,$$

and to choose $F(s, t_1, t_2)$ in such a way that

$$\alpha(s, t) = \alpha(s, t_1)\,\alpha(s, t_2) \qquad \text{for} \qquad t = F(s, t_1, t_2).$$

To deduce the kernel χ from these considerations is now relatively easy. Take $\tilde{g}$ as a δ-function, then $\tilde{f}$ has a simple pole in t. Furthermore, from (9), $a_l(s) = \alpha^l$. Then, coming back to f, we get

$$f_\alpha = \frac{1}{\sqrt{s}} \sum (2l+1)\alpha^l P_l(\cos\theta) = \frac{1}{\sqrt{s}} \frac{1-\alpha^2}{\{1 - 2\alpha\cos\theta + \alpha^2\}^{\frac{3}{2}}} ,$$

or, if we substitute $\cos\theta = 1 + (t/2s)$,

$$f_\alpha = s \frac{1-\alpha^2}{\{s(1-\alpha)^2 - \alpha t\}^{\frac{3}{2}}} . \tag{10}$$

We want to find a transformation χ carrying this singularity $1/(\tau - t)^{\frac{3}{2}}$ into a simple pole. As may be expected, this transformation may be chosen as a derivation of order $-\frac{1}{2}$, which is Abel's transformation (3). This transformation, however, brings in a branch point at $t = 0$, which we have to take care of by multiplying by $1/2\sqrt{t}$. We thus guess the kernel of our transformation:

$$\chi(t, t') = \frac{1}{2\sqrt{t}} \frac{1}{(t - t')^{\frac{1}{2}}} \theta(t^2 - t't) .$$

Let us verify that it works:

$$\int_0^t f_s(t')\chi(t, t')\,\mathrm{d}t' = \frac{\sqrt{s}(1+\alpha)}{s(1-\alpha)^2 - \alpha t} . \tag{11}$$

It is clear that all analyticity properties hold for the quantities with tilde as well as for the others, the asymptotic properties are the same (if there are no oscillations with phase increasing more rapidly than t at infinity, which is

(3) R. Courant: *Differential and Integral Calculus*, vol. 2 (New York, 1936), p. 340.

presumably the case). Therefore eq. (1) and (2) are still valid for quantities with tilde. Furthermore, eq. (11) tells us that if

$$\tilde{g}_\alpha = \frac{\pi\sqrt{s}\,(1+\alpha)}{\alpha}\,\delta\left(\frac{s(1-\alpha)^2}{\alpha} - t\right),$$

then $a_l = \alpha^l$, or taking $s(1-\alpha)^2/\alpha = \tau$ and expressing α as a function of τ, if $\tilde{g} = \delta(\tau - t)$,

$$a_l = \frac{(4s+\tau)^{\frac{1}{2}} - \sqrt{\tau}}{2\pi[s(4s+\tau)]^{\frac{1}{2}}}\left|\frac{(4s+\tau)^{\frac{1}{2}} - \sqrt{\tau}}{(4s+\tau)^{\frac{1}{2}} + \sqrt{\tau}}\right|^l.$$

Therefore, we may integrate over all values of τ with the actual $\tilde{g}$ as weight, and we get, putting $u' = -4s - t'$,

$$a_l(s) = \frac{1}{2\pi\sqrt{s}}\int_{-\infty}^{0}\frac{(-u')^{\frac{1}{2}} - (t')^{\frac{1}{2}}}{(-u')^{\frac{1}{2}}}\left|\frac{(-u')^{\frac{1}{2}} - (t')^{\frac{1}{2}}}{(-u')^{\frac{1}{2}} + (t')^{\frac{1}{2}}}\right|^l \tilde{g}(s, t')\,\mathrm{d}t' . \tag{12}$$

Then, eq. (5) reads

$$\frac{1}{2\pi\sqrt{s}}\int\frac{(-u')^{\frac{1}{2}} - (t')^{\frac{1}{2}}}{(-u')^{\frac{1}{2}}}\left|\frac{(-u')^{\frac{1}{2}} - (t')^{\frac{1}{2}}}{(-u')^{\frac{1}{2}} + (t')^{\frac{1}{2}}}\right|^l \tilde{\zeta}(s, t')\,\mathrm{d}t' =$$

$$= \frac{1}{4\pi^2 s}\int\frac{(-u_1)^{\frac{1}{2}} - (t_1)^{\frac{1}{2}}}{(-u')^{\frac{1}{2}}}\,\frac{(-u_2)^{\frac{1}{2}} - (t_2)^{\frac{1}{2}}}{(-u_2)^{\frac{1}{2}}}\left|\frac{(-u_1)^{\frac{1}{2}} - (t_1)^{\frac{1}{2}}}{(-u_1)^{\frac{1}{2}} + (t_1)^{\frac{1}{2}}}\cdot\frac{(-u_2)^{\frac{1}{2}} - (t_2)^{\frac{1}{2}}}{(-u_2)^{\frac{1}{2}} + (t_2)^{\frac{1}{2}}}\right|^l \cdot$$

$$\cdot\,\tilde{g}(s, t_1)\,\tilde{g}^*(s, t_2)\,\mathrm{d}t_1\,\mathrm{d}t_2 ,$$

which gives readily

$$\tilde{\zeta}(s, t) = \frac{1}{2\pi\sqrt{s}}\,\frac{(-u)^{\frac{1}{2}}}{(-u)^{\frac{1}{2}} - \sqrt{t}}\iint\frac{(-u_1)^{\frac{1}{2}} - (t_1)^{\frac{1}{2}}}{(-u_1)^{\frac{1}{2}}}\,\frac{(-u_2)^{\frac{1}{2}} - (t_2)^{\frac{1}{2}}}{(-u_2)^{\frac{1}{2}}}\cdot \tag{13}$$

$$\cdot\,\delta(t - F(t_1, t_2))\,\tilde{g}(s, t_1)\,\tilde{g}^*(s, t_2)\,\mathrm{d}t_1\,\mathrm{d}t_2 ,$$

where $t = F(t_1, t_2)$ is the solution of

$$\begin{cases}\dfrac{(-u)^{\frac{1}{2}} - \sqrt{t}}{(-u)^{\frac{1}{2}} + \sqrt{t}} = \dfrac{(-u_1)^{\frac{1}{2}} - (t_1)^{\frac{1}{2}}}{(-u_1)^{\frac{1}{2}} + (t_1)^{\frac{1}{2}}}\,\dfrac{(-u_2)^{\frac{1}{2}} - (t_2)^{\frac{1}{2}}}{(-u_2)^{\frac{1}{2}} + (t_2)^{\frac{1}{2}}}, \\ F(t_1, t_2) = t_1 + t_2 + \dfrac{t_1 t_2}{2s} + \dfrac{1}{2s}\{t_1 t_2(16s^2 + 4st_1 + 4st_2 + t_1 t_2)\}^{\frac{1}{2}} .\end{cases} \tag{14}$$

This derivation does not prove the equivalence between eq. (13) and eq. (3), but this equivalence presumably holds except for very pathological potentials, for which, for example, $\tilde{\sigma}(\mu)$ differs very much from $\sigma(\mu)$ in its asymptotic behavior.

One can simplify a little eq. (13), by noticing that, by virtue of (14),

$$\frac{[(-u_1)^{\frac{1}{2}} - (t_1)^{\frac{1}{2}}][(-u_2)^{\frac{1}{2}} - (t_2)^{\frac{1}{2}}]}{(-u)^{\frac{1}{2}} - \sqrt{t}} = 2\sqrt{s}\,,$$

so that

$$\tilde{\xi}(s,t) = \frac{\sqrt{u}}{\pi}\iint \delta[t - F(t_1, t_2)]\,\tilde{g}(s, t_1)\,\tilde{g}^*(s, t_2)\,\frac{\mathrm{d}t_1\,\mathrm{d}t_2}{(u_1 u_2)^{\frac{1}{2}}}\,. \tag{15}$$

A perhaps useful hint about the calculation of $F(t_1, t_2)$ is that, if we write $t = 2s(\cosh\varphi - 1)$ and similarly for t_1 and t_2, then the relation $t = F(t_1, t_2)$ reads $\varphi = \varphi_1 + \varphi_2$. Let us indicate now the inverse transformation [3]:

$$f(t) = \frac{2}{\pi}\frac{\partial}{\partial t}\int \frac{(t')^{\frac{1}{2}}\tilde{f}(t')\,\mathrm{d}t'}{(t - t')^{\frac{1}{2}}}\,. \tag{15}$$

This may be cast into a different form, which is perhaps more convenient for practical purposes:

$$f(t) = \frac{2}{\pi}\tilde{f}(t) - \frac{1}{\pi}\int_0^t \frac{(t')^{\frac{1}{2}}\,f(t') - \sqrt{t}\,f(t)}{(t - t')^{\frac{3}{2}}}\,\mathrm{d}t'\,. \tag{16}$$

We have of course to use this formula once, at the very end of the solution of the problem, as all iterations of eq. (2) (with tilde quantities) and (15) do not involve the original quantities.

In the case where there are exchange forces, one cannot use this transformation directly, and one is forced to split the problem in two: one solves the problem using first $V_{\mathrm{ord}} + V_{\mathrm{exch}}$ as an ordinary potential. The even partial waves are then obtained correctly. The odd ones are obtained by taking $V_{\mathrm{ord}} - V_{\mathrm{exch}}$ as an ordinary potential.

In the case of the relativistic problem [1], one has only to insert the proper kinematical factor in eq. (15). Of course, to have crossing symmetry, it is essential to return to the expressions without tilde.

Let us add some remarks about the mathematical aspects of this method. We may ask what replaces the Legendre polynomial expansion for the amplitude $\tilde{f}$.

If we apply our transformation to the particular function $(2l+1)\,P_l(\cos\theta)$, we get a polynomial $R_l(\cos\theta)$. We know from eq. (11) the generating function of R_l:

$$\sum_{l=0}^{\infty} R_l(x)\,\alpha^l = \frac{1+\alpha}{1 - 2\alpha x + \alpha^2}\,.$$

It is easy to verify with the generating functions that

$$R_l(x) = 2^{l-1}\left\{T_l(x) + \frac{x+1}{l}\, T_l'(x)\right\},$$

where T_l is the Tchebyscheff polynomial of 1st kind (4). This may be written

$$R_l(\cos\theta) = \frac{\sin\left((2_l+1)/2\right)\theta}{\sin(\theta/2)}.$$

On the other hand, if one applies term by term the transformation to the expansion of $P_l(\cos\theta)$ in powers of $(\cos\theta - 1)$, the result is expressed in terms of the Jacobi polynomial (4):

$$R_l(x) = (2l+1)G_l\left(1,\ \frac{3}{2},\ \frac{1-x}{2}\right).$$

At the present stage, it is not known to the author whether these results present any deep significance.

---

(4) R. Courant and D. Hilbert: *Differential and Integral Calculus*, vol. **1** (New York, 1953), pp. 88-90.

RIASSUNTO (*)

Ottengo la riduzione del numero di integrazioni necessarie per calcolare da un potenziale l'ampiezza di scattering con i metodi di dispersione teorica.

(*) *Traduzione a cura della Redazione.*

Mössbauer Effect Measurements on Superconducting Indium (*).

P. P. Craig, R. D. Taylor and D. E. Nagle

Los Alamos Scientific Laboratory, University of California - Los Alamos, N. Mex.

(ricevuto il 14 Agosto 1961)

Summary. — The amplitude and width of the Mössbauer's resonance in ^{57}Fe has been measured for ^{57}Fe as a very dilute impurity in metallic indium. The resonance amplitude is found to remain substantially unchanged in the temperature interval 0.35 °K ÷ 4 °K, showing that the Debye's temperature of In increases by less than 3 °K in this temperature range. Specific heat measurements on In had indicated a possible Debye's temperature change of 12 °K. As the source is cooled from 300 °K to 4 °K the resonance amplitude increases by only 50% in contrast to the minimum of 500% calculated from the Debye-Waller's factor.

Recent specific heat measurements on the superconductors In [1] ($T_c = 3.69$ °K) and Nb [2] ($T_c = 3.70$ °K) have indicated that for these materials the lattice specific heat measured at temperatures below the superconducting transition temperature T_c deviates substantially from the usual cubic temperature dependence. In the case of In the experimental lattice specific heat obtained by Bryant and Keesom [1] (by subtracting from the total specific heat the electronic and nuclear quadrupole contributions) may be represented by the empirical formula, valid in the range $2 < T_c/T < 10$

$$C_l = AT^3 \exp\left[-BT_c/T\right], \tag{1}$$

where $A = 1.75$ millijoule/mole·deg^4 and $B = 0.055$.

(*) Work performed under the auspices of the U. S. Atomic Energy Commission.

(1) C. A. Bryant and P. H. Keesom: *Phys. Rev. Lett.*, **4**, 460 (1960); *Phys. Rev.*, in press.

(2) H. A. Boorse, A. T. Hirshfeld and H. Leupold: *Phys. Rev. Lett.*, **5**, 246 (1960).

One possible way of interpreting eq. (1), suggested by BRYANT and KEESOM [1], is to assign a temperature-dependence to the Debye's temperature θ. They conclude that at the lowest temperatures studied (0.35 °K) the experimental specific heat is consistent with a Debye's temperature of 121 °K, as compared with 109 °K in the normal state. The Debye's temperature obtained from the elastic constant, extrapolated to 0 °K, is 111.3 °K [3]. Although a change in the Debye's temperature of such a large amount in the superconducting state should imply gross changes in many physical properties of the material, no changes were observed in the elastic constant measurements [3]. However, such measurements involve only long wavelength phonons, and it is conceivable that the specific heat anomaly is due to changes in the Debye's temperature θ arising from some other part of the phonon spectrum.

We have utilized the Mössbauer effect to determine whether such large implied changes in θ are indeed responsible for the observed specific heat. At low temperatures ($T \ll \theta$) the probability f of emission of recoil free γ-rays of energy E from a nucleus of mass m is simply related to the Debye's temperature

$$f = \exp\left[-3R/2k\theta\right], \tag{2}$$

where k is the Boltzmann constant and $R = E^2/2mc^2$. Since R is a known constant and f is experimentally measurable, information about the temperature variation of θ may be obtained. When the Mössbauer nuclide exists as a very dilute impurity in a host lattice, it is reasonable that some effective mass m' other than that of the Mössbauer nucleus should be used in evaluating R [4]. However, no temperature-dependent terms would be introduced, so that this possibility does not affect our experiment.

We have chosen the resonance in ^{57}Fe for our studies. This isotope has a 14.4 keV, 0.1 μs first excited state which may conveniently be populated by decay following electron capture in 270 day ^{57}Co. A source, composed of ^{57}Co in 99.97 % In, was prepared by electroplating onto a sheet of In metal about 2 mC of carrier free ^{57}Co (about $2 \cdot 10^{15}$ atoms). This source was diffusion annealed in vacuum for about 10 minutes at about $\frac{1}{2}$ °C below the melting temperature of In (156.4 °C). The source was mounted in a ^{3}He cryostat capable of producing and maintaining temperatures down to 0.30 °K. The 14.4 keV radiation passed out the of cryostat through a series of Be and aluminized mylar windows. The γ-ray then passed through a single line unsplit absorber (~ 1 mg/cm^2 ^{57}Fe electroplated onto and diffused into Ti) mounted on a loudspeaker Doppler shift drive, and into a detector whose signal was fed into the analyzing electronics. The 14 keV transmission was recorded as

[3] B. S. CHANDRASEKHAR and J. A. RAYNE: *Phys. Rev. Lett.*, **6**, 3 (1961).
[4] F. L. SHAPIRO: *Sov. Phys. (Usp.)*, **3**, 881 (1961).

a function of Doppler shift velocity on a RIDL 400 channel analyzer. Accumulated data were recorded on punched tape and later analyzed by an IBM 704 computer, which performed a least squares fit to a Lorenzian curve.

The resonance strength at room temperature was found to be about 7% with a full line width of about 0.8 mm/s. Most of the width is known to be due to the absorber (quadrupole splitting is much too small to explain the observed width). No background corrections have been made to the pulse-height spectrum, so the resonance amplitudes given are relative only. When the source was cooled to 4 °K (and below), the resonance amplitude was about 10% and the width the same as at room temperature. The absorber was always kept at room temperature. No changes were seen upon cooling through the superconducting transition temperature T_c (as expected [5]). Upon cooling from 2.12 °K to 0.35 °K the resonance amplitude was found to increase by $(-0.46 \pm 1.3)\%$, and the width to increase by $(1.1 \pm 1.5)\%$. The probability is about 1 in 3 that the resonance amplitude increases by as much as 0.8%. Such an increase would correspond to an increase in the Debye's temperature of In of about 3 °K. The increase required to explain the specific heat measurements of BRYANT and KEESON is about 12 °K. It thus seems certain that the anomalous specific heat does not arise from gross changes in the Debye's θ.

Two theories have been advanced to explain the lattice specific heat anomaly in In and Nb. DAUNT and OLSON [6] have suggested that if the Debye's temperature θ is a function of temperature, then in differentiating the internal energy to obtain the specific heat the zero point energy will yield a finite (negative) contribution to the specific heat. Quantitative estimates of the change in θ are made using the known temperature-dependence of the difference in compressibility between the superconducting and the normal states. FERRELL [7] has proposed a different mechanism, based upon anomalous dispersion in part of the phonon spectrum. The extra dispersion arises from the fact that the frequency of sound waves is dependent upon the response of the conduction electrons. While these two models seem to be considerably different from each other, both of them predict changes in the effective Debye's temperature of the superconductor which are too small to be distinguished by the Mössbauer's technique. Thus, our results are consistent with both theories, and are incapable of distinguishing between them.

An unexplained feature of our measurements is the extremely weak temperature-dependence of the resonance between 300 °K and 4 °K. According

---

[5] P. P. CRAIG, D. E. NAGLE and R. D. REISWIG: *Journ. Phys. and Chem. of Solids*, **17**, 168 (1960).

[6] J. G. DAUNT and J. L. OLSON: *Phys. Rev. Lett.*, **6**, 267 (1961)

[7] R. A. FERRELL: *Phys. Rev. Lett.*, **6**, 541 (1961).

to the Debye-Waller's factor, the resonance amplitude should change by a factor of roughly 30 over this temperature range if we use in eq. (2) the mass of the ^{57}Fe nucleus. If, following SHAPIRO ([4]), we use the mass of In (115) this factor is reduced to 5. This question is now under investigation.

* * *

A helpful discussion with professor J. G. Daunt is acknowledged. We would like to thank Dr. D. R. F. Cochran for assistance in the preparation of the source used in these experiments.

RIASSUNTO (*)

Abbiamo misurato l'ampiezza e la larghezza della risonanza di Mössbauer del ^{57}Fe nello stato di impurità molto diluita nell'indio. Troviamo che l'ampiezza della risonanza rimane sostanzialmente invariata nell'intervallo di temperatura fra 0.35 °K e 4 °K, mostrando che la temperatura di Debye dell'In aumenta di meno di 3 °K in questo intervallo di temperatura. Le misure del calore specifico dell'In avevano indicato una possibile variazione della temperatura di Debye di 12 °K. Quando la sorgente è raffreddata da 300 °K a 4 °K l'ampiezza di risonanza cresce solo del 50% in contrasto con il minimo di 500% calcolata dal fattore di Debye-Waller.

(*) *Traduzione a cura della Redazione.*

IL NUOVO CIMENTO Vol. XXII, N. 2 16 Ottobre 1961

The Effect of a Pion-Pion Interaction on the π^0 Photoproduction.

B. De Tollis

Istituto di Fisica dell'Università - Roma
Istituto Nazionale di Fisica Nucleare - Sezione di Roma

A. Verganelakis (*)

Scuola di Perfezionamento in Fisica Nucleare - Roma

(ricevuto il 14 Agosto 1961)

Summary. — It is shown that the results of the Chew, Goldberger, Low and Nambu dispersive theory, taking into account the pion-pion interaction in the resonance states $T=1$, $J=1$ of two pions and $T=0$, $J=1$ of three pions (with a suitable choice of some parameters that appear in the theory), are in good agreement with experimental data for π^0 photoproduction on protons for energies from threshold up to (400÷450) MeV.

1. – In previous papers [1,2] we have used a simple model based on the Cini-Fubini approximation [3] to the Mandelstam representation [4], in order to take into account the effect of a pion-pion interaction (in the resonance state $T=1$, $J=1$) in photoproduction processes. With this aim we have considered the ratio $(d\sigma/d\sigma^{\perp})_{90^\circ}$ of the π^- and π^+ photoproduction cross-sections, and the ratio $d\sigma^{\parallel}/d\sigma^{\perp}$ of the π^0 photoproduction with polarized γ's parallel and perpendicular to the production plane.

(*) With a scholarship of the Greek Atomic Energy Commission.

(1) B. De Tollis, E. Ferrari and H. Munczek: *Nuovo Cimento*, **18**, 198 (1960).
(2) B. De Tollis and A. Verganelakis: *Phys. Rev. Lett.*, **6**, 371 (1961).
(3) M. Cini and S. Fubini: *Ann. Phys.*, **3**, 352 (1960).
(4) S. Mandelstam: *Phys. Rev.*, **112**, 1344 (1958); **115**, 1752 (1959).

In this work we shall see that the relativistic dispersion theory of Chew, Goldberger, Low and Nambu (5) (CGLN), in which the effect of the pion-pion interaction in the $T=1$, $J=1$ (« bipion ») and in the $T=0$, $J=1$ resonance state of three pions (« tripion ») is included, is able to give a satisfactory fit to the available experimental data of π^0 photoproduction on protons at low energies. The presence of the « tripion » appears justified mainly on the basis of recent investigations on the isoscalar part of the nucleon's form factor (6,7). Its contribution is simply evaluated with an analogous model as in the « bipion » case (8).

2. – The results of our calculations are as follows. Assuming that only s- and p-wave contribute to the process, we write the differential cross-section for π^0 photoproduction by non polarized γ's, in the C.M. system, as

$$\sigma_{\text{unp}} = A + B\cos\vartheta + C\cos^2\vartheta\,, \tag{1}$$

with

$$\begin{cases} A = (q/k)\ \mathrm{Re}\left\{|E_{0+}|^2 + |M_{1-}|^2 + \frac{5}{2}|M_{1+}|^2 + \frac{9}{2}|E_{1+}|^2 + M_{1-}^* M_{1+} + \right. \\ \qquad \left. + 3E_{1+}^*(M_{1-} - M_{1+}) + \tfrac{1}{2}R^2 + E_{0+}^* R\right\}, \\ B = (2q/k)\ \mathrm{Re}\left\{E_{0+}^*(M_{1-} - M_{1-}) + 3E_{1+}^*(E_{0+} + R)\right\}, \\ C = (q/k)\ \mathrm{Re}\left\{-\tfrac{3}{2}|M_{1+}|^2 + \tfrac{9}{2}|E_{1+}|^2 - 3M_{1-}^* M_{1+} + 9E_{1+}^*(M_{1-} - M_{1-}) - \right. \\ \qquad \left. - \tfrac{1}{2}R^2 - E_{0+}^* R - 6E_{1+}^* R\cos\vartheta\right\}, \end{cases} \tag{2}$$

where $\boldsymbol{k}$ and $\boldsymbol{q}$ are the 3-momenta of the photon and the pion; ϑ is the pion production angle (angle between $\boldsymbol{k}$ and $\boldsymbol{q}$); E_{0+} and E_{1-} are the electric dipole and electric quadrupole scattering amplitudes; M_{1-} and M_{1+} are the magnetic dipole amplitudes with $J=\frac{1}{2}$ and $J=\frac{3}{2}$ in the final state, respectively; finally, the quantity R is connected with the nucleon recoil. The explicit expression

(5) G. F. Chew, M. L. Goldberger, F. E. Low and Y. Nambu: *Phys. Rev.*, **106**, 1345 (1957).

(6) G. F. Chew: *Phys. Rev. Lett.*, **4**, 142 (1960).

(7) S. Bergia, S. Fubini and A. Stanghellini: *Phys. Rev. Lett.*, **6**, 367 (1961); S. Bergia and A. Stanghellini: *Nuovo Cimento*, **21**, 155 (1961).

(8) M. Gourdin, D. Lurié and A. Martin: *Nuovo Cimento*, **18**, 933 (1960).

for the foregoing amplitudes, in the CGLN theory, are

$$
(3)\qquad \begin{cases} E_0 &= ef\{\omega\alpha(N^{(+)}-\mu)+i(2/3)(\delta_1-\delta_3)F_s\}\,, \\ E_1 &= -ef(2/9)kq^4F_Q h_{33}\,, \\ M_1 &= ef(1/3)kq\{\lambda(h_{11}+2h_{31})-2\mu(\alpha/\omega)\}\,, \\ M_{1+} &= ef(1/3)kq\{\lambda(h_{13}+2h_{33})+i(2/3)q^3F_M h_{33}+\mu(\alpha/\omega)\}\,, \\ R &= efq^2\alpha/M\omega\,. \end{cases}
$$

When the « bipion » and the « tripion » are included, the cross-section is still of the form (1), provided that in the expressions (2) for A, B and C the following substitutions are performed:

$$
(4)\qquad \begin{cases} E_{0+}\to E_{0+}+\varepsilon_{0+}^{(B)}+\varepsilon_{0+}^{(T)}\,; & E_{1+}\to E_{1+}+\varepsilon_{1+}^{(B)}+\varepsilon_{1+}^{(T)}\,; \\ M_{1-}\to M_{1-}+\mu_{1-}^{(B)}+\mu_{1-}^{(T)}\,; & M_{1+}\to M_{1+}+\mu_{1+}^{(B)}+\mu_{1+}^{(T)}\,; \\ R\to R+\varrho^{(B)}+\varrho^{(T)}\,; \end{cases}
$$

the superscript B and T refer to quantities (ϑ-dependent) connected to the « bipion » and the « tripion », respectively. Their explicit expressions are

$$
(5)\qquad \begin{cases} \varepsilon_{0+}^{(B,T)} = -\dfrac{A_{B,T}}{t_{B/T}-t}\cdot\dfrac{\varrho_1\alpha}{W}\left\{\omega^2-\beta_{B,T}\omega t+\dfrac{1}{2}(t-1)\right\}, \\ \varepsilon_{1+}^{(B/T)} = -\mu_{1+}^{(B/T)} = \dfrac{A_{B/T}}{t_{B/T}-t}\cdot\dfrac{\varrho_1\omega q\alpha}{6W}(\omega\beta_{B/T}-1)\,, \\ \mu_1^{(B/T)} = \dfrac{A_{B,T}}{t_{B/T}-t}\cdot\dfrac{\varrho_1\omega q\alpha}{3W}\left\{\omega\beta_{B/T}-1+\dfrac{3\varrho_2}{\varrho_1}\left|W-M+\beta_{B/T}t-\dfrac{t-1}{2(W-M)}\right|\right\}, \\ \varrho^{(B/T)} = -\dfrac{A_{B/T}}{t_{B/T}-t}\cdot\dfrac{\varrho_2\omega\alpha q^2}{W}\{1+\beta_{B/T}(W+M)\}\,. \end{cases}
$$

In (3) and (5) the notation is as follows ($\hbar=c=m_{\pi^0}=1$): M = proton mass; $W=k+(k^2+M^2)^{\frac{1}{2}}$; $\omega=W-M$; $\omega_0=(q^2+1)^{\frac{1}{2}}$; $\alpha=(1+\omega/M)^{-1}$; $E_1=(k^2+M^2)^{\frac{1}{2}}$ $E_2=(q^2+M^2)^{\frac{1}{2}}$; $\varrho_1=\big((E_1+M)(E_2+M)\big)^{\frac{1}{2}}$; $\varrho_2=\big((E_1+M)/(E_2+M)\big)^{\frac{1}{2}}$; $t=1-2k\omega_0+2qk\cos\vartheta$; $\mu=(g_P+g_N)/2M$. The constants β_B and β_T are connected

to the isovector and isoscalar part of the anomalous gyromagnetic ratio of the nucleon (and corresponds to C_2/C_1 and C_2'/C_1' that appear in ref. [8]). We have used the values [7]: $\beta_B = 0.266$, $\beta_T = -0.046$. t_B and t_T represent the quadratic « masses » of the « bipion » and the « tripion », and we have set [7]: $t_B = 23$, $t_T = 5$. Λ_B and Λ_T are proportional to « strength » of the two and three pions interaction, respectively. All the other symbols are as in ref. [5].

3. – The parameters which have more influence on the cross-section are essentially ω_{res} and $N^{(+)}$ of the CGLN theory, the small p-wave phase shifts, and Λ_B and Λ_T of the pion-pion interaction. We have taken the small p-wave phase shifts by a qualitative fit to experimental data [9], without using the effective range formula. The $\omega_{res} = 2.2$ ($f^2 = 0.081$) and $N^{(+)} = -0.07$ in order to be in agreement with the experimental data near the resonance (where the effect of the pion-pion interaction is negligible). Λ_B and Λ_T are considered as adjustable parameters; their effect is the following: by increasing Λ_B, the value of the backward cross-section decreases, while in the forward direction its effect is negligible. By increasing Λ_T, the cross-section increases around $\vartheta = 90°$.

Having in mind these remarks we have seen that a reasonable fit to the experimental data can be obtained by setting

$$\Lambda_B = 0.6\, ef\,, \qquad \Lambda_T = 0.4\, ef\,.$$

We note, by the way, that the presence of the « tripion » with $\Lambda_T = 0.4\, ef$, permits us to maintain the value of Λ_B within an interval necessary to be in agreement with the experimental data on the ratio $d\sigma^-/d\sigma^+$ at different angles [10].

We have computed the cross-section starting from $E_\gamma = 160$ MeV up to $E_\gamma = 450$ MeV (E_γ = energy of γ in the laboratory system). In Fig. 1 (*a*, *b*, *c*) we give the angular distributions for three representative energies: $E_\gamma = 220$, 320 and 400 MeV. In Fig. 1 the experimental data [11-14] are also shown. It

---

[9] B. Pontecorvo *et al.*: *Ninth Annual International Conference on High-Energy Physics* (Kiev, 1959), unpublished; S. W. Barnes, B. Rose, G. Giacomelli, J. Ring, K. Miyake and K. Kinsey: *Phys. Rev. Lett.*, **3**, 592 (1959); *Phys. Rev.*, **117**, 238 (1960).

[10] E. Ferrari: private communication. The value $\Lambda_B = 1.46\, ef$ used in ref. [1] so as to fit the experimental data of the $d\sigma/d\sigma^+$ ratio at $\vartheta = 90°$, seems unsuitable at other angles. It appears that a better agreement at all angles is reached with a lower value of Λ_B ($\sim 0.5\, ef$) (by setting the constant a of ref. [1] equal to zero).

[11] R. G. Vasil'kov, B. B. Govorkov and V. I. Gol'danskii: *Žurn. Èksp. Teor. Fiz.*, **37**, 11 (1959); translation: *Sov. Phys. JETP*, **37**, 7 (1960).

[12] D. C. Oakley and R. L. Walker: *Phys. Rev.*, **97**, 1283 (1955).

[13] W. C. McDonald, V. Z. Peterson and D. R. Corson: *Phys. Rev.*, **107**, 577 (1957).

[14] K. Berkelmann and J. A. Waggoner: *Phys. Rev.*, **117**, 1364 (1960).

appears that the fit is satisfactory. The same agreement holds at other energies.

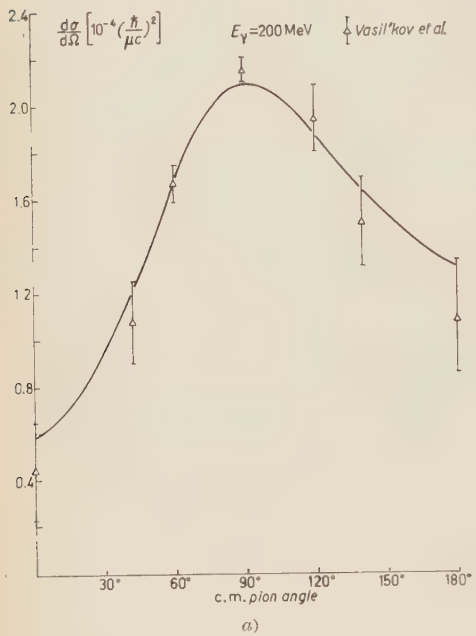

a)

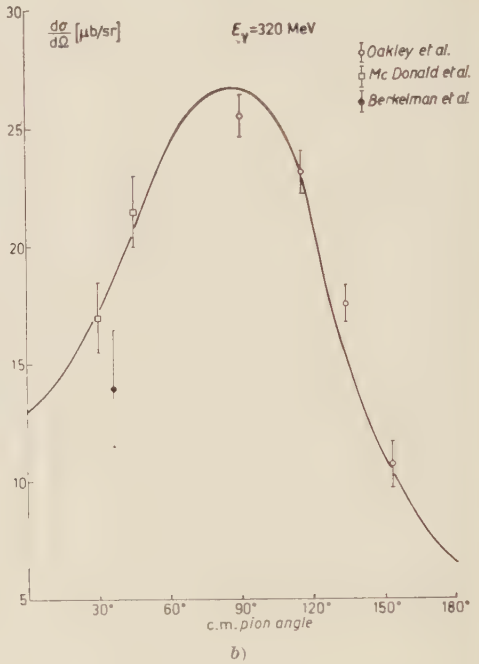

b)

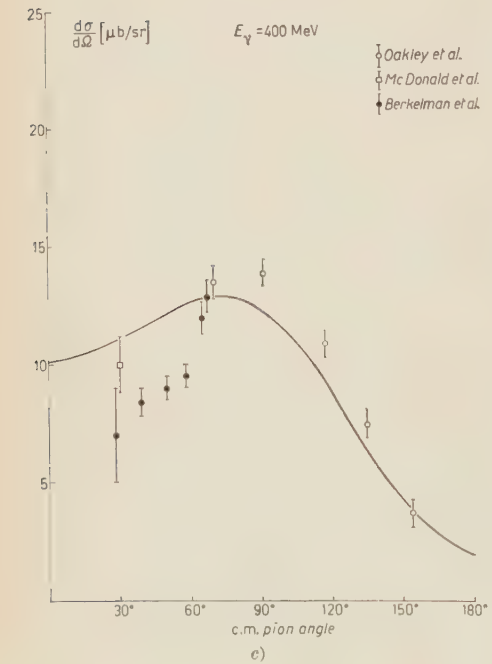

c)

Fig. 1. – *a*) The differential cross-section for π^0 photoproduction at fixed energy of the γ in the lab. system: $E_\gamma = 220$ MeV. The full line has been calculated by means of the CGLN theory ($f^2 = 0.081$, ω_{re} 2.2, $N^{(+)}$ 0.07), corrected by the « bipion » ($t_B = 23$, $\Lambda_B = 0.6$ *ef*) and the « tripion » ($t_T = 5$, $\Lambda_T = 0.4$ *ef*). The experimental points are taken from ref. [11]. *b*) The same at $E_\gamma = 320$ MeV. The theoretical curve has been calculated as in Fig. 1*a*. The experimental points are taken from ref. [12-14]. *c*) The same at $E_\gamma = 400$ MeV. The theoretical curve has been calculated as in Fig. 1(*a*, *b*). The experimental points are taken from ref. [12-14].

Furthermore we have calculated the constants $a_0^{(0)}$, $a_0^{(2)}$, $b_0^{(1)}$ and $c_0^{(2)}$ that appear in the expansion of the cross-section in series up to q^2 at threshold ($q < 0.7$):

$$\sigma_{\text{tot}} \approx (\hbar/m_{\pi^0}c)^2 \cdot 10^{-4} q\omega_0 (1 + k/E_1)^{-1}(1 + \omega_0/E_2)^{-1} \cdot \\ \cdot (a_0^{(0)} + a_0^{(2)} q^2 + b_0^{(1)} q \cos\vartheta + c_0^{(2)} q^2 \cos^2\vartheta) .$$

Using for the scattering lengths the values: $a_1 - a_3 = 0.283$, $a_{11} = -0.018$, $a_{13} = -0.049$, $a_{31} = -0.044$ and $a_{33} = 0.198$, we obtain

$$a_0^{(0)} = 0.1 ; \quad a_0^{(2)} = 1.7 ; \quad b_0^{(1)} = -0.5 ; \quad c_0^{(2)} = -0.7$$

in good agreement with the corresponding data which can be extracted by extrapolating at threshold the experimental coefficients of the angular distributions ([11]):

$$a_0^{(0)} \simeq 0.12 ; \quad a_0^{(2)} \simeq 1.5 ; \quad b_0^{(1)} \simeq -0.5 ; \quad c_0^{(2)} \simeq -0.8 .$$

4. – We have, on the other hand, been interested in the approach of the π^0 photoproduction with polarized γ-rays (for which experiments are in progress). In this case, the cross-section may be written as in (1) with the addition of the term: $D \sin^2\vartheta \cos 2\varphi$, where φ is the angle between the plane of polarization and the production plane, and D has the form

$$(6) \qquad D = (q/k)\, \mathrm{Re}\{-\tfrac{3}{2}|M_{1+}|^2 + \tfrac{9}{2}|E_{1+}|^2 - 3M_{1-}^* M_{1+} + 3E_{1+}^*(M_{1-} - M_{1+}) + \\ + [\tfrac{1}{2}R^2 + E_{0+}^* R + 6E_{1+}^* R \cos\vartheta]\} ,$$

(substitution (4), when the « bipion » and the « tripion » are included, should be borne in mind).

In Fig. 2 (*a*) the curves of the ratio $d\sigma_\parallel/d\sigma_\perp$ *vs.* E_γ are drawn for three angles: $\vartheta = 60°$, $90°$ and $120°$, calculated with the same values of the parameters as in the unpolarized case.

The effect of the pion-pion interaction on π^0 photoproduction with polarized γ's, can be summarized in the inequality; $D \neq C$ ([15]). On the contrary, in the CGLN theory (without the pion-pion interaction), as in other recent theories ([16]), $D \simeq C$; the difference between C and D (see form. (2) and (6))

([15]) Preliminary measurements of Prof. R. F. Mozley, at Stanford University, seem to give a clear evidence for $D \neq C$. We are particularly pleased to express our thanks to Prof. Mozley for sending us his experimental results.

([16]) L. D. Solovyov and Chen Jung-mo: *Application of the differential method for obtaining the photoproduction amplitude from dispersion relations* (preprint).

consisting in small terms connected to the electric quadrupole and nucleon recoil.

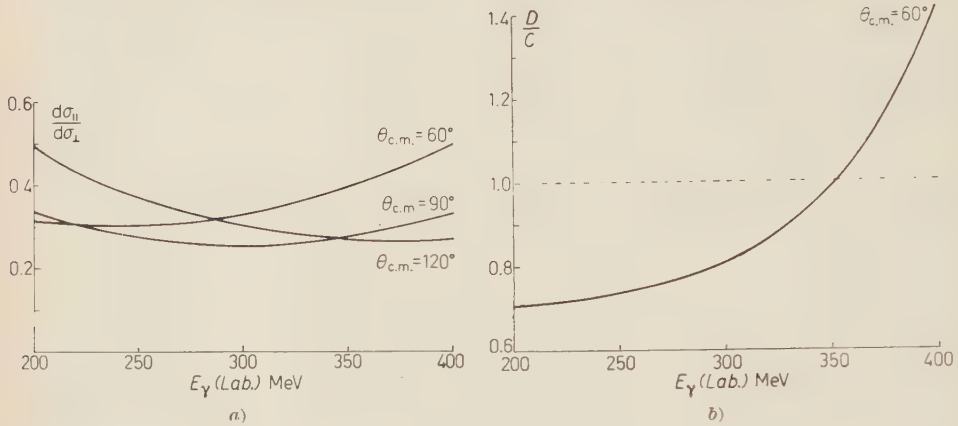

Fig. 2. – *a*) The ratio $d\sigma_\parallel/d\sigma_\perp$ *vs.* E_γ for $\vartheta=60°$, 90° and 120°. The three curves have been calculated as in Fig. 1 (CGLN+« bipion »+« tripion ») with the same values of the parameters. *b*) The ratio D/C *vs.* E_γ for $\vartheta=60°$. (D and C are the coefficients appearing in the cross-section for π^0 photoproduction by polarized γ's:

$$A + B\cos\vartheta + C\cos^2\vartheta + D\sin^2\vartheta\cos 2\varphi).$$

We give in Fig. 2 (*b*) the D/C ratio *vs.* E_γ for $\vartheta=60°$. The curves at $\vartheta=90°$ and 120° have the same behaviour.

Measurements with sufficiently good statistics of the following quantity (which coincides with $-D$) [17]:

$$\frac{1-(d\sigma_\parallel/d\sigma_\perp)\ \sigma_{unp}}{1+(d\sigma_\parallel/d\sigma_\perp)\sin^2\vartheta},$$

and comparison with the existing experimental values of C, will allow our calculations to be verified. Another test of the pion-pion interaction could be the dependence of D on ϑ [2,17].

5. – Finally, one can conclude that in CGLN theory, at its present state, it seems necessary to include a pion-pion interaction in order to have agreement with the experimental data.

The validity of the CGLN theory, the reliability of some of its approximations and consequently the necessity of other possible corrections (for instance *s*-wave relativistic corrections), remain, of course, an open question [18].

[17] This quantity (indicated with A) has been defined by R. C. Smith and R. F. Mozley: *Proc. of the 1960 Annual International Conference on High-Energy Physics at Rochester* (New York, 1960), p. 22.

[18] See, for example, K. Dietz, G. Hohler and A. Mullensiefen: *Zeits. f. Phys.*, **159**, 77 (1960).

* * *

We wish to thank Professor M. CINI for many fruitful discussions and for his constant helpful advice. We are also grateful to Professor M. AGENO who has permitted the use of the I.B.M. computer of the « Istituto Superiore di Sanità » at Roma, and Dr. A. REALE for his valid help in writing the computer program.

RIASSUNTO

Si dimostra che i risultati della teoria dispersiva di Chew, Goldberger, Low e Nambu, se si tiene conto dell'interazione pione-pione negli stati risonanti $T=1$, $J=1$ di due pioni e $T=0$, $J=1$ di tre pioni, sono in buon accordo (con una opportuna scelta di alcuni parametri che compaiono nella teoria) con i dati sperimentali sulla fotoproduzione di π^0 su protoni per energie dalla soglia fino a $(400 \div 450)$ MeV.

The Mass Difference of the Neutral K-Mesons and the Validity of the Pertubation Expansion in the Theory of Weak Interactions.

J. Nilsson (*)

CERN - Geneva

(ricevuto il 23 Agosto 1961)

Summary. — In the conventional $V-A$ theory of weak interactions, the selection rule $\Delta S \leqslant 1$ requires that the mass difference of the neutral K-mesons must be a second order effect in the weak interactions. This mass difference has actually been established by several experimental groups and it constitutes the single clear-cut piece of information on such higher order effects available at present. The experimental value of the mass difference could thus possibly give an estimate of the size of the cut-off entering the theory of weak interactions in order to make the individual terms in the perturbation expansion finite. Earlier attempts to determine the size of this cut-off have only established upper limits and in contrast to the mass splitting $\Delta m(K_1^0 - K_2^0)$ the results from the processes considered so far all critically depend on which version of the theory of weak interactions one applies. The theoretical interpretation of results from processes involving bosons are, however, partly obscured by the presence of strong interactions. One expects that the effective cut-off for such processes will be influenced by the strong interaction cut-off, which is of the order of the nucleon mass. It will be shown that the cut-off compatible with the observed value of $|\Delta m(K_1^0 - K_2^0)|$ is of the order of a few nucleon masses within two different schemes for the theory of weak interactions and the possible implications of these results are discussed. The two schemes both lead to the result that the K_2^0 meson is heavier than the K_1^0 meson. So far the sign of the mass difference has not been determined experimentally.

(*) On leave from the Department of Mathematical Physics, Chalmers University of Technology, Gothenburg.

1. – Introduction.

In processes involving weak interactions one usually treats the weak interaction part to first order only, arguing that higher order corrections, are negligible due to the smallness of the coupling constant. This would be a valid argument if the perturbation expansion for weak processes were an expansion in powers of the coupling constant G only, but the dimensional character of G leads to an effective expansion parameter $G\Lambda^2/(2\pi)^2$, where Λ is a cut-off introduced in the theory to make it convergent. It is, therefore, essential to determine the size of this cut-off in order to ensure the consistency of the theory of weak interactions, that is, to ensure the validity of the perturbation expansion in the theory.

In an earlier paper by the same author [1] the muon decay was considered in order to yield information with regard to the size of the cut-off. The muon decay was chosen because of the absence of strong interactions and the general belief that weak interactions involving leptons only are well understood. The information on the cut-off stems from the two modes $\mu \to e + \gamma$ and $\mu \to 3e$ which can proceed through second order diagrams [2] only. The main disadvantage with the choice of these two processes is that neither one has actually been observed. Experimentally, upper limits for the transition probabilities of these modes are given from which one can deduce an upper limit for the cut-off. However, the apparent absence of these decay modes has led some authors [3] to speculate whether these « unwanted processes » are strictly forbidden by means of some still unknown symmetry principle imposing new selection rules on weak processes or if possibly the neutrino in the electron component of the weak interaction current is different from the one in the muon component. The existence of two kinds of neutrinos would also make the $\mu \to e + \gamma$ and the $\mu \to 3e$ strictly forbidden as two different kinds of neutrinos cannot annihilate. Neither one of these hypothesis has been proved or disproved, but it should be noted that they are not needed either in order to save the theory. If the cut-off is small enough $(\Lambda \leqslant (50 \div 100)\,\mathrm{GeV})$, the expected transition probabilities are still smaller than the experimental upper

[1] J. Nilsson: *Nuovo Cimento*, **21**, 135 (1961).

[2] This is true if one assumes quadratic terms of the type (eν)(νe) and if there is only one kind of neutrinos. If self-coupling terms are omitted in the weak interaction Hamiltonian these processes can proceed through third order diagrams. If there are two kinds of neutrinos both processes are strictly forbidden.

[3] B. Pontecorvo: *Žurn. Èks. Teor. Fiz.*, **37**, 1751 (1959); G. Feinberg, P. Kabir and S. Weinberg: *Phys. Rev. Lett.*, **3**, 527 (1959); N. Cabibbo and R. Gatto: *Phys. Rev.*, **116**, 1334 (1959); N. Cabibbo, R. Gatto and C. Zemach: *Nuovo Cimento*, **15**, 1192 (1960); N. Cabibbo and R. Gatto: *Phys. Rev. Lett.*, **5**, 114 (1960); *Nuovo Cimento*, **19**, 612 (1961).

limits. Moreover, from the point of view of a unified description of elementary particle physics (4), the existence of a second kind of neutrinos would be very disturbing.

In view of these difficulties with the muon decay modes, it would be very appealing to find a process which can proceed through second or higher order diagrams only and which has been experimentally observed. Such a process would yield a definite value for the cut-off and not only an upper limit. At present, however, there are no such processes known unless one accepts processes for which the interpretation is obscured by strong interactions. For processes where also strong interactions play an important role, one would expect that the effective cut-off would be somewhere between the strong interaction cut-off and the corresponding weak interaction cut-off, provided that these two cut-offs are different. As the strong interaction cut-off is of the order of the nucleon mass it would, therefore, be difficult to understand if a cut-off considerably larger than the nucleon mass would be necessary to explain the experimental findings.

In spite of the inherent difficulty with processes affected by strong interactions, we shall in this paper consider such a « mixed » process, namely, the transition of a K^0 into a $\bar{K}^0$ meson. This transition must at least in part be due to weak interactions as it is strangeness non-conserving and, as will be shown below, it will give rise to an observable mass difference between the two decay states for the neutral K mesons usually denoted K_1^0 and K_2^0. The mass difference $\Delta m(K_1^0 - K_1^0)$ has been experimentally determined by several groups and the best value given so far is (5) $\Delta m(K_1^0 - K_2^0) = (0.84 \pm 0.29)h/\tau_1$, where τ_1 is the lifetime of the K_1^0 meson.

We shall compensate at least in part for the difficulties connected with the strong interactions by investigating the mass difference $\Delta m(K_1^0 - K_2^0)$ within two essentially different schemes for the theory of weak interactions involving baryons and mesons as well as leptons. It will be found that the final result does not critically depend on which scheme one adopts which gives some confidence in the calculations.

2. – The mass splitting between the two neutral K-mesons due to weak interactions.

The production of neutral K-mesons is due to strangeness conserving interactions, which means that the states produced are eigenstates of the strangeness operator if the initial states are, and that is usually the case. The states

(4) R. E. Marshak and S. Okubo: *Nuovo Cimento*, **19**, 1226 (1961); M. Gell-Mann: CTSL-report 20.

(5) R. H. Good: preprint.

corresponding to definite strangeness are conventionally denoted $|K^0\rangle$ and $|\bar{K}^0\rangle$ and we shall denote the corresponding field operators $\Phi(x)$ and $\Phi^+(x)$. In momentum space the field operators are defined by

$$(2.1)\qquad \begin{cases} \Phi(x) = \dfrac{1}{(2\pi)^{\frac{3}{2}}} \displaystyle\int \frac{\mathrm{d}^3\boldsymbol{k}}{\sqrt{2k_0}} \{\Phi_1^{(-)}(\boldsymbol{k}) \exp[-ikx] + \Phi_2^{(+)}(\boldsymbol{k}) \exp[ikx]\}\,, \\ \Phi^+(x) = \dfrac{1}{(2\pi)^{\frac{3}{2}}} \displaystyle\int \frac{\mathrm{d}^3\boldsymbol{k}}{\sqrt{2k_0}} \{\Phi_2^{(-)}(\boldsymbol{k}) \exp[-ikx] + \Phi_1^{(+)}(\boldsymbol{k}) \exp[ikx]\}\,. \end{cases}$$

The operator $\Phi_1^{(-)}$ thus annihilates a K^0-meson of strangeness $+1$ and $\Phi_2^{(+)}$ creates a $\bar{K}^0$-meson of strangeness -1. Similarly $\Phi_2^{(-)}$ annihilates a $\bar{K}^0$-meson while $\Phi_1^{(+)}$ creates a K^0-meson.

For discussions of decays of neutral K-mesons the states $|K^0\rangle$ and $|\bar{K}^0\rangle$ are no longer convenient as the decays are caused by weak interactions which contain strangeness non-conserving parts. The weak interactions are, however, invariant under the combined operation CP, and the appropriate states for discussions of the decays should, therefore, be chosen as eigenstates of the CP operator. As can be easily seen, the following states fulfil this requirement (6)

$$(2.2)\qquad \begin{cases} |K_1^0\rangle = \dfrac{1}{\sqrt{2}} \{|K^0\rangle + |\bar{K}^0\rangle\}\,, \\ |K_2^0\rangle = \dfrac{1}{i\sqrt{2}} \{|K^0\rangle - |\bar{K}^0\rangle\}\,. \end{cases}$$

For the corresponding field operators similar relations hold

$$(2.3)\qquad \begin{cases} \Phi_{K_1^0} = \dfrac{1}{\sqrt{2}} \{\Phi^+ + \Phi\}\,, \\ \Phi_{K_2} = \dfrac{1}{i\sqrt{2}} \{\Phi^+ - \Phi\}\,. \end{cases}$$

The factor i is inserted in the definition of $\Phi_{K_2^0}$ in order to make this operator hermitian.

The particles corresponding to the $|K^0\rangle$ and $|\bar{K}^0\rangle$ states are quanta of the same field. If then follows from TCP-invariance (7) that their physical masses are equal. This is for the K_1^0 and K_2^0 mesons in general no longer true as their relation to each other is not the one of particle-antiparticle. Indeed, the

(6) M. Gell-Mann and A. Pais: *Phys. Rev.*, **97**, 1387 (1955).
(7) P. Roman: *Theory of Elementary Particles* (Amsterdam, 1960), p. 342.

strangeness non-conserving part of weak interactions will give rise to a mass splitting between K_1^0 and K_2^0 in a way resembling mass renormalization in quantum electrodynamics as there will be diagrams of the type shown in Fig. 1*b*. which will affect the propagation of the K_1^0 and the K_2^0 fields differently. This difference in propagation for the two fields is simply a manifestation of their different physical masses.

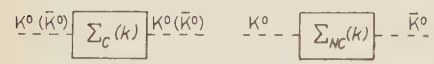

Fig. 1. – Feynman diagrams corresponding to « mass renormalization » of the K_1^0 and the K_2^0.

We shall first show that diagrams of the type shown in Fig. 1 actually correspondt o a kind of mass renormalization and later investigate how this mass renormalization acts differently in the case of K_1^0 as compared to K_2^0.

The contribution to the S operator from a diagram of the type shown in Fig. 2 is given by

$$S = -i\int \mathrm{d}^4k\, \Phi_{K_1^0}(k)\, \Sigma(k)\, \Phi_{K_1^0}(k)\,, \tag{2.4}$$

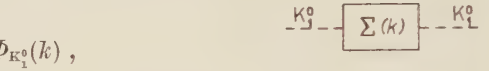

Fig. 2. – A diagram contributing to mass renormalization for K_1^0.

where $\Sigma(k)$ denotes the propagator carrying the $\Phi_{K_1^0}$ field in the initial state into the $\Phi_{K_1^0}$ field in the final state. In (2.4) we have absorbed numerical factors and phase factors in $\Sigma(k)$. The $\Phi_{K_1^0}(k)$ operator is the Fourier transform of $\Phi_{K_1^0}(x)$ defined by

$$\Phi_{K_1^0}(k) = \int \mathrm{d}^4x\, \Phi_{K_1^0}(x)\, \exp\,[-ikx]\,. \tag{2.5}$$

For the physical interpretation of (2.4) it is convenient to rewrite $\Sigma(k)$ in the following way

$$\Sigma(k) = a + b(k^2 - m^2) + \ldots\,, \tag{2.6}$$

where a and b are constants independent of k. If now the initial and the final K_1^0 meson are free, that is if the lines joining the box in Fig. 2 are external, then only the constant a in (2.6) will contribute to (2.4) as the field operators $\Phi_{K_1^0}(k)$ then satisfy the Klein-Gordon equation

$$(k^2 - m^2)\, \Phi_{K_1^0}(k) = 0\,. \tag{2.7}$$

Thus

$$S = -ia\int \mathrm{d}^4k\, \Phi_{K_1^0}(k)\, \Phi_{K_1^0}(k)\,. \tag{2.8}$$

This is, however, exactly the contribution to lowest order in the perturbation expansion from an additional term in the interaction Hamiltonian of the form

$$a\int \mathrm{d}^3x\, \Phi_{\mathrm{K}_1^0}(x)\, \Phi_{\mathrm{K}_1^0}(x)\,, \tag{2.9}$$

and the physical interpretation of the constant a, is, therefore, that of a mass renormalization. To get the exact relation between the constant a and the mass shift we recall that the free Lagrangian is of the form

$$\mathscr{L} = \tfrac{1}{2}\,\partial_\mu \Phi \partial^\mu \Phi - \tfrac{1}{2} m^2 \Phi^2\,. \tag{2.10}$$

If we now denote the observed mass m_0 and the mass shift δm, that is

$$m = m_0 + \delta m \tag{2.11}$$

we have for $\delta m \ll m_0$

$$\mathscr{L} \simeq \tfrac{1}{2}\,\partial_\mu \Phi \partial^\mu \Phi - \tfrac{1}{2} m_0^2 \Phi^2 - m_0\, \delta m \Phi^2\,. \tag{2.12}$$

We thus conclude

$$a = m_0\, \delta m\,. \tag{2.13}$$

To see how this mass renormalization affects the K_1^0 meson differently from the K_2^0 meson it is most convenient to classify all possible mass diagrams as it was done in Fig. 1. A diagram belongs to category (*a*) if it contains a strangeness conserving propagator function $\Sigma_c(k)$, that is, connecting external lines of the same strangeness. A diagram belongs to category (*b*) if it contains a strangeness non-conserving propagator function. A diagram belonging to category (*a*) can, of course, possibly contain strangeness non-conserving vertices, but then always so that they compensate for the change in strangeness with the net result that strangeness is conserved. In the same way, a diagram from category (*b*) can always contain strangeness-conserving vertices, but as a whole strangeness is not conserved for such a diagram. The contribution from all possible mass diagrams to the S operator for the K_1^0 meson can now be written

$$S_{\mathrm{K}_1^0} = -2\pi i \int \frac{\mathrm{d}^3\boldsymbol{k}}{2k_0}\, \delta(k_0 - k_0)\, \Phi^{(+)}_{\mathrm{K}_1^0}(\boldsymbol{k}) \{\Sigma_c(k) + \Sigma_{Nc}(k)\}\, \Phi^{(-)}_{\mathrm{K}_1^0}(\boldsymbol{k})\,, \tag{2.14}$$

where the δ-function assures energy conservation between initial and final

states. Inserting (2.3) we obtain

$$S_{K_1^0} = -2\pi i \int \frac{d^3\boldsymbol{k}}{2k_0}\,\delta(k_0 - k_0)\cdot\frac{1}{2}\{\Phi_1^{(-)}(\boldsymbol{k})\Sigma_C(k)\Phi_1^{(-)}(\boldsymbol{k}) - \Phi_2^{(-)}(\boldsymbol{k})\Sigma_C(k)\Phi_2^{(-)}(\boldsymbol{k}) + \Phi_1^{(+)}(\boldsymbol{k})\Sigma_{NC}(k)\Phi_2^{(-)}(\boldsymbol{k}) + \Phi_2^{(+)}(\boldsymbol{k})\Sigma_{NC}(k)\Phi_1^{(-)}(\boldsymbol{k})\}\,. \tag{2.15}$$

Similarly for the K_2^0 meson

$$S_{K_2^0} = -2\pi i \int \frac{d^3\boldsymbol{k}}{2k_0}\,\delta(k_0 - k_0)\Phi_{K_2^0}^{(+)}(\boldsymbol{k})\{\Sigma_C(k) - \Sigma_{NC}(k)\}\Phi_{K_2^0}^{(-)}(\boldsymbol{k})\,, \tag{2.16}$$

with (2.3) gives

$$S_{K_2^0} = -2\pi i \int \frac{d^3\boldsymbol{k}}{2k_0}\,\delta(k_0 - k_0)\cdot\frac{1}{2}\{\Phi_1^{(+)}(\boldsymbol{k})\Sigma_C(k)\Phi_1^{(-)}(\boldsymbol{k}) - \Phi_2^{(+)}(\boldsymbol{k})\Sigma_{NC}(k)\Phi_1^{(-)}(k) - \Phi_1^{(+)}(\boldsymbol{k})\Sigma_{NC}(k)\Phi_2^{(-)}(\boldsymbol{k}) - \Phi_2^{(+)}(\boldsymbol{k})\Sigma_{NC}(k)\Phi_1^{(-)}(\boldsymbol{k})\}\,. \tag{2.17}$$

From (2.15) and (2.17) it follows immediately that the mass splitting $\Delta m(K_1^0 - K_2^0)$ comes from the strangeness non-conserving part of the propagator function and that the mass difference is contained in the following part of the S operator

$$S = -2\pi i \int \frac{d^3\boldsymbol{k}}{2k_0}\,\delta(k_0 - k_0)\{\Phi_1^{(+)}(\boldsymbol{k})\Sigma_{NC}(k)\Phi_2^{(-)}(\boldsymbol{k}) + \Phi_2^{(+)}(\boldsymbol{k})\Sigma_{NC}(k)\Phi_1^{(-)}(\boldsymbol{k})\}\,, \tag{2.18}$$

or more precisely

$$\Delta m(K_1^0 - K_2^0) = -\frac{a_{NC}}{m_K}\,, \tag{2.19}$$

where a_{NC} is defined from $\Sigma_{NC}(k)$ in the same way as the constant a in (2.6) is defined from $\Sigma(k)$.

So far it has not been necessary to specify the explicit form of $\Sigma_{NC}(k)$. In doing so some arbitriness enters the problem as there is no unique way of coupling the bosons to the weak interaction currents. We shall carry through the discussion for two different models which we shall first briefly outline.

In the first model we shall follow an idea originally put forward by SUGAWARA ([8]), who extended the usual current × current type theory for weak interactions to include also meson currents. The total weak interaction Hamiltonian is then given by

$$\mathscr{H}_W = \frac{G}{\sqrt{2}}\mathscr{J}^\varkappa\mathscr{J}_\varkappa^+, \tag{2.20}$$

([8]) M. SUGAWARA: *Phys. Rev.*, **113**, 1361 (1959).

where

$$\mathcal{J}_\varkappa = \mathcal{J}^B_\varkappa + \mathcal{J}^M_\varkappa + \mathcal{J}^L_\varkappa \tag{2.21}$$

and

$$\begin{cases} \mathcal{J}^B_\varkappa = \overline{\psi}_n \gamma_\varkappa (1+\gamma_5)\psi_p + \overline{\psi}_\Lambda \gamma_\varkappa (1+\gamma_5)\psi_p , \\ \mathcal{J}^M_\varkappa = \sqrt{2}\,\{\varphi\,\partial_\varkappa \varphi - \varphi\,\partial_\varkappa \varphi\} , \\ \mathcal{J}^L_\varkappa = \overline{\psi}_e \gamma_\varkappa (1+\gamma_5)\psi_\nu + \overline{\psi}_\mu \gamma_\varkappa (1+\gamma_5)\psi_\nu . \end{cases} \tag{2.22}$$

We have here introduced the notation φ for the K_1^0 meson field operator and φ for the pion field operator. The reasons why only the K_1^0 meson field enters the meson current are discussed in detail in reference [8]. Within this scheme Feynman diagrams of the type shown in Fig. 3 will contribute to the mass splitting. As there is no coupling of the K_2^0 to the weak interaction currents within this scheme, there is no modification of the K_2^0 mass and the mass difference is solely due to the K_1^0 « mass renormalization ».

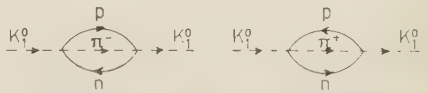

Fig. 3. – Feynman diagrams contributing to $\Delta m(K_1^0 - K_2^0)$ within the first scheme.

We shall also calculate the mass splitting within the more conventional theory in which there is no meson current in the weak interaction Hamiltonian. The K meson field is then coupled to the fermion by means of usual Yukawa type couplings and diagrams of the type shown in Fig. 4 will contribute to $\Delta m(K_1^0 - K_2^0)$.

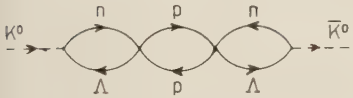

Fig. 4. – Feynman diagram contributing to $\Delta m(K_1^0 - K_2^0)$ within the second scheme.

3. – Calculation of the mass splitting within the first scheme.

To estimate the mass difference $\Delta m(K_1 - K_2)$ within the first scheme we consider the diagram shown in Fig. 5.

As the part of the S operator corresponding to this diagram is strongly divergent for large intermediate momenta, we shall introduce a cut-off in the theory by a regularization of the propagators in the following way

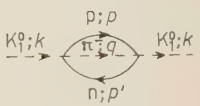

Fig. 5.

$$\frac{\mathbf{p}+m}{p^2-m^2} \to \frac{(\mathbf{p}+m)\Lambda^4}{(p^2-m^2)(p^2-m^2-\Lambda^2)^2} . \qquad \mathbf{p} = \gamma_\mu p^\mu . \tag{3.1}$$

By standard technique we now obtain for the S operator described by this

diagram

$$(3.2)\qquad S = -2\pi i \int \frac{\mathrm{d}^3\boldsymbol{k}}{2k_0}\,\delta(k_0 - k_0)\,\Phi^{(+)}(\boldsymbol{k})\left\{-\frac{G^2\Lambda'^2}{2(2\pi)^8}\int \mathrm{d}^4p \int \mathrm{d}^4q\cdot\right.$$

$$\cdot \mathrm{Tr}\left[\frac{\mathbf{p}-\mathbf{k}+\mathbf{q}}{[(p-k+q)^2-m^2][(p-k+q)^2-m^2-\Lambda^2]^2}\,I^\nu\,\frac{\mathbf{p}}{(p^2-m^2)(p^2-m^2-\Lambda^2)^2}\,I^\mu\right]\cdot$$

$$\left.\cdot\frac{q_\nu q_\mu + q_\nu k_\mu + k_\nu q_\mu + k_\nu k_\mu}{(q^2-m_\pi^2)(q^2-m_\pi^2-\Lambda^2)^2}\right\}\Phi^{(-)}(\boldsymbol{k})\,, \qquad I^\nu = \gamma^\nu(1-\gamma_5);\ m = \text{nucleon mass}.$$

We thus conclude from (3.2) and (2.14)

$$(3.3)\qquad \Sigma(k) = -\frac{G^2\Lambda'^2}{2(2\pi)^8}\int \mathrm{d}^4p \int \mathrm{d}^4q\cdot$$

$$\cdot \mathrm{Tr}\left[\frac{\mathbf{p}-\mathbf{k}+\mathbf{q}}{[(p-k+q)^2-m^2][(p-k+q)^2-m^2-\Lambda^2]^2}\,I^\nu\,\frac{\mathbf{p}}{(p^2-m^2)(p^2-m^2-\Lambda^2)^2}\,I^\mu\right]\cdot$$

$$\cdot\frac{q_\nu q_\mu + q_\nu k_\mu + k_\nu q_\mu + k_\nu k_\mu}{(q^2-m_\pi^2)(q^2-m_\pi^2-\Lambda^2)^2}\,.$$

After the integrations are carried out we expand $\Sigma(k)$ as indicated in (2.6) to obtain the mass renormalization part. From (2.13) and (3.3) we thus obtain

$$(3.4)\qquad \delta m \simeq \frac{1}{64(2\pi)^4}\cdot\frac{G^2\Lambda'^0}{m_\mathrm{K}(m^2+\Lambda^2)^2}\,.$$

It can be easily shown that the second diagram of Fig. 3 gives the same contribution. We, therefore, conclude that within this scheme

$$(3.5)\qquad \delta m \simeq \frac{1}{32(2\pi)^4}\cdot\frac{G^2\Lambda'^0}{m_\mathrm{K}(m^2+\Lambda^2)^2}\,.$$

With the experimental value given in reference [5] we obtain for the cut-off ($G \simeq 10^{-5}/m^2$)

$$\Lambda \simeq 1.4\,m\,.$$

From (3.5) and the definition of δm by (2.11) it then also follows that the K_1^0 meson is the lighter particle of the two neutral K mesons.

4. – Calculation of the mass splitting within the second scheme.

We shall next consider the mass difference generated by weak interactions as given by the second scheme. As mentioned above in the introductory discussion also strong interactions enter this scheme as the mesons are coupled

to the fermions by means of strong Yukawa couplings. Lacking any fully satisfactory method to handle strong interactions we resent to conventional perturbation theory.

We shall consider the diagram shown in Fig. 6. As within the first scheme the part of the S operator corresponding to this diagram is divergent although less strongly than in the earlier case. To make the individual terms in the perturbation expansion of the S operator convergent we regularize the propagators in the following way

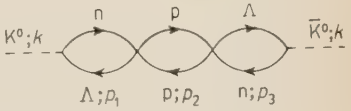

Fig. 6.

$$(4.1)\qquad \frac{\mathbf{p}+m}{p^2-m^2} \to -\frac{(\mathbf{p}+m)\Lambda^2}{(p^2-m^2)(p^2-m^2-\Lambda^2)} = -\int_0^{\Lambda^2} \mathrm{d}\lambda \frac{\mathbf{p}+m}{(p^2-m^2-\lambda)^2},$$

and we obtain

$$(4.2)\quad S = -2\pi i \int \frac{\mathrm{d}^3\boldsymbol{k}}{2k_0}\,\delta(k_0-k_0)\,\Phi_2^{(+)}(\boldsymbol{k})\left\{-\frac{ig_K^2G^2}{48(2\pi)^{12}}\int_0^{\Lambda^2}\mathrm{d}\lambda_1 \ldots \int_0^{\Lambda^2}\mathrm{d}\lambda_6 \int \mathrm{d}^4p_1 \int \mathrm{d}^4p_2 \int \mathrm{d}^4p_3 \cdot\right.$$

$$\cdot \mathrm{Tr}\left[\frac{\mathbf{p}_3+m}{[p_3^2-m^2-\lambda_1]^2}\,\gamma_5\,\frac{\mathbf{p}_3+\mathbf{k}+m_\Lambda}{[(p_3+k)^2-m_\Lambda^2-\lambda_2]^2}\,\Gamma^\mu\right]\cdot$$

$$\cdot \mathrm{Tr}\left[\frac{\mathbf{p}_2+m}{[p_2^2-m^2-\lambda_3]^2}\,\Gamma_\mu\,\frac{\mathbf{p}_2+\mathbf{k}+m}{[(p_2+k)^2-m^2-\lambda_4]^2}\,\Gamma_\nu\right]\cdot$$

$$\left.\cdot \mathrm{Tr}\left[\frac{\mathbf{p}_1+m_\Lambda}{[p_1^2-m_\Lambda^2-\lambda_5]^2}\,\Gamma^\nu\,\frac{\mathbf{p}_1+\mathbf{k}+m}{[(p_1+k)^2-m^2-\lambda_6]^2}\,\gamma_5\right]\right\}\Phi_1^{(-)}(\boldsymbol{k}).$$

From this we find

$$(4.3)\qquad \Sigma(k) = -\frac{ig_K^2G^2}{48(2\pi)^{12}}\int_0^{\Lambda^2}\mathrm{d}\lambda_1 \ldots \int_0^{\Lambda^2}\mathrm{d}\lambda_6 \int \mathrm{d}^4p_1 \int \mathrm{d}^4p_2 \int \mathrm{d}^4p_3 \cdot$$

$$\cdot \mathrm{Tr}\left[\frac{\mathbf{p}_3+m}{[p_3^2-m^2-\lambda_1]^2}\,\gamma_5\,\frac{\mathbf{p}_3+\mathbf{k}+m_\Lambda}{[(p_3+k)^2-m_\Lambda^2-\lambda_2]^2}\,\Gamma^\mu\right]\cdot$$

$$\cdot \mathrm{Tr}\left[\frac{\mathbf{p}_2+m}{[p_2^2-m^2-\lambda_3]^2}\,\Gamma_\mu\,\frac{\mathbf{p}_2+\mathbf{k}+m}{[(p_2+k)^2-m^2-\lambda_4]^2}\,\Gamma_\nu\right]\cdot$$

$$\cdot \mathrm{Tr}\left[\frac{\mathbf{p}_1+m_\Lambda}{[p_1^2-m_\Lambda^2-\lambda_5]^2}\,\Gamma^\nu\,\frac{\mathbf{p}_1+\mathbf{k}+m}{[(p_1+k)^2-m^2-\lambda_6]^2}\,\gamma_5\right].$$

In the same way as before we obtain from this

$$(4.4)\qquad \delta m \simeq \frac{g_K^2G^2}{96\cdot 4\pi}\cdot\left(\frac{\Lambda}{2\pi}\right)^2\frac{m_K}{2\pi}\left(\frac{m+m_\Lambda}{2\pi}\right)^2\ln^2\frac{\Lambda^2}{m_\Lambda^2}.$$

If we insert

$$G \simeq \frac{10^{-5}}{m^2}, \qquad g_K^2 = 4\pi,$$

(4.4) yields

$$\delta m \simeq \frac{10^{-10}}{96(2\pi)^4} \cdot \left(1 + \frac{m_\Lambda}{m}\right)^2 \cdot \frac{m_K}{2\pi} \cdot \left(\frac{\Lambda}{m}\right)^2 \ln^2 \frac{\Lambda^2}{m_\Lambda^2}. \tag{4.5}$$

One can easily show that the second term in (2.18) contributes the same. From (2.19) we, therefore, obtain

$$\Delta m(K_1^0 - K_2^0) \simeq -\frac{10^{-10}}{48(2\pi)^4} \cdot \frac{m_K}{2\pi} \left(1 + \frac{m_\Lambda}{m}\right)^2 \cdot \left(\frac{\Lambda}{m}\right)^2 \ln^2 \frac{\Lambda^2}{m_\Lambda^2}. \tag{4.6}$$

With the experimental value for $|\Delta m(K_1^0 - K_2^0)$ we thus get for the cut-off

$$\Lambda \simeq 3.7\, m.$$

From (4.6) we also conclude that the K_1^0 meson is the lighter of the two neutral K mesons. This is in agreement with our previous result within the first scheme.

5. – Conclusion.

In the introductory remarks it was stated that in order to explain the experimentally measured mass difference between the two neutral K mesons K_1^0 and K_2^0 one could expect a cut-off of the same order of magnitude as the strong interaction cut-off. This has been borne out in a very satisfactory way by the explicit calculations above. Whether this means that the weak interaction cut-off and the strong interaction cut-off actually are of the same order of magnitude, or if the result merely shows a very strong influence on the effective cut-off from the strong interactions cannot be decided from these calculations only. It is in this connection interesting to note that if we—for the diagram in Fig. 6—introduced a cut-off $\Lambda_s = 1.1\, m$ for the two loops containing strong vertices, then the experimental value for $|\Delta m(K_1^0 - K_2^0)$ requires a cut-off $\Lambda_w \simeq 20\, m$ for the middle loop. This result is of the same order of magnitude as the upper limit for the cut-off in weak interactions obtained from other processes. The result for Λ_w is, however, extremely sensitive to the choice of Λ_s and no firm conclusion about the size of Λ_w can be drawn for this argument.

The calculations for $\Delta m(K_1^0 - K_2^0)$ are carried out within two different schemes for the weak interactions which at first sight may seem completely independent of each other. The scheme proposed by SUGAWARA is, however, to be understood rather as a phenomenological way of handling strong interactions in « weak processes » than a fundamental interaction between bosons and fermions. SUGAWARA has shown that such a phenomenological description is in reasonable agreement with the experimental data available at present. If we take this point of view the two schemes are no longer completely independent. On the other hand, if the first scheme really is a consistent way of handling strong interactions within weak processes, that is, if such strong interaction parts are well described by an effective coupling of the type proposed by SUGAWARA, then one must interpret the cut-off obtained within the first scheme as the weak interaction cut-off since the underlying process causing the mass splitting between the neutral K-mesons then appears due to purely weak interactions. This would then lead to an expansion parameter in the perturbation expansion of the order $10^{-5} \div 10^{-6}$ and one can feel quite confident in applying perturbation methods within the theory of weak interactions.

Finally, we once more emphasize that within both schemes treated here the K_1^0 meson comes out as the lighter one of the two neutral K-mesons. With an entirely different approach to this problem, BARGER and KAZES (9), arrive to a similar conclusion. Assuming a direct K_1^0-2π interaction they find that the quantity $\tau_{K_1^0} \Delta m(K_1^0 - K_2^0)$ within a dispersion theoretic treatment essentially is given by the S wave, $I = 0$ π-π scattering phase shifts, and they reach the conclusion that only in case of huge, positive scattering length and with the phase shift within a rather limited range can $\Delta m(K_1^0 - K_2^0)$ be positive. With such a direct K_1^0-2π interaction they also state that a perturbation calculation yields a cut-off of 20 GeV with a negative sign for the mass difference. Up till now, no experiment has been performed in order to determine the sign of $\Delta m(K_1^0 - K_2^0)$ although different feasible experiments have been discussed in the literature. It is to be hoped that such an experiment will be carried out in a near future.

* * *

The author takes the pleasure to thank Professor R. E. MARSHAK, Dr. S. OKUBO and Dr. K. E. ERIKSON for many stimulating discussions. The kind hospitality at CERN is also gratefully acknowledged.

(9) V. BARGER and E. KAZES: preprint.

RIASSUNTO (*)

Nella teoria convenzionale $V - A$ delle interazioni deboli, la regola di selezione $\Delta S = 1$ richiede che la differenza di massa dei mesoni K neutri debba essere un effetto di secondo ordine nelle interazioni deboli. Questa differenza di massa è stata effettivamente accertata da molti gruppi di sperimentatori e costituisce la sola chiara informazione su questi effetti di ordine elevato disponibile a tutt'oggi. Il valore sperimentale della differenza di massa potrebbe così fornire una stima del cut-off che si introduce nella teoria delle interazioni deboli per rendere finiti i singoli termini dello sviluppo della perturbazione. Precedenti tentativi di determinare l'ampiezza di questo cut-off hanno solo stabilito dei limiti superiori, ed in contrasto con il frazionamento della massa $\Delta m(K_1^0 - K_2^0)$ i risultati dei processi sinora considerati dipendono tutti in modo critico dalla versione della teoria delle interazioni deboli, che si applica. L'interpretazione teorica dei risultati dei processi che coinvolgono bosoni però è parzialmente oscurata dalla presenza di interazioni forti. Ci si aspetta che il cut-off di questi processi sia influenzato del cut-off della interazione forte, che è dell'ordine della massa del nucleone. Si dimostrerà che il cut-off compatibile con il valore osservato di $\Delta m(K_1^0 - K_2^0)_1$ è dell'ordine di alcune masse nucleoniche in due differenti schemi della teoria delle interazioni deboli e si discuteranno le possibili implicazioni di questi risultati. I due schemi portano entrambi al risultato che il mesone K_2^0 è più pesante del mesone K_1^0. Sinora il segno della differenza di massa non è stato determinato sperimentalmente.

(*) *Traduzione a cura della Redazione.*

LETTERE ALLA REDAZIONE

(La responsabilità scientifica degli scritti inseriti in questa rubrica è completamente lasciata dalla Direzione del periodico ai singoli autori)

The Total Energy-Momentum Vector of a Closed System in General Relativity.

C. PELLEGRINI

Laboratori Nazionali di Frascati del C.N.E.N. - Frascati

(ricevuto il 15 Giugno 1961)

The difficulties connected with the concept of energy in the general theory of relativity have been widely studied by various authors [1,3] during recent years. In particular C. MØLLER [4] concluded that it is impossible to find an energy-momentum complex, θ_i^k, satisfying the following conditions:

1) $\theta_i^k(x^r)$ in the event point x^r is an affine tensor density that depends algebrically on the metric tensor g_{ik} and on its derivatives in the same point;

2) θ_i^k, $k=0$;

3) the total energy-momentum of a closed system, defined as

$$P_i = \int_{x_4=\text{cost}} \theta_i^4 \, \mathrm{d}^3x \, ,$$

is time independent; the P_i transforms as a four-vector under Lorents transformations and furthermore is unchanged under arbitrary transformations of the coordinates provided that the new system coincides with the original one at spatial infinity;

4) energy density and energy current must be a scalar and a 3-vector respectively under the group of purely spatial transformations

$$(1) \qquad \begin{cases} \overline{x}^\alpha - \overline{x}^\alpha(x^\beta) \\ \overline{x}^4 = x^4 \end{cases} \qquad \alpha = 1, 2, 3 \, .$$

As shown by MAGNUSSON [5] the conditions 1), 2), 4) determine the Møller energy-momentum complex T_i^k uniquely, but this does not satisfy the condition 3), *i.e.* it does not transform like a four-vector under Lorentz transformation. Furthermore MØLLER [4] showed that 1), 2), 3), lead uniquely to the Einstein energy-momentum complex Θ_i^k [6], but this does not satisfy 4).

It seems that the only way out of this situation is to drop or to modify at least one of the four conditions. If we take the point of viewt hat 4) is a necessary condition the only possibility

(1) J. N. GOLDBERG: *Phys. Rev.*, **111**, 315 (1958).

(2) P. G. BERGMANN: *Phys. Rev.*, **112**, 287 (1958).

(3) C. MØLLER: *Ann. Phys.* **4**, 347 (1958).

(4) C. MØLLER: *Ann. Phys.* **12**, 118 (1961).

(5) M. MAGNUSSON: *Mat. Fys. Medd. Dan. Vid. Selskab.*, **32**, 6 (1960).

(6) A. EINSTEIN: *Berlin Ber.*, 778, (1915); *Ann. Physik*, **49**, 769 (1916); *Berlin Ber.*, **24**, 448 (1918).

left is to change condition 1) or the definition of P_i.

The change of 1) means introducing some new variables to describe the gravitational field, as Møller recently did (7).

The other possibility is studied here, where an approach to the definition of a new total energy-momentum vector is made.

As assumptions 1), 2), 4) are supposed to be valid, the Møller complex T_i^k will be used.

We consider the case of a closed static system.

The new definition of the total energy and momentum of the system is

$$\mathscr{P}_i = \int_\sigma \frac{T_i^k}{\sqrt{-g}} \gamma_k \, \mathrm{d}\sigma \,. \tag{2}$$

In (2) $g = \det\{g_{ik}\}$ and σ is a three-dimensional surface orthogonal to γ_k.

γ_k is the unit vector tangent to the lines x^4 in the frame of reference in which the static closed system is at rest.

It is easy to show that $\mathscr{P}_i$ is a four-vector under Lorentz transformations. In the rest frame the metric is of the form

$$\mathrm{d}s^2 = a(r)(\mathrm{d}\overset{\circ}{x}_1^2 + \mathrm{d}\overset{\circ}{x}_2^2 + \mathrm{d}\overset{\circ}{x}_3^2) - b(r)\,\mathrm{d}\overset{\circ}{x}_4^2, \tag{3}$$

$$r^2 = \overset{\circ}{x}_1^2 + \overset{\circ}{x}_2^2 + \overset{\circ}{x}_3^2 \,,$$

where asimptotically rectilinear co-ordinates are used. In this frame we have

$$\overset{\circ}{\gamma}_k = 0, 0, 0, \sqrt{b} \,, \tag{4}$$

and as $\mathrm{d}\sigma_0 = \sqrt{\gamma_0}\,\mathrm{d}^3\overset{\circ}{x}$, $\gamma_0 = \det\{\overset{\circ}{g}_{\alpha\beta}\}$

$$\overset{\circ}{\mathscr{P}}_i = \int_{x_4=\mathrm{cost}} \overset{\circ}{T}_i^4 \,\mathrm{d}^3\overset{\circ}{x} \,, \tag{5}$$

which coincides with the old definition.

(7) C. Møller: to be published.

Using the transformation rules for T_i^k and γ_k the result

$$\mathscr{P}_i = \frac{\partial \overset{\circ}{x}_c}{\partial x_i} \overset{\circ}{\mathscr{P}}_c \,. \tag{6}$$

is obtained.

Since $\overset{\circ}{\mathscr{P}}_i$ satisfies the requirements of being time-independent and of being unchanged under arbitrary transformations which leave the co-ordinate system asimptotically invariant, and since $\mathscr{P}_i$ is a linear combination of $\overset{\circ}{\mathscr{P}}_i$ with constant coefficients it follows that condition 3) is now completely satisfied. Also condition 4) is satisfied as both T_4^k and γ_k are four-vectors under the transformation (1), and so $T_4^k \gamma_k$, which plays now the role of energy density, behaves like a scalar under the same group of transformations.

The total energy and momentum defined by (2) differs from the usual P_i since the integration must be performed always on the same surface and T_i^k must be saturated always with the same vector normal to this surface.

It is therefore necessary to give a geometrical definition of σ and γ_k or to define σ and γ_k in one frame of reference, which amounts to the same thing.

In the case of a closed static system γ_k coincides with the four-velocity of matter inside the matter tube.

It can be remarked that our definition of energy density is similar to that given by C. Cattaneo (8).

We hope to extend definition (2) to the case of a more general system.

* * *

I wish to thank Prof. C. Cattaneo and Prof. C. Møller.

(8) C. Cattaneo: *Nuovo Cimento*, **13**, 237 (1959).

The Spin of the μ-Meson (*).

P. K. Kabir

Carnegie Institute of Technology - Pittsburgh, Pa.

(ricevuto il 19 Settembre 1961)

Although all experimental evidence points to the similarity of the μ-meson to the electron, the evidence concerning the spin of the muon seems to be rather indirect.

For example, the earliest arguments (1), that a spin-value greater than $\frac{1}{2}$ would lead to cross-sections for high-energy electromagnetic processes much larger than those observed, are based on *theories* of the electromagnetic properties of higher-spin particles, regarding which we have no experimental evidence whatever. Later arguments based on the measured g-factor of the free muon (2) rest on the same theories. A separate measurement of the muon magnetic moment could provide a direct determination of the spin but, unfortunately, all such measurements (3) involve high-energy processes and consequently include theoretical assumptions regarding the form of the interaction. The measurement of the fine-structure (4) of the X-rays from μ-mesic atoms provides, in principle, a simple indication of the spin since the multiplicity is $2s+1$, s being the spin of the muon. However, the experiments are quite difficult and it does not seem possible at the present time to state with conviction that it is a doublet and not, say, a triplet or quadruplet structure which is observed (5). Another method, based on the comparison of the depolarization of polarized μ^--mesons when captured in spin-0 and in spin-$\frac{1}{2}$ nuclei, is open to the objection that it rests on the auxiliary assumption

(*) Work partially supported by U. S. Atomic Energy Commission.

(1) R. F. Christy and S. Kusaka: *Phys. Rev.*, **59**, 405, 414 (1941); J. Mathews: *Phys. Rev.*, **102**, 270 (1956); A. N. Mitra: *Nucl. Phys.* **2**, 383 (1956).

(2) R. L. Garwin, L. M. Lederman and M. Weinrich: *Phys. Rev.*, **105**, 1415 (1957).

(3) M. Avan and L. Avan: *Nuovo Cimento*, **6**, 1500 (1957); G. H. Rawitscher: *Phys. Rev.*, **107**, 274 (1957); S. Hirokawa and H. Komori: *Nuovo Cimento*, **7**, 114 (1958).

(4) W. Frati: Nevis Cyclotron Laboratory Report-90 (1960) haso bserved the expected fine structure splitting in the $3D$-$2P$ μ-mesic X-rays of Pb. He claims that a spin-$\frac{3}{2}$ muon would give rise to a third X-ray 0.25 MeV below the doublet and stronger in intensity than either component; since such an X-ray is not observed, he concludes that the possibility of spin $\frac{3}{2}$ is ruled out. It is obvious that this conclusion is not free from assumptions concerning the nature of the interaction between the μ-meson and the nucleus.

(5) I am grateful to Professor R. B. Sutton for helpful discussions regarding the measurement of mesic X-rays.

that there are no depolarizing mechanisms, other than the hyperfine interaction, which are different for the two materials and, also, that hyperfine transitions may be neglected.

Since the angular momentum of a state relates only to the transformation properties of that state under rotations, it should be possible to determine the spin of the muon without having to resort to additional assumptions regarding the detailed nature of its interactions. In view of the large asymmetry of the electrons from polarized μ-decay, it might have been hoped that an analysis similar to that carried out by LEE and YANG [6] for the Λ-particle might be fruitful. Unfortunately, this is complicated by the fact that there are three particles created in the decay and also that the spin of at least one of them is unknown [7]. Luckily, we can obtain the same information, with hardly any further assumption, from another experiment.

Recently, HUGHES, MCCOLM, ZIOCK and PREPOST [8] have detected the formation of muonium (μ^+e^-) through the observation of its Larmor precession. Whereas HUGHES *et al.* assume a muon spin of $\frac{1}{2}$ in analysing their results, it is the purpose of this note to point out that their experiment provides a measurement of this quantity for the positive muon [9]. Let us assume the muon spin to be s. In a weak magnetic field H, an S-state [10] of muonium will then precess about H with a frequency

$$g\left(\frac{e}{4\pi m_e c}\right)H,$$

where

$$g/g_e = \frac{1}{2s+1} + \frac{m_e}{m_\mu}\frac{2s}{2s+1},$$

for $F = s + \frac{1}{2}$, and

$$g/g_e = -\frac{1}{2s+1} + \frac{m_e}{m_\mu}\frac{2(s+1)}{2s+1}.$$

for $F = s - \frac{1}{2}$, and we have assumed for the sake of simplicity that the muon and the electron g-factors are equal (in terms of their respective magnetons), an approximation which is well justified experimentally [11]. The contribution of the muon magnetic moment will be detectable only if the accuracy of measurement exceeds 0.5%. The experimental observation of precession [8] with a frequency corresponding to $g = 1$ (within an error of 4%) therefore establishes that $s = \frac{1}{2}$.

We now make a further observation

[6] T. D. LEE and C. N. YANG: *Phys. Rev.*, **109**, 1755 (1958).

[7] L. M. BROWN and V. L. TELEGDI: *Nuovo Cimento*, **7**, 698 (1958) have shown that if both neutrinos are assumed to have spin $\frac{1}{2}$, it is not possible to reproduce the observed asymmetry and spectrum for a spin-$\frac{1}{2}$ muon if the decay interaction is restricted to non-derivative couplings.

[8] V. W. HUGHES, D. W. MCCOLM, K. ZIOCK and R. PREPOST: *Phys. Rev. Lett.*, **5**, 63 (1960).

[9] Professor V. L. TELEGDI has kindly drawn my attention to a paper by EGOROV, IGNATENKO and CHULTEM: *Sov. Phys. JETP*, **10** (37), 1079 (1960) reporting the observation of precession of μ^--mesons bound in phosphorus, in which he pointed out that this provided a measurement of the μ^--spin. I am glad to acknowledge Professor TELEGDI's priority in this matter.

[10] The formation of muonium is similar to the formation of positronium, cf. M. DEUTSCH: *Progr. Nucl. Phys.*, **3**, 131 (1953). Under the conditions of the experiment described in ref.[8], it is relatively unlikely that muonium will be formed in an excited state. Even if an excited state is formed, it will be de-excited by collision or radiation in a time short compared to the muon lifetime. I am grateful to L. WOLFENSTEIN, J. E. RUSSELL and G. B. YODH for valuable discussions of this question.

[11] R. L. GARWIN, D. P. HUTCHINSON, S. PENMAN and G. SHAPIRO: *Phys. Rev.*, **118**, 271 (1960); G. CHARPAK, F. J. M. FARLEY, R. L. GARWIN, T. MULLER, J. C. SENS, V. L. TELEGDI and A. ZICHICHI: *Phys. Rev. Lett.*, **6**, 128 (1961).

concerning the spin of the neutrino emitted in muonic decay processes. In the event that this neutrino, which we denote by ω, is physically distinct from the neutrino of β-decay, we could not formerly have said even whether the muon spin were integral or half-integral; we could say only that the spins of μ and ω were both integral or both half-integral. Now that the muon spin is fixed, the ω spin is correspondingly determined to be half-integral. Further, if we take the ω mass to be zero, its spin is determined as $\frac{1}{2}$. In the decay at rest of $\pi \to \mu + \omega$, consider the components of angular momentum along the direction of emission of the muon. There is no contribution from orbital motion and the μ-spin can have a projection of $\pm\frac{1}{2}$; conservation of angular momentum requires that the ω correspondingly have a spin projection of $\mp\frac{1}{2}$. Since a massless particle can only occupy states in which its spin is directed parallel or antiparallel to its direction of motion ([12]), we conclude ([13]) that the spin of ω is $\frac{1}{2}$.

* * *

I am indebted to many colleague for discussions concerning the muon spin, and in particular to H. Überall for a most helpful remark.

([12]) E. P. Wigner: *Rev. Mod. Phys.*, **29** 255 (1957).

([13]) A similar argument may, of course, be applied to $\pi \to e + \nu$.

Composite Pions.

P. E. Kaus (*)

University of Southern California - Los Angeles, Cal.

W. K. R. Watson

Jet Propulsion Laboratory, California Institute of Technology - Pasadena, Cal.

(ricevuto il 20 Settembre 1961)

At the present time, considerable doubt exists concerning the labeling of kaons, pions, and vector mesons as fundamental particles or dynamical resonances, in the sense that « fundamental » implies independent coupling constant and mass, whereas dynamical resonances possess constants which can, in principle, be determined in terms of the parameters (1) associated with other « more fundamental » fields.

Conversely, we may ask whether one should not regard the vector mesons as fundamental (2) and the pseudoscalar mesons as dynamic accidents. This notion indicates that the main contribution to the pion should arise from the binding of baryons to anti-baryons by vector mesons in a manner similar to that proposed originally by Fermi and Yang (3). If this is the case, the coupling would have to be sufficiently strong to produce a binding such that

$$\frac{E}{2m_N} \frac{m_\pi}{2m_N} \sim 0.07 .$$

There are indications that this is indeed possible if the nucleon B_0 meson coupling constant $(g^2/4\pi\hbar c)$ is of the order of 5, with the vector meson masses of the order of half a nucleon mass (4). The purpose of this paper is to point out that regardless of the accuracy of the computation (which is very poor), this philosophy coupled with the statements of unitary symmetry (1) leads to a contradiction with experience in predicting

(*) Consultant at the Jet Propulsion Laboratory, California Institute of Technology, Pasadena, Cal.

This paper presents the results of one phase of research carried out at the Jet Propulsion Laboratory, California Institute of Technology, under Contract, sponsored by the National Aeronautics and Space Administration.

(1) M. Gell-Mann: *The eightfold way: a theory of strong interaction symmetry*, California Institute of Technology Synchrotron Laboratory Report no. CTSL-20 (1961).

(2) J. J. Sakurai: *Ann. Phys.*, **11**, 1 (1960).

(3) E. Fermi and C. N. Yang: *Phys. Rev.*, **76**, 1739 (1949).

(4) P. Kaus and W. K. R. Watson: *Bull. Am. Phys. Soc.*, **6**, 377 (1961). The result of Fermi-Yang would give $(g^2/4\pi\hbar c) \sim 25$. However, the equation used in that reference is inconsistent and actually has no bound states at all.

a π_4 which is lighter than the conventional triplet π.

First, let us make some qualitative remarks about the binding. Since we shall always consider a baryon antibaryon pair, the B_0 « meson » which couples to the totally conserved baryon current is attractive for all pairs. The ω ($I=0$, $J=1$) « meson » which couples to the hypercharge is likewise always attractive or absent. (For example, the ω would not couple to a $\Sigma\bar{\Lambda}$, or $\Lambda\bar{\Sigma}$ pair.) Similarly, if we wished to regard the kaons as bound states, the ω coupling would be absent for all possible pairs, *e.g.*, $(\bar{\Sigma}\mathcal{N})$.

The ρ-mesons couple to the total isotopic spin current and can therefore either attract or repel depending upon the I-spin of the composite system. For those baryons which are genuine members of isotopic doublets, we can form either an isotopic vector (the usual pion $I=1$) or an isotopic singlet (the π_4, $I=0$). However, Σ has $I=1$, and one could again, within the framework of unitary symmetry, form a bound state $\Sigma^+\bar{\Sigma}^-$ system with $I=2$, $I_z=2$ and two units of charge. However, this point will be elaborated upon shortly.

If we regard the (n, p) and their corresponding anti-particles as typical building blocks, we will require the following combinations in the $^1S_0$ state in order to guarantee the correct spin, parity, and isotopic spin assignment for the various pions.

$$\left.\begin{array}{l} p\bar{n} \\ \dfrac{p\bar{p}-n\bar{n}}{\sqrt{2}} \\ n\bar{p} \end{array}\right\} I=1\,, \qquad \left.\dfrac{p\bar{p}+n\bar{n}}{\sqrt{2}}\right\} I=0\,.$$

In addition, we get similar contributions from the cascades. On the other hand the (Σ, Λ) groupings are slightly more complicated but may be understood in the following manner. As usual, the B_0 and ω mesons attract for all combinations of Σ, Λ and their antiparticles, however, a pair of Σ's can be arranged to form $I=2, 1, 0$ states. From the standpoint of single ρ exchange, it is clear that the $T=2$ state is repulsive and it can easily be shown that the $T=1$ and $T=0$ states are both attractive (the latter being twice as strong) [5]. Hence the $(\bar{\Sigma}\Sigma)$ contribution to the $I=0$ state is larger than to the corresponding $I=1$ state, (*i.e.*, the $I=0$ state is more tightly bound). Furthermore, we can form an $I=1$ state from a $(\Sigma\bar{\Lambda})$ pair, and an $I=0$ state from a $(\Lambda\bar{\Lambda})$ pair; in both cases, however, it is obvious that the ρ cannot couple. In calculating the ρ isodoublet contributions, one finds the projection $\tau^{(1)}\cdot\tau^{(2)}=1$ (repulsion), and -3 (attraction) for the $I=1$ and $I=0$ states respectively. Thus we conclude, (all other interactions being equal), that the total meson-baryon pair contribution causes the π_4 to be lighter than the conventional π. If this indeed were the case, it would have almost certainly been detected in pion production experiments, since $\pi_4 \to 2\gamma$'s would proceed at a rate determined by the π_4 mass [6]. Moreover $K^+ \to \pi^+ + \pi_4$ much faster than $K^+ \to \pi^+ + \pi^0$ since the first reaction is no longer forbidden by the $\Delta I = \frac{1}{2}$ rule. Thus the existence of a π_4 meson lighter than the usual pion appears highly improbable.

We are thus led to the conclusion [7], that the π-mesons are in fact « elementary », and the π_4 can therefore have essentially any mass consistent with the

---

[5] This arises from eigenvalues of $\boldsymbol{T}^{(1)}\cdot\boldsymbol{T}^{(2)}$ on the $I=2$, $I=1$, $I=0$ states, *i.e.*,

$$\boldsymbol{T}^{(1)}\cdot\boldsymbol{T}^{(2)}\,|\,I=2\rangle = |\,I=2\rangle\,,$$
$$\boldsymbol{T}^{(1)}\cdot\boldsymbol{T}^{(2)}\,|\,I=1\rangle = -1\,|\,I=1\rangle\,,$$
$$\boldsymbol{T}^{(1)}\cdot\boldsymbol{T}^{(2)}\,|\,I=0\rangle = -2\,|\,I=0\rangle\,.$$

[6] The reaction $\pi_0 \to \pi_4 + \gamma$ is forbidden by charge conjugation.

[7] The only way one could construct a pion from the vector meson themselves would be from a ρ-ω pair exchanging a pion; however, this could only contribute to the $I=1$ state.

aforementioned reactions not proceeding (*i.e.*, π_4 considerably heavier than the usual π). If this is the case, however, we must make sure that the baryon vector meson coupling constant (basic if the vector mesons are also elementary, phenomenological if they are dynamic) is not large enough to produce a set of bound $I=1$ and $I=0$ baryon anti-baryon states which would simulate a second set of dynamical pseudoscalar mesons. Order of magnitude calculations, using the projected Breit equation [4] indicate that this limits the baryon vector meson coupling constant $(g^2/4\pi\hbar c)$ to the order unity, if the vector mesons are assumed to have masses in the neighborhood of $(0.5 \div 1)$ nucleon masses. At the present time, there is no obvious contradiction to this statement [8] and it seems therefore more likely that the pseudoscalar mesons should be regarded as elementary particles.

---

[8] *E.g.*, W. K. R. WATSON: *Nuovo Cimento*, to be published. This work indicates that $\gamma^2_{\rho\mathcal{N}\mathcal{N}} \sim 0.12$ (at $k^2 = 0$).

IL NUOVO CIMENTO Vol. XXII, N. 2 16 Ottobre 1961

Knight Shifts in the Intermetallic Compound $PtSn_2$.

S. S. Dharmatti, V. Udaya Shankar Rao and R. Vijayaraghavan

Tata Institute of Fundamental Research - Bombay

(ricevuto il 25 Settembre 1961)

Rowland [1] has shown that the Knight shift of ^{195}Pt in platinum metal, measured with respect to chloroplatinic acid, is negative and large in magnitude (-3.52%). Its origin is probably similar to that of the negative hyperfine interaction in the Mn^{++} ion [1]. Heine [2], and Wood and Pratt [3] have shown that the above interaction arises as a consequence of the unpairing of the spins of the inner *s*-shell electrons due to exchange polarization by the outer 3*d*-electrons resulting in a non-vanishing and negative spin density at the nucleus. It is extremely probable [4] that the negative Knight shift in Pt metal is a result of the exchange polarization of the inner *s*-shell electrons by the unfilled *d*-electron band. Such a concept has proved fruitful in explaining the temperature dependence of the Knight shifts in vanadium alloys [5], where a correlation exists between the changes in the Knight shift and the magnetic susceptibility.

We undertook a study of the alloy $PtSn_2$ having a cubic structure, like CaF_2, to examine the effect of alloying on the Knight shift of Pt as a result of the possible filling of the *d*-electron band. It is observed that the Knight shift of Pt in $PtSn_2$ is -0.16% with respect to a molar chloroplatinic acid solution, showing a considerable decrease in the magnitude of the Knight shift from that of Pt metal. This is accompanied by a diminution in the magnetic susceptibility upon alloying. Platinum metal is paramagnetic with $\chi = 1 \cdot 10^{-6}$ e.m.u/G and a measurement of the susceptibility of the alloy showed that it has been reduced by a factor of four. This is an indirect evidence for the filling of the *d*-electron band. The peak-to-peak line-width of the derivative of the absorption curve is 2.1 G. All measurements were made at room temperature (20 °C).

The $^{117,119}Sn$ resonances in $PtSn_2$ showed a positive Knight shift of 1.06% with respect to the $SnCl_2$ solution. This is so far the highest reported Knight shift, for Sn. The absorption line of the Sn resonance was symmetric in the range of the magnetic field 2.5

---

[1] T. J. Rowland: *Journ. Phys. Chem. Solids*, **7**, 95 (1958).

[2] V. Heine: *Phys. Rev.*, **107**, 1002 (1957).

[3] J. H. Wood and G. W. Pratt, Jr.: *Phys. Rev.*, **107**, 995 (1957).

[4] D. A. Goodings and V. Heine: *Phys. Rev. Lett.*, **5**, 370 (1960).

[5] A. M. Clogston and V. Jaccarino: *Phys. Rev.*, **121**, 1357 (1961).

to 5 kG, unlike its resonance in the pure metal ([6]). This is consistent with the fact that the tin atom is located in a symmetric environment in the alloy $PtSn_2$. The line-width of the Sn resonance is 3.8 G.

All the measurements were made on a wide-line spectrometer of the Bloch type. The alloy was made by melting a mixture of platinum and tin in the appropriate proportion in an atmosphere of argon at 1100 °C. The alloy was powdered to have sample size less than the skin depth at the operating frequency and then annealed for five days at 700 °C. In the unannealed alloy, both ^{195}Pt and ^{119}Sn yielded two resonances each. X-ray analysis showed that a portion of the alloy was formed as Pt_2Sn_3. The other signals could therefore safely be attributed to the phase Pt_2Sn_3 which has a hexagonal structure. On this assumption the Knight shift of ^{195}Pt in the Pt_2Sn_3 phase is -0.01% and that of ^{119}Sn is $+0.72\%$. This means that the Pt resonance in Pt_2Sn_3 occurs very near the chloroplatinic acid point while the Sn resonance in this phase occurs at the tin metal point. Further confirmation is still to be obtained in this connection by preparing the alloy Pt_2Sn_3 separately (*). However, on annealing for five days, the phase Pt_2Sn_3 disappeared completely leaving the alloy in the phase $PtSn_2$ as revealed by X-ray analysis and also by disappearance of the signals corresponding to Pt_2Sn_3.

It is worth-while to point out that JACCARINO *et al.* ([7]) have observed a positive Knight shift for Pt in the intermetallic compounds $PtGa_2$, $PtAl_2$ and $PtIn_2$, all having cubic CaF_2 structure, whereas $PtSn_2$, having an identical structure, yields a negative Knight shift for Pt, as noted by us.

It would be interesting to study the temperature-dependence of the Knight shifts in $PtSn_2$ and similar platinum alloys and to correlate them with the temperature-dependence of the magnetic susceptibility. Efforts in this direction are in progress.

* * *

We are grateful to the Physical Metallurgy Group of the Atomic Energy Establishment, Trombay, for the help in taking the X-ray powder pattern of the alloys and to the Chemistry Division of the same Establishment for providing us with facilities for preparing the alloys.

([6]) N. BLOEMBERGEN and T. J. ROWLAND: *Acta Met.*, **1**, 731 (1953).

(*) *Note added in proof.* - The Knight shifts of ^{195}Pt and ^{119}Sn in Pt_2Sn_3 have been subsequently confirmed.

([7]) V. JACCARINO, W. E. BLUMBERG and J. H. WERNICK: *Bull. Am. Phys. Soc.*, **6**, 104 (1961).

Some Remarks about Low-Energy Pion-Pion Scattering.

C. Ceolin

Istituto di Fisica dell'Università - Padova

R. Stroffolini (*)

CERN - Geneva

(ricevuto il 30 Settembre 1961)

One of the most important questions in pion physics is the problem of pion-pion interaction at low energy. The knowledge of low-energy pion-pion phase shifts is of fundamental importance in the interpretation of many low-energy phenomena involving pions and nucleons and in the study of the main features of high-energy collisions.

Recently a p-wave pion-pion resonance has been found [1] with position and width not far from those predicted theoretically [2]. On the other hand, the situation concerning pion-pion interaction at low energy in the two s-wave states is not yet settled, since we do not yet have a unique choice for the phase shifts which is satisfactory both from the theoretical and the experimental point of view.

One interesting proposal has recently come from the interpretation of the observed anomaly in the ^{3}He spectrum in the p + d reaction [3], which has led to the hypothesis of a strong pion-pion interaction at threshold in the $T=0$ state. Using for the low-energy pion-pion amplitude the Chew-Mandelstam formula [4]

$$(1) \qquad A_0 = \left(\frac{\nu+\mu^2}{\nu}\right)^{\frac{1}{2}} \exp\left[i\delta_0\right] \sin\delta_0 = \frac{a_0}{1+\frac{2}{\pi}a_0\left(\frac{\nu}{\nu+\mu^2}\right)^{\frac{1}{2}} \ln\left[\frac{\nu^{\frac{1}{2}}+(\nu+\mu^2)^{\frac{1}{2}}}{\mu}\right] - ia_0\left(\frac{\nu}{\nu-\mu^2}\right)^{\frac{1}{2}}},$$

(ν=square of the c.m. momentum; μ=pion mass)

(*) On leave of absence from University of Naples.

(1) A. R. Erwin, R. March, W. D. Walker and E. West: *Phys. Rev. Lett.*, **6**, 628 (1961); D. Stonehill, C. Baltay, H. Courant, W. Fickinger, E. C. Fowler, H. Kraybill, J. Sandweiss, J. Sanford and H. Taft: *Phys. Rev. Lett.*, **6**, 624 (1961).

(2) J. Bowcock, W. N. Cottingham and D. Lurié: *Phys. Rev. Lett.*, **5**, 386 (1960).

(3) A. Abashian, N. E. Both and K. M. Crowe: *Phys. Rev. Lett.*, **7**, 35 (1961); see also T. N. Truong: *Phys. Rev. Lett.*, **6**, 308 (1961).

(4) G. F. Chew and S. Mandelstam: *Phys. Rev.*, **119**, 467 (1960); see also B. D. Desai: *Phys. Rev. Lett.*, **6**, 497 (1961).

a good fit of the experimental data has been obtained in correspondence of the scattering length $a_0/\mu=(2.5\pm0.4)\cdot 1/\mu$. This very large value of a_0 looks rather surprising because it means thresholds π-π cross-sections of the order of the barn which then decrease rapidly with energy.

On the other hand, such a value of a_0 seems hard to reconcile with the indications coming from the theoretical interpretation of the τ decay leading to $a_2 - a_0$ small and positive ([5]).

In this letter we want to point out another theoretical difficulty related to the effect of s-wave pion-pion interaction in pion-nucleon production processes. Let us consider the reaction $\pi^- + p \to \pi^- + \pi^+ + n$. In the hypothesis of a large pion-pion interaction the dominant contribution to the production cross-section will be due to the effect of the interaction of the incoming pion with the pions in the cloud of the target nucleon ([6]).

Disregarding the possible corrections due to rescattering which in any case do not alter appreciably ([7]) the order of magnitude of the result, the π-π contribution to production is simply given by formula ([8])

$$(2) \qquad d\sigma = \frac{8}{9}\frac{f^2}{\pi\mu^2}\frac{A^2}{A^2+\mu^2}\left(\frac{v}{v+\mu^2}\right)^{\frac{1}{2}}\frac{M}{(p^2+M^2)^{\frac{1}{2}}}\frac{d^3p}{q}\int |2A_0 + A_2 + 9A_1\cos\vartheta|^2 \, d\cos\vartheta \,,$$

$$A_T = \left(\frac{v+\mu^2}{v}\right)^{\frac{1}{2}} \exp[i\delta_T]\sin\delta_T \,,$$

where q is the momentum of the incoming pion;

p is the momentum of the recoil nucleon both in lab. system;

v is the square of the outgoing pions momentum in their own c.m. system;

ϑ is the angle of π-π scattering in the same system, and finally

$A^2 = 2M(\sqrt{M^2+p^2} - M)$, $M =$ nucleon mass.

Since, as shown by eq. (1), the large value of the threshold π-π cross-section decreases very rapidly with energy, the contribution of s-wave pion-pion interaction to production cross-section will be particularly important for energies of the incoming pion not too far from threshold. We shall therefore consider explicitly the energy range below 300 MeV. Before comparing the consequences of eq. (1) and (2) with experiment we want to discuss briefly the possible effects of A_1 and A_2 in eq. (1) and (2). For what concerns A_1 the contribution is positive definite without any interference with A_0 and A_2; reasonable estimates lead to a negligible contribution in our energy range.

We discuss the $T=2$ amplitude more in detail because of the possibility of a large $T=2$ scattering length a_2/μ interfering destructively with a_0/μ.

([5]) N. N. KHURI and S. B. TREIMAN: *Phys. Rev.*, **119**, 1115 (1960); R. F. SAWYER and K. C. WALI: *Phys. Rev.*, **119**, 1429 (1960).

([6]) The contribution due to the pion-nucleon interaction has beene alculated within the framework of the static model and has been found to contribute only a small fraction of the experimental cross-section. See L. S. RODBERG: *Phys. Rev.*, **106**, 1090 (1957); E. KAZES: *Phys. Rev.*, **107**, 1131 (1957); W. A. PERKINS, J. C. CARIS, R. W. KENNEY, E. A. KNAPP and V. PEREZ-MENDEZ: *Phys. Rev. Lett.*, **3**, 56 (1959).

([7]) C. GOEBEL and H. J. SCHNITZER: *Phys. Rev.*, **123**, 1021 (1961).

([8]) C. GOEBEL: *Phys. Rev. Lett.*, **1**, 337 (1958); G. F. CHEW and F. E. LOW: *Phys. Rev.*, **113**, 1640 (1959).

The possibility of a good estimate of a_2 is given by the analysis of the experimental results of $\pi^{\pm}+p\to p+\pi^{\pm}+\pi^0$ at 1.03 GeV ([9]). Both using the peripheral formula in the physical region and by performing a Chew-Low extrapolation in the energy range $5\mu^2 < 4(\nu+\mu^2) < 8.2\mu^2$ one obtains similar values for the low-energy $(\pi^{\pm}, \pi^0)$ cross-section ([10]) ~ 40 mb leading to a $T=2$ scattering length $|a_2/\mu| \simeq 0.54(1/\mu)$. This, naturally, excludes the possibility of a strong interference if one takes for a_0 the large value proposed by ABASHIAN, BOTH and CROWE.

Let us now finaly compare with experiment the theoretical results coming from eq. (1) and (2) in correspondence of different choices of a_0 and a_2. Such a comparison is shown in Table I. The large disagreement in order of magnitude between theory and experiment seems to exclude values of a_0 larger than 1. One might, of course, hope that the possible corrections to eq. (2) coming for example from rescattering might attenuate such a large discrepancy; however, we think this to be very unlikely especially in the low-energy region.

TABLE I. – *Total* $\pi^-+p\to\pi^-+\pi^++n$ *cross-section in* mb.

a_0	a_2	Incident energy (lab) 225 MeV	245 MeV	260 MeV	280 MeV	290 MeV	317 MeV
2.8	0.54	1.30	1.84	2.22	2.68	2.88	3.30
	— 0.54	0.83	1.16	1.39	1.65	1.76	1.98
2	0.54	0.90	1.33	1.65	2.03	2.20	2.59
	— 0.54	0.51	0.73	0.89	1.08	1.17	1.35
1.5	0.54	0.65	0.98	1.23	1.54	1.70	2.06
	— 0.54	0.30	0.46	0.57	0.70	0.77	0.91
1	0.54	0.39	0.62	0.78	1.00	1.10	1.37
	— 0.54	0.133	0.21	0.26	0.33	0.36	0.45
experiment		([11a]) 0.03±0.02	([11c]) 0.10±0.04	([11b]) 0.14±0.10	([11c]) 0.3±0.2	([11c]) 0.7±0.2	([11b]) 0.71±0.17

([9]) J. A. ANDERSON, V. X. BANG, P. G. BURKE, D. D. CARMONY and N. SCHMITZ: *Rev. Mod. Phys.*, **33**, 431 (1961); see in particular Fig. 3*a*.

([10]) Using the peripheral formula one obtains $\sigma_t=(35\pm 4)$ mb from $\pi^+\pi^0$ and $\sigma \simeq 27$ mb from $\pi^-\pi^0$. Finally, if one interprets the data by means of a Chew-Low extrapolation one obtains $\sigma=(40\pm 20)$ mb. The effect of the $T=1$ interaction in this energy range can be estimated to about 3 mb.

([11a]) J. DEAHL, M. DOVRICK, J. FETCOVIT, T. FIELDS and G. B. YODH: *Proc. of the 1960 Ann. Intern. Conf. on High-Energy Physics at Rochester* (New York, 1960), p. 185.

([11b]) W. PERKINS *et al.*: *Phys. Rev. Lett.*, **3**, 56 (1959); *Phys. Rev.*, **118**, 1364 (1960).

([11c]) The data at 245, 280 and 290 MeV have been obtained by the Dubna group (BATUSOV *et al.*). See, for example, B. PONTECORVO: *Report at the Ninth Annual Conference on High-Energy Physics* (Kiev, 1959).

We conclude that the interpretation of the ABASHIAN, BOTH and CROWE experiment in terms of a strong s-wave pion-pion interaction gives rise to very serious theoretical problems and that the situation concerning this experiment has to be considered by no means settled.

Therefore we think that a careful experimental analysis is very desirable. In particular, it would be very important to observe directly the charged pions in the reaction $p+d \to {}^3He+\pi^+ +\pi^-$ in order to study the mass spectrum of the $(\pi^+\pi^-)$ system. We also think that a study of the reaction $\pi^- + p \to \pi^+ + \pi^- + n$ for small masses of the $(\pi^+\pi^-)$ system will be very desirable because it would lead, through the peripheral formula, to a determination of a_0 analogous to that of a_2 discussed in this paper ([12]).

* * *

We thank Dr. S. FUBINI for having called our attention to the recent interpretation of the ABASHIAN, BOTH and CROWE's experiment and for a critical discussion of our results.

([12]) An analysis of this kind has been made by ERWIN *et al.*: ref. ([1]). Unfortunately, the number of events found for low $(\pi\pi)$ masses is too small to allow any estimate of a_0.

LIBRI RICEVUTI E RECENSIONI

Progress in Low Temperature Physics – Edited by C. J. Gorter; vol. III. North-Holland Publishing Company, Amsterdam, 1961; pp. 495.

Dopo alcuni anni di sospensione, appare questo terzo volume della serie « Progress in low temperature physics » e se ne promette il quarto a breve scadenza. Si deve essere grati al Prof. Gorter di curare questa serie di volumi sulla fisica delle basse temperature contenenti articoli aggiornati di rassegna e critica.

Questo terzo volume non delude le aspettative; esso ha un'impostazione spiccatamente sperimentale, in quanto tutti gli articoli sono diretti al chiarimento ed alla comprensione dei dati ricavati dall'esperienza, alla luce delle moderne teorie, mentre nessuno di essi è dedicato alla pura speculazione teorica o pecca di eccessivo formalismo matematico. Gli argomenti prevalentemente trattati sono l'elio liquido, la superconduttività e alcuni problemi di magnetismo.

Due dei quattro articoli sull'elio liquido riguardano argomenti di attualità, sviluppati dai rispettivi autori negli ultimi anni. Il primo articolo, chiarissimo, di Vinen, tratta le proprietà delle linee vorticali, che costituiscono oggi uno dei problemi più affascinanti del comportamento dell'elio superfluido. Il secondo articolo, compilato da Careri, tratta gli ioni positivi e negativi e le loro proprietà in elio superfluido e riguarda particolarmente il lavoro svolto dall'autore e dal suo gruppo a Padova. Buckingham e Fairbank, nel terzo articolo, discutono dettagliatamente la natura del punto λ, particolarmente alla luce dei loro più recenti esperimenti eseguiti entro alcuni milionesimi di grado dal punto λ e che dimostrano la presenza di una singolarità logaritmica. Il quarto articolo, sui recenti sviluppi della fisica dell'elio 3 liquido e solido, è stato preparato dai fisici di Los Alamos, Grilly e Hammel, ed è la continuazione di un articolo di Hammel, nel I volume dei Progress; molti progressi sono stati conseguiti da allora nella conoscenza di questo importante sistema di fermioni. (Per chi voglia gli ultimissimi sviluppi vi è il rendiconto del recente Simposio dell'Ohio State, 1960.)

La superconduttività è trattata molto dettagliatamente in un magistrale articolo di Bardeen e Schrieffer; la necessità di un articolo di rassegna e di critica dei risultati sperimentali e teorici dopo la formulazione della teoria di Bardeen, Cooper e Schrieffer era molto sentita e si deve dire che il compito è stato eseguito perfettamente.

La risonanza di ciclotrone e la risonanza paramagnetica dei metalli formano l'oggetto dell'articolo dei russi Azbel e Lifshitz, mentre il problema dell'orientamento dei nuclei a bassissima temperatura è trattato da Huiskamp e Tolhoek, che aggiornano l'articolo di Steenland e Tolhoek nel secondo volume dei « Progress ». Bloem-

BERGEN tratta molto chiaramente l'argomento dei maser a solido, illustrandone gli affascinanti aspetti e le utili applicazioni.

Vi sono alfine tre articoli dei fisici di Leiden su argomenti vari: BEENAKKER tratta, in dettaglio le proprietà termodinamiche e di trasporto degli idrogeni allo stato gassoso, cercando di mettere particolarmente in luce gli effetti quantistici alle basse temperature, mentre DOKOUPIL si occupa di alcuni equilibri solido-vapore. L'articolo di TACONIS, esclusivamente tecnico, illustra gli ultimi sviluppi nella costruzione dei criostati a elio 3.

Per concludere, questo volume sarà estremamente utile sia agli specialisti, sia a tutti quei fisici che vogliono aggiornarsi su alcuni tra i più interessanti progressi della fisica moderna.

G. BOATO

The Physical Examination of Metals – Edited by B. CHALMERS and A. G. QUARRELL. II Ediz.; Edward Arnold Ltd., London, 1960; pagine VIII-917, prezzo: 8 Guineas.

L'esame dei metalli mediante le loro proprietà fisiche interessa una così vasta categoria di tecnici e di studiosi, che un libro che porti questo titolo potrebbe avere contenuto assai vario, sia come profondità che come estensione. Il fisico dei solidi, il metallurgista, l'ingegnere ed il tecnico di officina hanno diverse esigenze, ma sono tutti interessati ai metodi ed agli strumenti di osservazione e di misura: è qui che si può trovare un punto d'incontro. Questo libro che appare completamente rinnovato, nella seconda edizione, sembra principalmente rivolto ai metallurgisti, e agli ingegneri, ma presenta anche per i fisici un indubbio interesse, specialmente come raccolta enciclopedica di molte tecniche diverse.

Il vastissimo materiale è suddiviso in capitoli, affidati a diversi Autori, specialisti nei vari campi, che formano un complesso abbastanza organico, benchè dall'uno all'altro si noti qualche differenza di impostazione.

Il tono generale si mantiene piuttosto elevato, anche se non tocca i più profondi problemi scientifici e le questioni più altamente specializzate come del resto non sarebbe opportuno in una rassegna di così vasto orizzonte. Il merito principale dell'opera è quello di raccogliere, in spazio relativamente breve, ed in forma facilmente accessibile, numerosi metodi che stanno diventando di sempre più largo uso, raggruppati ed inquadrati in modo da aprire la via allo studio più approfondito ed anche alla invenzione di procedimenti nuovi.

Passando ad un rapido esame del contenuto, notiamo che le più comuni prove meccaniche sui metalli, come quelle di trazione e di durezza, non sono prese in considerazione, come pure non sono trattate, o sono solo brevemente accennate, le questioni di più stretto carattere fisico.

Il primo capitolo riguarda le proprietà ottiche ed anche i metodi ottici di osservazione, il secondo le misure elettriche, principalmente misure di resistenza, il terzo quelle termiche, inclusa la termoelettricità. Alle proprietà magnetiche è dedicato un capitolo (il 4°) ed all'uso di metodi magnetici altri tre (13°, 14°, 15°), tutti piuttosto brevi, e prevalentemente di interesse pratico.

La diffrazione dei raggi X, degli elettroni e dei neutroni occupano tre ampie sezioni di notevole interesse generale, seguite da una rassegna estesa sulla microscopia. Il nono capitolo poi riunisce pirometria e spettrometria, con elementi di teoria e dati pratici.

Lo studio delle proprietà elastiche ed anelastiche, a mezzo di onde meccaniche, è svolto con ampiezza e con competenza; il fatto tuttavia che argomenti così strettamente connessi siano stati

trattati sperimentalmente e da diversi autori ne rende più difficile la visione unitaria. A nostro parere sarebbe stato più opportuno trattare in un capitolo tutti i metodi di misura, con le loro caratteristiche ed i loro limiti, e in un altro le cause fisiche che determinano le diverse proprietà.

Il dodicesimo capitolo è dedicato alla ricerca dei difetti (macroscopici) a mezzo di ultrasuoni: benchè questo argomento, di grandissimo interesse tecnico, non investa direttamente le proprietà fondamentali dei metalli, la raffinatezza dei metodi escogitati per la soluzione dei molti e non semplici problemi fa di questa sezione una brillante dissertazione sulla propagazione delle onde meccaniche nei solidi, il cui interesse va oltre i limiti che possono apparire a prima vista.

Le applicazioni dei radioisotopi fanno oggetto di una sezione piuttosto estesa che riunisce come ben si può comprendere, molti argomenti diversi. Microradiografia e autoradiografia sono trattate nel diciasettesimo capitolo. Il volume si chiude con una breve rassegna sulle moderne tecniche del vuoto che, benchè sia di innegabile interesse generale, sembra, in questa sede, un po' fuori posto.

Nell'insieme siamo di fronte ad un buon testo di consultazione per quanto riguarda le tecniche, che può anche servire egregiamente per lo studio introduttivo di molti argomenti.

F. A. Levi

L. D. Landau and E. M. Lifshitz: *Electrodynamics of Continuos Media*. Pergamon Press, London, 1960, pag. 428; prezzo 84 s.

Questo volume del corso di Fisica Teorica è certo all'alto livello dei volumi precedenti, ma presenta forse più marcata la limitazione di presentare solo argomenti sicuri ed incontrovertibili, e questi argomenti in forma categorica. Il libro inizia con capitoli di fisica matematica assai semplici e classici (elettrostatica di conduttori e dielettrici, campi magnetici, ecc.) per poi affrontare alcuni aspetti più fisici (superconduttività, ferromagnetismo, magnetoidrodinamica, passaggio di particelle cariche nella materia, scattering delle onde elettromagnetiche, fluttuazioni elettromagnetiche).

Purtroppo sono esclusi molti sviluppi teorici recenti e quindi non consolidati, ed anche i fatti sperimentali su cui la teoria si poggia non sono aggiornati convenientemente. Per esempio il capitolo sulla superconduttività presenta una situazione sperimentale come poteva essere prima della guerra, e una situazione teorica come poteva esserlo allora con esclusione di ogni tentativo fenomenologico. Passando ad altri argomenti, si rimane colpiti che Neél non sia nominato nell'antiferromagnetismo e Onsager a proposito dei dielettrici. Perciò il libro non può riuscire utile ai ricercatori, ma solo a chi si preoccupi di avere delle basi sicure su questioni fermamente stabilite.

G. Careri

R. E. Scott – *Linear Circuits;* Part I: *Time Domain Analysis*, pp. 510, £. 6.75. Parte II: *Frequency Domain Analysis*, pp. 928, £. 6.75; Addison Wesley, London, 1960.

Quantunque nel campo dell'editoria scientifica esistano già buoni libri che trattano la teoria dei circuiti lineari, il libro di Scott, dedicato agli studenti di ingegneria elettronica, si presenta come una delle opere didattiche più complete.

Il contenuto del libro può essere diviso in quattro argomenti:

Teorie dei circuiti resistivi.

Transienti.

Teorie dei circuiti *a-c*.

Trasformatore di Fourier e Laplace.

I primi due sono trattati nella parte I, e i secondi due nella parte II.

Nel primo argomento vengono trattati con le leggi fondamentali delle teorie dei circuiti, gli elementi di topologia delle reti, i metodi delle maglie e dei nodi e i metodi usati per la soluzione dei problemi relativi ai dipoli e ai quadrupoli.

Il secondo argomento tratta i metodi analitici per la soluzione delle equazioni integrodifferenziali relative a circuiti semplici eccitati da funzioni impulsive.

Il terzo argomento considera la risposta delle reti ad una eccitazione sinusoidale e tratta i metodi per ricavare le curve di ampiezza e fase.

Il quarto argomento tratta della risposta dei circuiti lineari ad eccitazione di forma d'onda complessa con il metodo della trasformata di Fourier e di Laplace.

Un importante bibliografia posta alla fine di ogni paragrafo, i numerosissimi esercizi risolti e le tavole riepilogative delle principali leggi completano l'opera e la rendono utile anche come elemento di consultazione.

F. Fioroni

Studies in Theoretical Physics. – Ministero per la Ricerca scientifica e gli Affari Culturali, Nuova Delhi, 1959; I e II volume.

In 339 pagine, tipo dispense, sono raccolte le lezioni e i seminari svolti dalla Scuola estiva di Fisica Teorica di Mussoorie (India) dal 22 maggio al 18 giugno 1959.

Il testo inizia con un messaggio del Presidente Nehru agli organizzatori ed alla direzione. Forse per non peccare di parzialità verso alcuna specializzazione della Fisica, nel suo primo anno di vita la Scuola ha svolto in questo corso inaugurale, diretto da S. N. Bose, ben 32 temi col concorso di circa altrettanti docenti, in prevalenza giovani, suddivisi in 5 sezioni: 1) Teoria dei campi; 2) Fisica nucleare; 3) Particelle strane; 4) Sciami; 5) Meccanica statistica. Le varie sezioni ospitano lezioni sia di carattere riassuntivo o panoramico, sia relative ad argomenti assai particolari. Le difficoltà tecniche per costringere entro i ridotti limiti di tempo imposti dal calendario un programma così vasto, hanno dato risultati abbastanza evidenti. Ogni tema svolto è aggiornato fino ai più recenti risultati ma spesso risulta eccessivamente conciso ed i commenti sono sacrificati. La sezione di Fisica nucleare è certamente la più completa e meno frammentaria, Fra gli altri sono apprezzabili il contributo di A. K. Saha sulla teoria dei sistemi dei fermioni applicata ai nuclei e per la sezione di Meccanica statistica quello di V. S. Nanda e R. K. Pathria sulla degradazione dei polimeri lineari e teoria dei numeri.

V. Nardi

A. Alberigi Quaranta and B. Rispoli – *Elettronica.* N. Zanichelli, Bologna, 1960; pp. 567, L. 6000.

Nella cultura professionale dei fisici e di molti ingegneri numerose nozioni di elettronica rappresentano oggi un elemento indispensabile. Si può d'altra parte constatare come scarseggiano o manchino del tutto, sopra tutto in lingua italiana, libri che aiutino i giovani a completare questo aspetto della loro cultura. Il volume di Alberigi Quaranta e Rispoli ha quindi il considerevole pregio di soddisfare un'esigenza realmente sentita da parecchi anni. Purtroppo, come apertamente avvertono gli autori nelle prefazioni, non tutti i campi dell'elettronica sono trattati in questo libro, ma esso si occupa principalmente dell'elettronica dei transienti.

A questo settore il volume introduce tuttavia con completezza e profondità dando inoltre la possibilità al lettore, per mezzo di numerose citazioni, di addentrarsi in quasi tutti gli argomenti, anche al di là dei limiti e degli scopi del volume. Un'esauriente trattazione della teoria dei circuiti, eseguita con i mezzi matematici più idonei alle applicazioni di elettronica dei transienti (trasformate di Laplace) è infatti seguita da un panorama dei componenti elettronici e quindi da una trattazione degli amplificatori lineari con e senza reazione negativa. Dopo un lungo capitolo sui circuiti non lineari (univibratori, circuiti multistabili, coincidenze ecc.) completa il volume un capitolo in cui vengono illustrati numerosi apparati elettronici, la cui comprensione è consentita al lettore dalla lettura dei capitoli precedenti. In tale modo quanto precede acquista ulteriore risalto e significato inquadrato nelle sue applicazioni.

Lo spazio dedicato ai transistori e ai circuiti transistorizzati andrebbe a nostro parere dilatato. Questo inconveniente è dovuto probabilmente al fatto che la stesura del libro è avvenuta in un periodo in cui il transistore era ancora un componente d'avanguardia.

Non dubitiamo tuttavia che gli autori non mancheranno di migliorare questo ed altri aspetti in successive edizioni di tale volume la cui utilità è già ora notevolissima per quanti vogliano introdursi con profondità all'elettronica dei transienti.

La lettura del volume è infatti consigliabile a chi voglia occuparsi in seguito di calcolatori numerici e di elettronica per la fisica nucleare; considerando tuttavia gli ultimi sviluppi di altri campi dell'elettronica e inoltre probabile che i futuri specialisti di altri settori (per esempio telecomunicazioni) troveranno frequentemente utile la lettura e la consultazione di questo libro.

M. Puglisi

J. Thewlis – *Encyclopedic Dictionary of Physics*: vol. I (A÷Compensated Bars). Pergamon Press, Oxford, 1961; pag. 800, s. 80.

L'identificazione di un pubblico per un dizionario di fisica è sempre impresa non facile. Ma è tuttavia indispensabile quando si vogliono stabilire i limiti e i criteri di stesura dell'opera. Secondo quanto viene detto nella presentazione del primo volume di questo dizionario, esso è destinato a tutti coloro che desiderano ottenere facilmente informazioni nel campo della fisica pura e applicata e di settori connessi. Questa definizione dei termini che ci si deve attendere di trovare nella consultazione dell'opera e del livello culturale richiesto al lettore è ancora alquanto vaga e l'opera risente a nostro parere di questa imprecisione di impostazione. Non è chiaro infatti come chi abbia bisogno di ricorrere a questo dizionario per chiarirsi la parola « aeroplano » sia poi in grado di comprendere l'illustrazione di argomenti di fisica trattati ad un livello che non è poi tanto elementare. Ma questo è un'inconveniente in certa misura inevitabile nella stesura di un'opera così vasta e ambiziosa, come in un certo senso lo sono anche gli altri che abbiamo rilevato, quali l'insufficiente aggiornamento di alcune voci, compilate evidentemente qualche anno fa (mancano completament i transistori negli esempi di circuiti elettronici; non vengono menzionati affatto gli amplificatori distribuiti) e la sproporzione tra lo spazio dedicato ad alcuni termini (poche righe per gli amplificatori).

È doveroso però riconoscere che l'opera ha non pochi pregi. I vocaboli sono spiegati con concisa competenza e semplice esattezza da esperti del settore e sono in molti casi corredati della bibliografia essenziale. È difficile trovare qualche termine non considerato, e se mai si è peccato accettando vocaboli

troppo indirettamente connessi alla fisica. Buona la veste tipografica, numerose e chiare le illustrazioni, mentre il costo del volume è mantenuto entro limiti ragionevoli. Naturalmente un giudizio completo su questa opera potrà essere dato soltanto dopo la comparsa di tutti i volumi.

A. Alberigi Quaranta

D. J. Thouless – *The Quantum Mechanics of Many Body Systems.* Academic Press, New York-London, 1961; pag. 175, $ 5.50.

Nella fisica dei molti corpi sta diventando urgente un processo di sintesi, che porti a precisare i punti fondamentali sia della fenomenologia, che delle tecniche di calcolo, perchè altrimenti ci si perde in mezzo al gran numero di articoli di tutti i generi che stanno uscendo sull'argomento. Il libro dà un ottimo schema delle techiche offrendone una rapida rassegna. Abbastanza estesa è la parte che introduce il formalismo perturbativo di Goldstone e Hughenholtz, presentata in modo elegante e sobrio, non ponderoso come nell'articolo di Hughenholtz del 1957. La teoria dello scattering multiplo di Brueckner viene illustrata in modo piuttosto sommario secondo il formalismo di Goldstone, più chiaro del linguaggio della teoria dello scattering usato negli articoli originali di Brueckner e Levison.

Le funzioni di Green sia per particella singola che per due particelle sono trattate con il duplice scopo di ricavarne le proprietà matematiche (relazioni di dispersione) e di calcolare con metodi perturbativi. In relazione alle funzioni di Green sono discusse le variabili collettive. Per temperature finite, sfruttando l'analogia tra l'equazione di Block per la funzione di ripartizione e quella di Schrödinger s'introduce il formalismo di Matsubra, che si serve della tecnica usuale della teoria dei campi in cui $it/\hbar$ è sostituito da $1/kT$ (t tempo, T temperatura). Il metodo di Bogoliubov è presentato solo in relazione alla superconduttività. Queste tecniche sono spiegate tenendo presente la materia nucleare e gli elettroni nella struttura atomica ma solo in modo fugace, l'elio nelle sue due forme isotropiche e i sistemi super-conduttivi. Però la fisica di questi sistemi è del tutto incompleta e non si può capirne nemmeno le linee essenziali senza precedenti conoscenze. Cioè la sintesi della materia, necessaria per chi voglia affrontare ex novo uno studio sistematico, è raggiunta in modo brillante ed unitario, ma ad un livello già specializzato. Quindi questo libro, ha il pregio rispetto all'altro già esistente del corso di Les Houches di una maggiore unitarietà, ma ha il difetto che la sintesi ragginta spesso va a discapito di una facile comprensione.

Per le tecniche non si richiede nulla che non sia ad un livello del 4° anno di fisica; man mano che si rendono necessarie conoscenze maggiori, come seconda quantizzazione dell'equazione di Schrödinger, teorema di Wick, ecc., esse vengono introdotte con sufficiente chiarezza; però, per quanto in modo minore, si risente lo stesso difetto della fisica dei sistemi. Ottima la bibliografia.

G. Di Castro

Handbuch der Physik; Bd. LIII: *Astrophysik IV: Sternsysteme.* Springer-Verlag, Berlin, Göttingen, Heidelberg; pp. VIII-566, con 189 Figure.

I quattro volumi dell'*Handbuch der Physik* che si riferiscono all'astrofisica, uscendo a 25 anni di distanza dall'*Handbuch der Astrophysik* presentano un quadro

sommamente interessante dell'enorme progresso realizzato in questo quarto di secolo. Per esempio, è assai notevole l'impostazione « evoluzionistica » che ricevono oggi quasi tutti i problemi astrofisici; essa rivela lo sforzo dei ricercatori attuali per riunire in un tutto coerente ed omogeneo i dati provenienti da fonti diverse. Un altro campo completamente nuovo sviluppatosi nel secondo dopoguerra è quello della Radioastronomia, a cui sono dedicati completamente 3 capitoli dei 14 che formano il 4° volume (53° di tutto l'*Handbuch*), a cui si riferisce questa recensione, per un totale di quasi 100 pagine su 537 del testo. I nomi degli Autori, alcuni dei quali, come HECKMANN HOGG, LINDBLAD, OORT, sono figure di primissimo piano fra gli Astronomi oggi in attività, costituiscono la migliore garanzia circa l'autorevolezza delle informazioni contenute nel volume che, siamo certi, resterà per vari anni una delle fonti più consultate nel campo dei sistemi stellari. Basterà quindi un elenco dei capitoli, senza ulteriori commenti: *Kinematical Basis of Galactic Dynamics* (F. K. EDMONDSON); *Galactic Dynamics* (B. LINDBLAD); *Radio Frequency studies of Galactic Structure* (J. H. OORT); *Star Clusters* (H. SAWYER-HOGG); *Discrete Sources of Cosmic Radio Waves* (R. H. BROWN); *Radio Frequency Radiation from External Galaxies* (B. Y. MILLS); *Classification and Morphology of External Galaxies* (G. DE VAUCOULEURS); *General Physical Properties of External Galaxies* (G. DE VAUCOULEURS); *Multiple Galaxies* (F. ZWICKY); *Clusters of Galaxies* (F. ZWICKY); *Large Scale Organization of the Distribution of Galaxies* (J. NEYMAN); *Distance and Time in Cosmology: the Observational Data* (G. C. MCVITTIE); *Newtonsche und Einsteinsche Kosmologie* (O. H. L. HECKMANN); *Andere Kosmologische Theorien* (O. H. L. HECKMANN).

L. GRATTON

I. I. GOLD'MAN, V. D. KRIVCHENKOV, V. I. KOGAN and V. M. GALITSKII – *Problems in Quantum Mechanics*, translated and edited by D. TER HAAR. Infosearch, London; pp. 394, s. 42.

I. I. GOLD'MAN and V. D. KRIVCHENKOV – *Problems in Quantum Mechanics*, edited by B. T. GEILIKMAN, translated by E. MARQUIT and E. LEPA. Pergamon Press, Oxford, London, New York and Paris; pp. 275, s. 50.

Sono state pubblicate quasi contemporaneamente due diverse traduzioni in lingua inglese di una raccolta di problemi di Meccanica Quantistica pubblicata in Russia, comprendente esercizi assegnati a studenti del quarto anno dell'Università di Mosca. La raccolta del primo volume (333 esercizi) è un poco più ampia di quella del secondo (283 esercizi), includendo oltre a tutti i problemi del testo russo di GOLD'MAN e KRIVCHENKOV, anche una selezione di problemi scelti da una raccolta pubblicata in Russia da KOGAN e GALITSKII. A sua volta il secondo volume comprende un piccolo numero di esercizi non contenuti nel primo, probabilmente perchè tale traduzione è stata condotta su una edizione più recente del testo russo di GOLD'MAN e KRIVCHENKOV.

Ambedue i volumi sono divisi in due parti: nella prima, che occupa una cinquantina di pagine, sono raccolti gli enunciati dei problemi; nella seconda vengono date le soluzioni. Queste sono esposte, specialmente per i problemi più complicati, molto dettagliatamente.

Ciascuna parte è a sua volta suddivisa, per argomenti, in nove capitoli.

I primi due capitoli sono dedicati all'equazione di SCHRÖDINGER unidimensionale; nel primo sono raccolti parecchi problemi su diversi tipi di buche di potenziale, nel secondo sulla trasmissione e riflessione da una barriera.

Il terzo capitolo è dedicato al principio di indeterminazione, relazioni di commutazione, comportamente dei pacchetti d'onda. Il quarto, al momento angolare e allo spin. Contiene anche qualche problema sui momenti di quadruplo e sui momenti magnetici degli atomi. Il quinto è dedicato ai potenziali centrali (stati legati). Il sesto, al comportamento di una particella in presenza di campi magnetici. Il settimo, che è il capitolo più ampio, è dedicato alla fisica atomica. L'ottavo è dedicato alle molecole. Il nono capitolo contiene problemi sullo scattering e sullo spin isotopico. Infine sono aggiunte due brevi appendici, la prima riguardante l'approssimazione semiclassica, la seconda il formalismo isotopico.

I problemi contenuti in questa raccolta sono di difficoltà variabile, cosicchè questi volumi costituiranno certamente un prezioso ausilio didattico per i corsi di meccanica quantistica ad ogni livello. Unico appunto che, a nostro avviso, si può sollevare è il carattere un po' troppo formale degli esercizi, compensato però dal pregio di costituite un « manuale » abbastanza esteso e completo.

F. Calogero
R. S. Liotta

Direttore responsabile: G. POLVANI Tipografia Compositori - Bologna

Questo fascicolo è stato licenziato dai torchi il 30-X-1961